

# AN INTEGRATED APPROACH TO TOOL LIFE MANAGEMENT



Thesis submitted in fulfilment of the requirement for the degree of

Doctor of Philosophy

By

**Zinah Jumaah Ahmed**

Institute of Mechanics and Advanced Material Engineering

Cardiff School of Engineering

Cardiff University

United Kingdom

**2018**

## **Publications:**

- Ahmed, Z. et al. 2017. Assessing Uneven Milling Cutting Tool Wear using Component Measurement. 30<sup>th</sup> Conference on Condition Monitoring and Diagnostic Engineering Management COMADEM2017 (University of Central Lancashire, UK).
- Ahmed, Z. J. et al. eds. 2016. The difficulties of the assessment of tool life in CNC milling. Students on Applied Engineering (ICSAE), International Conference for. IEEE.

# ABSTRACT

Tool wear is a complex phenomenon occurring in all metal cutting processes. It reduces dimensional accuracy, impairs the surface integrity of the component and can have profound effects on the overall quality of the machined workpiece. Tool condition monitoring methods can be broadly split based on the source of signals collected by sensors into direct and indirect methods. In real life, it is not simple to model or predict. This thesis considers current shortcomings in applied approaches to tool management to demonstrate the need for more accurate assessment of tool condition and particularly remaining tool life.

In this study, two kinds of indirect acquisition methods were used to estimate the tool wear. The post process method utilises the measurement of component geometry using a Coordinate Measure Machine. The in-process method utilises the acquisition and analysis of the applied spindle load from which tool wear can be estimated.

A series of tests were conducted based upon the machining of a set of cylindrical holes. Two different diameter tools, 10 mm and 16 mm end mills, were used. The CMM acquired component geometry was used to calculate the tool wear indirectly. The method was proved to provide a good indication of the tool wear behaviour. In particular the approach is shown to be helpful for identifying the important change in the rate of tool wear.

The developed online monitoring system, using the spindle motor load signal, is introduced in this thesis. It provides a practical method for detecting the progression of flank wear during machining. The results concluded that the signal amplitudes are increased when the flank wear increases. High cutting speed cause the flank wear to form quickly and shorten the tool life. This is an efficient and low-cost method that, with further development and testing, can be used in the real machining industry to predict the actual wear in the cutting tool.

# ACKNOWLEDGEMENTS

First, I would like to give thanks to Allah the almighty, the all great without whom I could not have completed this educational endeavour.

I would like to express sincere gratitude to Mr **Paul W. Prickett** and Dr **Roger I. Grosvenor** my immediate supervisors, for introducing me into this fantastic research area. They are generous and patient, guiding me in the research from the beginning to the end. Words cannot express my heartfelt gratitude for their efforts towards my development as a good researcher and a future academic. I consider myself ever so lucky to have been mentored by them. Their strong understanding and passion for academic quality resonates with me in every single way and has shaped my future goals as a researcher. They offered unquestionable support through the inevitable ups and downs of this research and kept me focused, giving me sound advice in all aspects of my studentship.

Further gratitude and appreciation is expressed to various people at Cardiff University including all the technical staff at Renishaw Lab, particularly Mr. Craig Ryan, for their help in overcoming the challenges of my experiments and all the staff of ENGIN Research Office for always keeping their door open for my inquiries. I wish to express my sincere thanks to my colleague Jacob Hill for his support in this research.

Finally, this research would not have been possible without the never-ending support of my family. My husband **Mohanad** Issa Ibrahim I hope to make you proud and thanks for your patience, encouragement and support over the past difficult years. Also, My Parents who has been a welcome distraction and ray of sunshine throughout. Thanks as well to Allah for his gift; my beloved **Tameem** and **Tasnim**.

During my time in Cardiff University, I had the privilege of knowing and working with many great people. Extra special thanks goes to my colleague Ali AL-Khafaji for his continued scientific support. Also, my deep gratitude to Ali Al-Zughaibi, Adnan AL-Amili, Raheem Al-Musawi and Zaynab Alraziqi for their consistent encouragement, invaluable guidance and strong support during the course of this study.

I will also take this opportunity to thank my sponsors at Baghdad the Ministry of higher education and scientific research, Al-Anbar University and Iraqi Cultural Attaché in London for their financial support but also for allowing me to gain an industrial perspective for my work.

*Zinah Ahmed*

*2018*

# TABLE OF CONTENTS

<b>DECLARATION AND STATEMENTS</b> .....	III
<b>ABSTRACT</b> .....	IV
<b>ACKNOWLEDGEMENTS</b> .....	V
<b>TABLE OF CONTENTS</b> .....	VI
<b>LIST OF FIGURES</b> .....	XII
<b>LIST OF TABLES</b> .....	XVIII
<b>Chapter 1 Introduction</b> .....	1
1.1 Background and Motivation.....	1
1.2 Research goals and objectives.....	2
1.3 Structure of the Thesis.....	3
<b>Chapter 2 Tool Condition Monitoring</b> .....	5
2.1 Introduction .....	5
2.2 Review of Various Techniques for Tool Condition Monitoring.....	6
2.2.1 Cutting Force.....	10
2.2.1.1 Direct Measurements of Cutting Forces.....	12
2.2.1.2 Measurement of the Cutting Forces Indirectly.....	14
2.2.2 Component Geometry .....	19
2.3 Summary .....	22

<b>Chapter 3 The Theory of the Tool Wear</b> .....	24
3.1 Introduction .....	24
3.2 Types of tool failure in milling cutting tools.....	25
3.3 Type of Wear Mechanism .....	29
3.3.1 Abrasive Wear.....	29
3.3.2 Adhesive Wear .....	31
3.3.3 Diffusion Wear.....	31
3.4 Parameters influencing tool wear .....	32
3.4.1 Machining parameters.....	32
3.4.1.1 Cutting Speed.....	32
3.4.1.2 Feed Rate .....	32
3.4.1.3 Depth of Cut.....	33
3.4.1.4 Cooling Fluid .....	33
3.4.1.5 Small chip load.....	33
3.4.2 Tool Properties .....	34
3.4.2.1 Rake Angle .....	34
3.4.2.2 Relief Angle .....	34
3.4.2.3 Tool Deflection.....	35
3.4.3 Workpiece Properties .....	36
3.4.4 Cutting phenomenon .....	36
3.4.4.1 Stiffness.....	37
3.4.4.2 Rigidity .....	37
3.4.4.3 Cutting Forces .....	37
3.5 Developing the Tool Life Modelling Methodology and Approaches .....	37
3.6 Tool Life Equations .....	41

3.7	Consideration of the Evaluation of Metal Removal Rate (MRR).....	48
3.8	Summary .....	51
<b>Chapter 4 Experimental Setup and Process Parameter Section.....</b>		<b>52</b>
4.1	Introduction .....	52
4.2	Experiment-based Approach to Tool Wear Assessment.....	53
4.2.1	Milling Machine.....	54
4.2.2	Test Piece Setup .....	55
4.2.3	Work Piece Material .....	55
4.2.4	Cutting Tool Setup.....	56
4.2.5	Cutting Conditions Setup.....	57
4.2.6	Coordinate Measure Machine .....	57
4.3	Experimental Procedure .....	60
4.4	Tool Diameter Measurements .....	67
4.4.1	Tool Wear Measurement.....	68
4.5	Assessment of the Volume Removed by the Cutter.....	72
4.5.1	Cutting Time .....	72
4.5.2	Calculation of the Volume of the Metal Removed .....	74
4.6	Summary .....	76
<b>Chapter 5 Experimental Results.....</b>		<b>77</b>
5.1	Introduction .....	77

5.2	Experimental Results.....	78
5.2.1	Cylinder Diameter vs. Hole Number .....	78
5.2.2	Tool Wear vs Hole Number .....	84
5.2.3	The Depth of Hole vs Hole Number .....	91
5.3	Summary .....	93
<b>Chapter 6 Discussion of the Initial Results .....</b>		<b>94</b>
6.1	Introduction .....	94
6.2	Tool Wear Mechanism .....	94
6.3	Tool Wear vs. Cutting Time.....	96
6.4	The Estimation of Remaining Useful Life .....	102
6.5	Detection of the Inflection Point of Tool Wear Curve .....	108
6.5.1	Substitution method .....	108
6.5.2	The Rate of Change.....	110
6.5.3	Multiple Linear Fit .....	111
6.5.4	The “Solver” Function .....	111
6.6	Volume Removed by Each Section.....	112
6.7	The Tool Wear in the Bottom cutting edges .....	114
6.8	The Results of Metal Removal Rate.....	116
6.9	Summary .....	121
<b>Chapter 7 Spindle Load /In-Process Monitoring .....</b>		<b>123</b>



7.1	Introduction .....	123
7.2	Spindle Current Measurement (Experimental setup) .....	124
7.3	Illustration and Analysis.....	128
7.3.1	Spindle Motor Load vs Cutting Time .....	128
7.3.2	Spindle Motor Load Profile during Milling One Cylinder .....	130
7.3.3	The Effect of Tool Wear on the Spindle Motor Load.....	133
7.3.4	Detecting Tool Breakage by the Spindle Motor Load .....	135
7.4	Assessment the Work Done by the Cutter.....	136
7.4.1	Cutting Time .....	136
7.4.2	Calculate the Work Done .....	137
7.5	The Relationship between Spindle Motor Load and Tool Wear.....	141
7.6	Summary .....	144
<b>Chapter 8 Conclusions, Contributions and Future Work.....</b>		<b>145</b>
8.1	Introduction .....	145
8.2	Conclusions .....	145
8.3	Contributions .....	149
8.4	Future Work and Recommendations .....	150
<b>References .....</b>		<b>151</b>
APPENDIX A The Tool Details.....		164
APPENDIX B CMM Program.....		165

APPENDIX C The Depth of the Holes.....	177
C.1 For The Large Cutter Series .....	177
C.2 For The Small Cutter Series .....	178
APPENDIX D Calculate the Metal Removal Rate.....	180
D.1 Introduction .....	180
D.2 10mm Cutter: series 10.6.....	180
D.2.1 Cycle 1: Plunge Milling .....	180
D.2.2 Cycle 2 Move Out .....	181
D.2.3 Cycle 3 Circular Cut.....	181
D.2.4 Cycle 4 Move Out .....	182
D.2.5 Cycle 5 Circular Cut.....	183
D.3 16mm Cutter: series 16.4.....	184
D.3.1 Cycle 1 Plunge Milling .....	184
D.3.2 Cycle 2 Circular Cut.....	185
D.3.3 Cycle 3 Move Out .....	185
D.3.4 Cycle 4 Circular Cut.....	185

# LIST OF FIGURES

Figure 2.1 Types of tool condition monitoring systems .....	7
Figure 2.2 Cutting tools monitoring options (Prickett and Johns 1999).....	10
Figure 2.3 Fishbone diagram with the parameters that affect cutting force (Bajić et al. 2012)	11
Figure 3.1 The wear in end milling cutter (ISO8688-2 2016) .....	26
Figure 3.2 Flank wear as a function of cutting time (Black and Kohser 2017) .....	28
Figure 3.3 Fishbone diagram with the parameters that affect tool wear and tool life..	29
Figure 3.4 Tool damage mechanisms and cutting speed (Childs et al. 2000).....	30
Figure 3.5 A: abrasive wear in the HSS milling tool and B: Microscopic image for Carbon steel (Hogmark and Olsson 2008).....	31
Figure 3.6 Geometrical parameters of an end-mill (Wang et al. 2014) .....	35
Figure 3.7 A schematic showing positive (left) and negative (right) rake angles.....	35
Figure 4.1 Mazak Vertical Centre Smart 430A (Mazakus.com) .....	53
Figure 4.2 CAD drawing of test piece .....	55
Figure 4.3 HSS end mill cutter.....	56
Figure 4.4 Coordinate Measuring Machine .....	59
Figure 4.5 The Diagram of Cutting Operation for Each Cylinder .....	61

Figure 4.6 Configurations of the workpiece and tool at each cutting cycle.....	62
Figure 4.7 The sketch of a sequence of four cylinders for one hole .....	63
Figure 4.8 Measurement position sketch .....	65
Figure 4.9 Workpiece plate after tool wear experiments .....	66
Figure 4.10 Determine the initial tool diameter .....	67
Figure 4.11 CMM commands to the user to establish alignment of the test piece .....	69
Figure 4.12 Sample of excel file for S16.4 test 10.....	70
Figure 4.13 The flowchart of using CMM to measure the diameter of the holes (one set) .....	71
Figure 4.14 Volume removed calculated position sketch .....	74
Figure 5.1 Variation in Cylinder Diameter/ Series 16.5 .....	79
Figure 5.2 Variation in Cylinder Diameter/ Series 16.1 .....	80
Figure 5.3 Variation in Cylinder Diameter/ Series 16.2 .....	80
Figure 5.4 Variation in Cylinder Diameter/ Series 16.3 .....	80
Figure 5.5 Variation in Cylinder Diameter/ Series 16.4 .....	81
Figure 5.6 Variation in Cylinder Diameter/ Series 10.4 .....	82
Figure 5.7 Variation in Cylinder Diameter/ Series 10.1 .....	82
Figure 5.8 Variation in Cylinder Diameter/ Series 10.2 .....	83
Figure 5.9 Variation in Cylinder Diameter/ Series 10.3 .....	83

Figure 5.10 Variation in Cylinder Diameter/ Series 10.5 .....	83
Figure 5.11 Variation in Cylinder Diameter/ Series 10.6 .....	84
Figure 5.12 Tool wear as a function of Hole Number/ Series 16.5 .....	85
Figure 5.13 Tool wear as a function of Hole Number/ Series 16.1 .....	85
Figure 5.14 Tool wear as a function of Hole Number/ Series 16.2 .....	86
Figure 5.15 Tool wear as a function of Hole Number/ Series 16.3 .....	86
Figure 5.16 Tool wear as a function of Hole Number/ Series 16.4 .....	86
Figure 5.17 Tool wear as a function of Hole Number/ Series 10.4 .....	87
Figure 5.18 Tool wear as a function of Hole Number/ Series 10.1 .....	88
Figure 5.19 Tool wear as a function of Hole Number/ Series 10.2 .....	88
Figure 5.20 Tool wear as a function of Hole Number/ Series 10.3 .....	88
Figure 5.21 Tool wear as a function of Hole Number/ Series 10.5 .....	89
Figure 5.22 Tool wear as a function of Hole Number/ Series 10.6 .....	89
Figure 5.23 Summary of the amount of tool wear occurs in different sections and tool wear average of the 10mm cutter .....	90
Figure 5.24 Summary of the amount of tool wear occurs in different sections and tool wear average of the 16mm cutter .....	90
Figure 5.25 Variation in the Depth of the Hole/ Series 16.1.....	91
Figure 5.26 Variation in the Depth of the Hole/ Series 10.1.....	92

Figure 6.1 End mill cutter: a) before and b&c) after tool wear experiment/ series 10.4.....	95
Figure 6.2 Tool wear as a function of Cutting Time / Series 10.4.....	96
Figure 6.3 The calculated cutting time for each section of all series (minutes).....	97
Figure 6.4 Tool wear as a function of Cutting Time / Series 16.1.....	98
Figure 6.5 Tool wear as a function of Cutting Time / Series 16.2.....	98
Figure 6.6 Tool wear as a function of Cutting Time / Series 16.3.....	99
Figure 6.7 Tool wear as a function of Cutting Time / Series 16.4.....	99
Figure 6.8 Tool wear as a function of Cutting Time / Series 16.5.....	99
Figure 6.9 Tool wear as a function of Cutting Time / Series 10.1.....	100
Figure 6.10 Tool wear as a function of Cutting Time / Series 10.2.....	100
Figure 6.11 Tool wear as a function of Cutting Time / Series 10.3.....	101
Figure 6.12 Tool wear as a function of Cutting Time / Series 10.5.....	101
Figure 6.13 Tool wear as a function of Cutting Time / Series 10.6.....	101
Figure 6.14 Calculate Remaining Useful Life/ series 10.4.....	103
Figure 6.15 the change in the component dimensions/series 10.6.....	105
Figure 6.16 the change in the component dimensions /series 16.1.....	105
Figure 6.17 Tool wear vs. cutting time/series 10.2.....	107
Figure 6.18 Tool wear vs. cutting time/ series 10.6.....	107

Figure 6.19 (A-C) Calculate the inflection point/ series 10.4 .....	109
Figure 6.20 The rate of change / series 10.4 .....	110
Figure 6.21 The multiple linear fit / series 10.4 .....	111
Figure 6.22 The transition point when using the Excel Solver/ series 10.4.....	112
Figure 6.23 Percentage of total Volume Removed by Each Segment for 16mm cutter .....	113
Figure 6.24 Percentage of total Volume Removed by Each Segment for 10mm cutter .....	114
Figure 6.25 Wear in the bottom cutting edges/ series 16.1 .....	115
Figure 6.26 wear in the bottom cutting edges/ series 10.1 .....	115
Figure 6.27 Metal Removal Rate for 16 mm cutter .....	119
Figure 6.28 Metal Removal Rate for 10 mm cutter .....	120
Figure 7.1 In- process tool condition monitoring.....	125
Figure 7.2 MAZAK monitoring system.....	126
Figure 7.3 Real-time monitoring system.....	127
Figure 7.4 The data stored in notepad.....	127
Figure 7.5 Spindle motor load percentage vs cutting time/series 10.4 .....	129
Figure 7.6 Spindle motor load percentage vs cutting time/series 10.6 .....	129
Figure 7.7 A schematic diagram of the power profile during milling one Cylinder for the small cutter /series 10.4 H1C1 .....	132

Figure 7.8 A schematic diagram of the power profile during milling one Cylinder for the large cutter /series 16.5 H1C1 .....	132
Figure 7.9 The spindle motor load signal Vs. The time during milling one Cylinder for new (H1C1) and fully worn (H32C1) tool/series 10.4.....	134
Figure 7.10 The spindle motor load signal Vs. The time during milling one Cylinder for new (H1C1) and fully worn (H48C1) tool/series 16.5.....	135
Figure 7.11 The spindle motor load signal for health cutter/series 10.5.....	136
Figure 7.12 The spindle motor load signal for broken cutter/series 10.5 .....	136
Figure 7.13 Total cutting time for each section (minutes).....	137
Figure 7.14 Percentage of the work done by each section.....	138
Figure 7.15 The work done by C4/ series 10.4 .....	139
Figure 7.16 The work done at different types of operation/series 10.4 .....	140
Figure 7.17 The work done in plunge operation/series 10.4.....	141
Figure 7.18 The relationship between the SML % and tool wear/series 10.4 .....	142
Figure 7.19 The relationship between the SML % and tool wear/series 16.5 .....	142
Figure 7.20 The relationship between the work done and tool wear/series 10.4.....	143
Figure 7.21 The relationship between the work done and tool wear/series 16.5.....	143
Figure D.1 .....	181
Figure D.2 .....	181



# LIST OF TABLES

Table 3.1 Representative values of $v$ and $T$ in Taylor Tool Life Equation for a combination of HSS cutter and Carbon Steel workpiece material.....	44
Table 3.2 Summaries Tool life equations with its advantages and disadvantages .....	47
Table 4.1 Milling Machine Specification.....	54
Table 4.2 machining parameters of verification experiment .....	58
Table 4.3 The series classification .....	64
Table 4.4 Feed rate at each cutting cycle .....	66
Table 4.5 CMM program .....	70
Table 4.6 The symbols used to calculate the volume removed.....	75
Table 6.1 The amount of Remaining Useful Life occurring in different sections of the 10mm cutter .....	103
Table 6.2 The effect of differential tool wear on the component geometry quantitatively .....	104
Table 6.3 The spindle speed, feed rate, cutting time, the area and the volume of metal removed for 16 mm cutter.....	116
Table 6.4 The spindle speed, feed rate, cutting time, the area and the volume of metal removed for 10 mm cutter.....	117

# Chapter 1

## Introduction

### 1.1 Background and Motivation

During machining operations, it is always hard to select suitable tools, machining parameters and a tool replacement time due to the vast variety of tool options and the complexity of the machining processes. Of particular interest are the complicated relationships between tool selection, cutting data calculation and tool life estimation and control. The cutting tool is one of the most crucial elements of a material processing system. Tool wear is a complex and varied process that cannot be described by a simple mechanism. The position and extent of wear varies and changes with the tool material, the operation, cutting conditions and the workpiece material.

To date, a relatively large number of research studies, which will be reviewed in Chapter 2 and Chapter 3, have investigated different techniques for this purpose. These can be broadly classified into direct and indirect techniques depending on the source of signals collected by sensors. Direct methods reviewed in this thesis include measuring the cutter itself. They may be said to be fast and accurate but cannot be applied online. Indirect methods involve measuring signals that related to tool condition. They may be online (in process) using measurements such as cutting force and power current. A final approach operates off line (post process) using the assessment of workpiece condition such as workpiece size and geometry.

Most of the reviewed published research has been concentrated on indirect methods measured online. There are a smaller numbers of studies about the indirect methods measured offline based upon workpiece condition with the milling process. These papers summarised that it is possible to measure the amount of the change in the tool dimensions based upon the machined parts. However, they did not take into account the

uneven tool wear because they did not consider this parameter as having a significant influence on the assessments of the degree of tool life and the component accuracy. This is not the case, as indicated by this research.

A comprehensive review of existing direct and indirect techniques will be presented in Chapter 2. The main conclusion from this critical review is that the assessment of the condition of the tool remains an area of open research. In particular, it is still of current scientific interest to develop tool condition monitoring techniques, which should be conducted in a simple, fast, and reliable manner.

## **1.2 Research goals and objectives**

In this context, the overall aim of the research reported in this thesis is to investigate the new engineering of technique for the assessment of the tool life. This technique relies on the analysing of information acquired from the component geometry.

Thus, the particular objectives of this thesis are:

- To develop an appropriate experimental methodology using a post-process technique for assessing the tool life which can be implemented based on measurement of the changes in machined component dimension.
- To validate the application of spindle load based monitoring by comparing its results with those obtained when using the component geometry based approach, considered for monitoring the tool condition online in this research.
- To explore the possibility of proposing additional approaches for assessing tool life based on the work done by monitoring the spindle motor load.

### 1.3 Structure of the Thesis

**Chapter 2** reviews knowledge about tool condition monitoring. It presents a critical analysis of the different techniques reported in the literature for characterising the condition of the cutter. Special attention is given to the current knowledge gaps, which affect reliability and predictability of the assessing tool life and feature geometry.

**Chapter 3** describes the types of tool wear mechanisms and the most common tool life criteria. The first attempt to predict the tool life based upon a theoretical approach represented in Taylor equations is explained in this chapter.

In **Chapter 4** the experimental approach to tool wear assessment based upon feature measurement is presented. A particular test piece to directly explore the level of tool wear was designed. The test piece and cutting parameters setup are presented. The experimental methodology for deploying this technique in practice is outlined.

**Chapter 5** reports the data obtained from a series of geometry experiments carried out on low carbon steel material for all series. These data are analysed and discussed later in Chapter 6.

**Chapter 6** the experimental results that were reported in Chapter 5 are discussed for all series. The cutting times and the metal removed by each segment were calculated. In addition, a method to assess the tool wear is also explained in this chapter.

**Chapter 7** presents a series of in process techniques to gain further insight into the monitoring of the cutting conditions. In particular, it focuses on the evaluation of the suitability of using the spindle load technique in monitoring the tool condition by comparing its outcome with the Coordinate Measure Machine (CMM) measurement obtained from the analysis of the component geometry data for all series considered. In addition, it presents the experimental setup utilised to measure the spindle load signals, which can be used to monitor the tool condition during the process.

Finally, **Chapter 8** provides a summary of the research reported in this Thesis. In particular, the most significant findings and contributions are highlighted. Recommended areas for future work are also provided in this chapter.

# Chapter 2

## Tool Condition Monitoring

### 2.1 Introduction

End milling is one of the most widely used material cutting operations in the industry. It is a discontinuous process in which the cutting tool edge enters and exits the workpiece several times. As a result, the life of the cutting tool can frequently be reduced because of chips, cracks, and breakage of the cutting edge (Vallejo et al. 2006).

Monitoring the condition of cutting tools and prediction of tool life plays an important role in improving machine productivity since it avoids possible damage to both products and machine tools. It can enable and support techniques aimed at maintaining the quality and integrity of the machined part, minimising material waste and reducing the cost and downtime of the machine and increase productivity. Therefore, it is necessary to be able to monitor tool wear during the material removal process.

The development of tool condition monitoring systems is crucially important for the advancement of technology. The conventional method to express machining parameters such as tool life is to conduct actual machining tests over a range of cutting conditions within a laboratory. However, the evaluation of the constants in these empirical equations and/or mathematical models is usually done in a conventional way one variable at a time. This is an expensive and time-consuming process. Additionally, in the case of constant cutting parameters, the tool failure will be a stochastic process. Hence, the need for both quickly and cheaply assessing the tool condition has attracted considerable attention in the past.

Accurate detection of tool wear is essential, since, in an industrial scenario, two possible situations could occur: the tool may be changed prematurely; i.e. changed before it reaches the end of the life. Alternatively, it may be used to produce several

defective parts before tool wear is noticed. In this case, more parts may need to be rejected and reworked. In the worst case, tool breakage could lead to damage of machine. Consequently, in both situations financial loss is unavoidable.

There has been a vast amount of research published on tool wear detection. This review does, however, present the most relevant and recent work in the field in order to highlight the complexity and challenges of the application area.

The rest of this chapter covers the highlighted indirect control methods of tool wear measurement using various techniques such as force, changes in machined component dimensions (component geometry), and current measurements that can be used to predict tool wear, as shown in Figure 2.1. This figure shows that a tool condition can be monitored based upon assessing tool life criteria, which can be divided into direct and indirect methods. The indirect methods could be on-line or off-line. Chapter 2 will review and focuses on the monitoring the tool condition indirectly, off-line by assessing the component geometry and online by assessing the tool load.

## **2.2 Review of Various Techniques for Tool Condition Monitoring**

One of the most crucial and determining factors enabling machine tool automation is the assessment of tool condition and the prediction or detection of tool failure. A variety of experimental sensing techniques has been applied to the automated tool wear monitoring problem in milling operations. The aim is to improve the quality of machined parts, reduce production time and costs.

- Tool life criteria
- Tool life equations

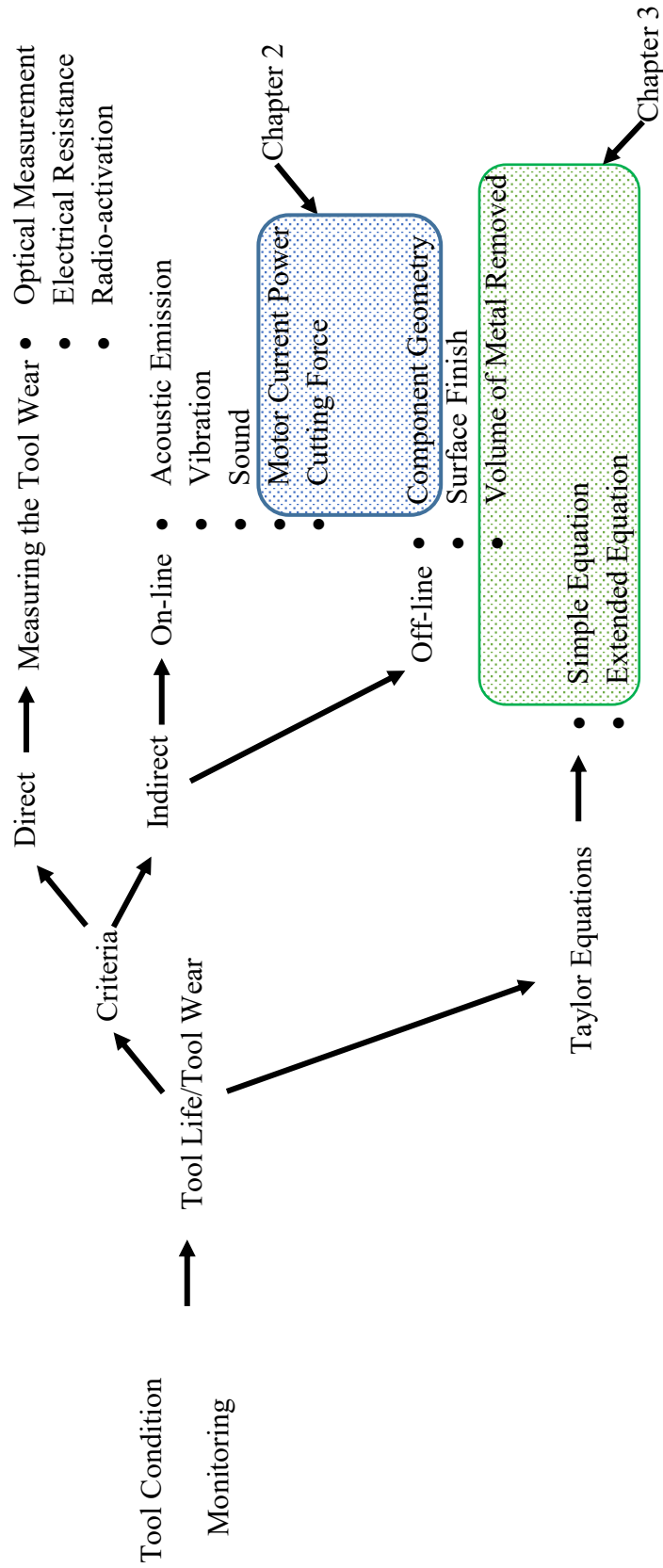


Figure 2.1 Types of tool condition monitoring systems



The tool life criterion that are most commonly used in the cutting process management can be classified as a being direct and indirect criterion. Direct criteria involves measuring the tool itself using different methods. These include optical measurement, radioactivation analysis, machine vision by using charged coupled device (CCD) or optical microscope (Kurada and Bradley 1997) (Castejon et al. 2007) (Byrne et al. 1995) (Shahabi and Ratnam 2009) and electrical resistance measurements. These can be fast and accurate. However, their implementations are avoided because they can be costly and cannot be applied online (Zuperl et al. 2011).

Direct criteria uses feature measurement such as the value of the width of flank wear land, the value of the maximum depth of crater and the extent of chip formation in the tool. Alternatively, indirect criteria sense the physical quantities which are mainly related to the cutting process. They may use the measurement of a parameter that is easy to measure, which can be used to assess tool wear. Indirect measurements may be online (in-process) and use machining process signals. These signals can be related to tool condition parameters that are known to be significantly affected by tool wear. They are used since cutting edges are generally inaccessible during cutting (Shao et al. 2004). The most commonly used signals are cutting force, acoustic emission, sound, current power for various drives and vibration. Other indirect measurements are mainly offline and relate to workpiece condition. This can be represented by workpiece size, geometry and condition. Methods include the measurement of the changes in machined component dimension or geometric form, the value of the volume of metal removed and component surface finish and roughness.

Measurements are commonly obtained offline because they can be very hard or impossible to perform in real time. This means that the cutting process must be stopped, causing lost machining time. In addition, the cutting tools are not in contact with the workpiece or acting under load and therefore tool wear-related problems, such as cracking, will not be easily discernible. Indirect methods can monitor the tool condition in real time. Thus, most of the reviewed research has been concentrated on indirect methods, due to the stability issues of the direct measurement methods. Indirect methods do not need to access the tool itself to measure the tool condition. Also, the

signals which refer the tool condition can be acquired in real time when the machine is running.

More recently, research has evolved towards the use of a multi-sensor approach. So-called sensor fusion brings together different signals in the same monitoring system in order to gather information from several sensors. This has supported research aimed at providing a comprehensive estimate of tool wear, especially under varying machining conditions.

Generally, all tool condition-monitoring systems (TCMS) consists of sensors, which are a fundamental element of any tool/process monitoring system; signal processing stages and decision-making systems. They use a strategy to analyse the signals from the sensors to provide reliable detection of tool and process failures (**Čuš and Župerl 2011**).

The ability of a TCMS depends on two basic elements: the number and type of sensors used and the associated signal processing methods applied. TCMS was initially associated with expensive hardware, including sensors, which affected the cost of the monitoring system. This consideration has been reduced by the increasing availability of more powerful yet lower cost sensors. The same evolution of more intelligent sensors has reduced the cost of signal processing and analysis. These have supported the development of methods that can be utilised to extract the necessary, important information from machining signals. The combination of enhanced sensors and powerful real-time analysis combine to affect the efficiency and the speed of the system (**Milfelner et al. 2005**). As a result, the right choice for sensors is a fundamental thing for a successful process monitoring system.

Many approaches have been proposed to accomplish tool condition monitoring. These are represented in Figure 2.2 (**Prickett and Johns 1999**). Although this figure is in some ways outdated, it does show the machine tool elements that can be the basis for TCM and indicate the most important options that can be exploited in the control systems for the study of the tool behaviour. In the machining process, a parameter such as cutting force is the most common important process quantities that are being

monitored either directly or indirectly. They are each discussed in more detail in the following sections.

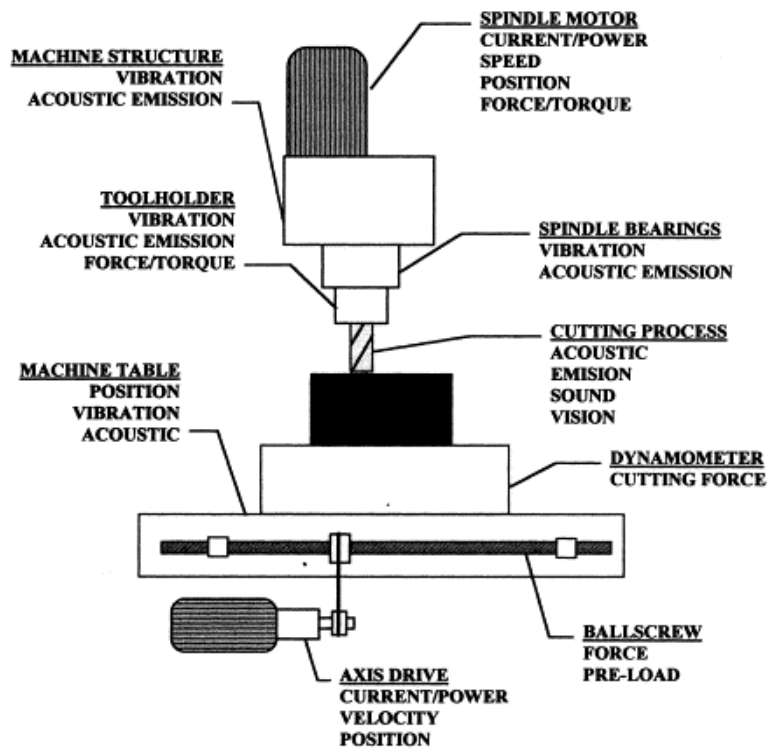


Figure 2.2 Cutting tools monitoring options (Prickett and Johns 1999)

### 2.2.1 Cutting Force

Cutting force has a great influence on tool life in milling operations. Therefore, measure the cutting forces produced during metal remove operation is a very logical common method of assessing the tool condition. The variation in the cutting force can be correlated to the tool wear due to a combination of mechanical, thermal, chemical, and abrasive phenomena acting on the cutting edge of the tool (Coromant 1994), or due to the friction between cutting tool flank and the workpiece (Choudhury and Kishore 2000) (Dimla 2000). As such, the measurement of cutting force provides precious information for tool wear monitoring. It is assumed that cutting force is approximately proportional to the cross-sectional area of the metal removed and that during normal

operation the volume of metal removed during one tool rotation is constant. However, as the tool gradually wears, the cutting force increases.

Cutting force can be measured directly and accurately by using a dynamometer. This may be mounted on the machining worktable (stationary dynamometer) or within a tool holder (rotating dynamometer) during machining. Restrictions to work holding and cost-related considerations limit the applicability of dynamometers in actual machining environments. As such, much attention has been placed on acquiring and measuring cutting forces indirectly. Either from the sensing currents of feed drive servo-motors (Altintas 1992) (Kim and Kim 1996) (Kim and Chu 1999) (Hongqi et al. 2010) or from sensing currents of the spindle motor (Kim et al. 2005) (Liang et al. 2002) or from both (Saraie et al. 2003). Cutting force is affected by many factors, which are represented in Figure 2.3.

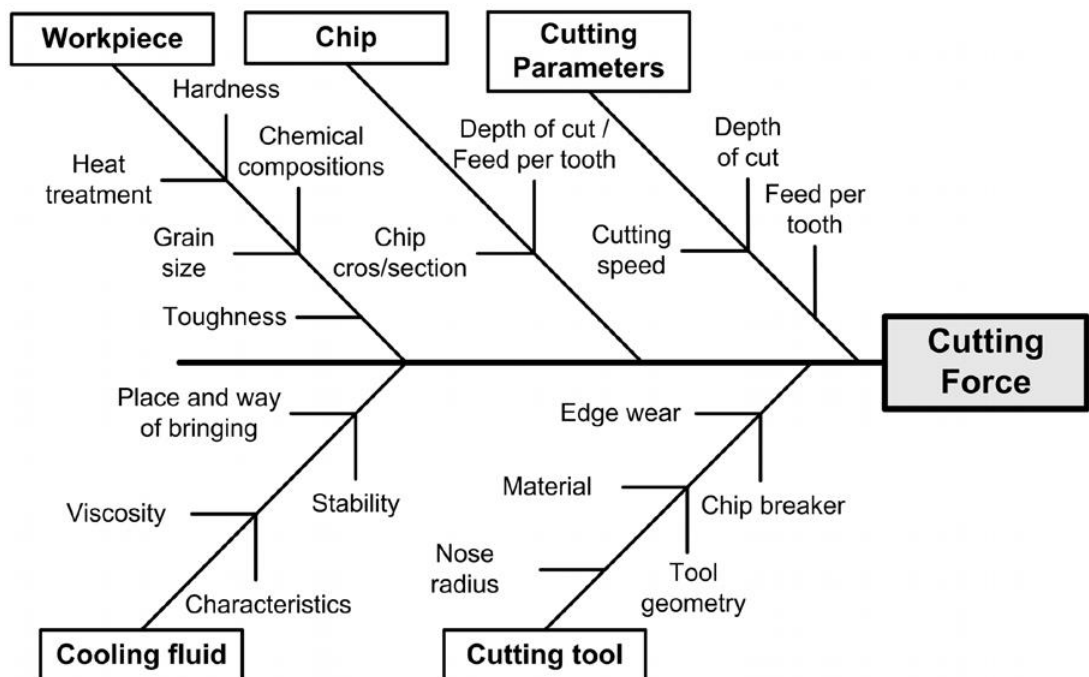


Figure 2.3 Fishbone diagram with the parameters that affect cutting force (Bajić et al. 2012)

### 2.2.1.1 Direct Measurements of Cutting Forces

Many researchers considered looking at tool wear as a related to the cutting parameters such as cutting speed, feed rate and depth of cut. Some of these then go on looking at cutting forces for predicting tool wear. They analysed the cutting force signals recorded by a dynamometer and characterized the tool wear by time domain and frequency domain via Neural Networks (NN) and Fast Fourier Transform (FFT).

**Lin and Lin (1996), Dong et al. (2006)** claimed that cutting forces in machining operations are actually related to tool wear and can be used in estimating the tool wear. In addition, they deduced that the results from the neural networks were found to be quite similar to the experimental results and the proposed model was more accurate in predicting flank wear.

**Sarhan and El-Zahry (2011)** used the FFT analysis. They found that the magnitudes of the cutting force and surface roughness changed with the flank wear at different rates.

**Čuš and Župerl (2011)** engineered a system for monitoring tool condition in real time based on an NN and Adaptive Neuro-Fuzzy Inference System. They conclude that the (ANFIS) system proposed model could predict flank wear for different cutting conditions with high accuracy.

Other researchers have engineered a statistical approach to analyse and identify the most significant cutting force signals recorded by a dynamometer for the tool wear monitoring system.

In **Choudhury and Rath (2000)**, a series of experiments were conducted according to the design of experiment Analysis of variance (ANOVA). The proposed model represented the relationship between flank wear, tangential cutting force coefficient and the cutting parameters.

A tool wear monitoring strategy for end milling operations when cutting steel with High-Speed Steel (HSS) tool has been presented (**Sarhan et al. 2001**). The cutting force signals were obtained using a sensitive strain gauge dynamometer. Signals were fed into

a FORTRAN program to plot responses in both the time and frequency domains. The results indicated that the cutting forces were more sensitive to the change of flank wear and increased significantly when the tool wears.

Three in-process tool wear monitoring systems based on cutting force were developed and tested (**Chen 2003**). These systems are using multiple linear regression, artificial neural networks, and a statistics assisted fuzzy-nets based in-process tool wear prediction system. This study demonstrated that the average peak cutting forces in the Y direction (the direction that is perpendicular to the table feed) is the most efficient cutting force representation for tool wear monitoring.

**Nouri et al. (2015)** employed a statistical method based upon a Cumulative Sum (CUSUM) control chart to detect the transition of the force model coefficient. They summarised that this approach could be used in real-time to monitor the wear of the tool and identify the transition point from the gradual wear region to the failure region.

A combination of signal processing techniques for estimation of tool wear in real time based on cutting force signals has been presented (**Bhattacharyya et al. 2007**). Discrete Wavelet Transform, Time Domain Average and Linear Filtering were adopted for extracting relevant features from cutting force signals when milling C-60 mild steel with a single cutting tool insert in face milling operations. Tests producing four different datasets were carried out covering a wide range of machining parameters. They summarised that the proposed model gives satisfactory prediction results by both laboratory and industrial implementations. It is important to note that in that technique, one insert tool was used, which simplified the algorithms, and the tool wear relationships established may not be applicable to multi-toothed cutters.

An approach for fault detection and a diagnosis based on an observer model of an uncertain linear systems was developed (**Huang et al. 2007**). They designed a model by using the observed variables and cutting force. Four sets of cutting tests were conducted under different working conditions defined by controlled variations to cutting speed, depth of cut, and feed rate. The results indicated that this approach could

be used for the detection of failures arising from sensor or actuator functions. However, it is hard to detect tool wear in industry.

The tool wear during end milling of AISI-D2 Steel was monitored using the resultant cutting force ( $F_R$ ) measured by a dynamometer (**Chandgude and Sadaiah 2014**). A series of experiments were conducted with TiAlN-coated flat solid carbide tools to determine the relationship between flank wear and cutting force as well as the cutting parameters such as cutting speed, feed rate, axial and radial depth of cut. They considered that the cutting force measurement method was the best method for in-process condition monitoring and observed that the resultant force increased as the tool wear progressed consistently.

Although many investigators agreed that cutting force is a reliable and sensitive method to estimate or detect tool wear. There continues to be disagreement on which force component is the most sensitive. Moreover, in some cases, it is hard to separate between cutting force increment due to other disturbances from those resulting from tool wear. For example, a sudden change from hard spots or inclusions in the workpiece material or unexpected changes of the depth of cut. Therefore, sensors for the spindle motor current and power signals are free from such limitations and have the potential of being effective indicators for indirect cutting force measurement.

### **2.2.1.2 Measurement of the Cutting Forces Indirectly**

The main task for the spindle in milling machining operations is to rotate the cutter. In doing so, it must transmit the required energy from the motor to the cutting zone for metal removal. The spindle function has a strong influence on the quality of the machined parts and the metal removal rates (**Abele et al. 2010**). In a milling machine, the spindle is the shaft to which the cutter is attached. Therefore, the rotational speed of the tool is equal to the spindle speed and is usually quoted in revolutions per minute (r.p.m).

During the cutting process, the current consumed by the spindle motor is related to the output torque of the motor and therefore the tool load. Hence, this current can be used

for monitoring the machining process since it is closely related to the cutting forces generated in machining (**Cuppini et al. 1990**). Similar observations may be applied to other motors driving the machine tool.

Spindle or feed motor current based tool wear monitoring systems have been presented in milling operations to overcome the disadvantages of other methods. This section discusses the published literature in the area of the prediction of tool wear in milling by using spindle current measurement.

The major advantages of using the measurement of a spindle motor current to monitor tool conditions is that it can be undertaken during the cutting process without the requirement for numerous added sensors. This does not influence machine integrity and stiffness (**Zuperl et al. 2011**) or disturb the machining process (**Reddy et al. 2012**). Access to the sensors used by the machine controller can allow this method to be applied to existing or new machines (**Zuperl et al. 2011**) (**Stavropoulos et al. 2013**). Consequently, the relative cost of installing and operating a power detection setup is reduced. If it is possible to access the motor controller, then power and control signals may be acquired directly without the need for a sensor. It is also important to state that this setup does not interfere with the operation of the machine tool.

The main advantage of monitoring the mechanical power instead of monitoring the electrical power is the electrical power monitoring can produce higher than actual estimates since many unavoidable losses will be added to the result. This includes the armature resistance, the spindle current, mechanical frictions at the bearings, etc. However, the mechanical power control provides a lower than actual estimate because many power-consuming sources would be omitted such as heat, sound and vibration generated during the process (**Al-Sulaiman et al. 2005**).

It is proposed however that a significant change in condition may be evident in changed electrical power levels rather than by using the absolute power measurements. In this way, the method may have considerable potential. In this investigation, the approach was based on monitoring such changes to reflect changes corresponding to tool condition.



The following researchers have based their work on the spindle measurement in order to enable the identification and detection of tool wear.

The tool failure in end milling operations using the spindle motor current has been tested by **Lee (1999)**. The author employed a discrete wavelet transform for the detection of a sudden change in the signal owing to tool failure. They confirmed the effectiveness of the proposed approach for monitoring the milling processes.

The sensitivity of spindle power for tool condition monitoring in milling, drilling and turning has been evaluated (**Axinte and Gindy 2004**). They calculated the cutting power based on cutting force/torque and compared between the theoretical cutting power and the spindle power signal. The time-domain diagrams of the output signals were analysed using MATLAB/LabView codes to identify tool malfunctions and to compute statistical measures in defined sampling windows. They concluded that tool condition monitoring using spindle power could be successful in continuous machining processes (turning and drilling), while for discontinuous machining operations (milling), the spindle power signal showed reduced sensitivity to detect small uneven events such as the chipping of one tooth.

A cutting power model for tool wear monitoring in face milling operation where cutting conditions and tool flank wear is taken into account has been developed by **Shao et al. (2004)**. Several machining experiments have been conducted when cutting a cast iron workpiece with carbide cutting tools covering wide range variations of machining conditions such as cutting speed, feed rate and depth of cut. They concluded that experimentally, it was difficult to use the power model in real time due to the inherent fluctuations in measured cutting power. However, the mean cutting power of measured and simulated power signals demonstrated good agreements. This has been used in an update strategy for the cutting performance threshold for tool wear monitoring during milling operations under variable cutting conditions.

A multiple linear regression model was used to predict tool flank wear and to evaluate the difference between the actual measurement and the expected value for face milling operation based on the measurement of a spindle motor current (**Bhattacharyya et al.**

**2006**). To achieve this aim, a number of experiments were carried out with constant cutting parameters (cutting speed, depth of cut, and feed rate) when milling C-60 mild steel workpiece using a single cutting insert. In this research, the authors measured cutting force signals and spindle motor current to estimate flank wear. Cutting force signals were considered only to compare the performance. The results showed that the average absolute error between predicted and measured values were lower than 5%. Therefore, it is possible to replace force signals by the spindle motor current signal for tool condition monitoring in face milling.

A real-time cutting tool condition monitoring by measuring the current variations of the main spindle and feed motors using Hall effect sensors has been developed by **Shin et al. (2006)**. The connection between the cutting force and the spindle motor Root Mean Square current at various spindle rotational speeds was established. The research concluded that the current of the main spindle motor and the cutting force are proportional to each other so confirming previous findings (**Kim and Chu 1999**) (**Lee and Kwon 2001**).

**Kim and Jeon (2011)** monitored the cutting forces indirectly by using motor current in CNC milling process. They concluded that the proposed system to predicting cutting forces could be used under limited conditions. For example, spindle speed > 4500 rpm and depth of cut > 4mm.

In a new hybrid approach for cutting tool wear monitoring, the influence of force components from different parameters on the measured spindle current was assessed (**Lee et al. 2007**). The researchers removed the impact of each parameter not related to tool wear from the measured signals such as the force variation by non-homogeneity of the workpiece, then employed this approach to cutting force regulation with merits of both the off-line and the real-time feed rate controls.

Monitoring the tool condition in real time based upon the low-cost spindle motor current has been introduced (**Bhattacharyya et al. 2008**). A multi-linear regression model was used to estimate tool wear in real time for face milling operations. Experimentally, two different data sets were conducted when cutting C-60 mild steel workpiece with a single

cutting insert. The first one for rough machining, the second set for finish machining. It was concluded that the estimations based on current or power can accurately and reliably estimate tool wear, especially when choosing a suitable signal processing technique. The proposed model predicts tool wear with an accuracy, which reached to 95% and has the potential for industrial acceptance.

A tool wear observer model to monitor flank wear that predicts the actual state of tool wear in real time by measure spindle power consumption has been developed by **(Niaki et al. 2015a)**. They applied a Kalman filter disturbance observer and Root Mean Square Error method. Spindle power information was integrated to predict tool flank wear when cutting. While machining, the progress of tool wear was relatively fast due to the high strength and hardness of the workpiece. Therefore, the authors considered tool wear progress as a linear function of the volume of material removed. They concluded that the models created with the above technique provided a reasonable prediction of tool flank wear. Stochastic model-based filtering such as Kalman and particle filter in predicting tool flank wear in machining difficult-to-machine materials through spindle power consumption measurements have been further considered by the same authors **(Niaki et al. 2015b)**. The result indicates a good potential of using stochastic filtering techniques in estimating tool flank wear since the maximum error was less than 15%.

**(Abbass et al. 2015)** detected the tool wear by monitoring the fluctuation in the motor of a CNC spindle in comparison with eddy current sensors during the machining operation in milling processes. They concluded that the eddy current sensors and the Kurtosis value of the power are more successful and sensitive to monitor the tool conditions.

The machine spindle power to predict the remaining useful life of tools using the neural network technique with different MATLAB<sup>TM</sup> training functions has been employed **(Drouillet et al. 2016)**. The results show a good agreement between the predicted and actual remaining useful life of tools since it takes into account the uncertainty in tool life.

### 2.2.2 Component Geometry

In order to evaluate tool life criteria indirectly, measuring the changes in the machined component dimension can be used.

Studies have been conducted to investigate the correlation between cutting parameters and product quality; they agreed that cutting parameters have a direct effect on the machined parts quality (**Iliescu et al. 2010**) (**Shyha et al. 2009**) (**Hocheng and Tsao 2006**). It is therefore suggested that the relationship may apply and that component quality will reflect tool health.

A considerable amount of research has been directed towards the component-based indirect measurement of tool wear. This is typically based upon measuring the changes in geometric form or machined component dimensions such as cylindrical form and quality.

An optimisation of cutting conditions for hole-making processes of a nickel-base superalloy has been presented (**Axinte and Andrews 2007**). The holes were machined with two steps, roughing (drilling) and finishing (reaming or plunge milling). These holes were evaluated using various criteria, such as tool life, hole accuracy. CMM, surface roughness using (Talysurf CLI 1000), and level of cutting torque using (Kistler 9272). The profiles of the holes were constructed at seven levels (0.5, 1, 2, 3, 4, 5, and 5.5mm) from the top of the holes from which the values of the “average diameters” of each hole were evaluated. They concluded that plunge milling cutter resulted in the lowest levels of cutting torque and spindle power, as well as a good tolerance on the circularity of the finished holes. However, the main point in that research is that the authors established the hole diameters based upon the average measurement. They measured the hole at seven levels and values of the average diameters for each hole were evaluated. In this case, it is possible for the authors to over or underestimate the advisable limit of tool life.

Methods of measuring tool wear experimentally based on the direct measurement the radius of a tool’s cross-section using a CMM have been proposed (**Liu et al. 2010**)

(Zhang et al. 2011). A series of experiments were carried out using a wide range of different machining parameters including cutting depth, feed rate and spindle speed. The tool flank wear was calculated based on the radial wear, which was measured directly using the CMM. An approach was outlined in which the flank wear for each hole was measured at different depths, and the difference in the radius between the reference hole and other holes at a certain depth were plotted. The researchers proposed that this method was effective and that it was feasible to apply it to conduct tool wear investigations. However, they did not take into account the differential tool wear at different depths when evaluating the flank wear in the cutter at each hole.

Similarly, the modelling of tool wear based on shape mapping using theoretically and experimentally acquired measurements from using a ball end milling cutter have been investigated (Zhang and Zhou 2013). They obtained the tool wear for each experiment from the tool wear estimation model by using multiple linear regression methods and concluded that on average the tool wear could be predicted within 10%, although a useful approach 10% remains a significant level of inaccuracy. The proposed model of tool wear was specific to a certain range of cutting conditions for a milling operation.

Tool wear and its influence on the machined hole quality (geometrical accuracy and surface roughness) in the dry helical milling of Ti-6Al-4V has been evaluated (Li et al. 2014). To observe the tool wear mechanism arising for a 6 mm cutter, a CMM was used to measure the diameter and roundness error. These tests were stopped, and the tool was rejected when the tool wear met one of the International Organization for Standardization ISO 8688 criteria (0.3mm). The experiment was also halted by excessive chipping/flaking or catastrophic failure. The researchers concluded that the tool wear at bottom cutting edges does not affect the hole geometry and surface roughness. This may be due to the fact that they made a through-hole, which reduces the work done by the bottom cutting edges. Interestingly they observed the smooth wear pattern at the periphery cutting edge, and the quality of the machined hole was still high even near the end of tool life. They did not mention how or where each hole was measured and this makes an assessment of their method more difficult. It may be that it would not have a sufficient resolution. They only used a Scanning Electron Microscope SEM and a digital camera to measure the tool wear mechanisms.

The tool life and hole surface integrity for hole-making of titanium alloy by traditional drilling and helical milling technologies have been investigated. (Zhao et al. 2015). The results conclude that using helical milling operation to produce a hole is better than that of using a drilling operation under the same cutting conditions regarding low cutting force, low surface roughness, high cutter tool life and no plastical deformation layer in holes produced by helical milling. In this investigation, the tool wear was measured by using SEM.

### 2.3 Summary

Evaluating the performance of a machining process is important. There are various characteristics used to monitor the tool condition including online (classified as in-process) or off-line (post- process). However, no one characteristic has been adopted as the standard. Measuring the changes in machined component dimension is one of the indirect measurements conducted offline and that relates to workpiece condition. These include the measurement of the changes in machined component dimension or geometric form, the value of the volume of metal removed and component surface finish or roughness. This method forms the first part of this research.

The review has indicated that there is no reported research with regard to the measurement of differential tool wear in the milling of cylindrical forms. From the reported research it is apparent that existing approaches to the assessment of tool wear have been based upon the measurement of diameters at different heights within the cylindrical form. These measurements are then averaged to provide an estimated level of tool wear. Using this approach it is likely that the level of tool wear could be subject to either an under or over estimation. This can be very important as the level of tool wear reaches a critical point. No researchers paid attention to the potential for differential tool wear and effected tool life management, which means machine tool operations may be continued using a cutter that is near to or has exceeded the end of its life. It is also likely that the geometric form of a component machined using this cutter will be less than optimal.

Cutting force provides valuable information; it is expected that the cutting force will increase as the tool gradually wears. It can be measured directly by using the dynamometer or indirectly by monitoring the spindle current or load. However the cost of the dynamometer can be too high, and using it could disturb the machining process. Spindle power and current are less expensive solution to monitor tool condition than the method that is usually employed (traditional methods) and robust. They are used more often than other sensor-based methods and are more suitable for industrial environments since they can be installed on both new and existing machines. This method forms the second part of this research.

In terms of using the spindle power and current to monitor the tool condition, most of the reviewed published research has been reliant on the addition of a sensor on the power supply. However, there is no requirement for adding such a sensor in this research. Due to the limitations of the information obtained from the additional sensor previous research has been based upon monitoring the total electrical power used by the machine tool. In this thesis, the changes in mechanical power required for metal removal is being represented by the changes measured in the values of spindle power. This work uses relative changes to the spindle power to investigate the progressive effect of tool wear.



# Chapter 3

## The Theory of the Tool Wear

### 3.1 Introduction

One of the most important influential factors for tool life arises due to tool wear weakening the cutting edge. In all machining operations, tool wear is a critical and complex aspect, since it effects the machined part's quality and the economics of machining.

In tool wear management, two main issues could occur. Firstly, the workpiece dimension might become out of tolerance as the tool wears, and thus, the tool position must be adjusted through the program to compensate for the tool wear. Secondly in continuously applying such compensation it is possible that levels of tool wear may become higher than acceptable. If this process is not carefully managed, this could lead to tool breakage. It is therefore important to also monitor tool wear rate.

Tool wear can be defined as the gradual failure of cutting tools over the time due to normal operation. It is always associated with the portion of the tool that contacts with a workpiece (**Jindal 2012**). The dynamic interactions between the cutting tool and the workpiece causes change in the tool geometry, which in turn, results in a reduction in the quality of the machined parts and the associated reduction in productivity because more components can be rejected and possibly reworked and machining may be slowed down to safer speed.

### 3.2 Types of tool failure in milling cutting tools

Tools can fail via various mechanisms. These mechanisms are complicated because of the number of factors affecting the cutting operations. According to **Creese (1999)**, there are five different mechanisms, classified into two categories: primary and secondary.

The primary failure mechanisms are:

1. Flank wear
  - a. Rough cuts,  $VB = 0.76$  mm [VB defined in Figure 3.1]
  - b. Finish cuts,  $VB = 0.38$  mm
2. Crater wear

The secondary (subsequent) failure mechanisms are:

3. Oxidation
4. Breakage (shock, fatigue)
5. Chipping of the tool (chatter, vibrations)
6. Plastic deformation

Tool wear is most often associated with flank wear (VB), which can be defined as the loss of tool material from the tool flanks during cutting. It is not always uniform along the major and minor cutting edges of the tool, and it occurs along the flank or relief face below the cutting edge. It becomes progressively deeper (more in-depth) as the tool wears, as shown in Figure 3.1. Tool wear is a complex phenomenon occurring in different metal cutting processes and is an event inherent in any cutting process. It can happen gradually by adhesion, abrasion and diffusion or may be subject to very rapid catastrophic mechanisms. Flank wear most commonly forms by the friction between the flank face of the tool against the newly machined surface of the workpiece, which leads to the loss of the cutting edge. Flank wear affects the dimensional accuracy and surface finish quality. Increasing the cutting speed leads to decreasing of adhesion wear and slightly oxidation wear, while all other types of wear increase. (**Vučina et al. 2013**).

From the process point of view, flank wear is the most important wear mechanism that needs to be controlled and it is easier to measure. The mechanism of the material loss is better understood for most machining situations. It was often used as a criterion of tool life since it can be described using the Taylor tool life equation. According to the temperature distribution on the tool face, flank wear is mainly dominated by abrasive wear due to the change in the metallurgy properties of the workpiece material (Xie et al. 2005). In the other word, during the cutting oprations, the cutter will effect the workpiece, in particular, the temperature of the workpiece will rise and therefore, the metallurgy properties of the workpiece will change.

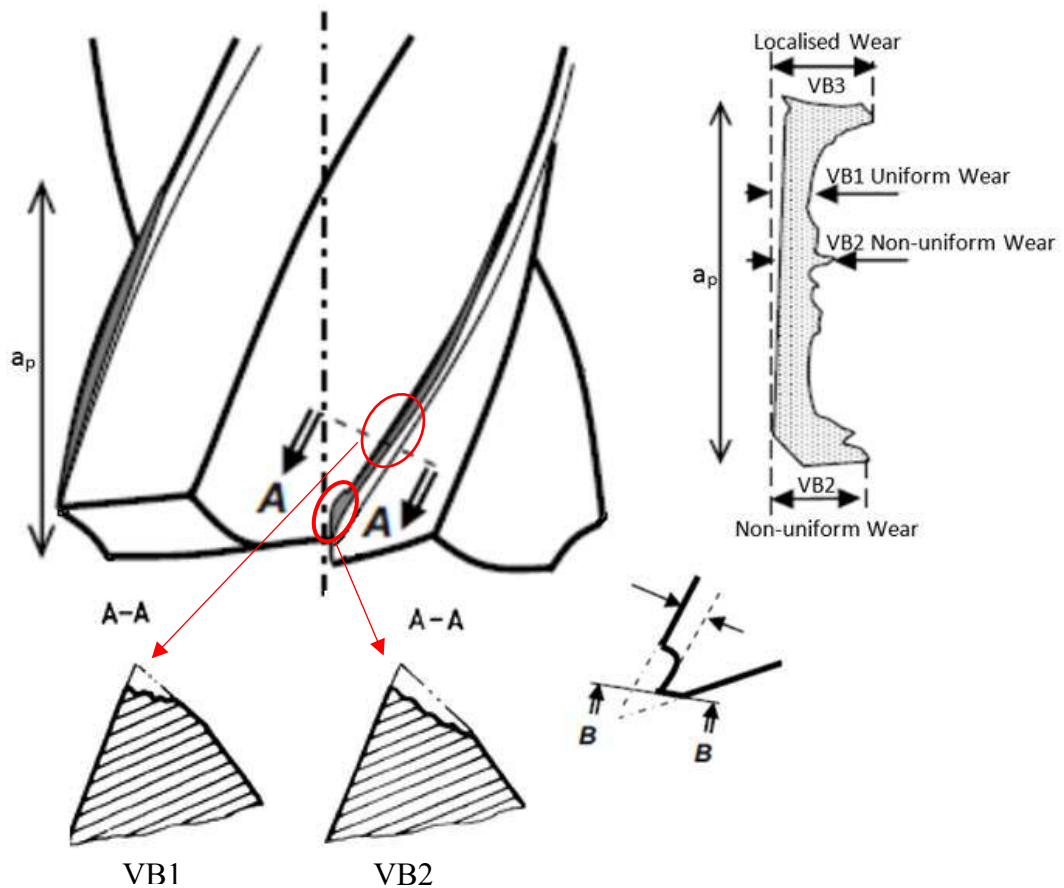


Figure 3.1 The wear in end milling cutter (ISO8688-2 2016)

Figure 3.2 shows the generally accepted relationship between flank wear and tool life. The behaviour of the tool wear curves is roughly divided into three regions (**Koren et al. 1991**). Nonlinear at the initial stages (running in), linear at intermediate steps (stationary) refers to a linear function of time and the slope is affected by work material as well as cutting conditions and nonlinear at the final stages (severe) when the flank wear is considerable before the tool breaks/fails completely. In the third state, the flank wear is substantial, and the cutter will wear much faster than to the other phases. Intensive vibration, higher cutting forces and raised temperature will have been induced in the latter phase. It is, therefore, highly recommended that the cutter is monitored more carefully to avoid tool breakage that arises at the end of this stage.

Each tool wear curve can be considered as;

Stage I: when the initial contact between the new cutter and the workpiece happens, the sharp cutting edge wears rapidly. It is relatively short and occurs within the first few minutes of tool use. In this phase, a high rate of initial wear results from the small contact area associated with the sharp cutting edge and with high contact pressure. These contribute to the breakdown or rounding off of the cutting edge. The initial wear value is usually given as  $VB=0.05-0.1\text{mm}$ .

Stage II: in this stage, the cutting edge was rounding thus, this leads to improve the micro-roughness. The wear rate is proportional to the cutting time and is relatively constant. Tool wear will normally occur over a prolonged period at a minimal rate.

Stage III: in this stage, the flank wear rate is increasing rapidly. This leads to increasing cutting force and temperature, and then the tool loses its cutting ability.

When the wear rises to a critical value, the component surface roughness will be increased, mainly when chipping occurs. The cutting force and temperature will increase rapidly due to increasing friction in the tool-workpiece and tool-chip interfaces. The flank wear will affect and change the shape of the component produced. Practically, this region of wear should be avoided. The stages of wear combined with a variety of

wear modes make wear prediction difficult. This problem requires a systematic approach.

Despite the changes of the cutting conditions (for example cutting speed,  $V_1, V_2, V_3,$  and  $V_4$ ), the general shape of the flank wear curve remains the same as shown in Figure 3.2. However, changes do affect the tool life, i.e. the gradient of the curve, especially the straight (linear) section. Cutting speed, feed rate and depth of cut are important cutting parameters in relation to tool wear. Tool wear is affected by many factors represented in fishbone diagram shown in Figure 3.3.

Contact between the cutting tool and the removed material chip can produce the most extreme conditions that apply only to the actual cutting area (Li 2012). This wear will change the tool geometry, which in turn will influence the cutting force, the power being consumed, the component surface finish and they can have profound effects on the overall quality of the machined workpiece and the dynamic stability of the process (Alamin 1996) (Jindal 2012). It is therefore crucial and necessary to understand tool wear in cutting operations in order to plan tool changes and avoid failure-related costs.

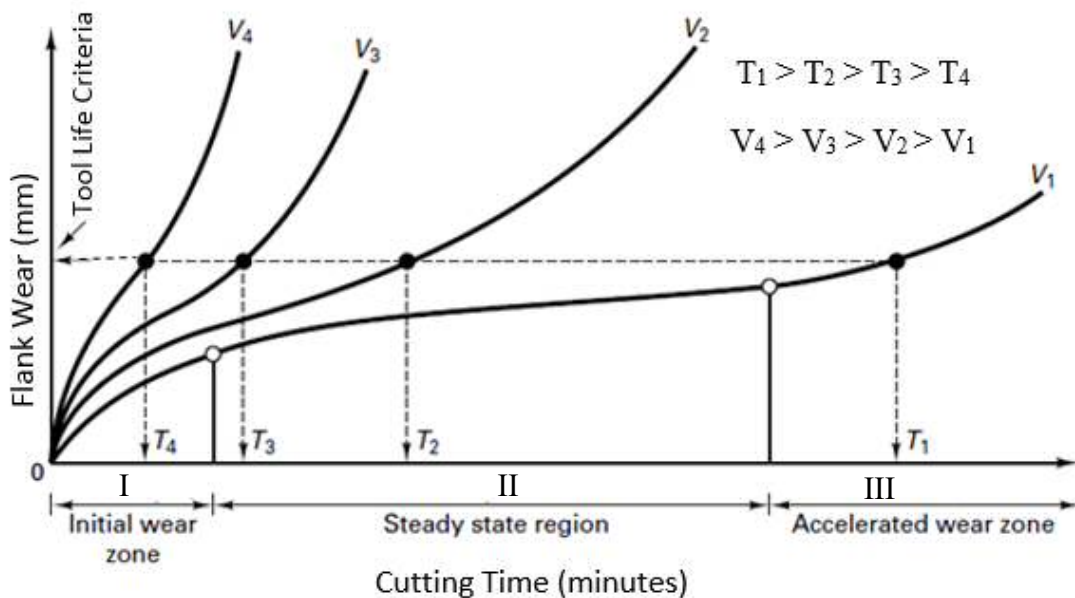


Figure 3.2 Flank wear as a function of cutting time (Black and Kohser 2017)

The analysis of the information is challenging because the tribological behaviour of tool wear is not clearly defined and requires expertise for the interpretation of data. Nevertheless, wear analysis is recognised as a valuable source of information when managing machine performance.

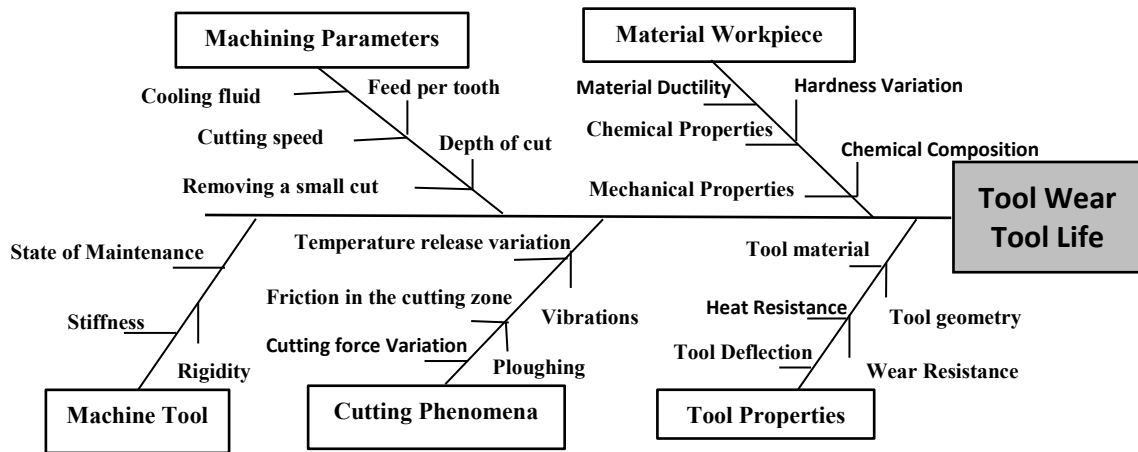


Figure 3.3 Fishbone diagram with the parameters that affect tool wear and tool life

### 3.3 Type of Wear Mechanism

Shaw (2005) classified tool wear mechanisms into three types: adhesive, abrasive and diffusion wear. However, Childs et al. (2000) presented the three causes of tool failure in Figure 3.4, including adhesive, thermal damage and mechanical damage. Regardless of the mechanism of tool failure, the cutting temperature is the main reason behind it.

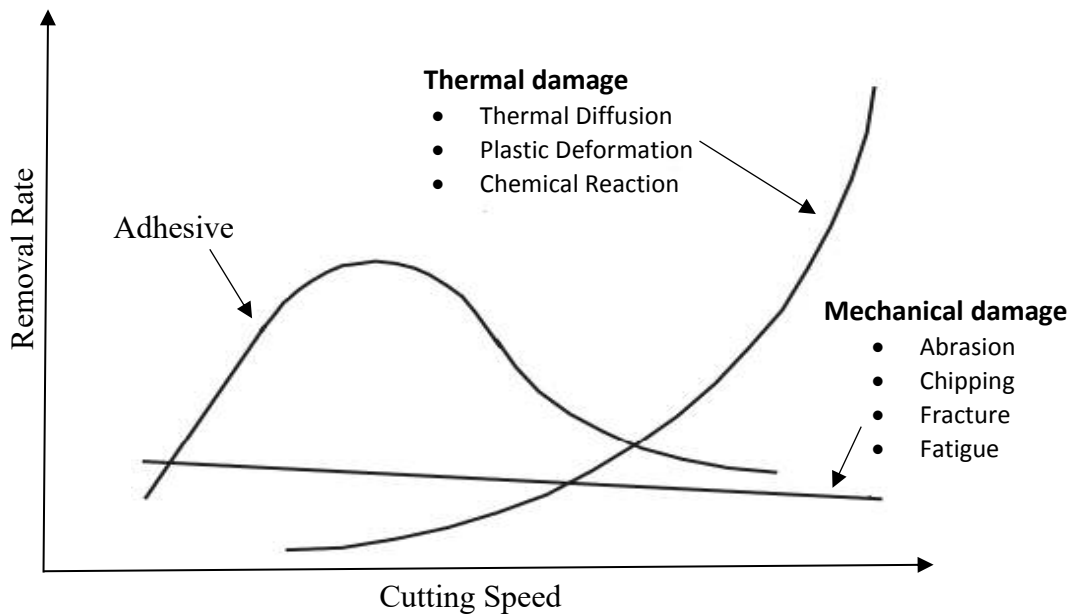
#### 3.3.1 Abrasive Wear

Abrasive wear is the widely dominant wear mechanism especially in many industrial applications. It is the loss of tool material on the tool face due to the friction of the cutting flank face and the machined workpiece surface (Davoodi and Eskandari 2015;

**Hao et al. 2011; Xue and Chen 2011**), and the cutting edge's ability to resist abrasive wear depends on the tool and the workpiece hardness (**Gu et al. 1999**).

Carbon steel is a ductile metal, which contains a hard constituent known as cementite. These constituents are very hard and contribute to the tool degradation by abrasion wear (**Hogmark and Olsson 2008**).

Figure 3.5 (A) shows abrasive wear dominates the crater and flank wear of a milling tool. The arrows point at ridges of HSS material relatively resistant to abrasion. Figure 3.5 (B) shows the workpiece material from Carbon-steel, an extremely fine-scaled abrasion, only resisted by the hard carbides, dominates the tool wear (**Hogmark and Olsson 2008**).



**Figure 3.4 Tool damage mechanisms and cutting speed (Childs et al. 2000)**

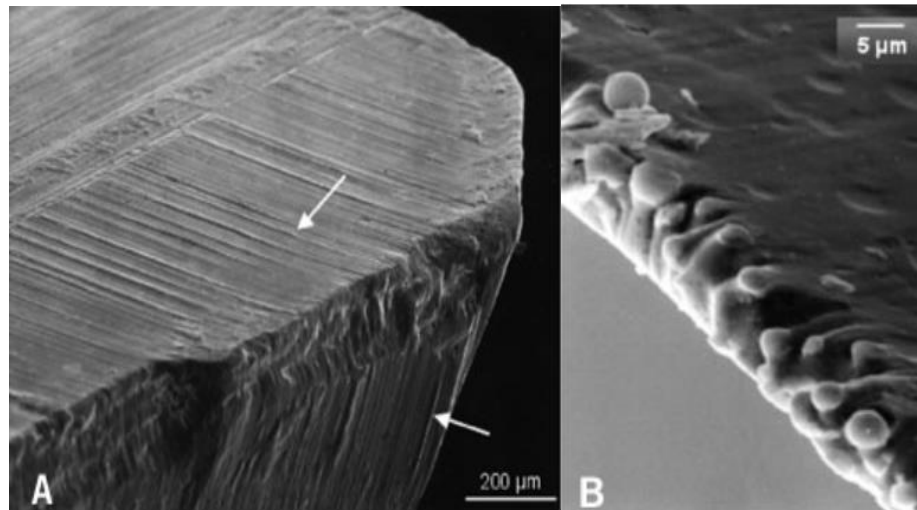


Figure 3.5 A: abrasive wear in the HSS milling tool and B: Microscopic image for Carbon steel (Hogmark and Olsson 2008)

### 3.3.2 Adhesive Wear

Adhesive wear occurs at low machining temperatures on the face of a tool; it is associated with a shear plane deformation. Successive layers are welded from the chip and become part of the cutting edge in a dynamic process. This mechanism frequently leads to the formation of a built-up edge on the cutting edge, especially when machining ductile materials at low to medium cutting speeds. This arises because the friction between the tool and the chip tends to cause a portion of the work material to adhere to the rake face of the tool near the cutting edge. Junctions between the chip and the tool materials form strong bonds as part of the friction mechanism. When the built-up edge breaks away, it takes a part of the cutter with it and thus increases the wear rate.

### 3.3.3 Diffusion Wear

Diffusion wear occurs at high surface temperatures, it is not the direct cause of tool damage. However, it causes the tool surface to be weakened and thus, the abrasive or adhesion can then more easily cause tool damage (Childs et al. 2000). The chemical properties of the tool material and the affinity of it to the workpiece material will determine the development of the diffusion wear mechanism. The hardness of the tool



material will not affect the process significantly. Whereas, the metallurgical relationship between the materials will determine the amount of wear (**Gu et al. 1999**).

### **3.4 Parameters influencing tool wear**

As shown in figure 3.3, machining parameters, tool properties, cutting phenomenon, and material workpiece affect the tool wear and tool life to varying degrees. The following section will discuss these factors.

#### **3.4.1 Machining parameters**

The volume of metal, which is removed by a cutting tool, depends on the cutting speed, depth of cut, and feed rate. Increasing these cutting parameters lead to increasing metal removal rate. It is likely that increased cutting conditions result in accelerated tool wear causing reduced tool life.

##### **3.4.1.1 Cutting Speed**

Most of the authors agreed that cutting speed has a more significant effect on tool wear than feed rate and depth of cut (**Luo et al. 2005; Rogante 2009**). A lower cutting speed result in tool wear by built-up edge formation. However, higher speeds result in costly penalties concerning tool life as well as vibration, higher cutting temperature, and softening of the tool material (**Juneja 2005**). It may affect the performance of specific machine tool components causing damage to element such as bearing, and reduced safety. Therefore, it may be the least desirable means of improving productivity.

##### **3.4.1.2 Feed Rate**

The change in the feed rate results changes in MRR. However, increases in feed rates are limited by many factors such as the capability of the machine tool, workpiece,

cutting tool, and set-up to withstand the higher cutting forces. The surface finish required in the case of finishing operations must also be considered. A significant feed rate increase raises the likelihood of chipping of the cutting edge through mechanical shock.

#### **3.4.1.3 Depth of Cut**

The depth of cut has a significant influence on MRR. It leads to an increase in the area of the chip-tool contact. The associated rise in tool temperature is relatively small, in the case when the feed is constant and low. For large increases, the change in temperature is large. This can result in a shorter tool life by accelerating the abrasive, adhesive, and diffusional types of tool wear occurring.

#### **3.4.1.4 Cooling Fluid**

Using the cooling fluid acts on the chip and workpiece and can reduce the frictional stress between the tool and chip. Consequently, the cutting temperature is reduced. There is an appreciable increase in tool life because of using cutting fluids, especially when using a low value of hot hardness tools such as carbon steel and HSS. Otherwise, the effect of cutting fluid on tool life can be negligible (**Juneja 2005**).

#### **3.4.1.5 Small chip load**

Any change in the feed per tooth leads to a corresponding change in the cutting temperature. As a result, the cutting feed influences the tool wear rate. Low feed rates mean a small chip load per tooth; it may cause the tool to rub or burnish instead of shearing off a real chip. Regarding cutting with very low feed rate and hence chip load, the cutter edge radius will be too large relative to the depth of cut (bottom), and, thus, all the force goes to pushing the chip under the edge (**Warfield 2016**) (**Dasarathi 2016**).

Even this can actually produce a decent surface finish due to the burnishing effect, but it is extremely tough on the tool. The rubbing will heat the tool and material and reduce tool life drastically (**Warfield 2016**). Removing a small cut from a material such as carbon steel which is prone to work hardening, could increase the tool wear (**Warfield**

**2016**). The cutting edge cuts the transient surface formed on the previous tool pass. This means it removes the surface located between the surface to be machined and the machined surface by the cutting edges. This surface has greater strength and higher hardness compared to those of the original work material. As such, the tool wear rate increases (**Astakhov 2007**).

### **3.4.2 Tool Properties**

Tool geometry and tool material have a significant impact on tool wear. For example, the rake angle should be positive and large when machining ductile materials. Likewise, a smaller rake angle is preferred when machining brittle materials. Figure 3.6 gives an overview of the Geometrical parameters of an end mill.

#### **3.4.2.1 Rake Angle**

The rake (radial and axial) becomes an essential factor for the chip formation and chip flow direction. For example, a positive rake angle gives a better chip sliding that offers a better engagement of the cutting edges. In contrast, a negative rake angle guides the chip towards the workpiece that increases the cutting forces and friction, and thus, the tool becomes blunter. However, it makes the cutting edge stronger as shown in Figure 3.7.

#### **3.4.2.2 Relief Angle**

The relief angle is the angle between a cutter and the workpiece material it has just cut. A large relief angle increases the flank wear more slowly. Consequently, a significant tool life values are obtained although decreases the strength of the cutting edge and tool is more (susceptible) liable for chipping or fracture. Therefore, the relief angle should be optimised to maximise both the tool life and the work achievable per tool.

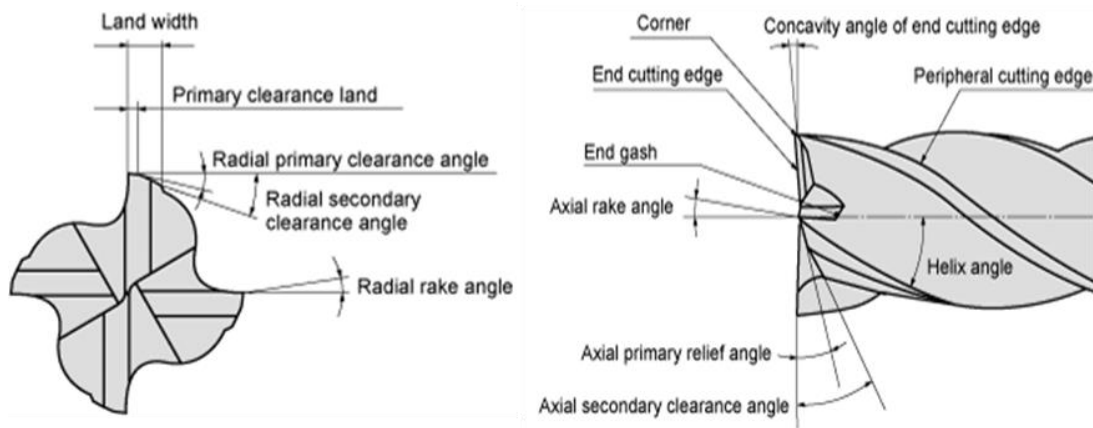


Figure 3.6 Geometrical parameters of an end-mill (Wang et al. 2014)

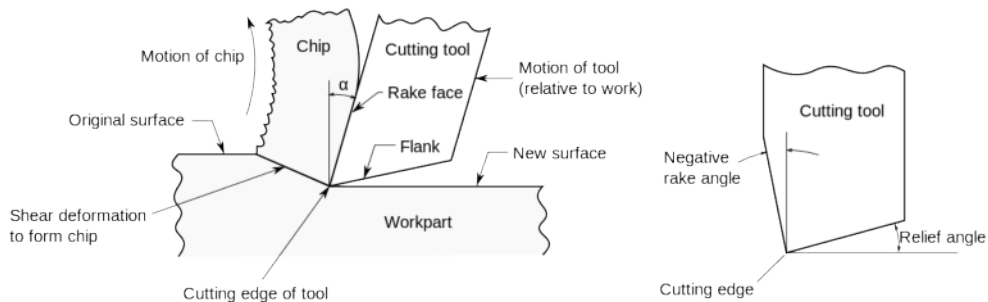


Figure 3.7 A schematic showing positive (left) and negative (right) rake angles

### 3.4.2.3 Tool Deflection

Tool wear on the cutting edges of end mills is a critical issue affecting the tool deflections and surface roughness, especially when machining difficult-to-cut materials such as titanium alloys and stainless steel. Therefore, an understanding of the interactions between tool wear and tool deflections is essential to maintain component quality.

The bending, displacement or distortion of the cutter under cutting pressure/forces may be included in the definition of tool deflection. It can be measured indirectly through its effect on the workpiece. However, practically this is difficult. It is very hard to predict

the direction of the deflection without sophisticated analytical models, since it changes throughout the cut. There are many ways that can be used to reduce tool deflection. One choice is to reduce the forces acting on the cutter regardless of the effect this will have on the productivity. Another is to increase the cutter's rigidity by increasing the cutter diameter and decreasing the length of the cutter as well as the number of flutes.

Generally, tool deflection is dependent on the axial load which is mostly constant for all the uncoated tools since the HSS tool base material is quite similar. While for the coated tools this coefficient depends strongly on the microstructure of the coating layer (Iliescu et al. 2010).

Many researchers study the tool deflection in a milling machine using experimental, mathematical (Kim et al. 2003) (Ikua et al. 2001) or computational techniques (simulation) (Layegh et al. 2013) or both together (Huo et al. 2017); (Oliaei and Karpal 2016). They concluded that the cutting force components that increase with tool wear affects the tool deflection.

### 3.4.3 Workpiece Properties

Machining a material that has low strength and hardness tends to reduce cutting forces, abrasive wear, and cutting temperature. As a result, large tool life values are obtained.

### 3.4.4 Cutting phenomenon

There are several properties that must be considered in this category, as shown in Figure 3.3. They include:

#### **3.4.4.1 Stiffness**

The high stiffness of the machine, tool and workpiece, and high levels of inherent or inbuilt damping leads to great of dynamic rigidity of the system. This leads to less vibration or chatter, which may cause fatigue failure or catastrophic failure of the tool.

#### **3.4.4.2 Rigidity**

The cutting mode whether turning or milling has excellent effects on system rigidity as well as the tool wear especially on the job when the cutting edge has frequently entered and exit from the workpiece.

#### **3.4.4.3 Cutting Forces**

Cutting forces were higher when using worn tools due to the high ploughing forces induced owing to the increased contact area of the large flank wear face of the cutter acting on the workpiece.

### **3.5 Developing the Tool Life Modelling Methodology and Approaches**

Tool life is usually determined by using criteria based on tool wear (**Carrilero et al. 2002**). There are several types of tool wear commonly occurring in end milling cutter as shown in Figure 3.1. However, only flank wear and crater wear are widely used as tool life criterion. This is because they have adverse effects on the final surface finish quality and the dimensional accuracy of the component.

The most frequent way to judge tool life in factories is to determine the condition of the cutter. However, this is not always easy, timely or cost-effective. Hence, an alternative way is proposed based upon the monitoring of the tool wear by considering the state of

the component. This will then enable the application of the most suitable tool wear criterion.

The life of any cutting tool may be defined in terms of the time interval for which the tool may be said to work safely and effectively. Traditionally this period was typically measured as being between two successive grinding and re-sharpening actions, which were applied to reinstate the cutting capabilities of the tool (**Gokulachandran and Mohandas 2012**).

The tool life of the cutting tool is governed by many contributing factors, as indicated in Figure 3.3. These include cutting related parameters: cutting speed, feed rate, depth of cut, and tool geometry. Machining process parameters also have an influence. They include the application of the coolant, chip formation and the rigidity of the work holding and machine tool. Moreover, the chemical and physical properties of the workpiece material also influence tool life and play a role in affecting the rate of tool wear.

It is normal practice to assert that a tool should be considered to have reached the end of its useful life when flank wear has been attained to a predetermined wear level. Tool life is related to the wear magnitude in different areas of the cutting tool, and the tool life criterion can be set to a certain level of wear.

In previous work **Niklasson (1962)** considered the tool life criteria occurs when the flank wear width is 0.7mm. However, the life criteria for the coated tools is different, sometimes it is 0.1mm (**Diaz et al. 2012**) or 0.25mm (Li et al. 2010; Toh 2006) depends on the thickness of the coated layer, so, the tool life criteria would be the point at which the coating is no longer protect the cutter.

According to ISO 8688-2 a tool may be considered as worn out once the VB1 exceeds 0.3mm for uniform flank wear or VB2 exceeds 0.6mm for non-uniform/localised flank wear to both roughing and finishing cuts, as shown in Figure 3.1 (**ISO8688-2 2016**).

In practice it is often the case that the above criteria is of limited usefulness, subjective and insufficient. It does not take into account the tool geometry (such as the flank, the

rake and the cutting edge angles). As such it may not be suitable for comparing cutting tools having different geometry. In addition, there is no account for the cutting regime. The resulting tool life criteria do not reflect the real amount of the work material removed by the tool during the machine operating time. That is normally defined as the time needed to achieve the chosen tool life criterion (**Astakhov 2004,2006**); (**Li et al. 2012**) (**Li 2012**). Ultimately, however, this standard is widely applied to support the use of smaller cutters, having a diameter of less than 12 mm (**ISO8688-2 2016**). The most important point is that the measure recommended by these standards has limitations. The main concern relates to the tool geometry itself, which may vary. However, it may provide a useful guideline since regardless the size of the cutter in most aspects the geometry of the cutting teeth is the same. For example, the tooth (tooth height and tooth width) of 16 mm cutter is basically the same as the tooth of 10 mm cutter, but the actual tool (core diameter) is different.

The ISO 8688-2 was published in 1989-04, and the first edition was done in the 1<sup>st</sup> of May 1989, and the last reviewed and confirmed in 2016. Therefore this version remains valid.

It should be noted that the ISO 8688 does not consider the subsequent failure mechanisms such as edge fracture or plastic deformation and only covers the primary failure mechanisms (flank and crater wear).

According to **Armarego and Brown (1969)**, the active end of life of the cutter can be judged by the following possible prompts:

- Cutter edge failure. Complete failure of cutting edge
- Visual inspection of flank wear or crater wear by the machine operator.
- A fingernail test of cutting edge (this involves running a nail along a tooth edge).
- The changes in the sound of cut.
- Changes to the chips being formed as they become stringy and hard to handle.
- Surface roughness degrades.
- Increased power consumption.
- The volume of material removed to failure



According to **Astakhov (2004)**, the measurement of tool life can be characterised by the time required for the wear land to increase from zero (sharp tool) to some value at which the tool is considered as dull. It may also be assessed by the number of parts produced, or by the length of the tool path, by the area of the machined surface, and by the linear relative wear.

In spite of numerous investigations carried out over the last seven decades, the nature of tool wear in metal cutting is not yet clear enough (**Li 2012**).

Considerable research has been directed towards measuring the cutting tool life based upon the empirical relation of tool life to the cutting machine variables and the material properties by using a microscope, some of their findings will be explained below.

**Jawaid et al. (2001)** come to conclude that at lowest cutting speed, the uncoated tool performed better than the PVD-TiN coated tools. However, at cutting speed of 50 m/min, the situation is reversed. In addition, both tools gave tool lives of less than one minute at a feed rate of 0.14 mm per tooth and cutting speed of 75-100 m/min, which means that the cutting speed and feed rate have a great effect on the tool life than the depth of cut. **Filho and Diniz (2002)** found that cutting speed has a significant effect on tool life regardless of whether feed velocity or feed per tooth varies followed by the feed rate, lastly, the axial depth of cut. The empirical results from **Li et al. (2012)** showed the similar results that cutting speed has a great effect on tool life. **Krain et al. (2007)** summarised that an increase in the radial depth of cut and feed per tooth resulted in an overall reduction in tool life.

**Shah and Gaw (2012); Kiran and Kumar (2013)** demonstrated that the cutting speed and depth of cut are the main parameters that influence the tool life of end milling cutters when using a solid carbide flat as the cutting tool and stainless steels S.S-304L as the material.

However, **Nagaanjeneyulu et al. (2015)** found that only the depth of cut has significant effects on tool life when using Poly Crystalline Cubic Boron Nitride (PCBN) as the

cutting tool material and En8 steel (HRC 46) as workpiece material to predict the tool life that calculated by Taylor's tool life equation.

The **Aykut et al. (2007)** experimental result showed that cutting force increase when the feed rate and depth of cut increases. However, the effect of cutting speed on cutting force has not been observed.

**Jozić et al. (2012)** summarised that in down milling, the time of insert engagement has the most significant influence on flank wear. However, the radial depth of cut has least influence. Also, the time of inserts engagement and cutting speed were found to have an equal influence on flank wear in up milling.

Some authors then go on looking at effect of cutting tool's geometry as well cutting parameters on the tool wear.

**Sivasakthivel (2010)** concluded that the helix angle has the most significant effect on tool wear. The tool wear is minimal when helix angle value was between  $40^{\circ}$  -  $45^{\circ}$ , spindle speed and axial depth of cut were high, and the radial thickness (depth) of the cut was low.

**Lin et al. (2006)** deduced that the large rake angle means more wear on the tool. Likewise, the smaller rake angle was more significant on the chips flow constraints. Moreover, the signals of cutting noise exhibit a regular fluctuation and are increased gradually as the tool wear increases during phase one and two of the cutting process. However, after that, the cutting noise may increase abruptly. Therefore, this comparison can be used to judge whether the tool is still useful or not.

### 3.6 Tool Life Equations

Predicting the tool life based on the theoretical equation is a most challenging task in the case of various metal-cutting processes.

Extensive investigations have been carried out in the material cutting field to express the tool life of cutting tools in a mathematical form. Most of these present the tool life equations as a function of various machining variables involved in different material cutting operations.

The earliest useful empirical approach to determine tool life for a given cutting speed was proposed by Taylor (**Taylor 1907**). This approach suggested that, for progressive wear, the relationship between the time to tool failure for a given wear criterion and cutting speed was of the form:

$$(Taylor\ 1907)\ (3.1)$$

Where:  $v$  is the cutting speed (m/min) and  $T$  is the tool life. This is normally measured in the most relevant time base (i.e. minutes).  $C_1$  is spindle speed coefficient.  $C_2$  is a constant of proportionality that varies considerably with the rake angle of the tool (**Stephenson and Agapiou 2016**). It can be traditionally set to provide a value for the cutting speed that gives a tool life of one minute.

Taylor's fundamental Equation (3.1) describes the linear section of the tool life curve. However, it does not include the effect of cutting feed, depth of cut, cutting tool geometry and is limited to a certain range of speed (**Li 2012**). Also, it is not possible to know the wear of the tool at any time during the machining. Equation (3.1) has been extended to take into account feed rate and depth of cut. Incorporating those parameters as variables affecting tool life;

For milling, Taylors equation can be improved to take into account feed rate and depth of cut (**Colding 1961**). Incorporating those parameters as variables affecting tool life, Taylor tool life equation has been modified to give:

$$- - - (Creese\ 1999;\ Shaw\ 2005)\ (3.2)$$

Or

---


$$(Spitler \text{ et al. } 2003); (Juneja \text{ } 2005) \text{ (3.3)}$$

Or

$$\text{—————} \text{ (Saranya et al. 2016)(3.4)}$$

Or

$$\frac{\text{—}}{\text{— — —}} \text{ (Kiran and Kumar 2013; Shah and Gaw 2012) (3.5)}$$

Where:  $v$  is the feed rate (mm/min),  $d$  is the depth of cut (mm),  $K$  is the feed rate coefficient, and  $C$  is the depth of cut coefficient.

In this simplest form Equation (3.1), the constant Taylor tool life exponent  $n$  is defined to match the particular combination of tool material with the workpiece.  $n$  is traditionally set to provide a value for the cutting speed that gives a tool life of one minute. Applying this approach each combination of tool and workpiece has its own values for  $n$  and  $K$ . These can be obtained from published data or standard tables for different workpiece materials and various cutting tools. This process requires many experiments with different combinations of cutting speed and workpiece properties. The nature of this process and the potential difference in conditions arising mean that variations in the parameter estimates will result even for the simplest form of the tool life equation. This can be seen in Table 3.1, which shows the ranges of  $n$  and  $K$  values according to different authors. All these cases were for HSS cutters and steel workpieces.

**Table 3.1 Representative values of  $n$  and  $K$  in Taylor Tool Life Equation for a combination of HSS cutter and Carbon Steel workpiece material**

References		(m/min)			Tool Life (min)
(Creese 1999)	0.1	70			99
Juneja et al. 1986	0.08-0.2	/			5-46
(Juneja 2005)	0.15-0.2	40-100			0.5-231
(Black and Kohser 2017)	0.16	60			6.8
(Groover 2010)	0.125	70			39.6
(Kalpakjian 1984; Kalpakjian and Schmid 2014)	0.08-0.2	/			5-46
(Pilafidis 1971)	0.09-0.55	/			1.7-30
(Spitler et al. 2003)	0.1-0.15	/	0.5-0.8	0.2-0.4	111-451
(Nee et al. 2010)	0.1-0.15	/	0.5-0.8	0.2-0.4	111-451
(Stephenson and Agapiou 2016)	0.17	/	0.77	0.37	213.7

Where, in general,  $n$  and  $K$  are

It can be observed from the basis of the above assumption of Taylor's equation that cutting speed has a decisive effect on tool life. This is particularly for HSS cutters when the tool life exponent  $n$  is small. However, this simple model neglects other factors including feed and depth of cut (Karandikar et al. 2014). These and other factors have been shown to exert a direct influence on tool life, and as a result, equation (3.1) is almost never utilised in milling.

The extended Equations (3.2 - 3.5) provide more appropriate consideration of cutting variables than the basic formula. However, Equations (3.2, 3.3, 3.4, and 3.5) should only be used to estimate tool life and do not relate directly to tool wear. The number of variables contributing to tool life means that several different empirical constants are required to obtain a meaningful result. The estimation of the parameters needed to provide these values requires a significant amount of experimental based investigation with controlled changes to the cutting conditions. The experimental data can then be used to define the parameters needed for use in the specific application being analysed.

In addition, there are many types of workpiece material and cutters used in industrial operations and developing an empirical tool wear model for each combination is time-consuming, meaning that tool life equations are not usually applied (**Xiaoli and Zhejun 1998**). This approach is however usefully applied by cutting tool manufacturers to establish the properties of a specific tool, which can be used as a guide for comparative purposes.

Under the scenario imagined by equations (3.1 and 3.2-3.5), tools should be replaced when the indicated tool life is reached regardless of the actual tool condition. This may result in a tool management strategy under which replacement rates can be unnecessarily increased and consequently valuable production time is lost. It is usual for such a conservative strategy to be applied in the application that involves expensive workpieces where the cost of potential damage is significant. This is even more important in safety-critical applications, such as aerospace, where any failure may result in the scrapping of the element being machined. In many such cases, this can mean that the full lifetime of tools is not taken into account and the tools retain an element of useful life, which is not used. It must also be remembered that these unnecessary actions bring with them additional machine downtime, associated with the tool replacement and/or resetting process.

However, there will be circumstances under which tools can become worn out and/or broken before reaching the expected tool life. This type of failure can be especially costly in modern, automated facilities; as such automated production control is not possible without a means for tool wear monitoring.

Regardless of the cutting operations, tool life equations will attempt to provide an expected tool life. In practice, tool wear is a complex phenomenon occurring in different ways, and these simple equations will not be capable of taking into account all of the variables. Another factor is that the majority of tools being used in industry will not be used on a single task for their entire life, but will be utilised in a variety of different operations with slightly different materials, cutting speeds, cutting depths and feed rates. In order to provide a basis for comparison and prediction these cutting process

variables are often combined into one; metal removal rate. This is usually defined in terms of volume of metal removed per set time, such as cubic millimetres per minute.

In conclusion, it can be stated that Taylor's equations were intended to be applied where the appropriate constants of the equation have been determined. The approaches mentioned above assume that the tool life is deterministic. Unfortunately, the combined effects of cutting tool material, type of workpiece and cutting conditions, influence tool wear and variations are inherent in every cutting process. Therefore, tool wear is considered to be a stochastic and complicated process, and the tool life is difficult to predict.

Table 3.1, column 6 summarises the output from using Taylor approach equations and shows how this approach depends significantly on the workpiece constant. Small changes, therefore, result in considerable differences in tool life. Estimated tool life of 40-255 minutes based upon Kalpakjian coefficient, for example, is not very meaningful because of the range calculated. Moreover, the values of tool life that result from Juneja, Black and Kohser, and Groover are so far to those derived from these experiments.

It is worth mentioning that Taylor approaches have a different version that considered the cutting parameters and tool geometry. Several of these are presented in Table 3.2 for completeness this basic form and features are compared.

Where:  $r_n$  or  $r$  refers to the tool nose radius,  $\alpha$  and  $\beta$  refer to the rake and clearance angle, Figure (3.6),  $H$  refers to the hardness of the material workpiece

**Table 3.2 Summaries Tool life equations with its advantages and disadvantages**

Reference	Equations	Advantages	
(Creese 1999)		Easy to use	The const workpiece
(Creese 1999)	- - -	Gives better accuracy Than simple Taylor equation	more exp
(Spitler et al. 2003)			
(Saranya et al. 2016)	_____		
(Barrow 1972)	_____ - _____ - _____	Considers important machining variables	Complica
(Colding 1961)	_____ _____ - _____	Feed, depth of cut, and tool geometry	Complica
(Lau et al. 1980)		Considers tool geometry	Difficult relationsh angles
(ben Wang and Wysk 1986) (Hoffman 1984)	_____ _____	Considers feed, depth of cut and Brinell hardness	Materials different t
(Spitler et al. 2003)			
(Kronenberg 1970)		Easy to use	Required



The major limitation with this approach is that tool life is dependent on more than just the material it is machining; other factors include cutting tool material, cutting tool geometry, machine condition, cutting tool clamping, cutting speed, feed, and depth of cut.

As a result of these complications, it is hard to predict which tool wear mechanism will dominate and result in a tool failure in a particular situation, tool life is usually treated as a stochastic variable and not as a deterministic quantity (**Alamin 1996**). The reason for varying tool life could be due to the inhomogeneity in the workpiece and tool materials and the irregularities in the cutting fluid motion.

It is however generally assumed that tool life decreases, and tool wear increases with increasing metal removal rates and cutting time.

As can be seen what is achieved appears to be a relatively fairly simple formula that can be used to represent tool life. This, or similar equations, can be used under carefully defined and controlled “laboratory” conditions to test and quantify tool performance. Such tests will provide valuable performance data, allowing tool characteristics to be measured and compared. This, in turn, will enable more informed tool selection and process setting actions when the tools are in use. It is not the intention that this approach should be used to manage actual machining operations because of the numerous combinations of material and component machining operations that can render such an approach impractical.

### **3.7 Consideration of the Evaluation of Metal Removal Rate (MRR)**

Metal removal rate can be defined as the volume of metal removed from an unfinished part per set time; it is measured in cubic centimetres per minute, it can be calculated from the basic equation (3.6). Metal removal rate can also be defined based upon “the rate at which the cross-section area of material being removed moves through the workpiece” (**Black and Kohser 2017**). Cutting speed, depth of cut and feed rate have

a major effect on the volume of metal and MRR. Whenever any one of those variables is changed, MRR will change also. In terms of constant cutting conditions, the progress of flank wear in the steady wear phase (phase II) of the tool life curve is directly proportional to the actual machining time or the volume of metal removed. Under such constraints, this relationship can be used as a criterion for tool wear and tool life and must be clearly understood. Practically, it may be more helpful to assess the tool life regarding the volume of metal removed since the wear is related to the area of the chip passing over the tool surface.

The simple direct basis for MRR considers the volume removed from the workpiece and the time is taken for the material removal.

(Creese 1999)(3.6)

Where:  $V$  is the volume of the workpiece removed in ( $\text{mm}^3$  or  $\text{cm}^3$ ), and  $t$  is the machining time in (minute).

In a milling operation, the tool is rotated about its axis as well as moving in the axial and radial directions. Thus, it is important to specify the radial  $r$  and the axial  $a$  depth of cut per revolution

Using these defenitions it is posible to calculate MRR

For plunge milling MRR is

————— (SandvikCoromant 2017)(3.8)

Where:  $D$  is the cutter diameter (mm), feed rate  $f$  is a function of the feed per tooth per revolution ( $\text{mm/rev}$ ), and the spindle revolution speed  $S$  (rpm), and it is expressed as below:

---

---

(mm/min)

(Creese 1999)(3.9)

Therefore, equation (3.7) can be written in another form (3.10).

The radial depth of cut is often defined relative to the cutter diameter and called immersion ratio. This can be further developed to give;

---

Many researchers have determined that there is a correlation between metal removal rate and tool wear or tool life.

The effect of MRR for a 3-axis machining centre on energy consumption of milling machine tools have been characterised (**Diaz et al. 2011**). They summarised that increasing MRR translates to faster machining time but with an increase in the loads on the spindle motor. The power concerning the process parameters and tool wear was empirically modelled (**Yoon et al. 2014**). The model used a response surface methodology under three kinds of tool wear condition, mild, moderate and severe. They found that the material-removal power increased with the flank wear of the tool. However, these increases were not proportional to the total cutting power value. Hence, the optimum power consumption point can vary, regarding tool wear.

The effects of cutting parameters on TiAlN-coated carbide tool life and volume of workpiece material removed during machining a hard material were also evaluated by using response surface methodology (RSM) (**Davoodi and Eskandari 2015**). The results indicated a good agreement between the mathematical model and its respective variables with less than 2% error.

### 3.8 Summary

The wear of the cutting tool, which develops due to the dynamic interactions between the cutting tool and the workpiece, results in a reduction in the quality of the machined parts and the associated reduction in productivity because more components can be rejected and /or reworked possibly. Many criteria can be used as an advisable limit for tool life in process planning and machining optimisation. Such as the time required for wear to increase to the tool life criteria, a number of the parts produced, and length of the tool path. However, the ISO recommendations are the commonly used in evaluating the tool life.

In this chapter, data from a survey of the literature and other available information on Taylor's Equations have been reviewed to obtain a coherent picture of current knowledge about the validity of these equations in industry. This work suggests that versions of the equation can be used to describe the levels of tool flank wear and thus provide the basis for the monitoring of tool condition. Poor predictability of the tool life in Taylor's approach is mostly due to the following: it neglects the cutter geometry, the wide range of the empirical constant (  $K$  ), and the tool life is treated as a deterministic instead of as a stochastic variable.

In conclusion, it can be stated that Taylor's equations were intended to be applied where the appropriate constants of the equation have been determined. The approaches mentioned above assume that the tool life is deterministic. Unfortunately, the combined effects of cutting tool material, type of workpiece and cutting conditions, influence tool wear and variations are inherent in every cutting process. Therefore, tool wear is considered to be a stochastic and complicated process, and the tool life is difficult to predict.

# Chapter 4

## Experimental Setup and Process Parameter Section

### 4.1 Introduction

When compared to the machine and workpiece, the cutting tool is often the least expensive component. However, much of the process monitoring effort reported to date has concentrated on ensuring that the tool is in good working condition. This is because cutting tool failure can cause severe damage to the workpiece and possibly the machine tool. It may ultimately result in catastrophic failure leading to significant downtime and loss in productivity.

The extensive level of empirical verification of tool wear, usually conducted by tool manufactures, allows to the production engineer to adjust the settings of the machine in a systematic manner. It is common practice and to examine the impact of such cutting parameters on the part quality before the part is passed on for production. This is essential in most machining operations since most process control models are created based on the empirical data, and no universal mathematical models exist. This research consideres potential limitation in existing approaches to tool wear assessment and the impact this may have on milled components.

## 4.2 Experiment-based Approach to Tool Wear Assessment

The experiments aimed to establish and verify an approach which would be adopted to form and feature measurement. This was designed to directly explore the potential level of tool wear using the measurement of tool flank wear based on component metrology. This method was established to enable in depth the consideration of the extent and nature of tool wear. The key concept embedded within the method was to employ the appraisal of the form and dimension of features of a milled cylindrical cavity to quantify and classify the levels of differential tool wear assessment.

Workpiece setting was enabled using an on-machine probing system. As the testing of tools needed more than one workpiece, this function allowed the replacement of workpieces as required. The cutting tool used for each test series was retained in the machine between tests without the resetting of tool offsets. All of the experimental work was performed on a Mazak Vertical Center Smart 430A (MVCS) shown in Figure 4.1. The test pieces were bright mild steel and all tools were HSS Cylindrical end milling cutters.



Figure 4.1 Mazak Vertical Centre Smart 430A (Mazakus.com)

### 4.2.1 Milling Machine

The MVCS's ability to machine in three-axes of direction enables the production of complex components and shapes. The range of allowable spindle speed is limited by the maximum 12000 rpm. The relevant technical details of the machine are specified in Table 4.1.

Another feature that made the MVCS a suitable machine was its capacity to hold multiple tools. As complete testing of tools could need more than one sitting, it allowed the cutting tool to be left in the machine without having to be removed and re-set by a technician. This could have potentially caused the tool to be positioned differently, affecting results.

Another feature of the MVCS is the CNC controller that operates it, the Mazatrol Matrix Nexus 2. The controller allows a CAD design to be converted into the Mazatrol programming language. The generated program can then be viewed and altered by the technician using local commands in the controller.

**Table 4.1 Milling Machine Specification**

Maximum feed rate	15 m/min (rapid)
Maximum spindle speed	12000 r.p.m
Spindle power	30 KW
Tool holding style	HSK 100A
Table Right/Left	900 mm
Table Longitudinal	430 mm
Movement Increment	0.0001 mm
Number of Tools	30
Feed Axes (X-Axis)	560 mm
Feed Axes (Y-Axis)	430 mm
Feed Axes (Z-Axis)	510 mm

### 4.2.2 Test Piece Setup

Details of the test piece dimensions, which were uploaded to the MVCS and later used by the CMM, are given in Figure 4.2. Rectangular blocks of bright mild steel approximately 125 mm x 220 mm x 25 mm were used. The feature labelled with P0 as a reference plane, which is 0.5 mm deep with 5mm wide. Each test piece was machined to produce a sequence of 8 x 40 mm diameter, 20 mm deep holes. These were formed from 4 x 5 mm deep cylinders. A sequence of machined slots were included to support future surface finish assessments, not considered here. The cutting order was P0, H1, SA, H2, SB, H3, SC, H4, SD, H5, SE, H6, SF, H7, SG, H8, SH.

### 4.2.3 Work Piece Material

In this study, bright mild steel was used as machining material. It was selected because of its extensive use in research laboratories and industry, due to its relatively low cost, and availability. Mild steel is classified by carbon content less than 0.25% with no other alloying elements in its structure. Bright steel is a steel that has been cold drawn through a die; this increases its mechanical properties of hardness, tensile and yield strengths. In each case, the hardness of the test piece was assessed using a hardness tester; the results are shown in Table 4.2.

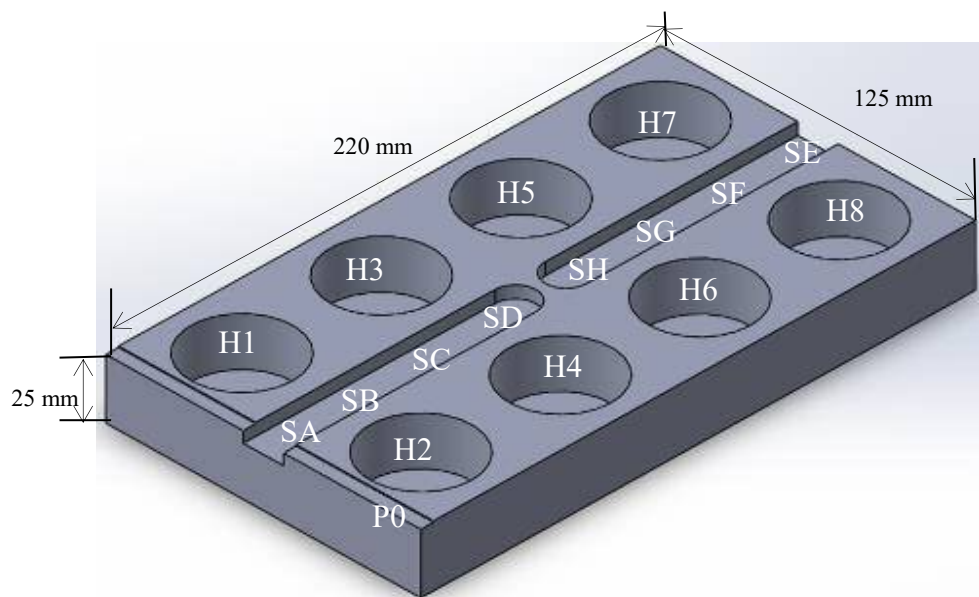


Figure 4.2 CAD drawing of test piece



#### 4.2.4 Cutting Tool Setup

HSS is a very common tool material for machining steels and its alloys. Figure 4.3 shows one of the high-speed steel, 16 mm diameter 4-flute end mill cutters. The cutter is made from 18% Tungsten W, 4% Chromium Cr, 1% Vanadium V, 0.7% carbon C and the rest is Iron Fe (**Rassouli 2011**). The main reasons for using HSS in many cutting operations is the relatively high toughness and the affordability of these cutters. It may be the case that more advantageous tools are becoming more widely used. However, HSS tools are still vastly used. HSS was chosen for the following reasons:

1. The expected tool life of HSS cutters when milling mild steel is considerably lower than carbide tools. This meant that tests could take a shorter space of time.
2. The HSS end mill cutter is capable of plunging directly into the workpiece as well as milling slots across it. This is in contrast to tools using carbide inserts, which often have particular roles, such as face milling or boring.
3. The geometry shape of the carbide inserts is limited, usually have a rounded edges. However, the HSS tools have a significantly sharp edge (**Fairbrother 2010**).
4. The carbide inserts are more brittle than the HSS tool. Hence, for interrupted cut, to avoid tip breakage, the tool movement should be reduced at the beginning of the cut (**Fairbrother 2010**). Therefore, HSS tools are suitable for most cutting operations.

The main limitation of HSS tools is that the range of the cutting speed is lower than carbide tools. In this case, speed and feed were carefully selected to produce specific levels of tool wear.



**Figure 4.3 HSS end mill cutter**

The tools utilised in this study were (HSS-E-Type N), they are available in a range of diameters from 2.5 to 25mm and different flute lengths. Two cutting tools diameters were used; 16 mm and 10 mm. Both were end mills with four flutes. The flute length and the overall length of the tools were 22 mm and 72 mm for the small cutter, 32mm and 92 mm for the large cutter (Appendix A). It should be noted that the reason for using the 10 mm diameter cutter was to promote a short life cycle.

#### **4.2.5 Cutting Conditions Setup**

Eleven series of experiments were carried out with parameters detailed in Table 4.2. The convention used to identify series was (cutter diameter.tool number). The first (in time) four series (16.1, 16.2, 16.3, and 10.1) were intended to verify the development of tool wear utilising the CMM. The next two series (16.4 and 10.2) were designed to investigate the use of data related to the cutting power in the time domain. The last five series 10.3,10.4, 10.5, 10.6 and 16.5 were carried out to verify the establishment of the relationship between VB and identified tool wear and the mean cutting power.

The conditions for the initial tests were selected by taking the recommended cutting speed for a milling operation involving a HSS cutter and bright mild steel workpiece. These were selected using the experience of the technician machinist, and with usual reference to a machinist's handbook. The particular combination of cutter, cutting speeds and feeds was selected to induce tool wear on a realistic but accelerated basis. The setting for each series are presented in Table 4.2.

#### **4.2.6 Coordinate Measure Machine**

The Coordinate Measure Machine (CMM) is an advanced, multi-purpose quality control system used to help inspection keep pace with modern production requirements. It replaces long, complicated and inefficient conventional assessment methods with simple procedures. It is used to check the dimensional and geometrical feature accuracy of an object by a probe supported on three mutually perpendicular (X, Y & Z) axes (**Manufacturing-Terms 2007**). It is also used in manufacturing and assembly processes to test a part or assembly against the design intent. There are mainly two

major parts in CMM; the structural system and the probing system or measuring probe. Also, the control system and the measuring software, incorporating an advanced high-speed scanning system, which enables high-quality data to be collected quickly and accurately. The structural system includes bridge, bearings for moving the bridge, a large granite table to support the workpiece, air bearings along each component allow for smooth independent movement along the X, Y and Z directions, and vibration isolation system. The probing system includes the probe tip that is made of spherical ruby; it is mounted to a motorised indexing head which in turn is attached to CMM structure.

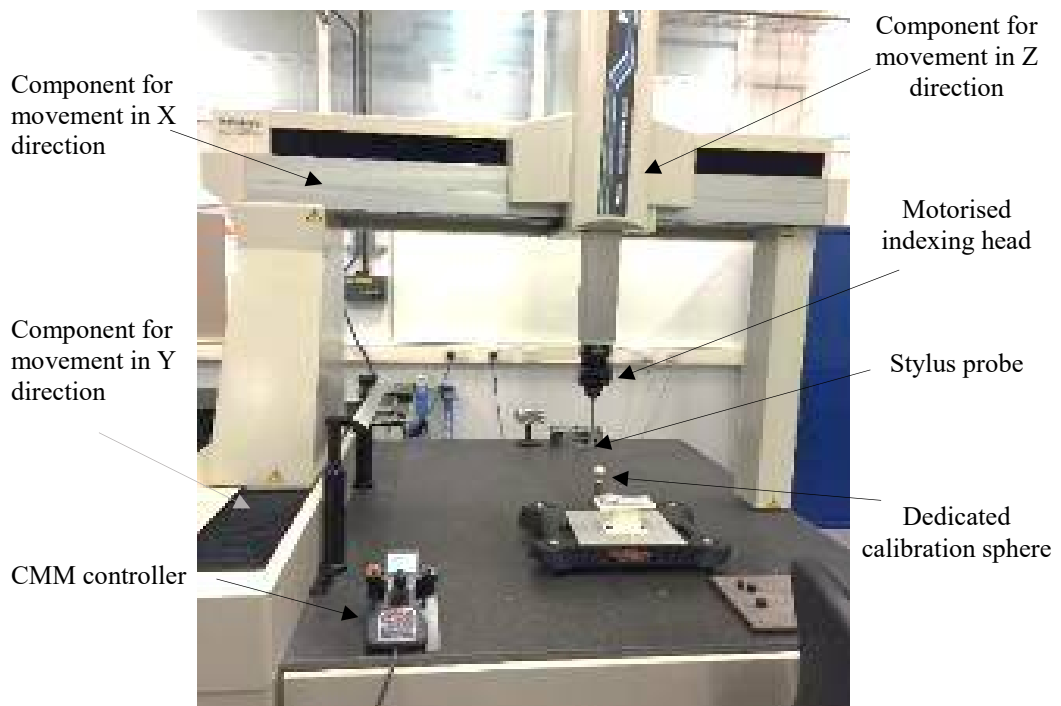
**Table 4.2 machining parameters of verification experiment**

Series number	Cutter diameter (mm)	Spindle speed (rpm)	Feed* (per cut) (mm/rev)	Feed rate (mm/min)	Cutting speed (m/min)	Hardness HV
Series 16.1	16	717	0.25	179.2	36	208.5
Series 16.2	16	856	0.25	214	43	209
Series 16.3	16	1035	0.25	258.7	52	209.5
Series 16.4	16	1035	0.25	258.7	52	207.6
Series 16.5	16	1028	0.25	257	52	209.1
Series 10.1	10	1656	0.17	281.5	52	208.6
Series 10.2	10	1157	0.17	196.7	36	210
Series 10.3	10	1656 /1157	0.17	281.5 /196.7	36 & 52	207.4
Series 10.4	10	1656	0.17	281.5	52	206.9
Series 10.5	10	1646	0.17	279.8	52	211.3
Series 10.6	10	1153	0.17	196	36	208.3

\* The chip load (the size of cut per tooth of the cutter) was changed for each cycle as shown in Table 4.4.

In this study, a Mitutoyo Euro-C-A121210 CMM was employed to measure the dimension of the machined components, a photograph of the CMM is shown in Figure 4.4. This bridge structure is in turn attached perpendicularly to a large granite bed. The motorised indexing head can rotate about two more axes, allowing for the probe to be positioned in varying angles. The probe can rotate from  $+90^\circ$  to  $-115^\circ$  about the X-axis and from  $+180^\circ$  to  $-180^\circ$  about Z- axis. When the stylus at the end of the probe comes into contact with an object or the required location, as positioned manually by the operator or automatically via programmer.

The CMM is capable of providing dimensions such as length, diameter, angle, circularity, cylindricity, straightness, and surface roughness. The measuring dimensions of CMM are 400 mm x 700 mm x 400 mm (**Mazakus.com**). As the CMM is so precise; the resolution is  $0.1 \mu\text{m}$ ., the temperature can affect its accuracy. To avoid this the CMM is located in a temperature controlled laboratory. Also, the large granite bed has a high thermal mass to ensure further that changes in temperature will not affect any gathered results.



**Figure 4.4 Coordinate Measuring Machine**

### 4.3 Experimental Procedure

The following section present the machining operations applied to the test piece. There were designed specifically to use for this research. An expert machine operator provided the support needed to the machine. In each test series, a brand new tool was fixed in the tool holder of the machine; the tool had to be firmly tightened into the holder in order to prevent loosening which could lead to the tool moving in its holder, and affecting the results. Similarly, the prepared workpiece was fixed to the work table of the machining centre using a standard vice. The test piece machining file was then uploaded to the CNC controller along with the information relating to the tool and workpiece materials. The required cutting speed and depth of cut were included. From this, the controller then set the optimum feed per cut and calculated the other cutting parameters. These were defined using built-in capabilities provided with the MAZAK machine. The controller also generated the tool paths as required. Once the test process was setup, the protective screen was closed and the machining process started.

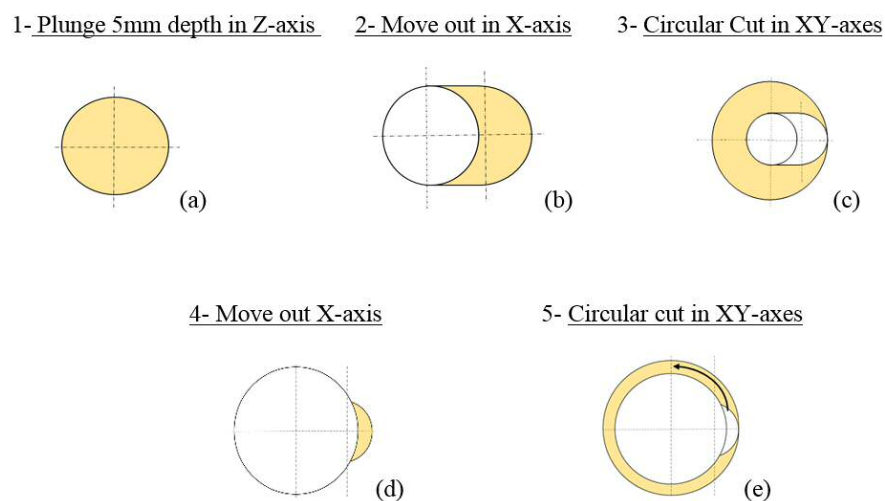
The tests were based upon milling a series of eight 40 mm diameter cylinders into a series of workpieces as shown in Figure 4.2. Initially, a new cutter was deployed and used to machine a 125 x 5 x 0.5 mm slot along the edge of the workpiece, as shown in Figure 4.2. This machined surface was utilised as a reference plane from which feature depths could be measured. This approach was designed to facilitate the transfer of tool length related parameters between workpieces.

The next cutting operation was for Hole 1 Cylinder 1, the cylinder is generated by a milling tool which executes a defined tool path in the workpiece as shown in Figures 4.5 and 4.6 (2D in Figure 4.5 and 3D in Figure 4.6). For the 10 mm cutter, the machining cycle started with an initial plunge into the centre of the workpiece down to 5mm depth, Figure 4.5a. After that, the cutter then proceeds to move out following a straight line to complete move 2, Figure 4.5b. The initial bore by a radius increase of 7 mm, Figure 4.5c. Once finished with this procedure the cutter then moves out again to the second part remaining 8 mm, Figure 4.5d, then removed producing the cylinder, Figure 4.5e. Hence termed Cylinder 1, repeating cycles moving down 5 mm each time produced cylinders 2, 3, and 4, and ultimately Hole 1. For the large cutter, it started with an initial

plunge into 3mm from the centre of the workpiece down to 5mm depth, Figure 4.5a and open out the initial bore, Figure 4.5c. Once finished with this procedure the cutter would then move out, Figure 4.5d and cut the remaining 9 mm in a large cutter width left surrounding the cylinder, Figure 4.5e. With these cutting parameters, the amount of metal removed from each hole is the same, which allows us to compare the tools more easily.

In these validation tests, the blind hole was milled by using a pocket milling operation. It can be regarded as one of the most common operations in machining (**Kramer 1992**). The metal is removed to a fixed depth on a flat surface of a workpiece inside an arbitrarily closed boundary. Normally end mills are used, and it can be carried out mainly by two tool paths, viz. linear and nonlinear (**Choy and Chan 2003**) or by three tool paths unidirectional, zig-zag, and arachnoid (like a spider web) (**Kramer 1992**). It is also necessary to specify the cutting conditions (spindle speed, feed rate, axial and radial depth of cut) which are to be applied to this operation.

In summary, a sequence of four cylinders (C1 to C4) was machined in each of the eight holes (H1–H8) on a workpiece. These four cylinders were milled to depths of 5, 10, 15 and 20 mm as shown in the Figure 4.7. The schematic of the way in which each hole was machined and formed using four cylinders to support this process is shown in Figure 4.8.



**Figure 4.5 The Diagram of Cutting Operation for Each Cylinder**

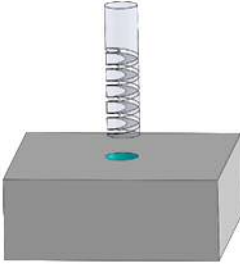
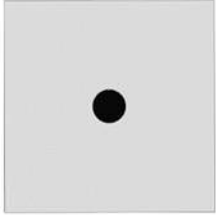
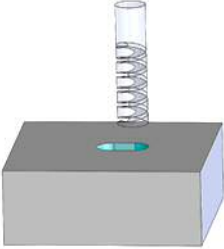

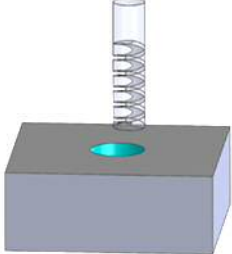
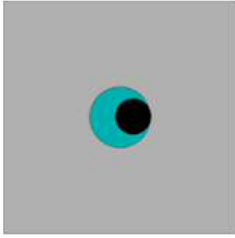
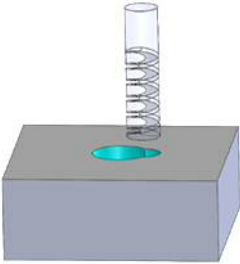
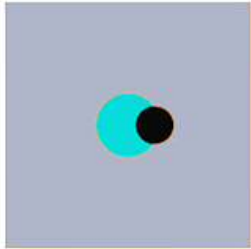
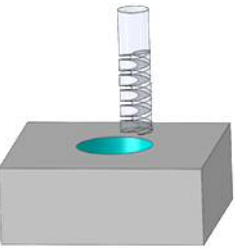
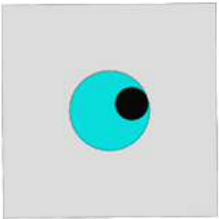
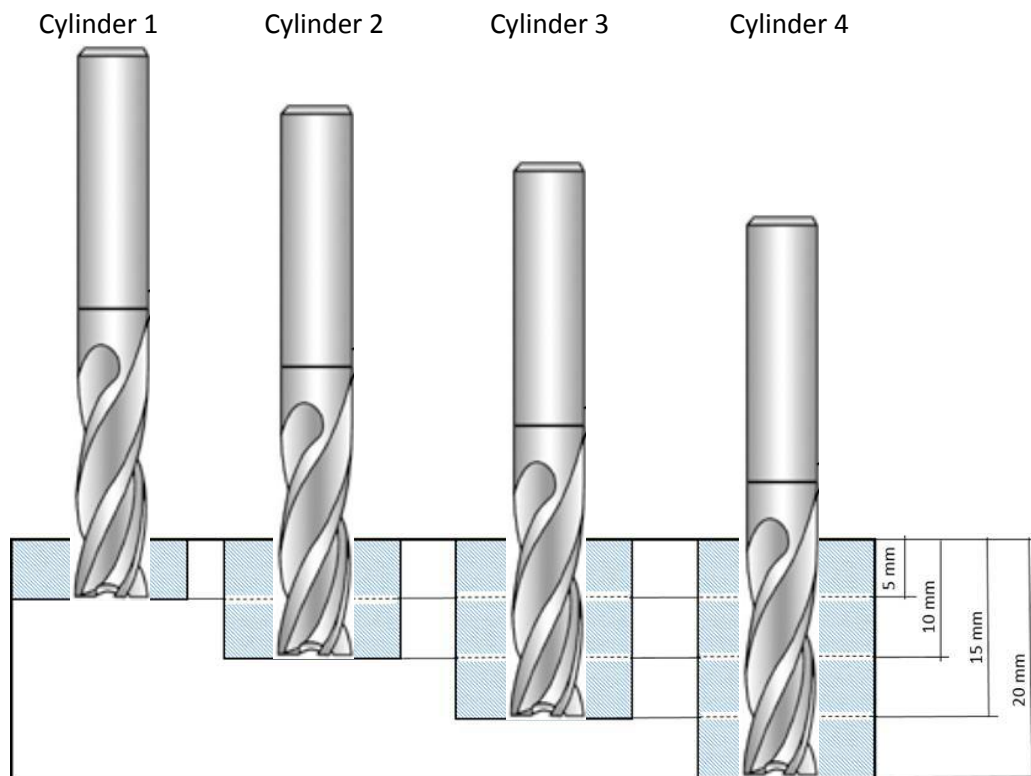
Sequence Number	Operation	Sequence Name	Side View	Top View
Cycle 1	Plunge into workpiece	Plunge		
Cycle 2	Move out*	Loop1		
Cycle 3	Open out initial bore			
Cycle 4	Move to outer			
Cycle 5	Cut cylinder	Loop2		

Figure 4.6 Configurations of the workpiece and tool at each cutting cycle

\* Does not exist for the large cutter path

At the end of this process, each workpiece had been machined to produce eight times 20 mm depth holes, as shown in the Figure 4.9. In this manner, 40 holes were machined for series 16.1 with constant cutting parameters. The same processes are also carried out to produce 32 holes for series 16.2, 16.3, 10.4, 10.5, and 10.6. The first eight holes in series 10.3 were done with 36 m/min cutting speed and the other 24 holes were done with different cutting speed. In series 10.1 and 10.2 a 24 and 25 holes were produced. However, 34 holes and 48 were machined in series 16.4 and 16.5, respectively. There are listed in Table 4.3.



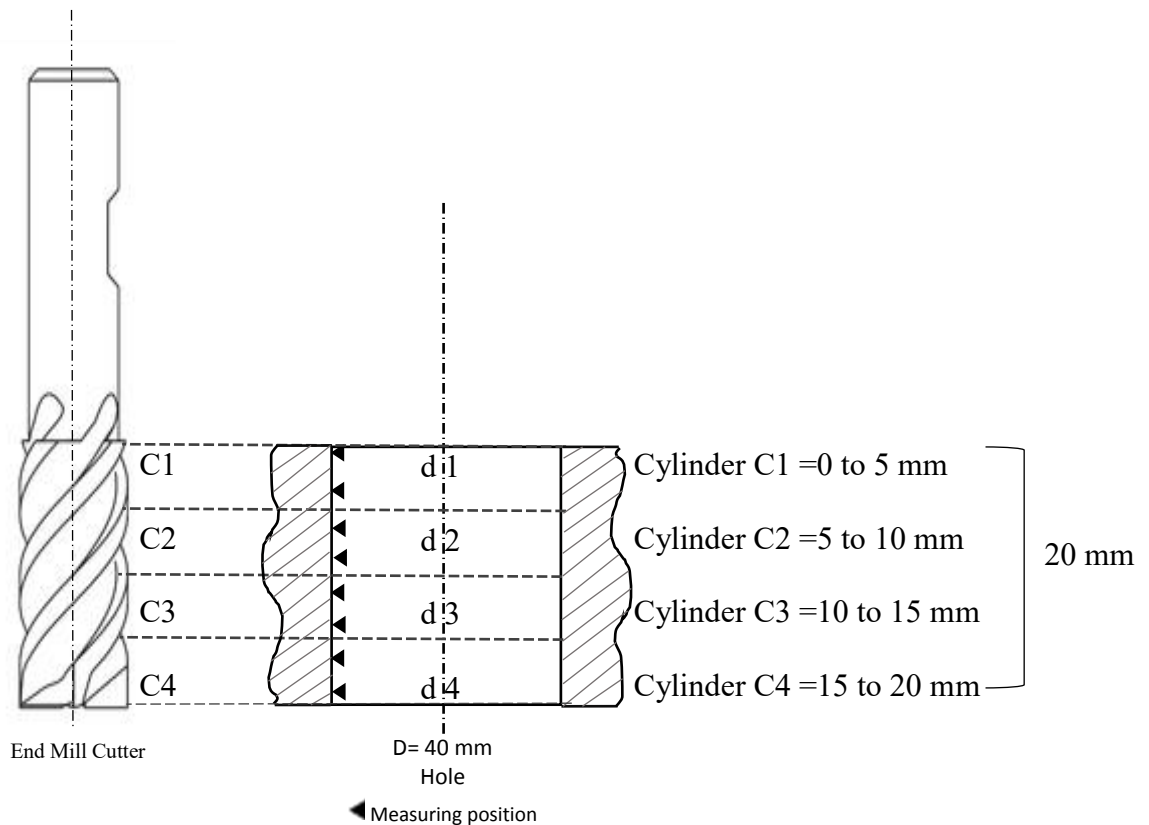
**Figure 4.7** The sketch of a sequence of four cylinders for one hole



Table 4.3 The series classification

Series number (cutter diameter. tool No.)	Hole number (in series)	Hole number (in set)	Set number (physical identification)
Series 16.1	1-8	1-8	Set 4
	9-16	1-8	Set 5
	17-24	1-8	Set 6
	25-32	1-8	Set 7
	33-40	1-8	Set 8
Series 16.2	1-8	1-8	Set 9
	9-16	1-8	Set 10
	17-24	1-8	Set 11
	25-32	1-8	Set 12
Series 16.3	1-8	1-8	Set 13
	9-16	1-8	Set 14
	17-24	1-8	Set 15
	25-32	1-8	Set 16
Series 16.4	1-8	1-8	T 4
	9-16	1-8	T 5
	17-24	1-8	Set 8
	25-32	1-8	Set 9
	33-34	1-2	Set 10
Series 10.1	1-8	1-8	Set 2.1
	9-16	1-8	Set 2.2
	17-24	1-8	Set 2.3
Series 10.2	1-7	2-8	Set 2
	8-15	1-8	Set 3
	16-23	1-8	Set 6
	24-25	1-2	Set 7
Series 10.3	1-8	1-8	This set was done with 36m/min cutting speed These sets were done with 52m/min cutting speed
	1-8	1-8	
	9-16	1-8	
	17-24	1-8	
Series 10.4	1-8	1-8	Set 1
	9-16	1-8	Set 2
	17-24	1-8	Set 3
	25-32	1-8	Set 4
Series 10.5	1-8	1-8	Set 1
	9-16	1-8	Set 2
	17-24	1-8	Set 3
	25-32	1-8	Set 4
Series 10.6	1-8	1-8	Set 5
	9-16	1-8	Set 6
	17-24	1-8	Set 7
	25-32	1-8	Set 8
Series 16.5	1-8	1-8	Set 1
	9-16	1-8	Set 2
	17-24	1-8	Set 3
	25-32	1-8	Set 4
	33-40	1-8	Set 5
	41-48	1-8	Set 6

The total machining time for each test piece varied depending on the cutting speeds and diameters of the tools. Throughout the cutting operation, the feed per cut was changing for each cycle as shown in the Table 4.4. Once a test piece had been completed, the operator could then open the protective screen and remove it from the work holder before fixing a new test piece. In order to increase the repeatability and reliability of the tests, only one work holder was used throughout all the testing processes.



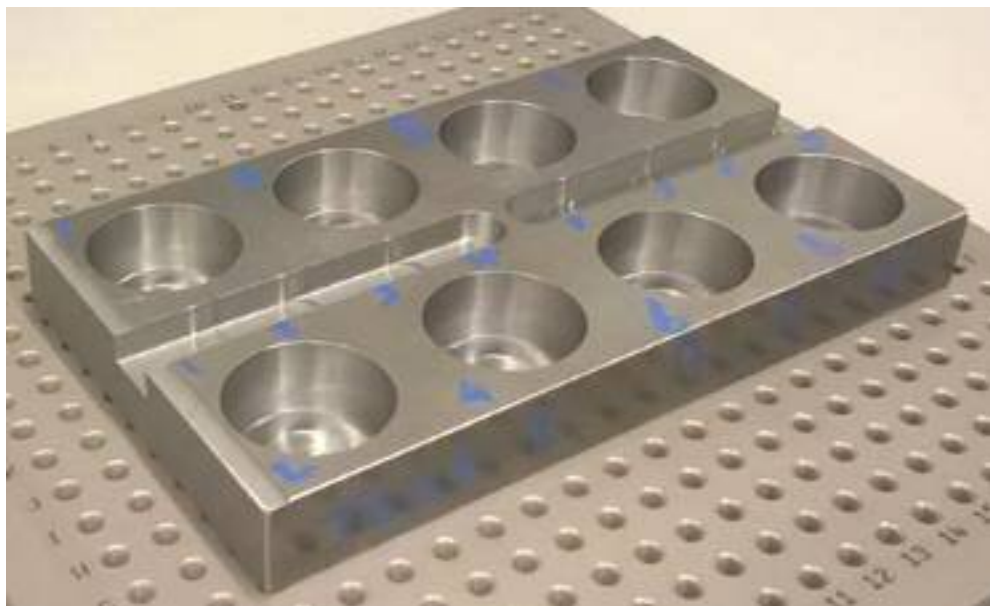
**Figure 4.8 Measurement position sketch**

**Table 4.4 Feed rate at each cutting cycle**

Sequence Number	Sequence Name	Operation	Feed per Revolution in Large Cutter (mm/rev)	Feed per Revolution in Small Cutter (mm/rev)
			Series 16.3, 16.4, and Series 16.5	Series 10.2, 10.3, 10.4, 10.5 Series 10.6
Cycle 1	Plunge	Plunge into workpiece	0.1	0.068
Cycle 2	Loop1	Move out	Not used	0.136
Cycle 3		Open out initial bore	0.2	0.136
Cycle 4		Move to outer	0.25	0.17
Cycle 5	Loop2	Cut cylinder	0.25	0.17
Slot		Move out	0.2	0.136

The method described was applied to support the measurement of tool wear across tests undertaken on several workpieces.

Two considerations needed to be made to support this investigation. They were the work done by the cutter and changes in its dimensions. The work done by the cutter is assessed in section 4.5.

**Figure 4.9 Workpiece plate after tool wear experiments**

#### 4.4 Tool Diameter Measurements

In this investigation, the initial tool diameter was measured online on the MAZAK machine by using the tool-setting probe (a physical contact tool-setter). This provided the input needed to start machining.

To provide a more accurate measure, the cutting tool dimension was acquired after machining using the CMM to measure a feature designed for this process [appendix B]. It can be seen that C1 in H1 was formed using the portion of the cutter that had undertaken minimal cutting. This hole was thus used as the reference to determine the initial tool diameter. Figure 4.10 represents this procedure and relates to the simple calculation given in equation (4.1). An exaggerated view of the tool wear effects on dimensions is shown for illustration discussion purposes. This was then utilised as the reference diameter for the entire series. It was used to define the diameter of the other holes at different depths. The assumption made was that the difference between diameter may treated as the tool flank wear.

$$\text{Initial Tool Diameter } D_i = d_{\text{nom}} - (D_{\text{nom}} - D_{\text{ref}}) \quad (4.1)$$

Where;  $D_{\text{nom}}$  = Nominal cylinder Diameter = 40 mm,  $D_{\text{ref}}$  = Reference Diameter (reference point), and  $d_{\text{nom}}$  = Nominal Tool Diameter = 10mm or 16mm

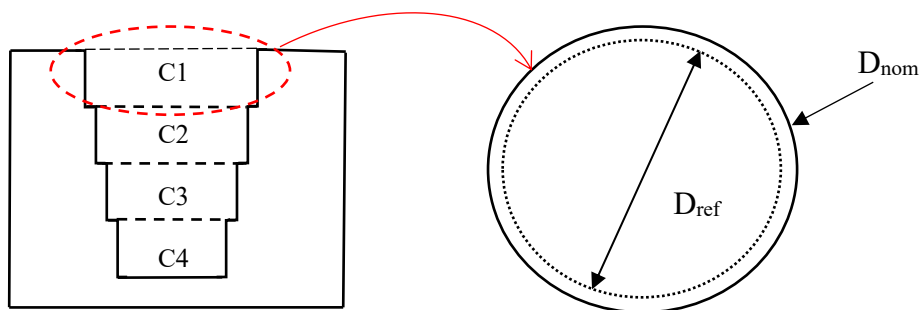


Figure 4.10 Determine the initial tool diameter

It should be noted that  $d_{\text{nom}}$  may have been set by a tool-setting probe but would still be updated in this manner. In this study, the  $D_{\text{nom}}$  was assumed to be 40 mm to start with, and that information was used to assess how much the tool wear has been.

#### 4.4.1 Tool Wear Measurement

This section describes the tool wear measurement method based upon the assessment of the features and the metrology of the components.

After completion of the above-mentioned experiments, the flank wear (VB) of the cutting edge of the tool was adopted as the tool life criteria and measured indirectly based upon shape mapping. In general, when a tool is new, dimensional accuracy will be controllable and thus satisfactory. However, over time, as the tool gets worn out, dimensional accuracy may be reduced. This is particularly true in cases of uneven wear.

In this investigation, the dimension (i.e. diameter) and form (i.e. circularity and cylindricity) of the machined cylinders were assessed for each of the features indicated in the Table 4.3 using the CMM.

In order to operate the CMM, the CAD model was uploaded to the CMM's controlling computer. From the uploaded file, a programme could be created using the CMM's programming language. This used the geometries of the design as a reference. A program was then created that enabled the CMM to measure the required features.

The finished workpiece was located within a fixture that allowed for it to be positioned within the CMM. This meant that following tests would also be located in the same position each time.

The measurement process started with the operator using the joystick on the controller to manoeuvre the tip of the probe to follow the commands detailed in Figure 4.11. The reason for this initial operation was to locate its datum points, enabling it to reference the part. The heading at the bottom of Figure 4.11 '\$\$ CNC Alignment \$\$' signals the

beginning of the CMM's auto-alignment, where these reference datums are determined more accurately.

The CNC alignment process used is performed for each measurement cycle. In this way, every test piece is measured using the same initial reference datums, meaning more accurate measurements can be applied.

The next stage was the actual measurement process of the cylinders (C1–C4) in the holes (H1-H8). The probe first moved to the coordinates above the hole to be measured, then proceeded to lower into the hole.

```
$$ Manual Alignment $$  
  
TEXT/OPER, 'Take 4 Points on Top Plane Bores 1 3 5 7'  
  
TEXT/OPER, 'Take 6 Points in Bore 1'  
  
TEXT/OPER, 'Take 6 Points in Bore 7'  
  
TEXT/OPER, 'Move Probe to Safe Position Above Bore 1'  
$$ CNC Alignment $$
```

**Figure 4.11 CMM commands to the user to establish alignment of the test piece**

As detailed in Figure 4.8, each hole was measured in eight positions to establish d1, d2, d3, and d4 for each of the four cylinders. Measurements were taken using a circular scan of the inside of the designated cylinders, and an average diameter was established. Then the tip of the probe ran around the circumference to determine the circularity. After each cylinder was completed the next cylinder 5mm down was measured for a total of 4 cylinders per hole, the programme represented in the Table 4.5 (the whole programme is in **Appendix B**). Once completed for all 8 Holes, the CMM provided an output for hole diameter directly into the separate excel sheet in the format of Figure 4.12. Figure 4.13 summarise the procedure of utilising CMM to measure one test piece.

Table 4.5 CMM program

CMM program	Meaning
P(PArc8)=PATH/ARC,CART,0,0,0,0,0,1,20,0,360,1,0,0 P(PArc9)=PATH/ARC,CART,0,0,-2.5,0,0,1,20,0,360,1,0,0	In Cylinder 1, the two circles at 0.0 and 2.5mm depth have been scanned, and an average diameter was established.
P(PArc10)=PATH/ARC,CART,0,0,-5.5,0,0,1,20,0,360,1,0,0 P(PArc11)=PATH/ARC,CART,0,0,-8,0,0,1,20,0,360,1,0,0	In Cylinder 2, the two circles at 5.5 and 8.0mm depth have been scanned and an average diameter was established.
P(PArc12)=PATH/ARC,CART,0,0,-10.5,0,0,1,20,0,360,1,0,0 P(PArc13)=PATH/ARC,CART,0,0,-13,0,0,1,20,0,360,1,0,0	In Cylinder 3, the two circles at 10.5 and 13.0mm depth have been scanned and an average diameter was established.
P(PArc14)=PATH/ARC,CART,0,0,-15.5,0,0,1,20,0,360,1,0,0 P(PArc15)=PATH/ARC,CART,0,0,-18.5,0,0,1,20,0,360,1,0,0	In Cylinder 4, the two circles at 15.5 and 18.5mm depth have been scanned and an average diameter was established.

	A	B	C	D	E	F	G	H
1	Start Template							
2	#####							
3		ACTUAL	NOMINAL	LO-TOL	HI-TOL	DEVIATIO	GRAPHIC	ERROR
4								
5	Bottom of Hole 1							
6	Hole 1 Cylinder 1							
7	Cylinder:CYL006							
8	Diameter	39.8	40	-0.5	0.5	-0.2	--*+---	
9	Circularity	0.143	0.1				+-->	0.043
10								
11	Hole 1 Cylinder 2							
12	Cylinder:CYL007							
13	Diameter	39.725	40	-0.5	0.5	-0.275	-*+---	
14	Circularity	0.187	0.1				+-->	0.087
15								
16	Hole 1 Cylinder 3							
17	Cylinder:CYL008							
18	Diameter	39.675	40	-0.5	0.5	-0.325	-*+---	
19	Circularity	0.22	0.1				+-->	0.12
20								
21	Hole 1 Cylinder 4							
22	Cylinder:CYL009							
23	Diameter	39.621	40	-0.5	0.5	-0.379	-*+---	
24	Circularity	0.255	0.1				+-->	0.155

Figure 4.12 Sample of excel file for S16.4 test 10

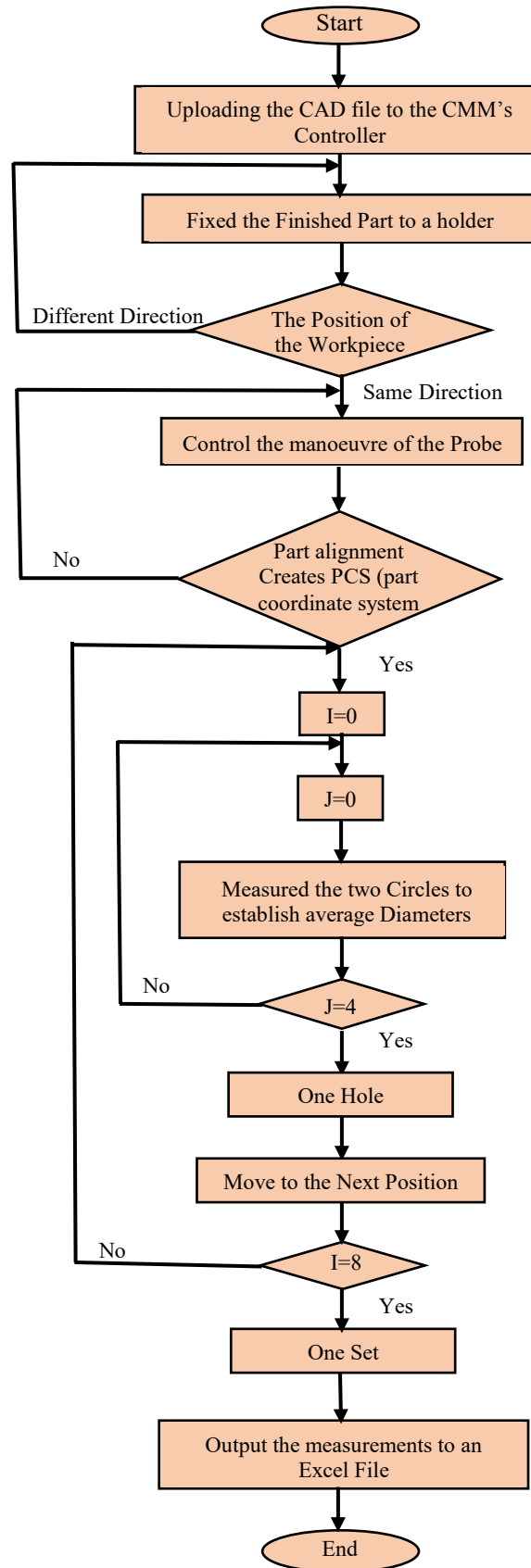


Figure 4.13 The flowchart of using CMM to measure the diameter of the holes (one set)



The same procedure that utilised to measure the diameter of the four cylinders was used to assess the wear in the bottom cutting edge. The bottom of the hole was measured at three places and an average value was established. In this technique, the P0 ‘reference plane’ was used as a reference point to measure the depth of holes. The depth of the first hole H1 (normally 20 mm) was used as a reference depth for the entire series regarding to tool wear.

The assumption made was that the difference between the reference depth H1 and the other depth may be treated as the tool wear in the bottom cutting edges.

After assessing the cylinder diameters of all the holes and calculating flank wear, it was possible to produce plots from which underlying trends could be determined. This process is considered in full in section 5.2.2.

## 4.5 Assessment of the Volume Removed by the Cutter

### 4.5.1 Cutting Time

In all machining processes, actual cutting time is an essential parameter to evaluate tool wear. From the economic perspective, the time to produce a part is the most important factor that effects on the cost of the process. In the experiment design, the length of each cut was used to derive the cutting time. It is generally expressed in minutes, since the speed units are often in m/min. For each series, the cutting speed was constant, and both the depth of cut and length of cut are fixed. Therefore, as in single-pass cutting, the time is calculated based on feed rate and the approach is called “the feed-based method” (Creese 1999). The time to produce one cylinder can be obtained from:

1- For the plunge milling will be given as.

---

(4.2)

Or

$$\text{---} \quad (4.2a)$$

2- For a straight tool path, machining time (T2 and T4) will be given as.

$$\text{-----} \quad (4.3)$$

Or

$$\text{---} \quad (4.3a)$$

Or

$$\text{---} \quad (4.3b)$$

3- For a circular tool path, machining time (T3 and T5) will be given as:

$$\text{-----} \quad (4.4)$$

Or

$$\text{---} \quad (4.4a)$$

Or

$$\text{---} \quad (4.4b)$$

### 4.5.2 Calculation of the Volume of the Metal Removed

Calculation of the metal removed by each section of the cutting tool is a very logical method of assessing the work done by the different sections. The information provided will be linked later in this thesis to the measured level of tool wear (in Section 6.6). This information is also important as it is used (in Section 7.4) to consider how to proportion the total work done by the cutter to each section of the tool. The total work done is assessed by plotting the spindle load against time data, which is transformed into an estimation of work done by calculating the area under the resulting curve. This can then be divided into work done by each section, based upon the respective volumes removed.

In order to establish the metal removed by each section a number of equations 4.5 through 4.8 have been used. These equations included calculating the volume of metal removed to make each cylinder based on the diameter of the cylinder that assessed by using CMM, as well as the depth of cut. The schematic of the way in which the volume removed was calculated for four cylinders is shown in Figure 4.14, the Table 4.6 represents the symbols used to support this process.

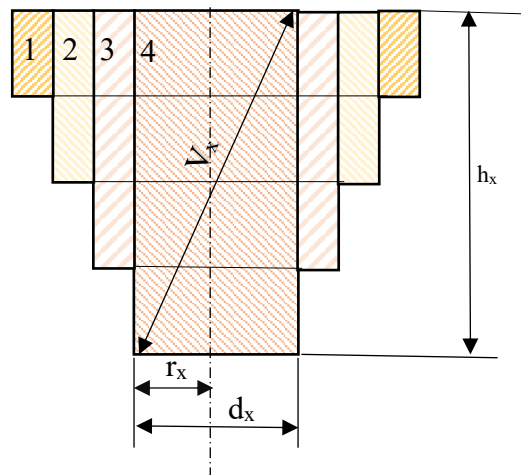


Figure 4.14 Volume removed calculated position sketch

Table 4.6 The symbols used to calculate the volume removed

	1	2	3	4
V	$V_1$	$V_2$	$V_3$	$V_4$
A	$A_1$	$A_2$	$A_3$	$A_4$
d	$d_1$	$d_2$	$d_3$	$d_4$
r	$r_1$	$r_2$	$r_3$	$r_4$
h	$h_1$	$h_2$	$h_3$	$h_4$

(4.5)

-

(4.6)

-

(4.7)

-

(4.8)

## 4.6 Summary

The present investigation focuses on the evaluation of the approach adopted to the feature measurement. This was designed to obtain the tool flank wear directly. A series of milling experiments were performed on bright mild steel test pieces using HSS end mill cutters. The aim was to investigate the consideration of the effect of machining condition on tool wear. In particular, a new methodology has been developed to measure the diameter and the depth of the hole to assess the tool flank wear based on component metrology.

In this work, both 10 mm and 16 mm diameter tools were used to machine a series of 40 mm diameter cylinder by firstly axial plunging at a fixed increment and followed by subsequent circular milling operations, which is performed in the x-y plane.

In this technique, the diameter of the first cylinder in the first hole (H1C1) established the initial diameter of the new cutter. This was used in the entire series to determine the differential tool diameter and the tool wear measurement. The depth of the first hole was used to determine the tool wear in the bottom cutting edges. The designed approach for assessing tool flank wear was supported by the CMM.

# Chapter 5

## Experimental Results

### 5.1 Introduction

This study focuses on multiple cutting edge tools, and tool life is considered by monitoring changes in the cutting process as indicated by component features rather than by assessing the state of the cutting edges directly.

A number of experimental techniques and tests for evaluating the tool wear in metal cutting have been developed. Many of these tests actually aim to assess the tool wear based upon the changes to the component of measured using CMM.

This chapter presents the findings relating to tool wear behaviour in the context of these initial experiments. The intention is to consider how this data can determine when the tool wear is sufficiently high to change the tool. The tool-wear level is assessed by the CMM for each set of tests. These results were used to calculate the amount of tool flank wear.

The experimental research involves quantifying the effect of process parameters, i.e. spindle speed, feed, and tool wear on hole quality during the milling of bright mild steel. Milling tests were conducted for a range of spindle speeds and feed rates, as shown in Table 4.2, with a 10 and 16 mm diameter standard flat end mill cutter. The depth of cut was kept constant. This investigation extended the milling approach to evaluating the tool life and differential tool wear, which, was not explored or reported in the open literature.

## 5.2 Experimental Results

After evaluating the initial diameter of the milling cutter, the measurements of the diameter of the cylinders of all the holes enabled the estimation of the wear of the tool flanks. It should be noted that this results section will consider in depth one series for a 10 mm cutter and one for a 16 mm cutter of these experiments.

### 5.2.1 Cylinder Diameter vs. Hole Number

Figures 5.1 present the results for test series 16.5. Figures 5.2, 5.3, 5.4, and 5.5 present the result to series 16.1 -16.4. The figures show the relationship between the cylinder diameter with hole number for all series. Excluding the repeating anomaly has been seen occurring in series 16.1 Figure 5.2 in the 3<sup>rd</sup> Hole of every test piece (Hole 3, 11, 19, 27, and 35) and abnormally high results recorded for Hole 33 and 34. The results represent the reduction in the measured cylinder diameters down the hole as the cutting operations went on in all series. Diameters loss is lowest in the top section of the cutter corresponding to d1 in Figure 4.8. Where it refers to the initial tool diameter  $D_{ref}$  when compared to the other tool segments.

The results show how the level of change to cylinders diameter varies with the hole depth. There is a clear difference in each section (C1 to C4). The effect can be understood by considering the metal removal process used to form the hole. Section C4 is at the lower level of the tool and removes most of the metal.

The average diameter ( $D_{ave.}$ ) was calculated at each hole. This was to enable the comparison of actual tool wear and the average value that would be used to represent tool wear. This will be considered in the discussion section of the thesis.

The result concluded that, for the 16 mm cutter as the cutting operations went on, a tapering effect become evident on the workpiece. The measurement of this continuous decrease in the cylinder diameter down the tool length would essentially be proportional to the amount of radial wear occurring on the tool.

The initial result from the Figure 5.1 shows that the diameter of the cylinders at the same depth of the corresponding regions (C4) became smaller from 39.80 mm to 39.43 for series 16.5 as the milling experiments went on. There are variations between the values of the actual diameters at the different levels (d1, d2, d3, and d4) with the value of the calculated average diameter ( $D_{ave.}$ ). Given that the average diameter could have been adopted as the input into tool-related calculations. This analysis suggests that the geometric form of a component machined using the uneven wear cutter will be less than optimal. It is also possible that incorrect assessments of the degree of tool life will be made. In the figures 5.1 to 5.5 the d1 values appear to be inconsistent. At this stage it was thought that this could be due to the very small amount of metal being removed. This will be discussed in more detail in Chapter 6.

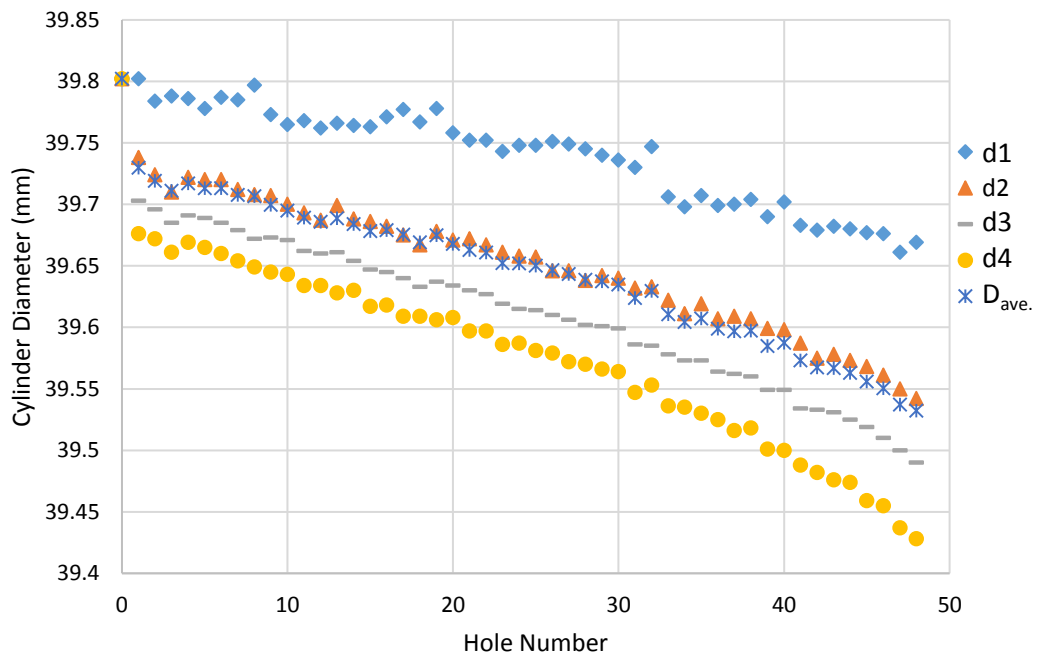


Figure 5.1 Variation in Cylinder Diameter/ Series 16.5



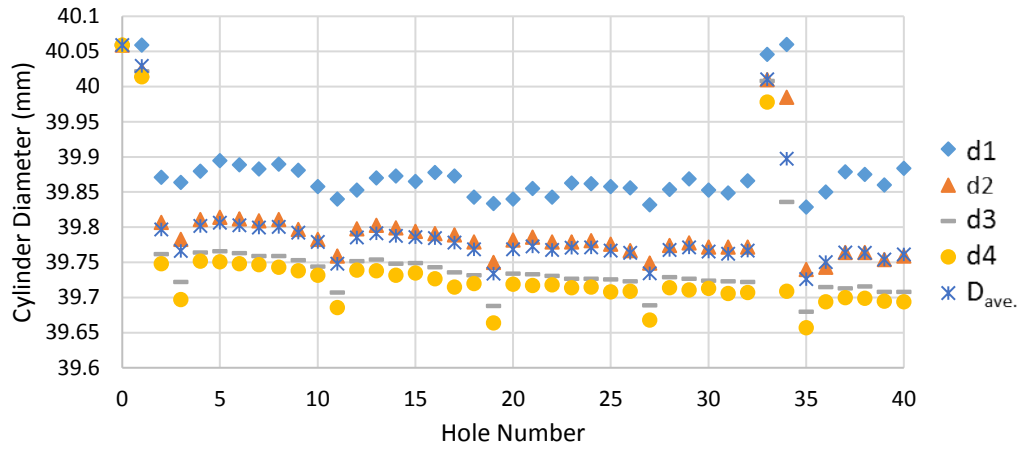


Figure 5.2 Variation in Cylinder Diameter/ Series 16.1

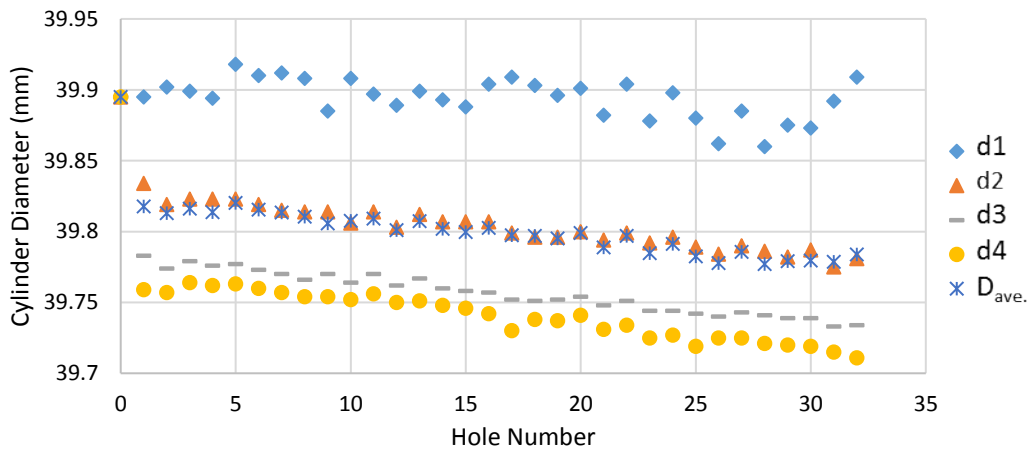


Figure 5.3 Variation in Cylinder Diameter/ Series 16.2

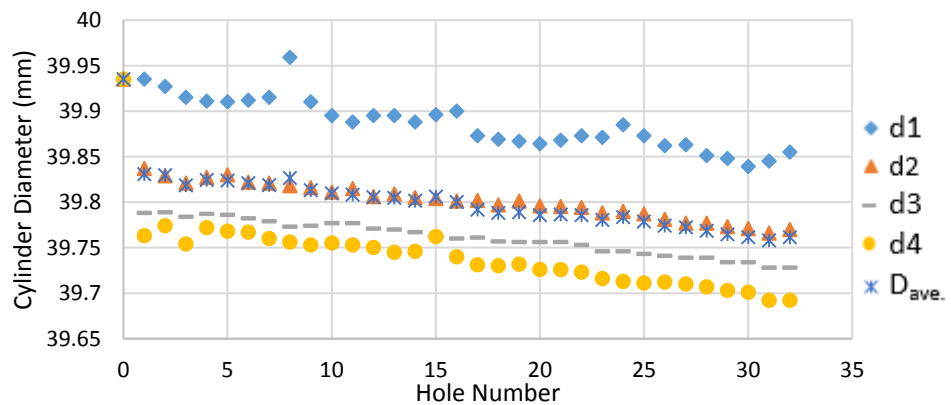


Figure 5.4 Variation in Cylinder Diameter/ Series 16.3

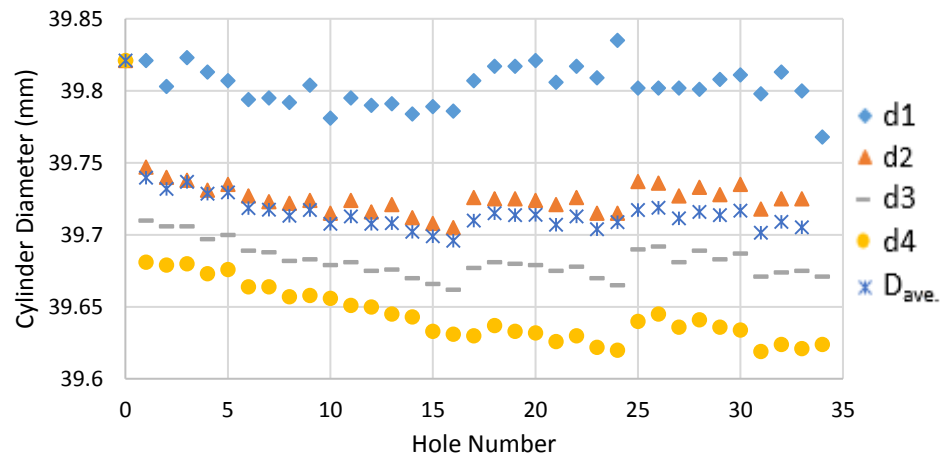


Figure 5.5 Variation in Cylinder Diameter/ Series 16.4

Figures 5.6 present the results for test series 10.4. Figures 5.7 to 5.11 present the result to series 10.1, 10.2, 10.3, 10.5, and 10.6. In each case, the cylinder diameters are again seen to vary with each hole. It also be noted that the number of holes produced is lower due to the use of the smaller tool.

It can be seen from the initial results of the CMM measurement in Figure 5.6 that the diameter of the cylinders at the same depth of the corresponding regions (C4) became smaller from 39.87 mm to 39.36 for series 10.4 as the milling experiments went on. There are also variations between the actual diameters at the different levels (d1, d2, d3, and d4) with the value of the calculated average diameter ( $D_{ave.}$ ). For example, at the end of series 10.4, the diameter of the cylinders at the same depth of the corresponding regions C1, C2, C3, and C4 is 39.77 mm, 39.6 mm, 39.54 mm, and 39.36 mm. The calculated average diameter ( $D_{ave.}$ ) is 39.56 mm. It is clear that there is a difference between 39.36 mm and 39.56 mm which refer to d4 and ( $D_{ave.}$ ) respectively. This meant that incorrect assessments of the tool life will be made.

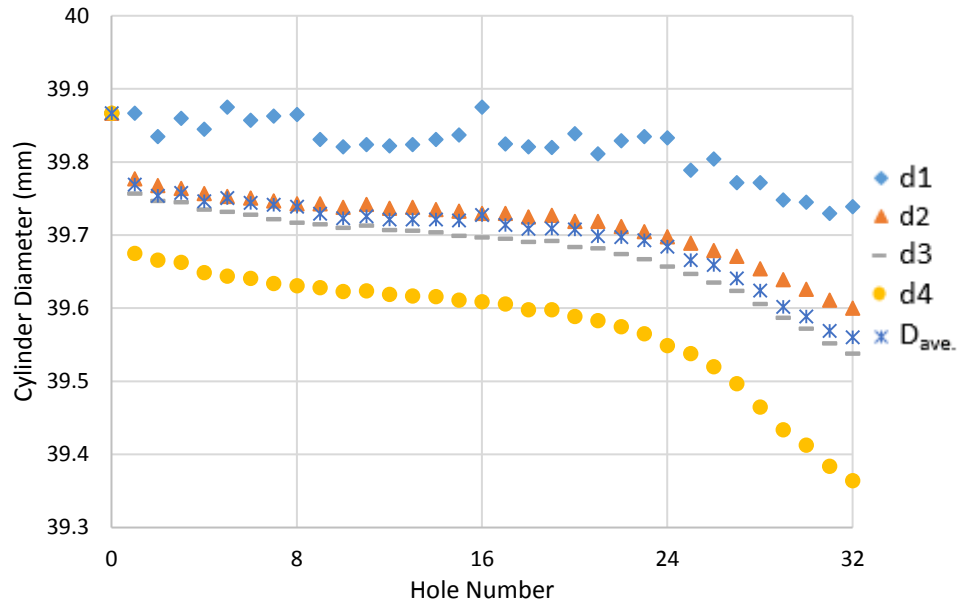


Figure 5.6 Variation in Cylinder Diameter/ Series 10.4

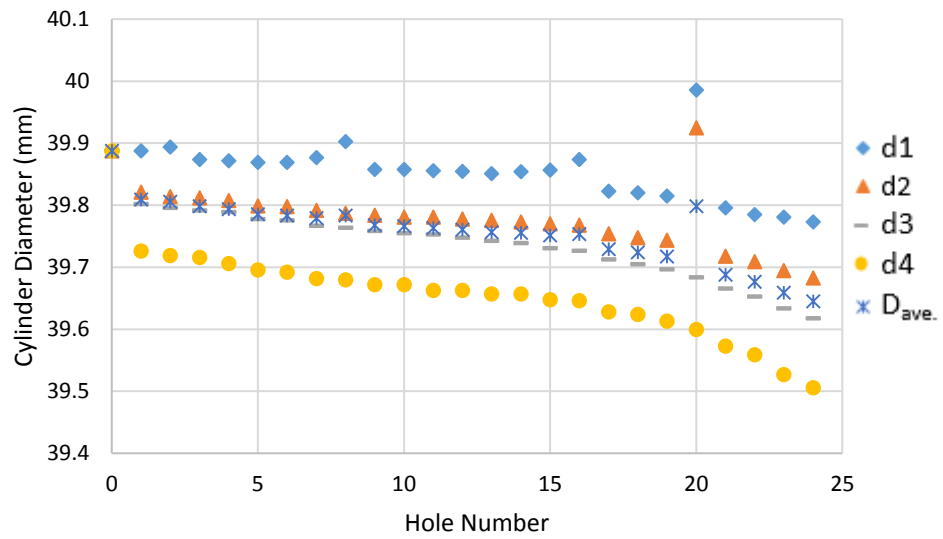


Figure 5.7 Variation in Cylinder Diameter/ Series 10.1

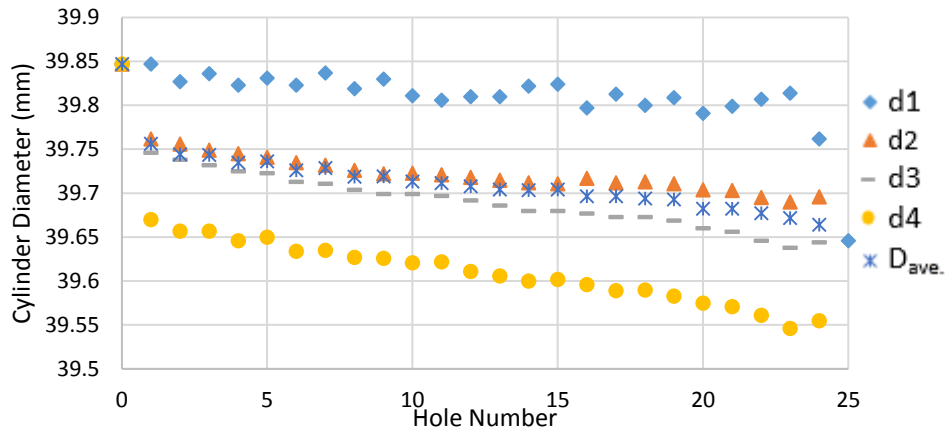


Figure 5.8 Variation in Cylinder Diameter/ Series 10.2

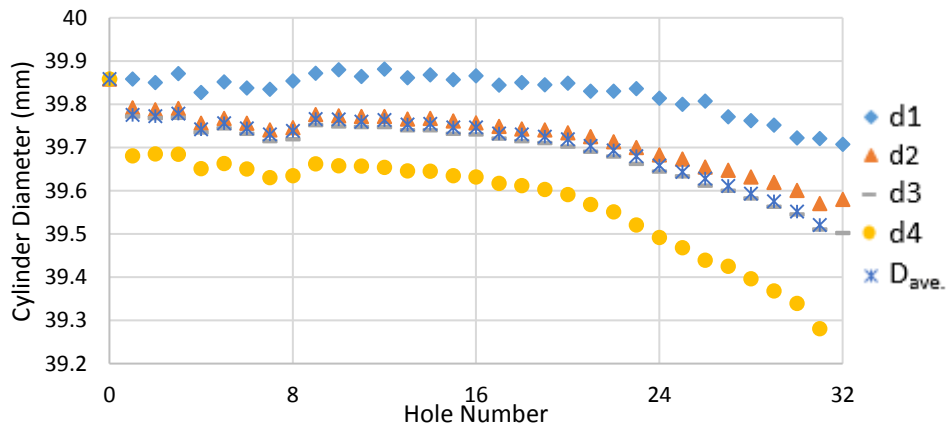


Figure 5.9 Variation in Cylinder Diameter/ Series 10.3

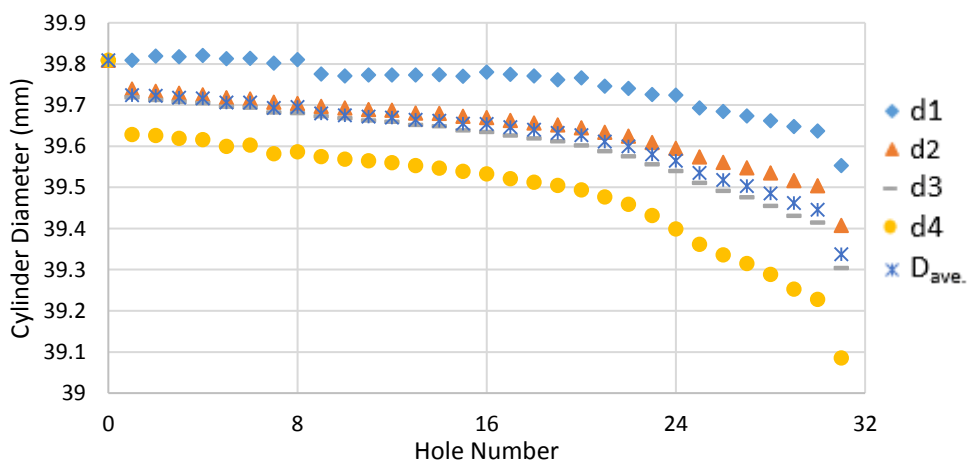


Figure 5.10 Variation in Cylinder Diameter/ Series 10.5

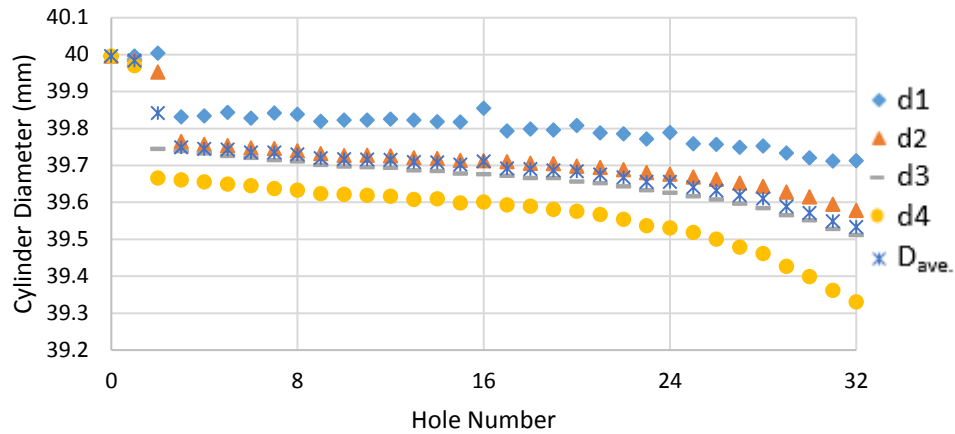


Figure 5.11 Variation in Cylinder Diameter/ Series 10.6

### 5.2.2 Tool Wear vs Hole Number

The analysis of tool wear in this study is derived from the observations made by employing the proposed wear method based on the component geometry measurements. The procedure deployed allows the data represented in Figure 5.1 to be transformed into the results given in Figure 5.12. Similar processing provided the tool wear plots generated for the other test series Figures 5.13 to 5.16 for the 16mm cutter and Figures 5.17 to 5.22 for the 10mm cutters.

The effect of reduction in the measured cylinder diameters can also be used to calculate the levels of tool wear. These values were calculated from the changes in cylinder diameter which represent the apparent wear of the tool at each of the corresponding levels.

The level of tool wear arising in the 16 mm cutter tests was lower than anticipated. Initial test were conducted with a view to reaching the ISO 0.3 mm limit. However, this was shown to be likely to require extended numbers of tests. For this reason, the decision was taken to use a smaller cutter.

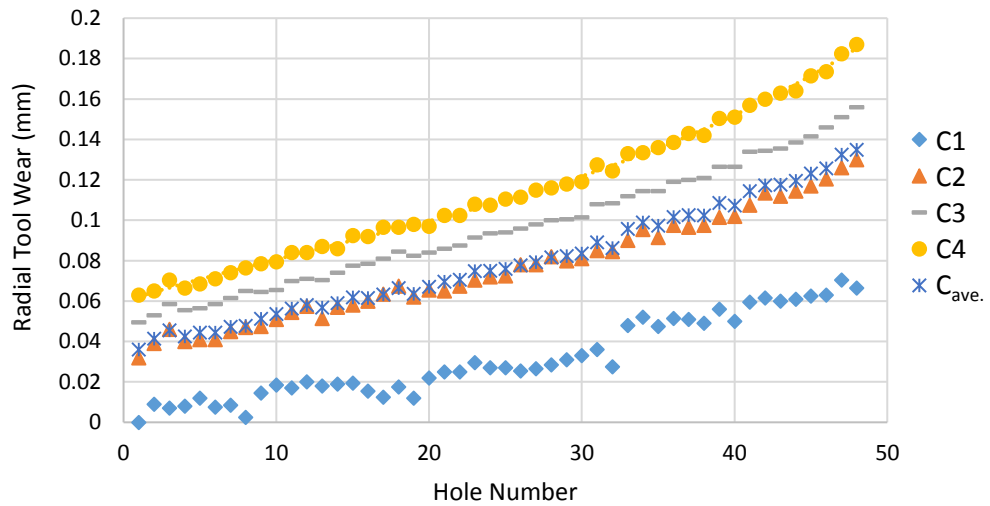


Figure 5.12 Tool wear as a function of Hole Number/ Series 16.5

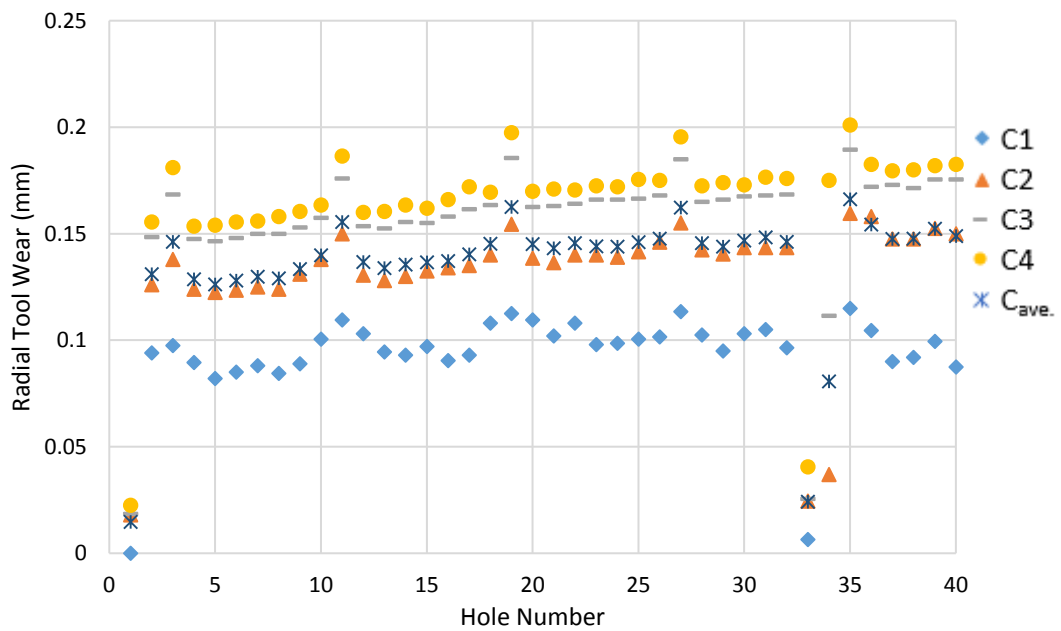


Figure 5.13 Tool wear as a function of Hole Number/ Series 16.1

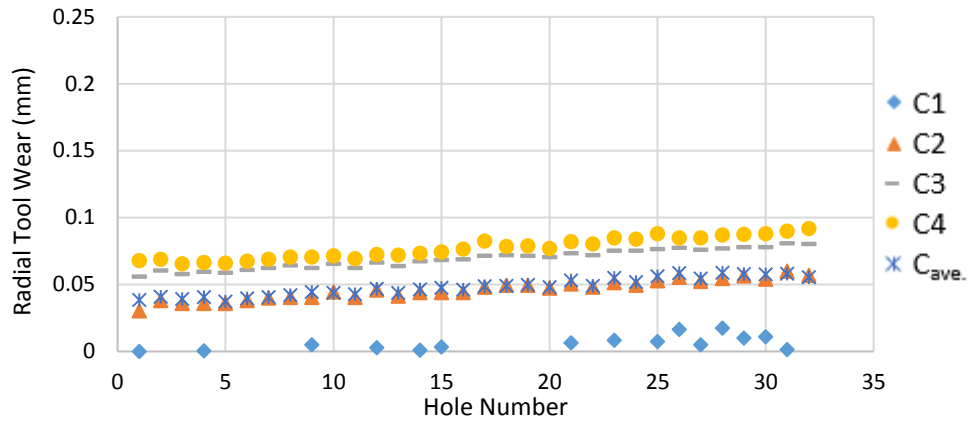


Figure 5.14 Tool wear as a function of Hole Number/ Series 16.2

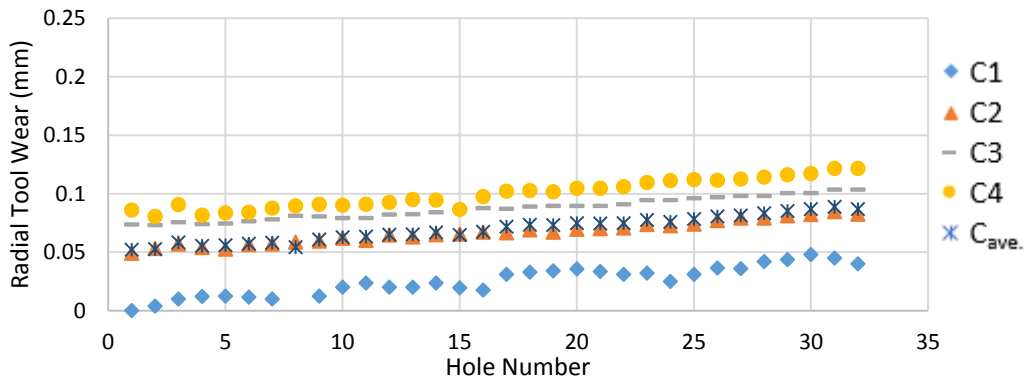


Figure 5.15 Tool wear as a function of Hole Number/ Series 16.3

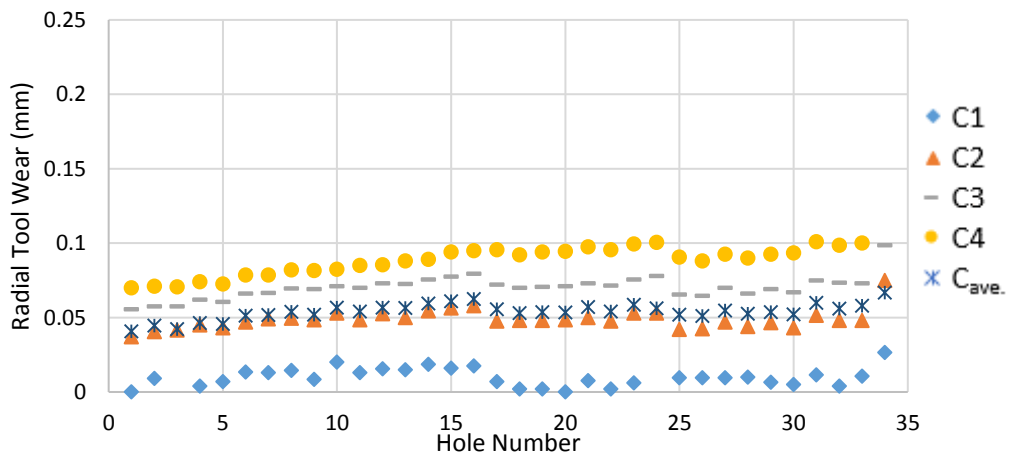


Figure 5.16 Tool wear as a function of Hole Number/ Series 16.4

The general trend indicated in all of the 16 mm cutter series is as anticipated. Tool wear is shown to be occurring to different amounts for the four cylinders. It is difficult to assess in the early stages since it is not possible to establish levels of tool wear arising in hole 1. This means that the indicated wear of C4 in hole 1 is measured with this portion of the tool having removed all the material above.

The effect of using the 10mm cutter is evident. Levels of tool wear were increased and tools reached the anticipated 0.3 mm limit with a reasonable number of tests. However, the cutter was broken in series 10.2, 10.3, and 10.5 before it reaches to the end of its life.

Regarding the tool wear result for the 10 mm cutter, Figure 5.17 in series 10.4, the three phases which correspond to the three wear stages present after milling 32 holes appear to follow the overall shape of the resulting curve associated with the established tool wear curves shown in Figure 3.2.

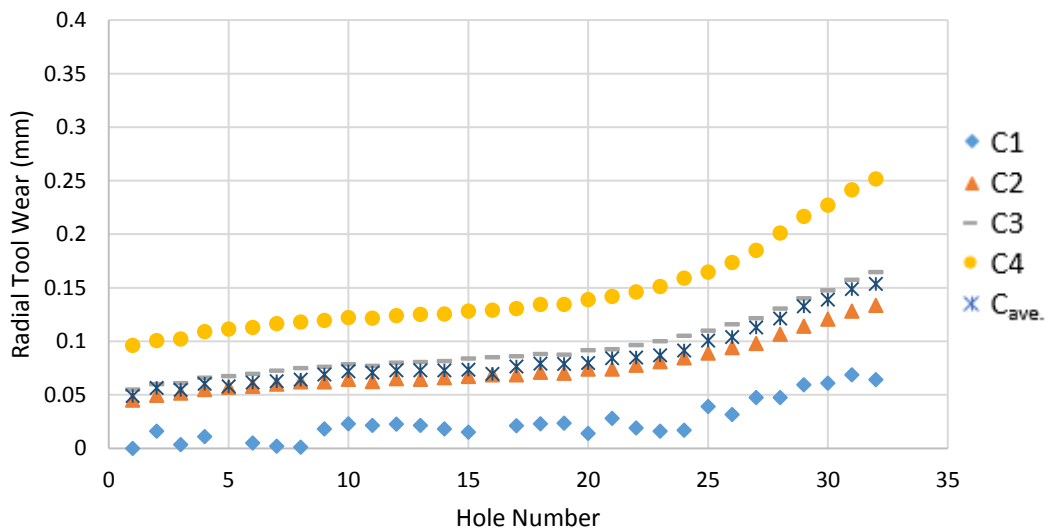


Figure 5.17 Tool wear as a function of Hole Number/ Series 10.4



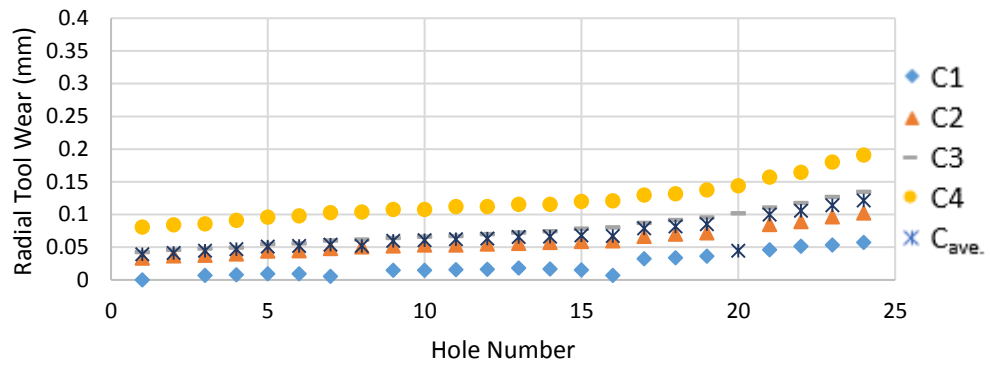


Figure 5.18 Tool wear as a function of Hole Number/ Series 10.1

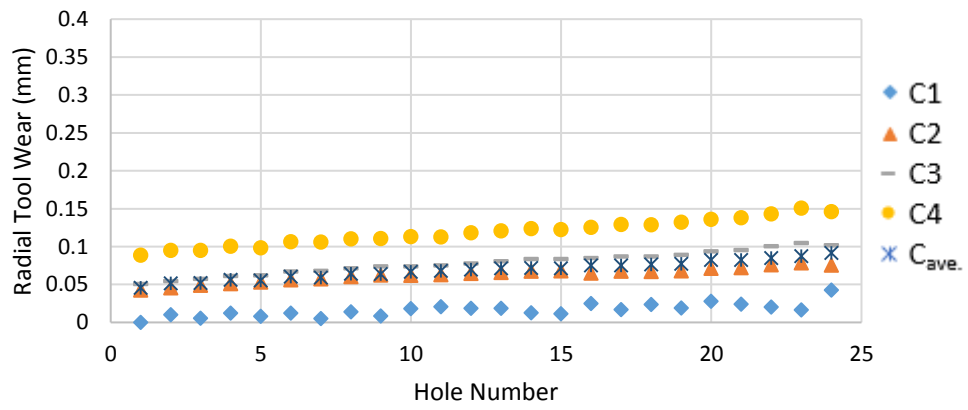


Figure 5.19 Tool wear as a function of Hole Number/ Series 10.2

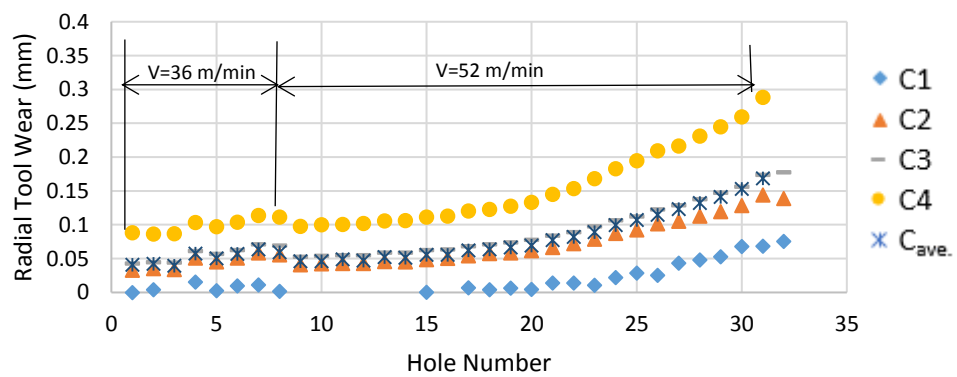


Figure 5.20 Tool wear as a function of Hole Number/ Series 10.3

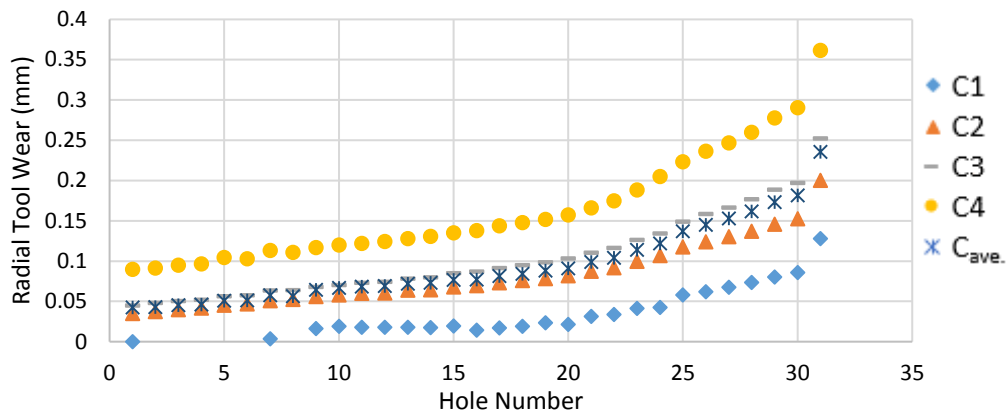


Figure 5.21 Tool wear as a function of Hole Number/ Series 10.5

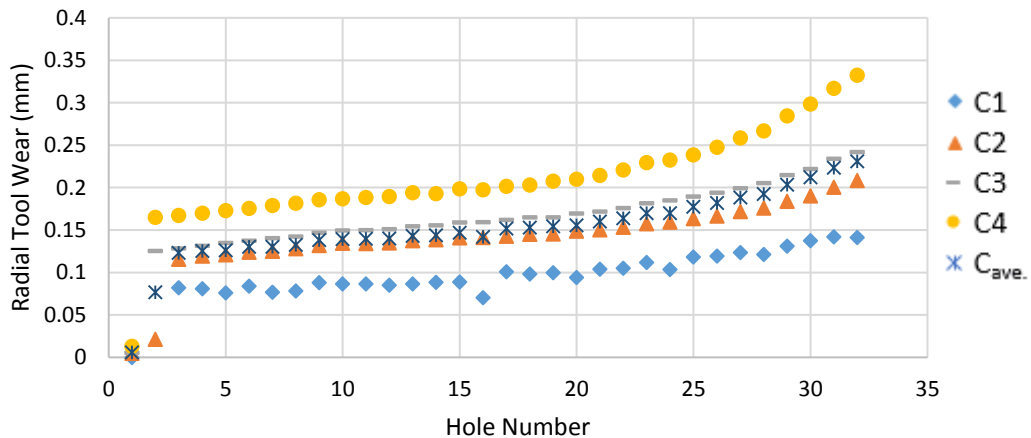
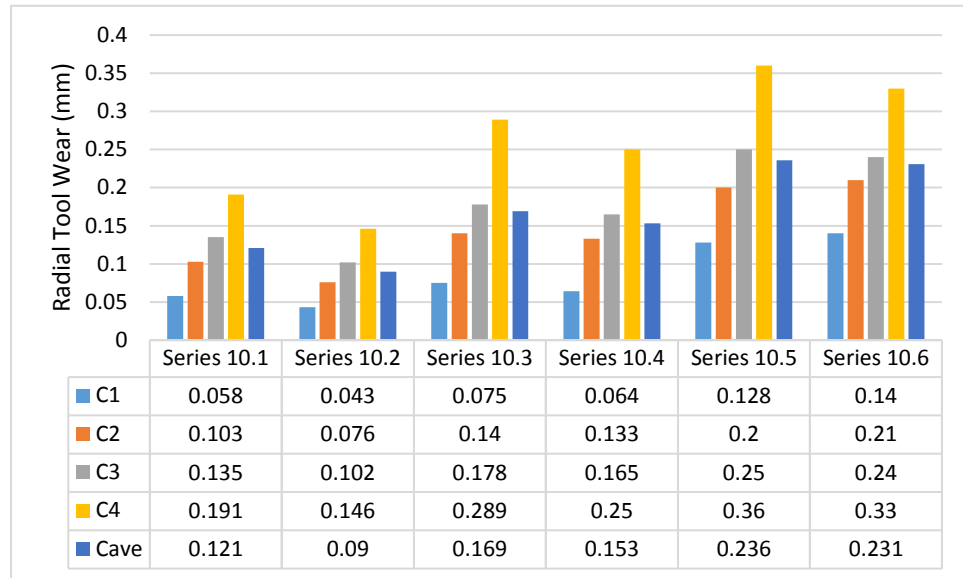


Figure 5.22 Tool wear as a function of Hole Number/ Series 10.6

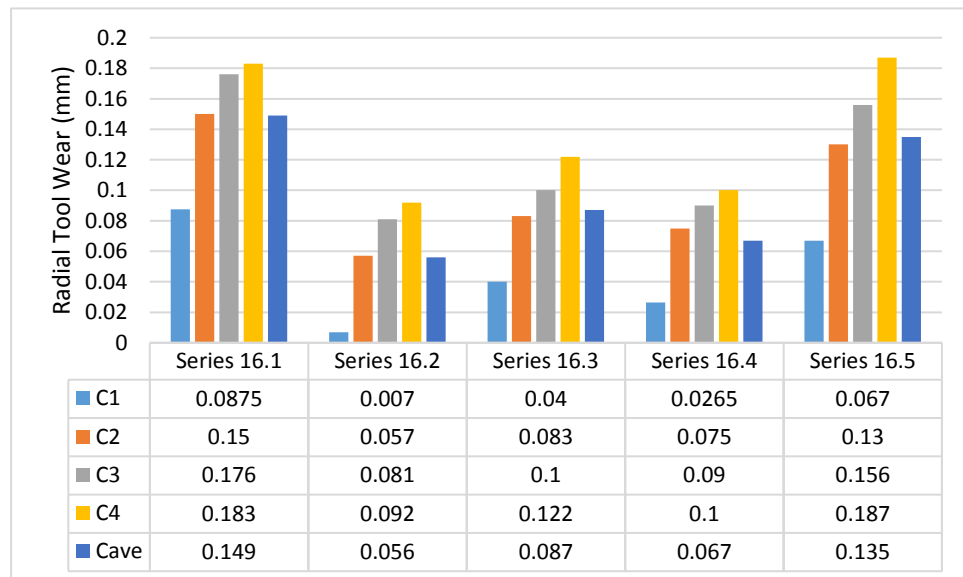
As anticipated, the amount of tool wear indicated in all series, Figures 5.12 to 5.22 is least in the top section of the cutter (C1). For example, in series 10.4 Figure 5.17, the maximum value reaches 0.064 mm. The highest level of tool wear occurs in the section C4, which corresponds to the bottom section of the cutter, where the maximum approaches 0.25 mm. Figure 5.17 also indicates the results of the average wear value of the tool,  $C_{ave.}$  is reaches 0.153 mm.

Figures 5.23 and 5.24 summarise the values of C1, C2, C3, C4, and  $C_{ave.}$  for the other test series, representing the data provided in Figures 5.12 to 5.22. This confirms that the potential exists for error associated with the non-allowance for differential tool wear in the cutter when using the average value to inform the re-set of the tool offset. This also

shows how this can reduce the dimensional accuracy of the product. Resetting the tool offset could hide the problem of differential tool wear, but it creates another problem that either makes the hole too big or too small depending upon which measure will be used as a reference point.



**Figure 5.23 Summary of the amount of tool wear occurs in different sections and tool wear average of the 10mm cutter**

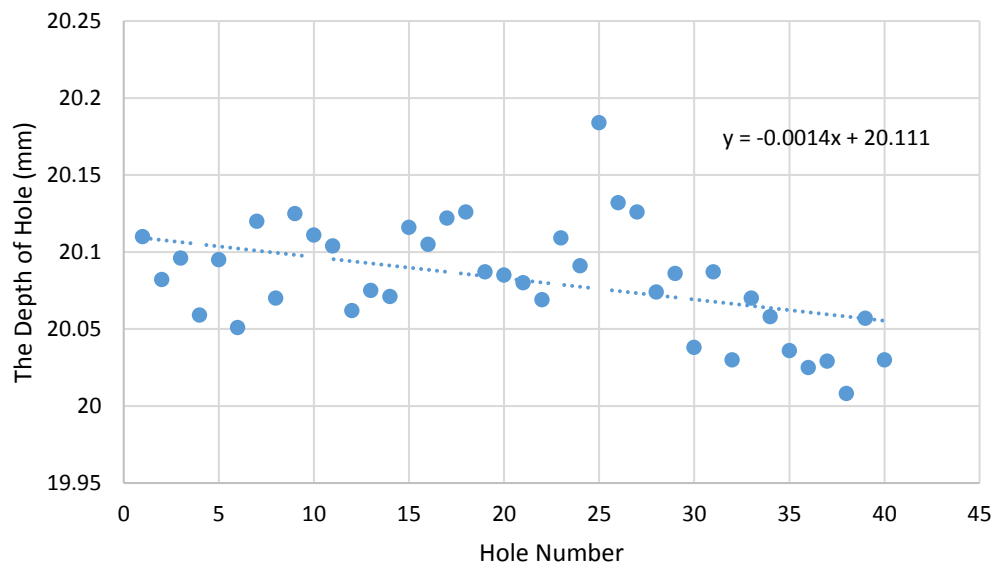


**Figure 5.24 Summary of the amount of tool wear occurs in different sections and tool wear average of the 16mm cutter**

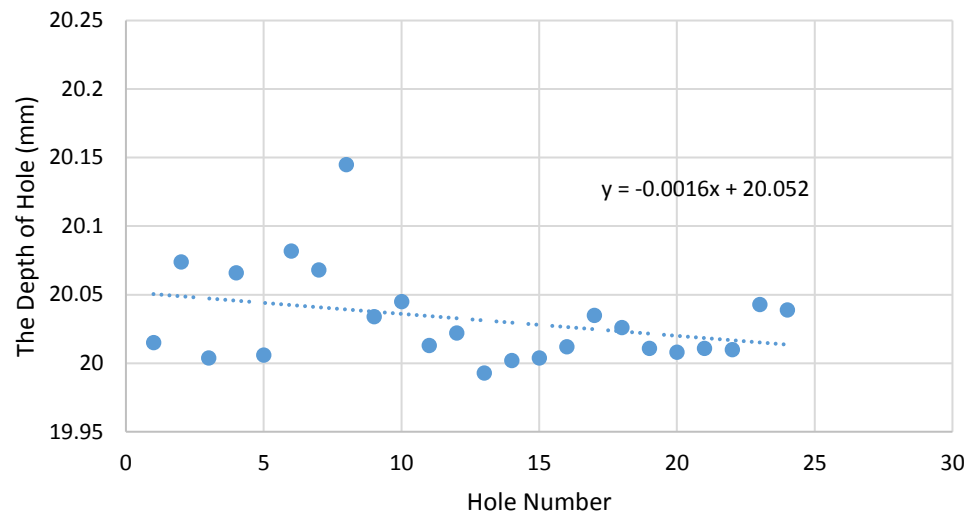
### 5.2.3 The Depth of Hole vs Hole Number

Figure 5.25 presents the results for test series 16.1. Figure 5.26 presents the results for test series 10.1, the rest of the data is existing in **Appendix C**. Figures 5.25 and 5.26 show the relationship between the depth of hole with hole number for the whole series. Although there is no specific pattern for the direction of the curve during the series, the trend line represents the reduction in the measured depth of the hole as the cutting operations went on. Which, refers to the loss in lowest part of the cutter corresponding to the bottom cutting edges. The method used to evaluate the tool wear in the bottom cutting edges relied upon the values of the depth of the hole. This was assessed based on the reference plane (P0) shown in Figure 4.2, which changes from piece to piece. This process was found to be inconsistent and thus these measurements were not considered further other than to indicate the trends.

The results show how the depth of hole varies with the hole number. The effect can be understood by looking at the metal removal process used to form the hole, section C4 which is located at the lower level of the tool, removes the major part of the metal.



**Figure 5.25 Variation in the Depth of the Hole/ Series 16.1**



**Figure 5.26 Variation in the Depth of the Hole/ Series 10.1**

### **5.3 Summary**

In this chapter, the results obtained from measuring the component geometry using the CMM were presented. This has shown that the CMM can be used effectively to measure tool wear at different positions down the cutting edge of end milling cutter. It should be noted that the wear analysis in this study was related to observations made employing component geometry measurement. The results concluded that there is differential tool wear which could reduce the dimensional accuracy of the product. Also, the tool wear in the bottom cutting edges was measured based upon the variation in the depth of the holes.

# Chapter 6

## Discussion of the Initial Results

### 6.1 Introduction

The work conducted in Chapter 5 shows how the level of the cylinders diameter varies with the depth in each section (C1 to C4). It confirms the existing of differential wear in the cutter which has a significant influence on the component accuracy and assessment of the degree of tool life when adopting the average diameter value as the input into tool-related calculations.

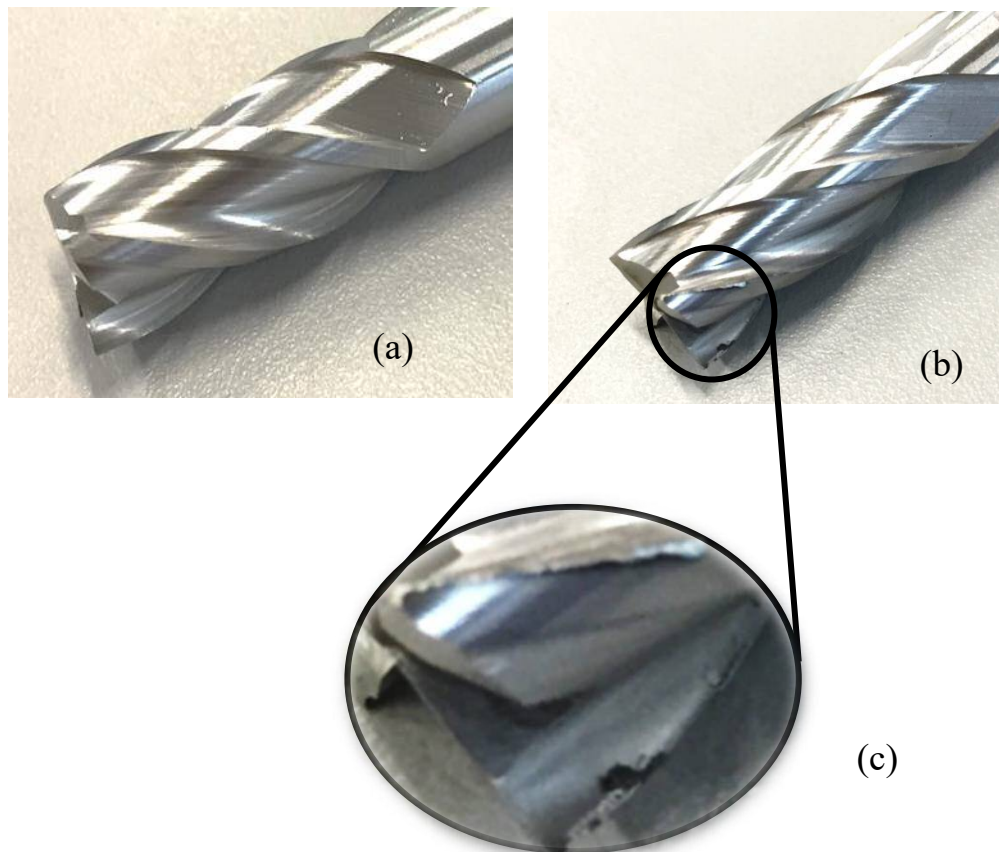
This chapter will discuss all the consequences resulting from the incorrect identification of the level of tool wear due to the differential tool wear and the difficulties of assessing the tool geometry because of the occurrence of uneven tool wear.

### 6.2 Tool Wear Mechanism

In this investigation, each test series was started with a new tool and stopped when the worn tool was anticipated (by the machinist and observers during the cutting operation) to have reached a dangerous condition.

The milling process can be considered as a discontinuous process on the periphery cutting edge and a continuous drilling process on the bottom cutting edge. During the machining of a hole in this study, the front and periphery cutting edge are working at the same time. The periphery materials of the hole is removed by the periphery cutting edges, while the bottom cutting edges remove the material at the bottom of the hole. An attempt to qualify the work done by a tool is introduced later in section 6.7.

An example of the consequences of these operations is shown in Figure 6.1 which shows the new cutter used in test series 10.4 and the state it reached after machining for 81 minutes. The main cutting edge (longitudinal direction) for the HSS tool has experienced abrasion mainly on the flank face and suffered flank wear. The tool flank wear was observed in both the front and periphery cutting edges. This is an expected outcome as reported by other researchers. For example, **Li et al. (2014)** observed that the abrasive wear was more dominant than any other wear mechanism on the flank face of the periphery cutting edge.



**Figure 6.1** End mill cutter: a) before and b & c) after tool wear experiment/ series 10.4



### 6.3 Tool Wear vs. Cutting Time

The information presented in Chapter 5 in Figures 5.12 to 5.22 can be used to consider the relationship between the tool wear with hole number. This is useful because the technician would know how many components (holes) can be made between changing the tool. However, that is of limited use in real life, since the tools in industry will not be used on a single task or to always make the same component. They will be utilised in a variety of different operations possibly with different materials, cutting speeds, cutting depths and feed rates. To support the further assessment of the nature and level of tool wear the flank wear of all test runs was calculated for each test and the time taken for each hole was calculated. This allowed the generation of tool wear versus cutting time data.

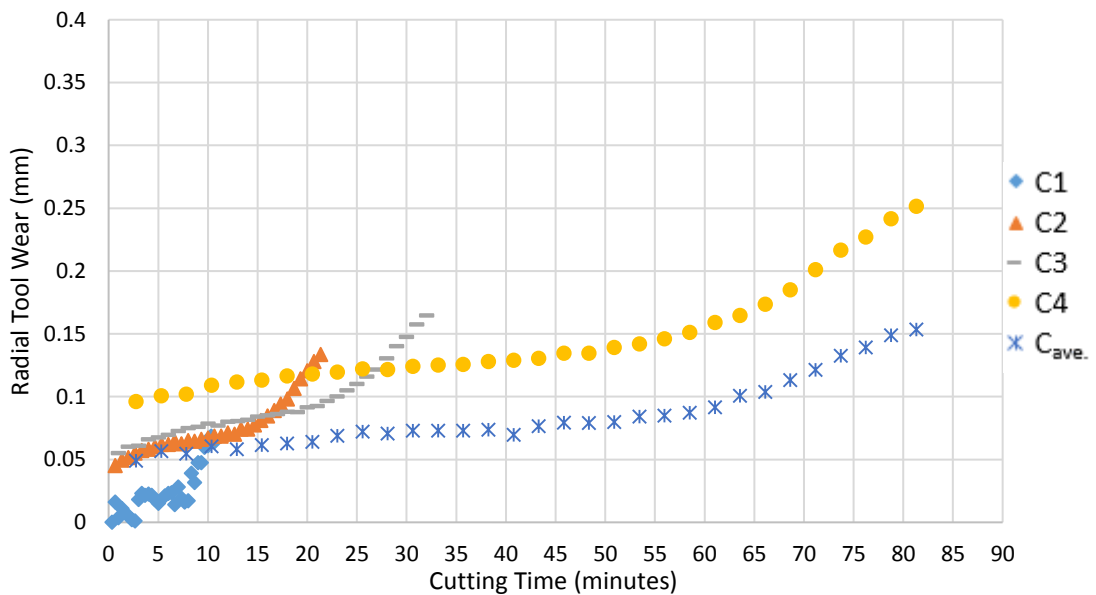


Figure 6.2 Tool wear as a function of Cutting Time / Series 10.4

Cutting time is one of the main factors that is used in order to evaluate the level and rate of tool wear in machining operations. To produce the data as shown in Figure 6.2, a

number of equations (4.2 - 4.4) were used to calculate the cutting times for C4. The nature of these calculations was discussed in section 4.5.1. It important to note that the cutting times for C1, C2, and C3 refer to the contact of the cutter with the circular (inner) surface of the cylindrical hole in loop 2 ( ), not the actual cutting time. This was calculated by using equation 4.4 (Creese 1999). As previously outlined in section 5.2.2, C4 is the most worn section and is the best guide for tool wear estimation. Thus, only C4 and  $C_{ave}$  will be considered in full. Figure 6.3 summarises the cutting time for each segment of all series and more clearly illustrates the nature of the cutting times arising.

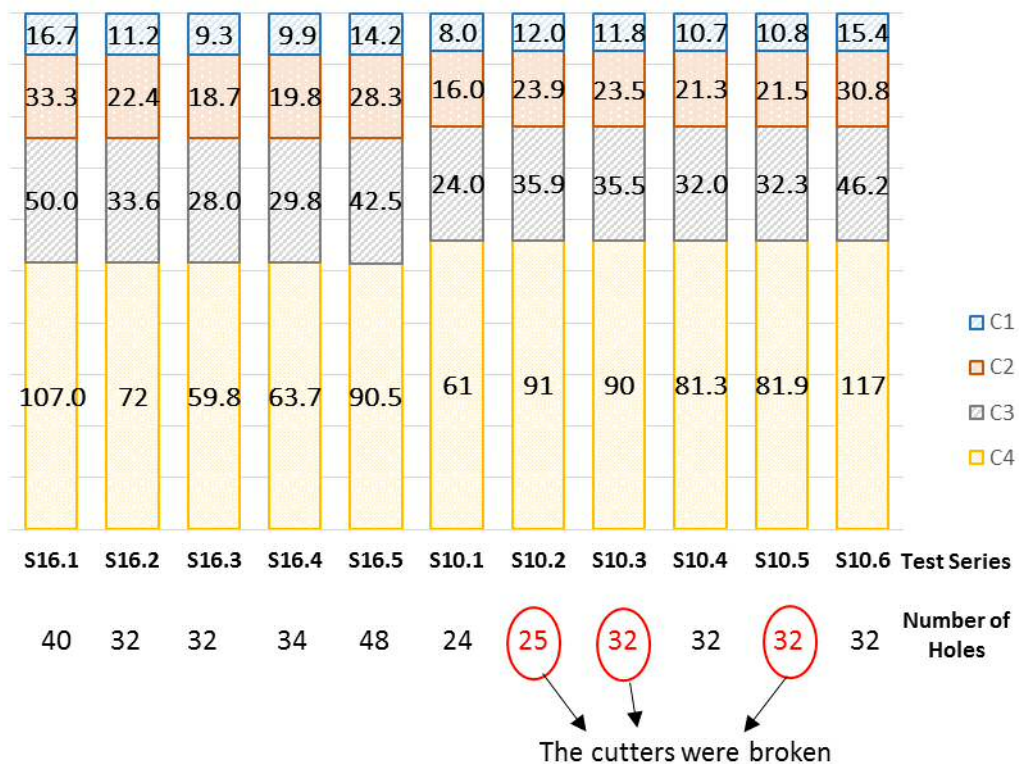


Figure 6.3 The calculated cutting time for each section of all series (minutes)

Similar processing provided the tool wear plots for all of the test series. There are shown in Figures 6.4 to 6.8 for series 16.1 -16.5 and Figures 6.9 - 6.13 for series 10.1-10.3, 10.5 -10.6.

Consideration of the estimated cutting times can explain the behaviour depicted in Figure 6.2. The bottom of the cutter (C4) worked longer than the upper regions and removed more metal as will be discussed later. Therefore, the cutting time for C4 is the main parameter used in this initial analysis to predict the remaining useful life.

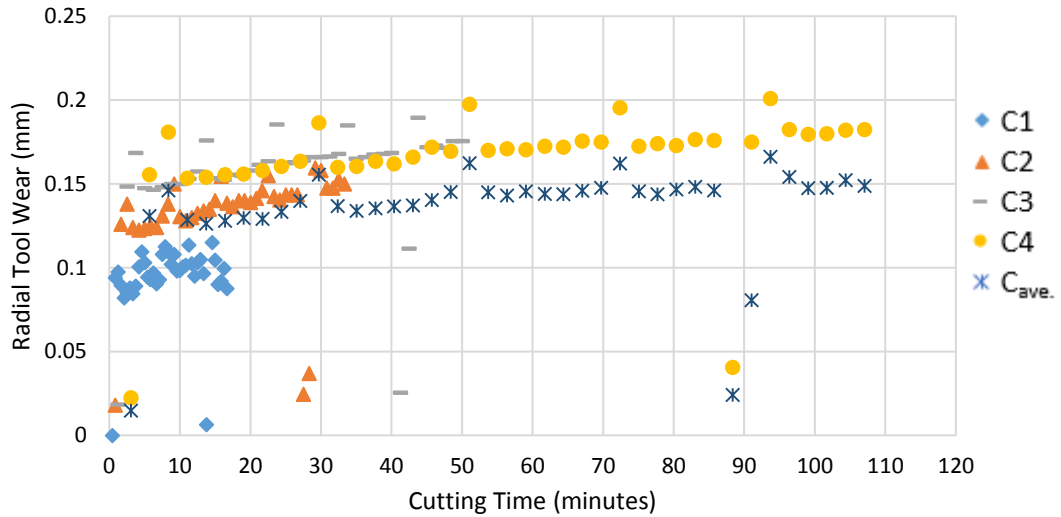


Figure 6.4 Tool wear as a function of Cutting Time / Series 16.1

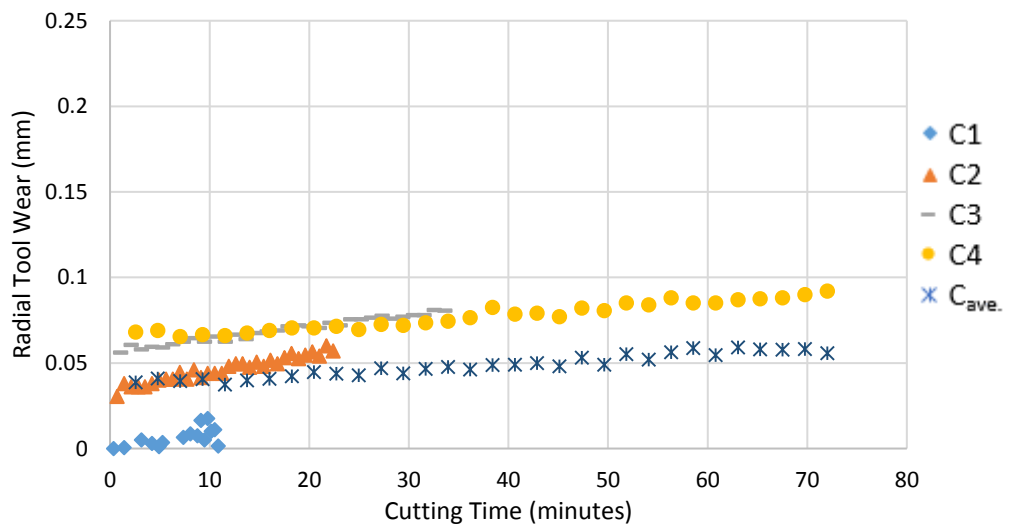


Figure 6.5 Tool wear as a function of Cutting Time / Series 16.2

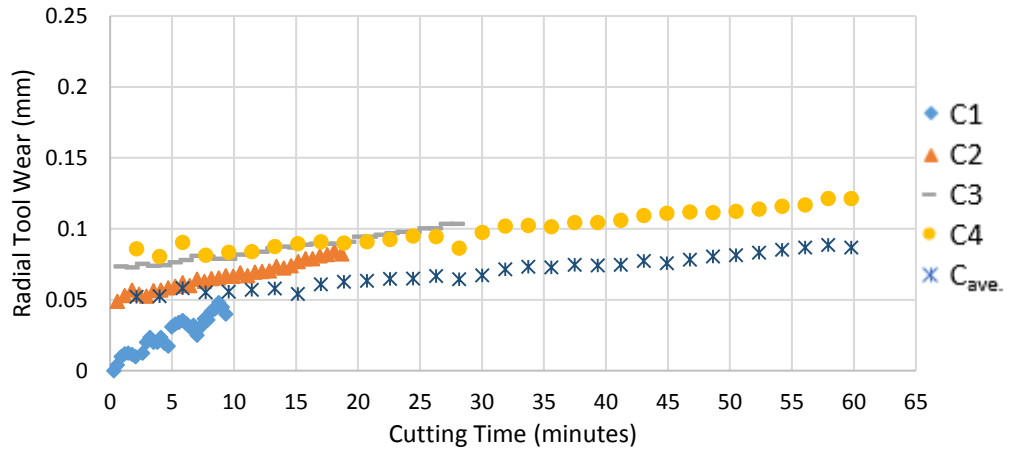


Figure 6.6 Tool wear as a function of Cutting Time / Series 16.3

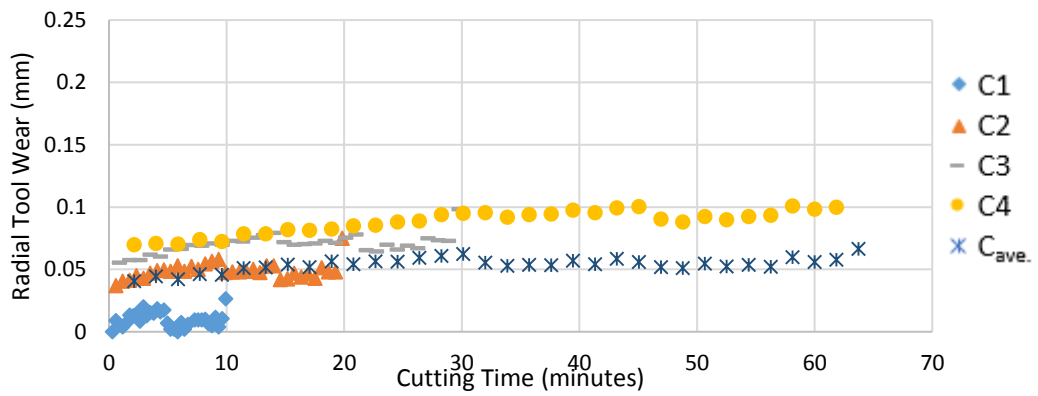


Figure 6.7 Tool wear as a function of Cutting Time / Series 16.4

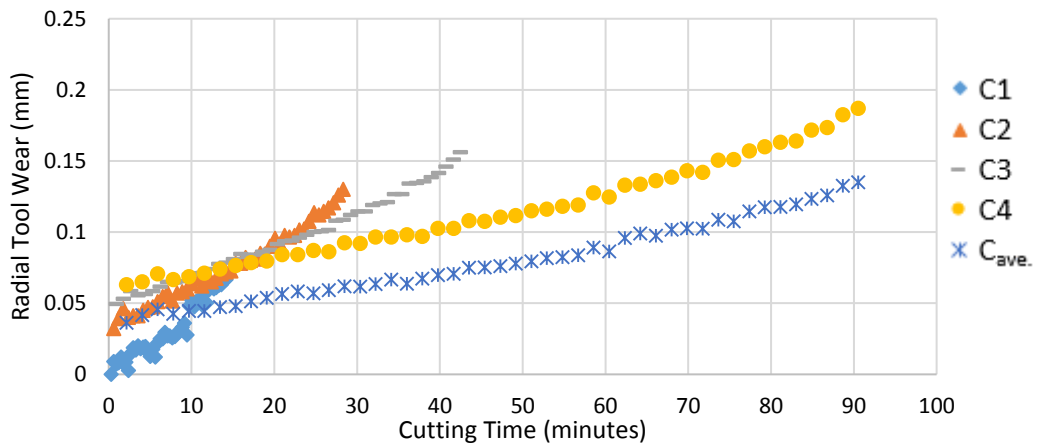


Figure 6.8 Tool wear as a function of Cutting Time / Series 16.5

The results for test series 16.1 to 16.5 indicate that tool wear does not approach the 0.3 mm limit. The decision was therefore made to use the smaller 10 mm cutter.

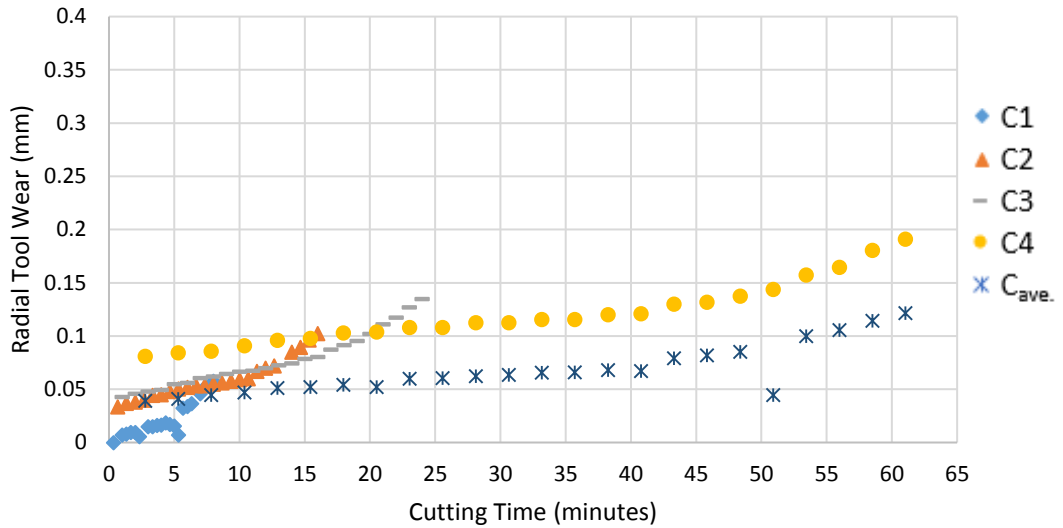


Figure 6.9 Tool wear as a function of Cutting Time / Series 10.1

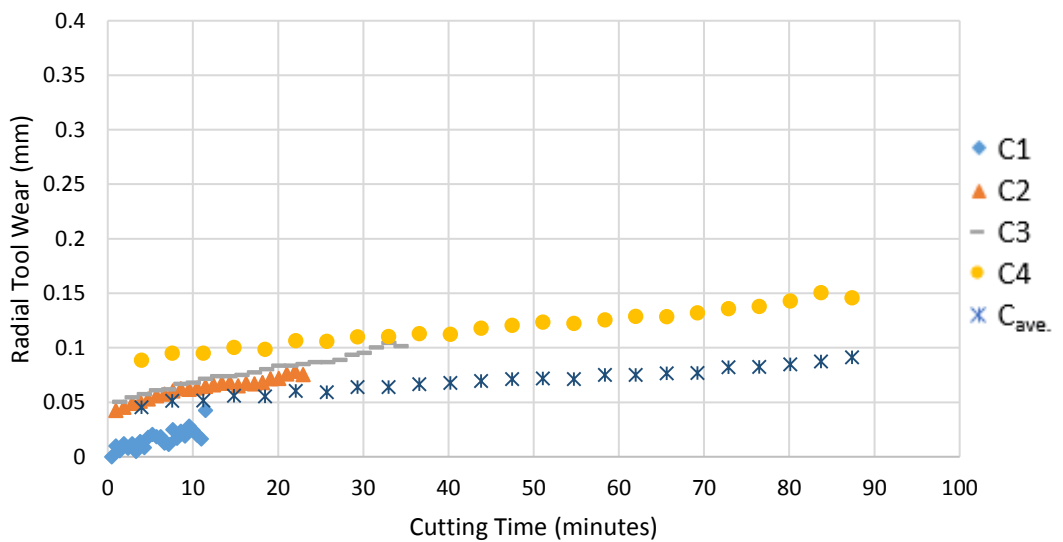


Figure 6.10 Tool wear as a function of Cutting Time / Series 10.2

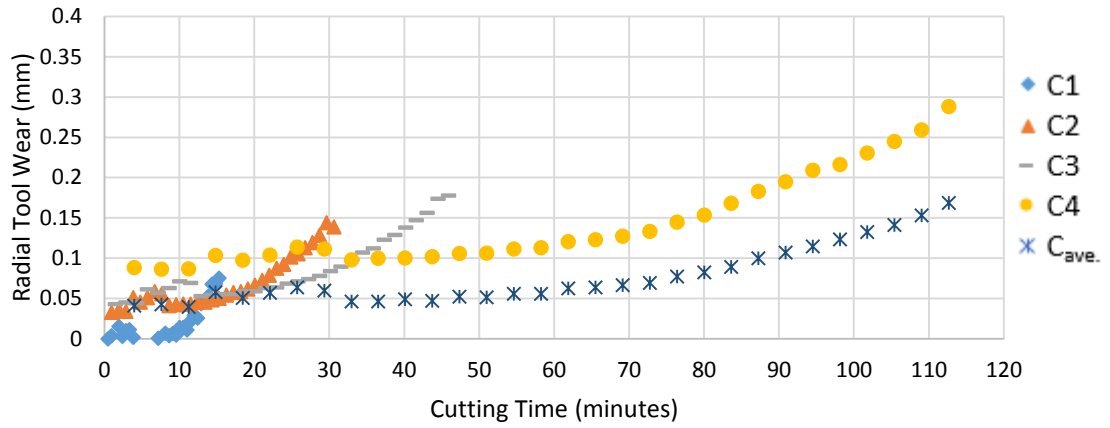


Figure 6.11 Tool wear as a function of Cutting Time / Series 10.3

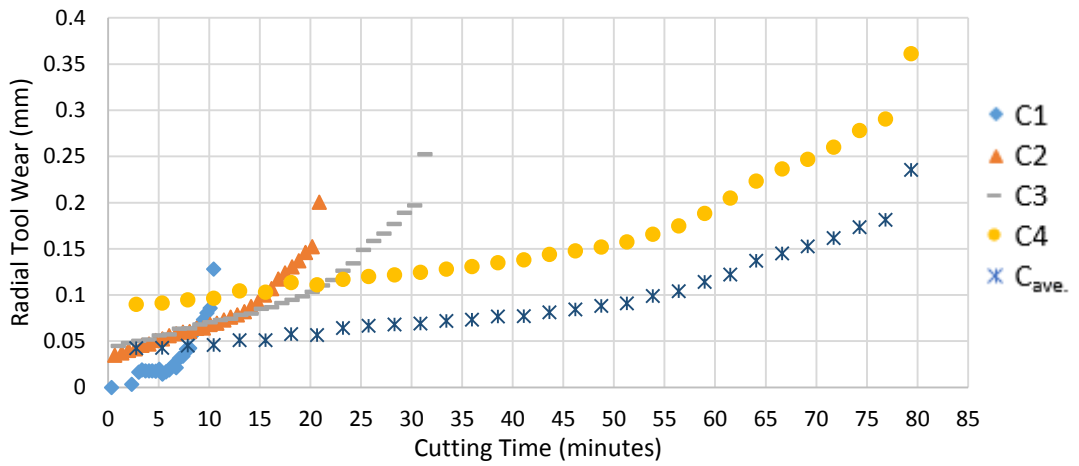


Figure 6.12 Tool wear as a function of Cutting Time / Series 10.5

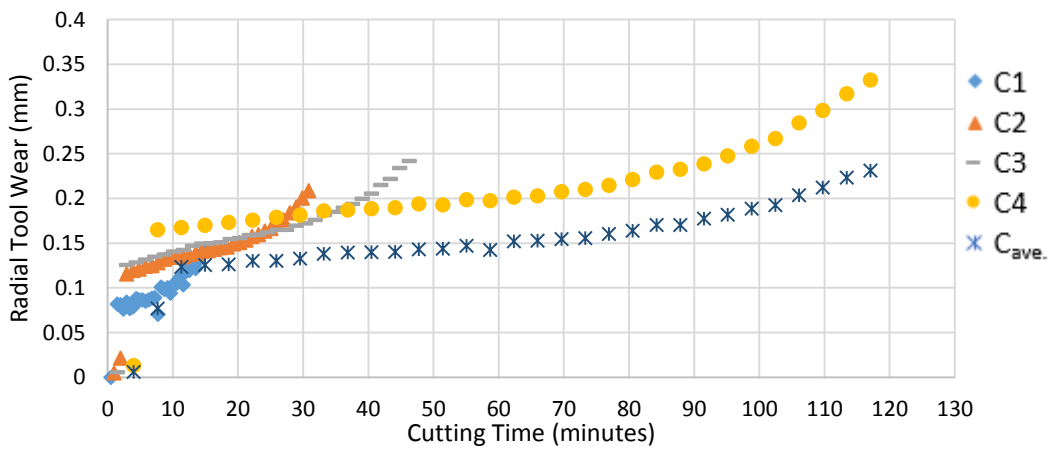


Figure 6.13 Tool wear as a function of Cutting Time / Series 10.6

## 6.4 The Estimation of Remaining Useful Life

Using the data for  $C_4$  and  $C_{ave}$  from the experimental results from series 10.4. Figure 6.14 can be drawn; it is then possible to consider how this can be used to predict tool life. In Figure 6.14, anticipated tool life was extrapolated for the  $C_4$  and  $C_{ave}$  tool wear curves acquired using a third order polynomial regression trend lines (plotted in Figure 6.14). This approach was intended to explore the potential variation in indicated tool life by estimated the cutting time at which tool wear trend line intersects with the maximum advisable 0.3mm limit. This was discussed in section 3.2 and the identification of the anticipated wear reaching this level has been enacted as shown in the Figure 6.14. From this analysis, it was determined that the bottom section,  $C_4$ , will reach the end of tool life criteria after 86 minutes of work. While based on the average tool wear  $C_{ave}$ , the cutter will reach this point after 103 minutes of cutting.

The effect of basing anticipated remaining useful tool life on the measurement of tool wear is clearly important. Based on the difference between the trendline intersection of these two tool wear curves with the tool life criteria in the y-axis in Figure 6.14, taking the last test as a basis, the assessment of remaining useful life for the average tool wear  $C_{ave}$  would indicate a value of 20 minutes. Applying a tool management strategy on this basis would mean, in this instance, the section of tool performing most of the cutting, section  $C_4$ , would be at risk of failing once the cutting time passes 5 minutes. This is clearly not a viable position as it could result in tool breakage. At the other extreme, the remaining useful life of the lightly used sections of cutter would be more than allowed for by using the average value. This is less important as it is not possible to make use of this section of the tool and no tool failures would result.

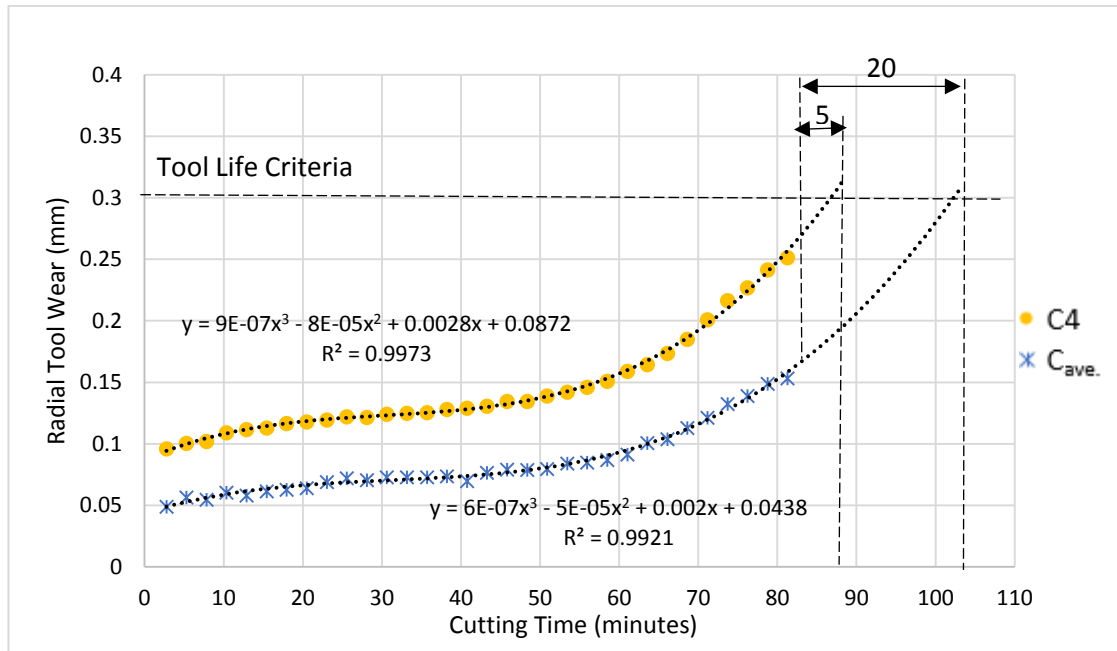


Figure 6.14 Calculate Remaining Useful Life/ series 10.4

Table 6.1 summarises the remaining useful life values of C4 and  $C_{ave}$  for the other 10 mm cutter test series, representing the data provided in Figures 6.9 to 6.13. It shows there is a potential exists for error in assessing the remaining useful life when using the average value as a reference measure. In this table, the negative values mean that the cutter was over the advisable limited without being broken.

Table 6.1 The amount of Remaining Useful Life occurring in different sections of the 10mm cutter

Series Number	Remaining Useful Life (minutes)	
	C4	$C_{ave}$
Series 10.1	14	22
Series 10.2	64	79
Series 10.3	-2	16
Series 10.5	-4	4
Series 10.6	-7	11

Figure 6.14 can also be used to confirm the potential for errors in component machining due to differential tool wear. The difference between the level of tool wear is obvious



and depending upon which curve/ parameter is used the tool wear related compensation will vary. To illustrate this consider the effect at the final measure point.  $C_{ave.}$  would suggest a wear value of 0.15mm, whereas C4 would provide a value of 0.25mm.

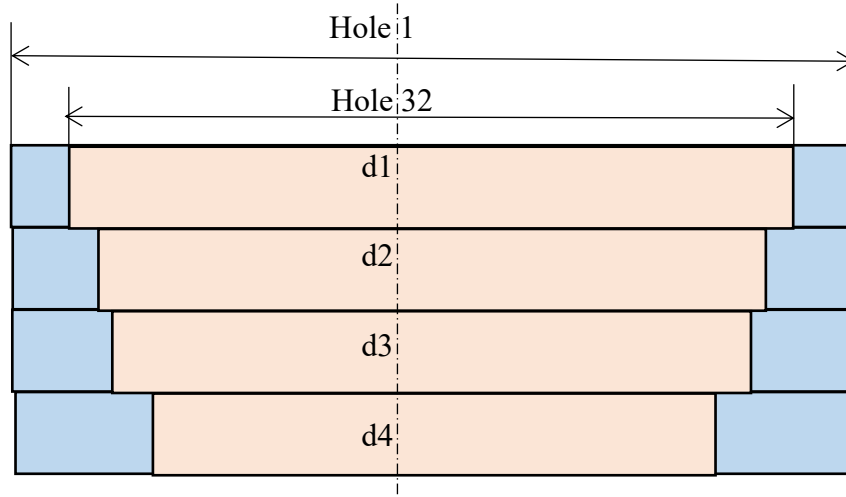
According to the results in Tables 5.1 and 5.2, C1 would suggest the lowest values of the tool wear. Whereas, C4 provides the highest amounts of the tool wear. Based on the difference between these values and using the uneven wear cutter, the geometric form of a component machined will be less than the optimal and incorrect assessment of the degree of tool life made, and needs careful consideration from the technician.

As previously discussed, the results point out the differential wear in the cutter happened, which in turn effects on the dimension components accuracy. In all series, for example series 10.6, when the bottom of the cutter C4 was taken as a reference to reset the tool offset and machine the hole, the component dimensions d1, d2, and d3 will be oversize and getting more significant than the required measurements all the times. It will be equal to 40.38, 40.25, and 40.18 mm, respectively, instead of 40 mm. However, the case is reversed when taken C1 as a reference. d2, d3, and d4 will be undersized and smaller than the required dimensions all the times and it will get worst till the tool breaks. It will be equal to 39.87, 39.8, and 39.62 mm, respectively. Used C2, C3, or even  $C_{ave.}$  as a reference measure points will make d1 oversize and d2, d3, and d4 undersized. Table 6.2 illustrates if the tool diameter was measured at any of these points (C1, C2, C3, C4, and  $C_{ave.}$ ) and made the component, the geometry will be different based upon which one have to use as the tool diameter.

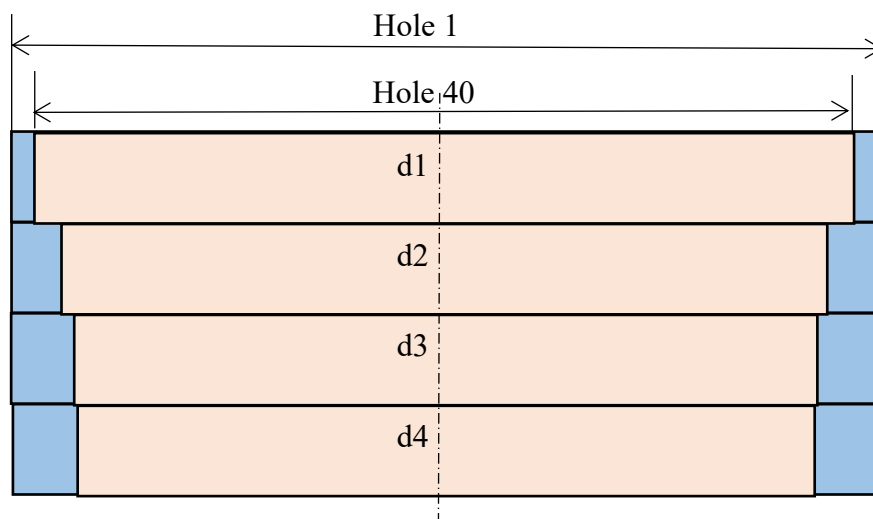
**Table 6.2 The effect of differential tool wear on the component geometry quantitatively**

The component diameter (mm)	The measured point				
	C1	C2	C3	C4	$C_{ave.}$
d1	40	40.13	40.2	40.38	39.94
d2	39.87	40	40.07	40.25	39.81
d3	39.8	39.93	40	40.18	39.75
d4	39.62	39.75	39.82	40	39.56

Figures 6.15 and 6.16 show precisely the difference between the level of the tool wear for the 10mm and 16 mm cutters. The blue area refers to the hole 1, and the peach area refers to the last hole in the series. In both series, the difference between d1, d2, d3, and d4 in hole 1 was very small because the tool did not actually removes a lot of material. Whereas, the difference between d1, d2, d3, and d4 in hole 32 and 40 in Figures 6.15 and 6.16 was clearly evident.



**Figure 6.15 the change in the component dimensions/series 10.6**



**Figure 6.16 the change in the component dimensions /series 16.1**

Removing a small cut could be the main cause of accelerated tool wear in C1, C2, and C3 because the chip load per tooth was small. In this case, the cutter edge radius will be too large relative to the depth per tooth, thus, all the force goes to pushing the chip under the edge. Consequently, the tool rubs or burnish instead of shearing off a real chip. Alternatively, could be due to the cutting edge cuts the transient area that was formed during the previous tool pass. This means it removes the surface found between the surface to be machined and the machined surface through the cutting edges. This surface is stronger and harder than the original material due to the change of the local condition of the material due to the work hardening.

In the large cutters series, the absence of an increase in gradient towards the end of the results is evidence that the tool has not yet reached the rapid tool wear third phase. Therefore, using both  $C_4$  and  $C_{ave}$ , the remaining useful cannot be estimated with any real confidence. For example remaining remaining useful life that extrapolated from Figure 6.6 indicates a value of 110 minutes for  $C_4$  and 200 minutes for  $C_{ave}$ .

In taking this research forward, it is evident that these trend line may support an important aspect of technical analysis in providing an indication of remaining tool life. They may be considered as being a source of valid support since this indicate the general tendency of the curve. However, when the steepness of a trend line increases, the validity of the support level decreases and this is what happened in the top segment of the cutter C1 in Figures 6.8 to 6.13.

The behaviour of a tool under a particular set of cutting conditions seems reproducible to a certain extent. However, the identification of a limit value for the tool life is continually subject to many variables that cause the cutter to fail prematurely or be underestimated. For example, in series 10.2, Figure 6.17, the cutter fails prematurely in the hole 25 before 90 minutes, whereas, in series 10.6, Figure 6.18, the cutter was still working although the value exceeds 0.3 mm at 110 minutes. This means that the tool might be used without a break over 0.3 mm under a very low feed or speed, or just continuously cut without interruption. Therefore, it is possible that the use of 0.3 mm as the tool life standard will avoid any tool break, but will not use all the tool life. As a

result, the tool life standards is more useable than Taylor's tool life equations based assessments, but 0.3 mm showed be used only as a guide in advance.

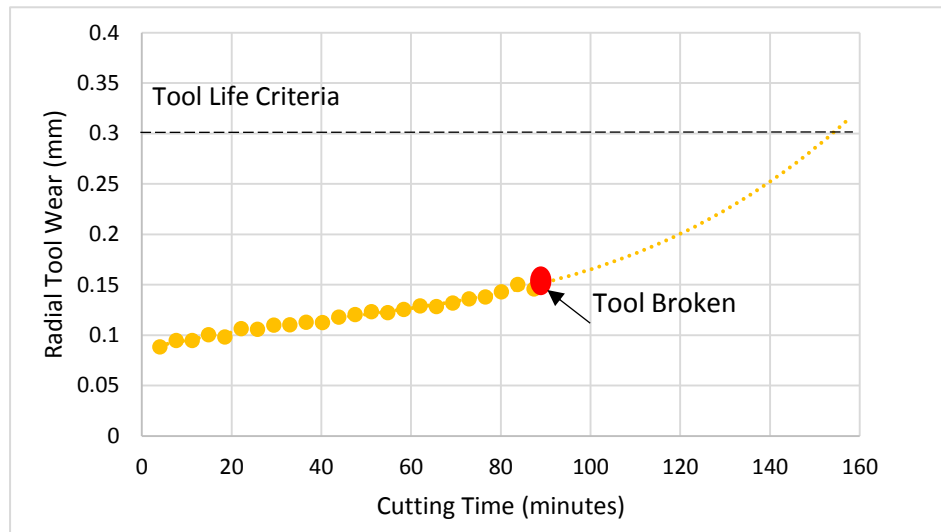


Figure 6.17 Tool wear vs. cutting time/series 10.2

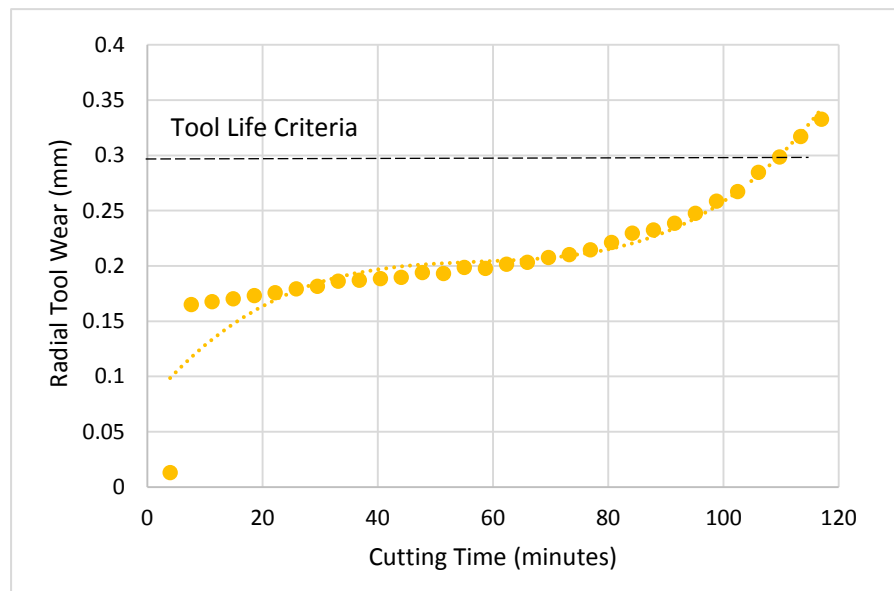


Figure 6.18 Tool wear vs. cutting time/ series 10.6

## 6.5 Detection of the Inflection Point of Tool Wear Curve

The nature of the tool life curve depicted in Figure 3.2 means that the transition point from the second to the third stage in the tool wear curve is very important. Clearly identifying when it arises can be used if some estimation of remaining tool life is to be considered. Four methods were used to detect the inflection point in this study; these methods will discuss below:

### 6.5.1 Substitution method

In this method, the tool wear curve was divided into two sections, Figures 6.19: the first indicates the steady-state wear region  $L_1$ , where the cutter wears very slowly and the second to the accelerated wear  $L_2$ , where the wear is rapid. Using a curve fitting procedure to find the equation of the two curves and calculate the intersection point for the two trendline curves identifies the transition following which the rate of tool wear will accelerate. For example, in Figure 6.17 (A) for series 10.4, the two section lines have the form  $Y=mX+b$ .  $L_1: y = 0.001x + 0.0951$  and  $L_2: y = 0.0052x - 0.1723$ . First, take any of the lines,  $L_1$  will take, then substitution  $L_2$  into  $L_1$ . The result will be:

$$0.0052x - 0.1723 = 0.001x + 0.0951 \quad (6.1)$$

Now this 1-variable linear equation have to be solved, and getting the x-coordinate of our intersection:

$$X=63.7$$

Thus the x-coordinate of our intersection is 63.7. To find the y-coordinate, any of the lines can be taken and set  $x$  to be 63.7 to get the corresponding  $y$  coordinate. The choice of the equation does not matter, though it is usually best to pick the easier equation. Let us choose  $L_1$  again:

$$y = 0.001x + 0.0951, y = 0.159$$

Therefore, the coordinates to which our lines intersect is (63.7, 0.159). The same procedure can be applied to calculate the inflection point in Figures 6.19 (B) and 6.19 (C). The results are as follows: (57.8, 0.145) for Figure 6.19 (B) and (54, 0.14) for Figure 6.19 (C). The previous results indicated that the transition point occurred in the 63<sup>rd</sup>, 57<sup>th</sup>, and 54<sup>th</sup> minutes when the tool wear is 0.159mm, 0.145mm and 0.14; this means after 54 minutes work the technician have to monitor what is going on with the tool and work carefully.

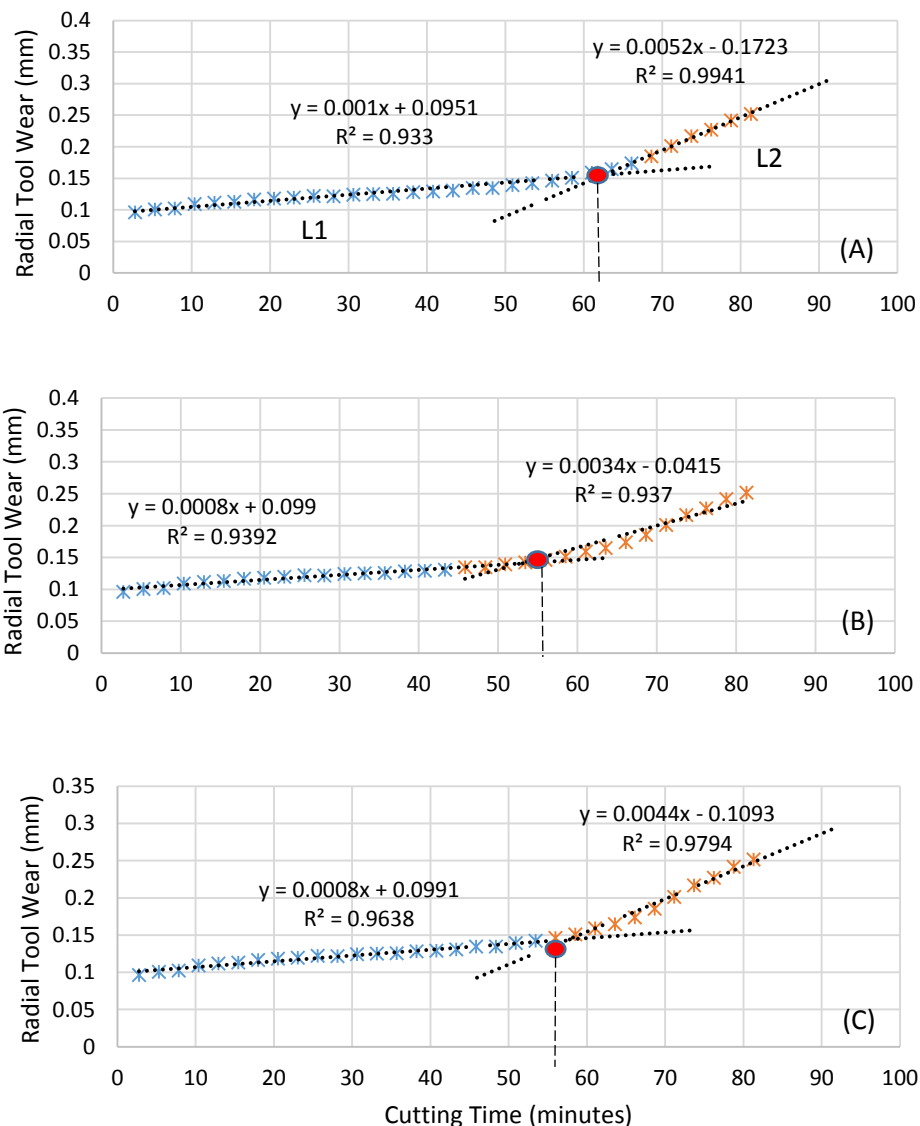


Figure 6.19 (A-C) Calculate the inflection point/ series 10.4

This technique can be applied to any cutting process; it is easy to understand that the machining process after that point needs to be performed knowing that the cutter is reaching the end of its life and is being used in a potentially dangerous condition. The main deficiency of this approach is that the number of points is selected randomly, without any rules.

### 6.5.2 The Rate of Change

Another method that can be used to detect the transition point is by taking the difference for every two points for the tool wear curve in y-axis and select the highest difference as the transition point as shown in Figure 6.20. In this Figure, the result shows that the transition point will be after 60 minutes from the beginning of the work.

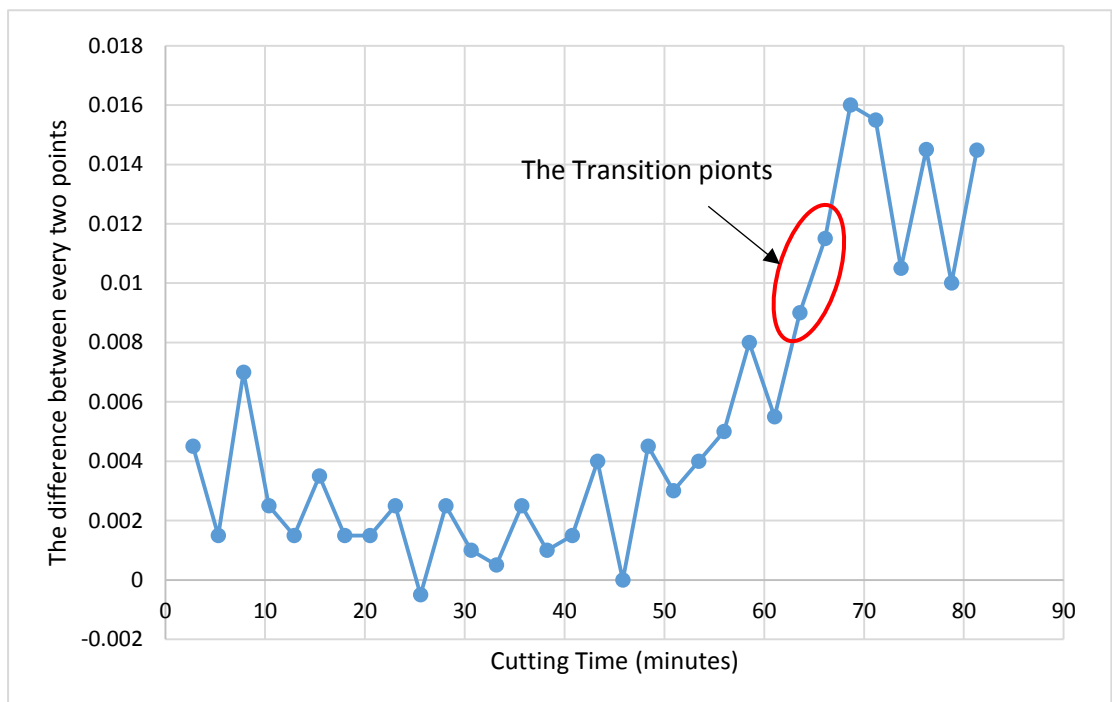
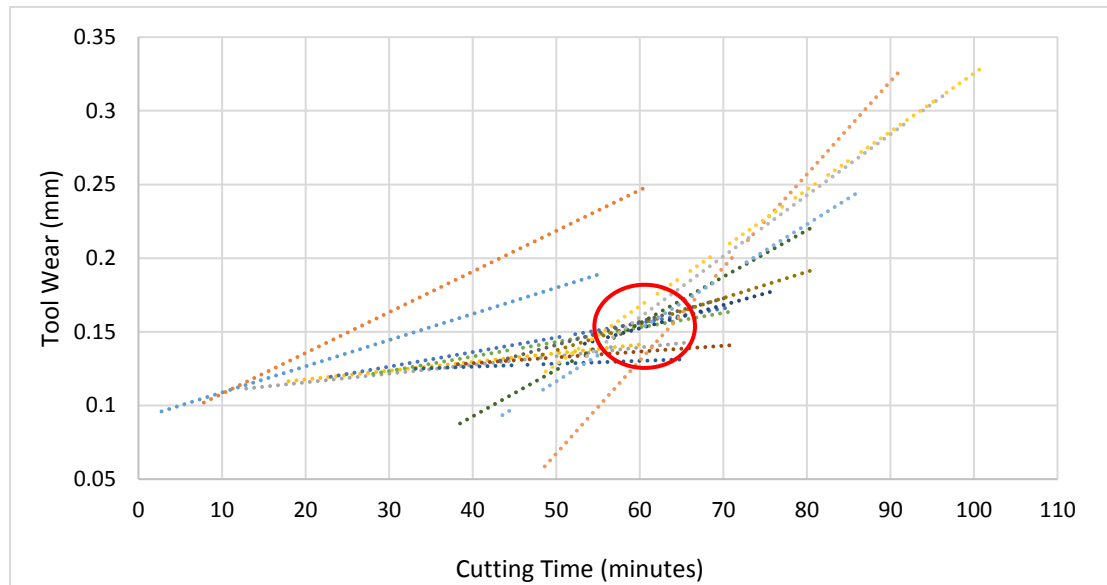


Figure 6.20 The rate of change / series 10.4

### 6.5.3 Multiple Linear Fit

The last method to detect the inflection point is by drawing the trend-line for every two points in tool wear curve. The most prominent intersection point is considered as the point of transition as explained in Figure 6.21. In this Figure, the result shows that the transition point is among 55 to 65 minutes.



**Figure 6.21** The multiple linear fit / series 10.4

The main deficient of the rate of changes and multiple linear fit approaches is it depends on a personal decision or vision. This could be introduced an error in detecting the transition point.

### 6.5.4 The “Solver” Function

Another method of determining the transition point was more refined because of the variability of the data is by using the so-called “Solver” function of the Excel programme (John et al. 2000). This is a mathematical function that considers progressively change between the cells to solve linear, nonlinear and integer problems.



“Solver” identifies a "Target cell" or "Objective cell" which is subject to a limited value. It also identifies "Change cells" or a "Decision function" which are used to find the optimal value for a "Target cell". To solve nonlinear optimisation problems, which is the case of the tool wear curve, the results show that a reliable measurement of the transition point could be estimated. This then represents the best fit to the experimental tool wear curve data, as shown in Figure 6.22.

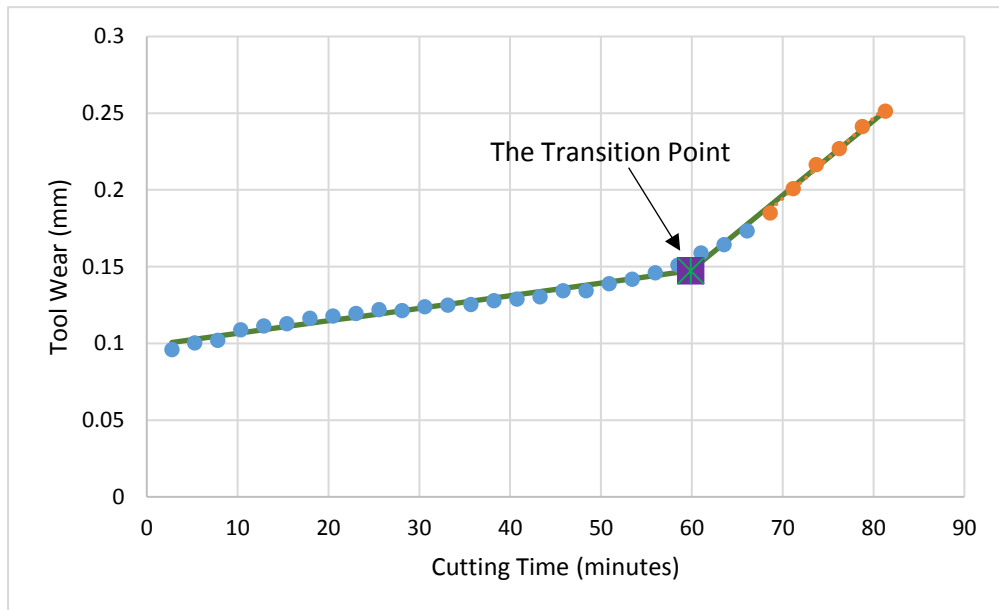


Figure 6.22 The transition point when using the Excel Solver/ series 10.4

## 6.6 Volume Removed by Each Section

Consideration of the cutting time can produce the analysis shown in Figure 6.3. The bottom of the cutter C4 works for longer and removes more metal than the upper regions. In addition, each of the four segments of the cutter removes a different amount of metal. The difference between the amounts of material each section removes was calculated based upon equations 4.5 through 4.8 and is shown in Figure 6.23 for 16 mm cutter diameter and Figure 6.24 for 10 mm cutter diameter.

In terms of cutting time versus the volume removed, Figures 6.23 and 6.24 prove the result of Figure 6.3, which is that the bottom of the cutter removes more than 99% from

all of metal and equivalent to the working cutting time. This can be consider as the effective cutting time. However, the percentage of volume removed by sections C1, C2, and C3 is not compatible with the corresponding cutting time. The same amount of the metal has been removed by segments C1, and C2 in Figures 6.23 and 6.24 during different cutting time in Figure 6.3, which means the cutting times for the upper sections of the tool (C1, C2, and C3) are misleading and they do not refer to the effective cutting time.

It is possible to measure the metal removed in C1, C2, and C3 but, because they are undertaken concurrently, it is not possible to separate the work done during cutting for each of these. Therefore, focusing on monitoring the behaviour of the bottom C4 of the tool is important since it has impact on estimation the remaining useful tool life.

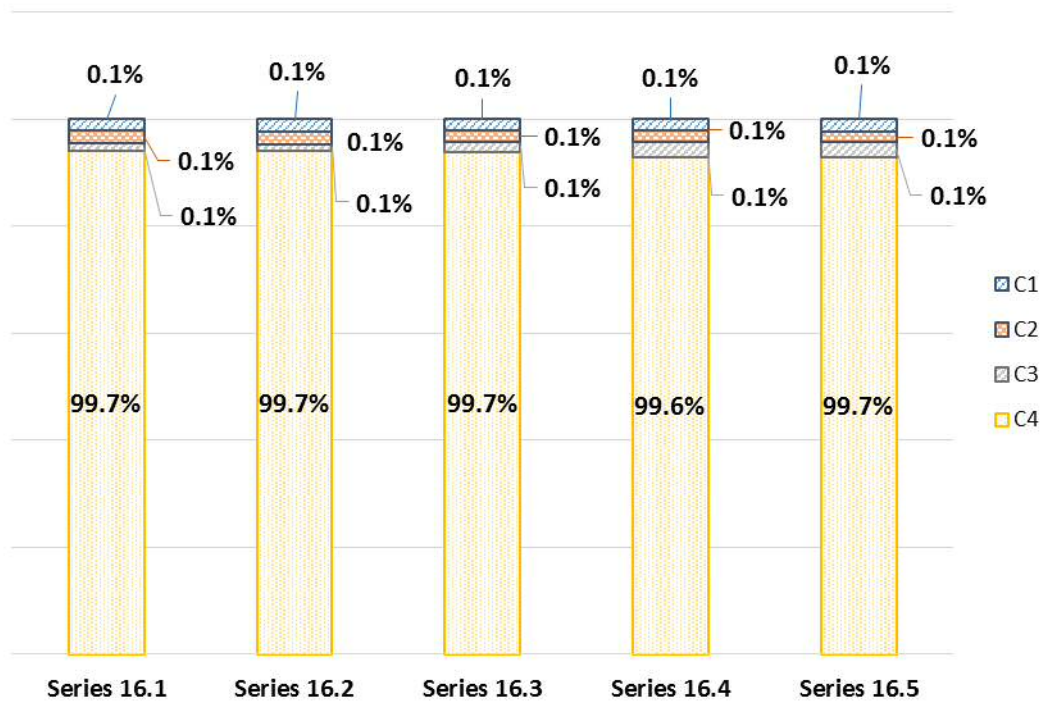


Figure 6.23 Percentage of total Volume Removed by Each Segment for 16mm cutter

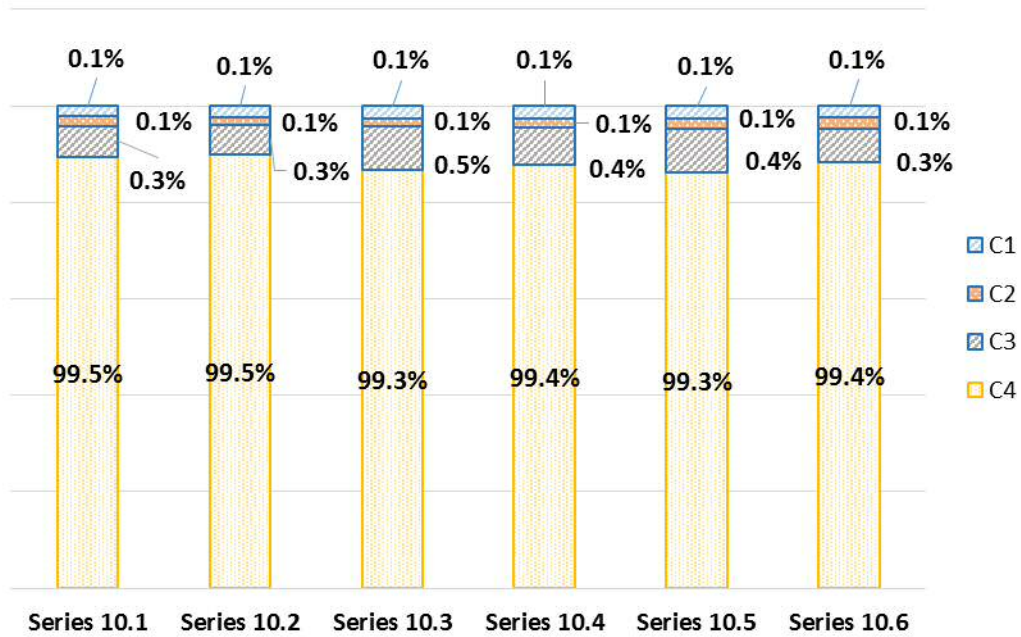


Figure 6.24 Percentage of total Volume Removed by Each Segment for 10mm cutter

## 6.7 The Tool Wear in the Bottom cutting edges

The effect of reduction in the depth of holes can also be used to calculate the level of the tool wear in the bottom cutting edges. The values of the tool wear were calculated based upon the measured depth of hole. The comparison between the depths of any measured hole with the reference hole (H1) when the tool wear is equal zero provided a measure of the front tool wear. Figure 6.25 presents the results for test series 16.1. Figure 6.26 present the results for test sreies 10.1.

The results show how the tool wear in the bottom cutting edges varies with the hole number however, it is inconclusive. The problem with assessing the depth of hole as well as tool wear in bottom cutting edges is it relies on the transfer of the reference point P0 in Figure 4.2. After finish the set 1, the slot was machined firstly in the next set and assumed the length of the slot P0 in set 2 relative to the tool as the length of the slot P0 in set 1. Therefore, it is difficult to transfer reference for one set to another. In addition,

the way of measure the basis of the hole may affect the results where it was measured in three places and it is not good enough to evaluate the depth of the hole as well as the wear in the front edges.

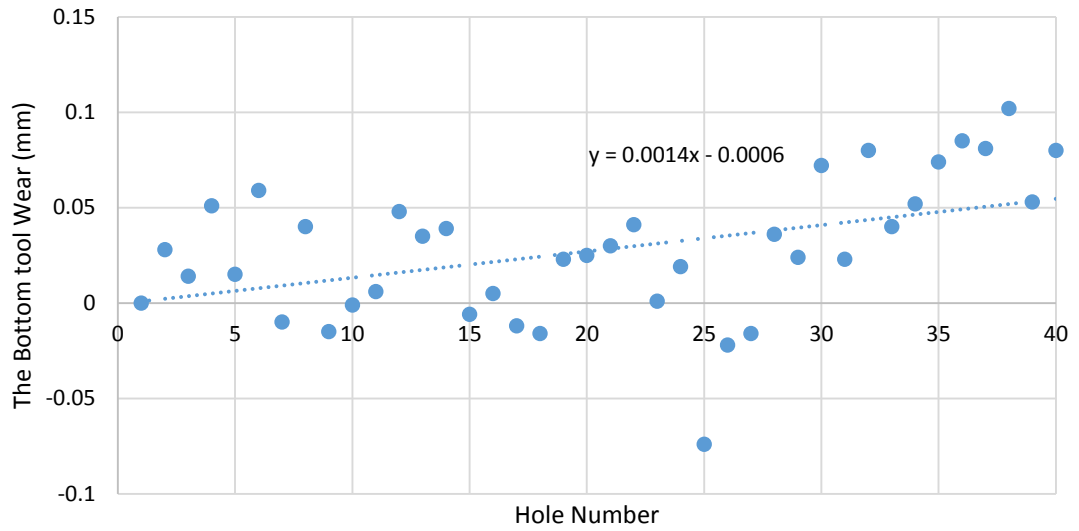


Figure 6.25 Wear in the bottom cutting edges/ series 16.1

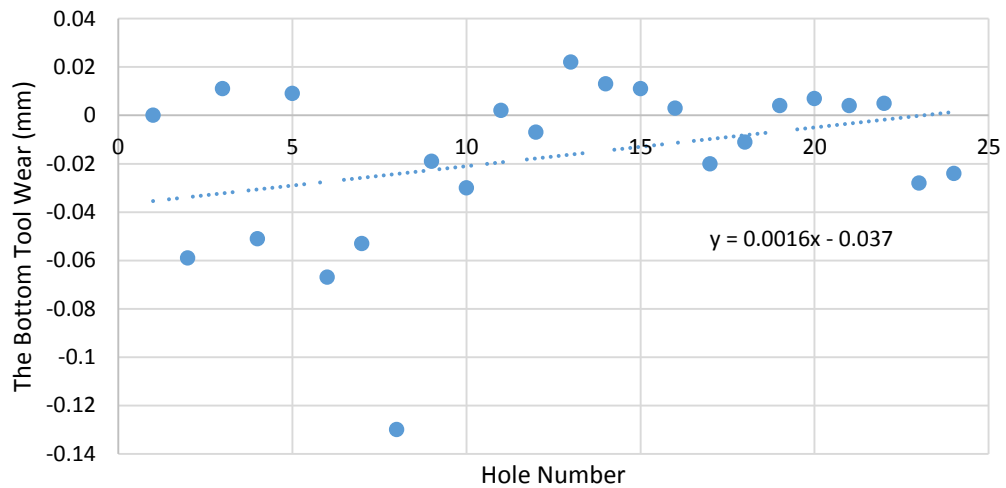


Figure 6.26 wear in the bottom cutting edges/ series 10.1

## 6.8 The Results of Metal Removal Rate

Some experiments were held to the effect of the tool wear in MRR to be studied. To mill a 40 mm diameter cylinder, by a 16 and 10 mm diameter cutter in end milling process, a number of cycles have been used. These cycles are explained in Figure 4.5 (a-e). It is difficult to assess the MRR since the metal removed from the workpiece changes with the tool wear that result in changes in tool geometry.

In this study, MRR has been calculated through the five cycles shown in Figure 4.5 (a-e) in two ways. Firstly, based on the volume and cutting time by using equation (3.6), the value calculated in this way is called  $MRR_1$ .

Secondly, based on the cutting parameters included feed rate, radial and axial depth of cut by using equations (3.7 and 3.8), the value calculated is called  $MRR_2$ . **Appendix D** shows the sample of how the feed rate, cutting time, and the volume of metal removed for each cycle for 10mm and 16 mm cutters were calculated.

Table 6.3 and 6.4 summarise the spindle speed (N), feed rate (f), cutting time (t), the volume of metal removed (V), and metal removal rate for all series refer to the Table 4.4.

**Table 6.3 The spindle speed, feed rate, cutting time, the area and the volume of metal removed for 16 mm cutter**

Series No.	Parameters	Cycle 1	Cycle 2	Cycle 3	Cycle 4	Slot
	(mm <sup>3</sup> )	1005	895	668	3714	
Series 16.1	N (r.p.s)	11.95				
	(mm/sec)	1.195	2.39	2.99	2.99	2.39
	(sec.)	4	8	3	25	22
	(mm)	/	9.5	16	9.7	
	(mm)	/	5	5	5	
	(mm <sup>3</sup> /sec)	251.3	111.9	222.7	148.6	
	(mm <sup>3</sup> /sec)	241	113.5	239	145	
Series 16.2	N (r.p.s)	14.3				
	(mm/sec)	1.43	2.86	3.58	3.58	2.86
	(sec.)	3.5	6.6	2.5	21	18.5
	(mm)	/	9.5	16	9.7	

	(mm)	/	5	5	5	
	(mm <sup>3</sup> /sec)	287.1	135.6	267.2	176.9	
	(mm <sup>3</sup> /sec)	287.5	135.58	286	173.6	
Series 16.3	N (r.p.s)	17.25				
	(mm/sec)	1.725	3.45	4.3	4.3	3.45
	(sec.)	3	5.5	2	17.5	15.4
	(mm)	/	9.5	16	9.7	
	(mm)	/	5	5	5	
	(mm <sup>3</sup> /sec)	335.0	162.7	334.0	212.2	
	(mm <sup>3</sup> /sec)	346.8	163.9	344	208.6	
Series 16.4	N (r.p.s)	17.25				
	(mm/sec)	1.725	3.45	4.3	4.3	3.45
	(sec.)	3	5.5	2	17.5	15.4
	(mm)	/	9.5	16	9.7	
	(mm)	/	5	5	5	
	(mm <sup>3</sup> /sec)	335.0	162.7	334.0	212.2	
	(mm <sup>3</sup> /sec)	346.8	163.9	344	208.6	
Series 16.5	N (r.p.s)	17.1				
	(mm/sec)	1.71	3.42	4.28	4.28	3.42
	(sec.)	2.9	5.5	2.11	17.7	15.6
	(mm)	/	9.5	16	9.7	
	(mm)	/	5	5	5	
	(mm <sup>3</sup> /sec)	346.6	162.7	316.6	209.8	
	(mm <sup>3</sup> /sec)	343.8	162.5	342	207.6	

**Table 6.4 The spindle speed, feed rate, cutting time, the area and the volume of metal removed for 10 mm cutter**

Series No.	Parameters	Cycle 1	Cycle 2	Cycle 3	Cycle 4	Cycle 5	Slot
	(mm <sup>3</sup> )	392.7	350	1519.3	365	3655	
Series 10.1	N (r.p.s)	27.6					
	(mm/sec)	1.88	3.75	3.75	4.69	4.69	3.75
	(sec.)	2.7	1.9	11.7	1.7	20	13.85
	(mm)	/	10	7	10	7.68	
	(mm)	/	5	5	5	5	
	(mm <sup>3</sup> /sec)	145.4	184.2	129.9	214.7	182.8	
	(mm <sup>3</sup> /sec)	147.7	187.5	131	234.5	180.1	
	N (r.p.s)	19.3					
	(mm/sec)	1.3	2.6	2.6	3.28	3.28	2.6

Series 10.2	(sec.)	3.8	2.7	16.8	2.4	28.7	19.8
	(mm)	/	10	7	10	7.68	
	(mm)	/	5	5	5	5	
	(mm <sup>3</sup> /sec)	103.3	129.6	90.4	152.1	127	
	(mm <sup>3</sup> /sec)	102	130	91	164	126	
Series 10.3	N (r.p.s)	19.3 and 27.6					
	(mm/sec)	1.88	3.75	3.75	4.69	4.69	3.75
	(sec.)	2.7	1.9	11.7	1.7	20	13.85
	(mm)	/	10	7	10	7.68	
	(mm)	/	5	5	5	5	
	(mm <sup>3</sup> /sec)	145.4	184.2	129.9	214.7	182.8	
	(mm <sup>3</sup> /sec)	147.7	187.5	131.3	234.5	180.1	
Series 10.4	N (r.p.s)	27.6					
	(mm/sec)	1.88	3.75	3.75	4.69	4.69	3.75
	(sec.)	2.7	1.9	11.7	1.7	20	13.8
	(mm)	/	10	7	10	7.68	
	(mm)	/	5	5	5	5	
	(mm <sup>3</sup> /sec)	145.4	184.2	129.9	214.7	182.8	
	(mm <sup>3</sup> /sec)	147.7	187.5	131.3	234.5	180.1	
Series 10.5	N (r.p.s)	27.4					
	(mm/sec)	1.86	3.7	3.7	4.66	4.66	3.7
	(sec.)	2.7	1.9	11.8	1.7	20.2	13.96
	(mm)	/	10	7	10	7.68	
	(mm)	/	5	5	5	5	
	(mm <sup>3</sup> /sec)	145.4	184.2	128.8	214.7	180.9	
	(mm <sup>3</sup> /sec)	146.1	185	129	233	178.9	
Series 10.6	N (r.p.s)	19.2					
	(mm/sec)	1.3	2.6	2.6	3.26	3.26	2.6
	(sec.)	3.8	2.7	16.8	2.45	28.87	19.9
	(mm)	/	10	7	10	7.68	
	(mm)	/	5	5	5	5	
	(mm <sup>3</sup> /sec)	103.3	129.6	90.4	149.0	126.6	
	(mm <sup>3</sup> /sec)	102	130	91	164	126	

The results in Figures 6.27 and 6.28 show there are difference between and in each cycle for one cylinder, this is may be due to the nature of the used equation. For example, equation (3.6) neglects important changes in cutting operations, such as feed rate. Alternatively, due to the machine did the mission with slightly different path that is not possible to predict. In real life, the MAZAK machine has an intelligent control element; it will adapt the tool path and reduce the cutter load that makes the tool blunt. As a result, the cycle time will change too. For example, the tool path for 10mm cutter in cycle 2 and 4, does not go across and stop and get around, it was going across and accelerate into the next circular cut.

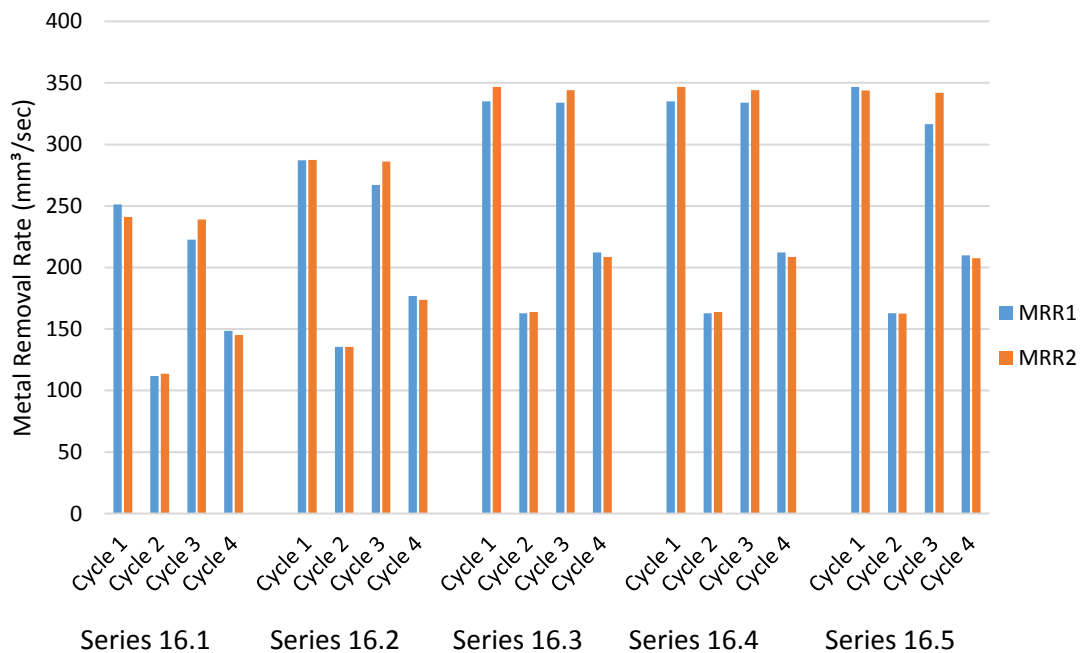
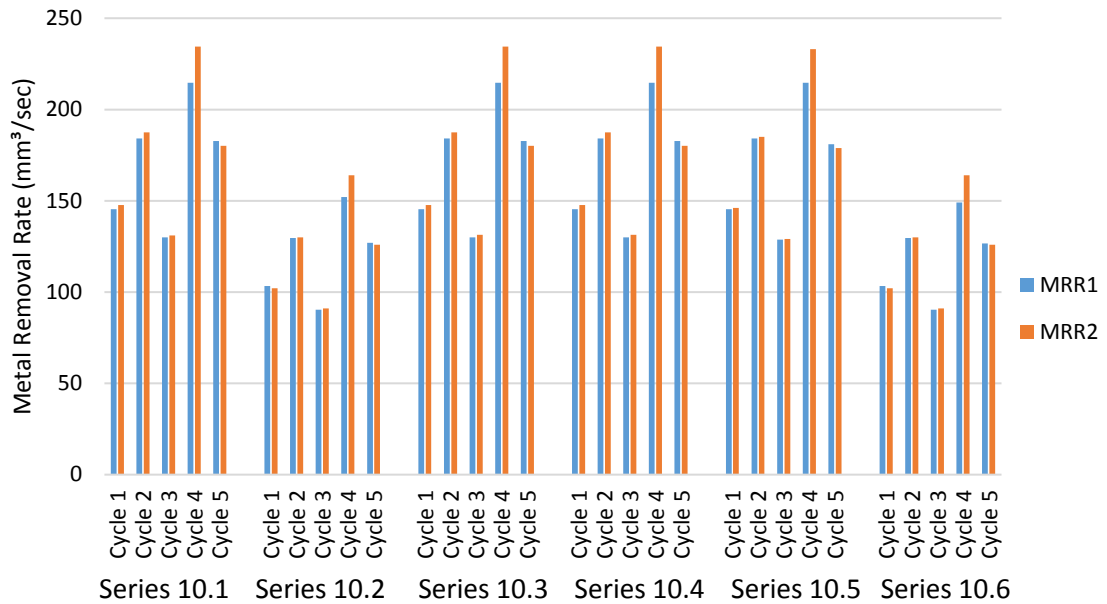


Figure 6.27 Metal Removal Rate for 16 mm cutter





**Figure 6.28 Metal Removal Rate for 10 mm cutter**

Two main points can be concluded in this section, the first point is there is an indication that the change in MRR has an effect on the tool life. In Table 6.4, two different MRR were used in series 10.3, which leads to decrease the tool life. In series 10.2 and 10.6 the MRR was less than that used in series 10.1, 10.4, and 10.5. Although the tool was broken in series 10.2, it was not broken due to MRR. The tool breakage is not just associated with tool life, it can occur at any time. Sometime the brand new tool breaks by hitting something in the workpiece, so that can happen any time. MRR is only the link that shows how hard the tool is working and that can be used as the indicator.

The second point is the volume of metal removed per set time is not a suitable way to predict tool wear since it can get the same MRR with various cutting parameters. For example, if the cutting speed is very quick and the feed is slow or cutting speed is very slow and feed is quick. These two cases have the same MRR but the others thought the second case is better than the first case, however, as indicated previously, removing small metal has an effect on the tool wear. Moreover, it can be seen that depth of cut is the primary parameter, which affects MRR, and thus, doubling the DOC means doubling MRR, as well as the amount of the tool flute length used, but not duplicating the tool wear quantity.

## 6.9 Summary

The results agree with the literature review and ISO recommendation that the flank wear is the dominant wear mechanism in milling carbon steel. It concludes that the wear rate for the small cutter is higher than for large cutter due to the lower feed per tooth values were used. The cutting time for each segment was calculated. The results indicated that the bottom of the cutter (C4) was work longer and removes most of the metal than the other segments.

Remaining useful life was calculated for C4 and  $C_{ave}$ . The results show that using  $C_{ave}$  as the input into the tool life leads to incorrect assessment remaining useful life. In addition, the geometric form of the component will be less than the optimal.

On the arithmetic scale, different trend lines could be acquired for each state. Therefore, the tool life criteria that extrapolation from the linear section of tool wear-time curves will be changed too over an extended period with a change of tool geometry.

Using extrapolation tool wear curve is not sufficient to meet the requirements of quantifying the tool life or monitor the changes in tool conditions. Since the changes in tool geometry increase as tool wear increase. this contributes to reducing in identifying the point that the tool reaches the end of useful life. In particular, towards the end of a tool's life, the wear rate increases so fast. therefore, online identification is necessary to monitor its state accurately.

A range of methods has been used to find the transition point explained in this chapter. A special optimisation tool, called “Solver”, available within the Excel software was applied to determin the transition point. This method has the potential to be useful because of the variability of the data to which it can be applied. Although some of these methods are a subjective analysis which means the results depend on the personal decision, they have given us a range of data close to each others. This confirms the validity of these methods for use in detecting the transition point. potentially if any of the data changes, the inflection point going to change as well. Identified the transition point not means the tool has to be changed but it means the technician should be aware

that the cutter is starting work in a dangerous zone and use the tool carefully. Finally, the change in metal removal rate has an effect on the tool life. However, it is not sensitive to the tool wear.

The results concluded that this was a promising approach, but in order for the method to be applied effectively it obviously needs to be closely related to the condition of the actual cutter. Therefore, to monitor tool condition in an efficient manner, an indirect method that can actually apply directly was used in the next part of this project. The spindle motor load with a standard milling tool appears to have significant potential for monitoring and improving the performance of the cutter.

# Chapter 7

## Spindle Load /In-Process Monitoring

### 7.1 Introduction

During a machining process, such as milling, the cutting edges are subjected to forces, high-temperature and sliding wear. Thus, become progressively blunt as the machining time increases. Consequently, the quality of the workpiece also deteriorates (**Kurada and Bradley 1997**). The main focus of this chapter is to develop a reliable method to predict flank wear during the end milling process based upon the tool force signal. One of the most common ways of tool wear prediction is by low-cost spindle current sensing technology that is used to measure spindle power consumption in CNC machines and relate power increase to tool wear. In this contribution, tool wear can be measured and predicted in the process based on spindle motor load. The primary reason for this approach is to study the possibility of monitoring the work done by the spindle motor that drives the cutting tools to measure tool wear. The reason for considering a system such as this is the potential difference in cost between this system and other tool condition monitoring systems that could be used. The system that is to be studied could be very economical.

The idea of this tool condition monitoring structure is to merge the off-line cutting condition monitoring and the online tool condition monitoring based on spindle load. The end milling tests were performed on the same type of low carbon steel workpiece at different cutting speeds. In each set of tests, both the component geometry and spindle load was recorded.

To establish the tool wear model, the monitoring system extracts the spindle motor load, since the latter can potentially measure changes in the cutting conditions of the machine in real time. The reason for using a spindle to measure the overall power consumed instead of using directional piezoelectric dynamometers is the latter are usually three-component piezoelectric dynamometer to measure the tool force in x, y, and z directions. Hence, the spindle takes away from any of the problems with which direction are cutting.

In this investigation, the spindle power (load) consumption is acquired and employed to predict the tool wear. It is assumed that tool wear is proportional to the torque resulting in a correlation between the power and the cutting forces.

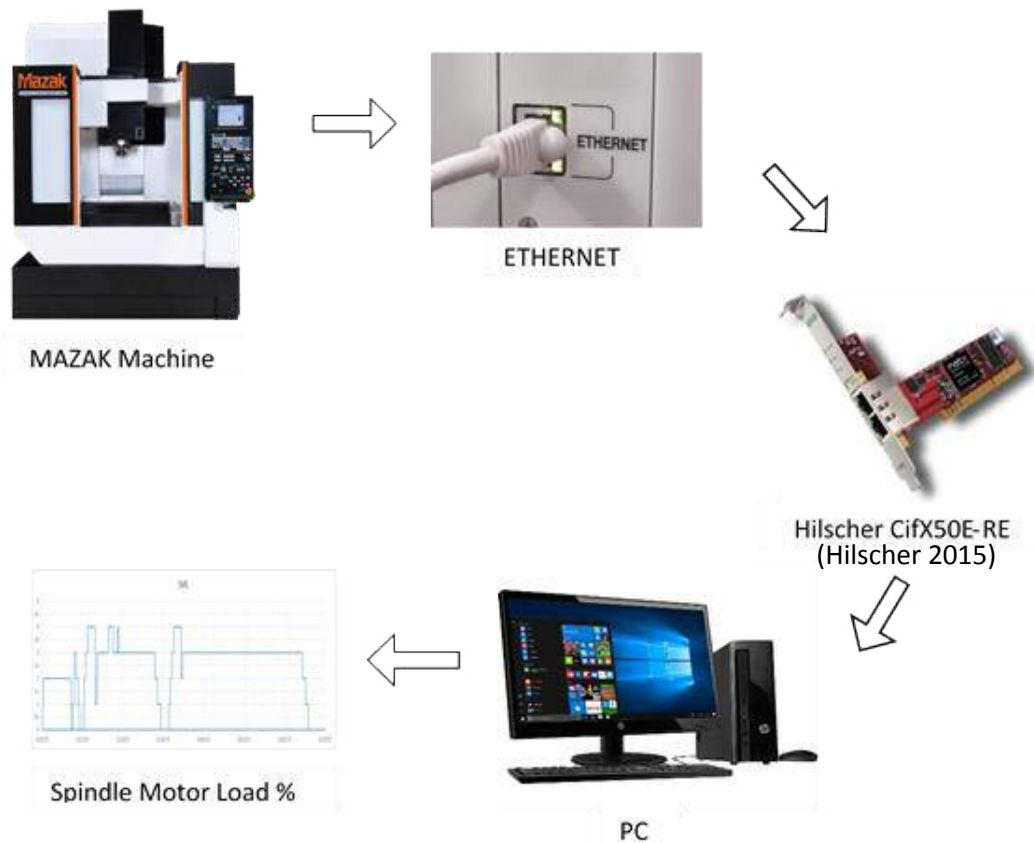
It is assumed that the load on the motor that is driving a machine tool spindle gives valuable information and that this motor could reflect the changes of the machining condition by the change of load.

In order to examine the validity of the suggested cutting power model, seven series of experiments, which is 16.4, 16.5, 10.2, 10.3, 10.4, 10.5, and 10.6 were carried out with parameters detailed in Table 4.2. In this case, the first two series (16.4 and 10.2) were designed to investigate the use of data related to the cutting power in the time domain. The other five were carried out to verify the establishment of the relationship between identified tool wear and the mean cutting power.

## **7.2 Spindle Current Measurement (Experimental setup)**

The spindle current was measured directly from the CNC machine as a percentage value. The spindle current was measured directly through monitoring the CNC process signals by using the VMC PLC. Embedded Ethernet protocols in 504-byte packets were used to transfer the CNC process signals to an external computer. The acquired data was transferred to the Hilscher CifX50E-RE interface board (HIB) (Hilscher 2015) with a per-packet delay of 100ms and processed through the application of a

simple C++ executable to monitor the VMCs and the acquisition of spindle motor load (SML) data, as shown in Figure 7.1. In these experiments, the Mazak controller output was the spindle load percentage quantised in 1% steps, how or where the percentage comes from being hidden.



**Figure 7.1 In- process tool condition monitoring**

The tests were conducted at the same settings as stated previously in chapter four and the same procedure was followed to monitor tool usage.

The experiment setup for validating the proposed monitoring system is presented in Figure 7.2. This system can be utilised to capture continuous sampling as well as

collecting and recording the real-time signal as shown in Figure 7.3. Data is saved so it could be exported to another computer for analysis. The data is then analysed to be stored in the database. In addition, a particular time can be set to store data on the computer automatically. The details of this method can be found in a paper produced by our research group (Hill et al. 2018).

Figure 7.4 shows an example of data, which has been stored in notepad by using this system.

The first step towards all of these aims was taken by the author. Data was plotted to see if any impressions could be made immediately. Figures 7.5 and 7.6 show the plots received by the spindle motor for 10mm cutters.



**Figure 7.2 MAZAK monitoring system**

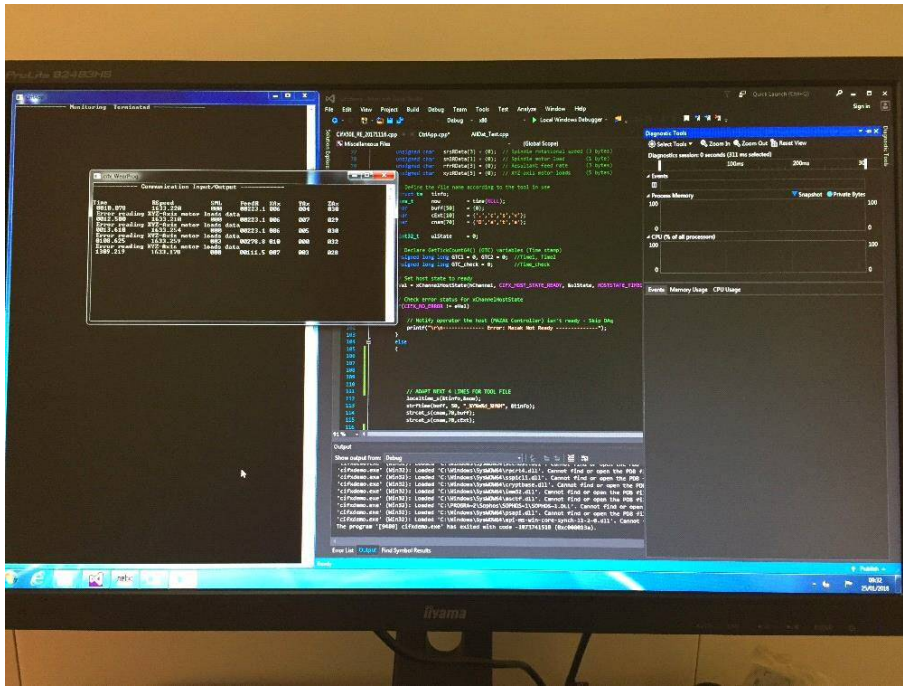


Figure 7.3 Real-time monitoring system

Time	RSpeed	SML	FeedR	XAX	YAX	ZAX
0156.6880	1637.144	000	00075.2	008	008	031
0156.7030	1637.144	000	00075.2	008	008	031
0156.7190	1636.983	000	00223.6	002	008	030
0156.7350	1636.983	000	00223.6	002	008	030
0156.7500	1636.983	000	00223.6	002	008	030
0156.7660	1636.983	000	00223.6	002	008	030
0156.7820	1636.983	000	00223.6	002	008	030
0156.7970	1636.983	000	00223.6	002	008	030
0156.8130	1637.233	001	00223.6	013	007	032
0156.8280	1637.233	001	00223.6	013	007	032
0156.8440	1637.233	001	00223.6	013	007	032
0156.8600	1637.233	001	00223.6	013	007	032
0156.8750	1637.233	001	00223.6	013	007	032
0156.8910	1637.233	001	00223.6	013	007	032
0156.9070	1637.233	001	00223.6	013	007	032
0156.9220	1637.220	001	00223.6	005	005	030
0156.9380	1637.220	001	00223.6	005	005	030
0156.9530	1637.220	001	00223.6	005	005	030
0156.9690	1637.220	001	00223.6	005	005	030
0156.9850	1637.220	001	00223.6	005	005	030
0157.0000	1637.220	001	00223.6	005	005	030
0157.0160	1637.129	002	00223.6	011	010	031
0157.0320	1637.129	002	00223.6	011	010	031
0157.0470	1637.129	002	00223.6	011	010	031
0157.0630	1637.129	002	00223.6	011	010	031
0157.0780	1637.129	002	00223.6	011	010	031
0157.0940	1637.129	002	00223.6	011	010	031
0157.1100	1637.129	003	00223.6	009	007	031
0157.1250	1637.129	003	00223.6	009	007	031
0157.1410	1637.129	003	00223.6	009	007	031
0157.1570	1637.129	003	00223.6	009	007	031
0157.1720	1637.129	003	00223.6	009	007	031
0157.1880	1637.129	003	00223.6	009	007	031
0157.2030	1637.129	003	00223.6	009	007	031
0157.2190	1637.127	003	00223.6	008	008	032
0157.2350	1637.127	003	00223.6	008	008	032
0157.2500	1637.127	003	00223.6	008	008	032
0157.2660	1637.127	003	00223.6	008	008	032
0157.2820	1637.127	003	00223.6	008	008	032
0157.2970	1637.127	003	00223.6	008	008	032
0157.3130	1637.253	004	00223.6	010	010	032
0157.3280	1637.253	004	00223.6	010	010	032
0157.3440	1637.253	004	00223.6	010	010	032
0157.3600	1637.253	004	00223.6	010	010	032
0157.3750	1637.253	004	00223.6	010	010	032
0157.3910	1637.253	004	00223.6	010	010	032
0157.4070	1637.253	004	00223.6	010	010	032
0157.4220	1637.213	004	00223.6	007	011	031
0157.4380	1637.213	004	00223.6	007	011	031
0157.4530	1637.213	004	00223.6	007	011	031
0157.4690	1637.213	004	00223.6	007	011	031
0157.4850	1637.213	004	00223.6	007	011	031
0157.5000	1637.213	004	00223.6	007	011	031
0157.5160	1637.163	004	00223.6	011	008	032
0157.5320	1637.163	004	00223.6	011	008	032
0157.5470	1637.163	004	00223.6	011	008	032
0157.5630	1637.163	004	00223.6	011	008	032
0157.5780	1637.163	004	00223.6	011	008	032
0157.5940	1637.163	004	00223.6	011	008	032
0157.6100	1637.162	004	00223.6	012	009	028

Figure 7.4 The data stored in notepad



## 7.3 Illustration and Analysis

### 7.3.1 Spindle Motor Load vs Cutting Time

Figure 7.5 presents the plot of the spindle motor load (SML) versus time during the full length of series 10.4. The data-sampling rate was 10 Hz. It has been noted that the magnitude of spindle noise increases with the time. The idea behind monitoring spindle load is evident. The gradual loss of sharpness of cutting edges causes a decrease in the capability of the tool to cut the material. This leads to an increase in cutting force. The rise in tool wear would degenerate the material removal mechanism progressively (Isbilir and Ghassemieh 2013).

The explanation for this behaviour is, as flank wear width increases, the contact area between side face (flank) and the workpiece increase too. This, in turn, requires more cutting force, and as a result of that, the spindle motor needs more power to rotate the cutter at the desired speed to overcome the increasing friction force on the cutting contact area.

The tool wear can be identified as an increasing magnitude of the SML together with irregular changes. The signal is gradually increasing over the process of the operations by a small rate till the middle of them indicating a plateau in the tool wear development and then increases again until the end of the test. The same tendency is observed when the cutting speed is decreased but less as shown in Figure 7.6.

It is observed from the Figures 7.5 and 7.6 that using low cutting speed consumes power less than when using the high cutting speed, but it cannot assume that the trend would keep going on the same way.

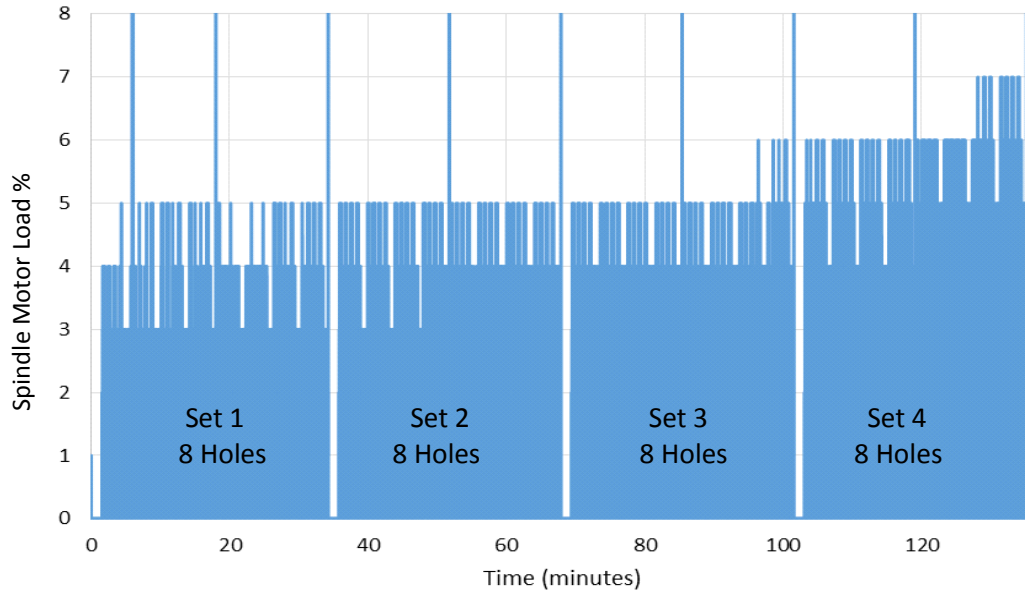


Figure 7.5 Spindle motor load percentage vs cutting time/series 10.4

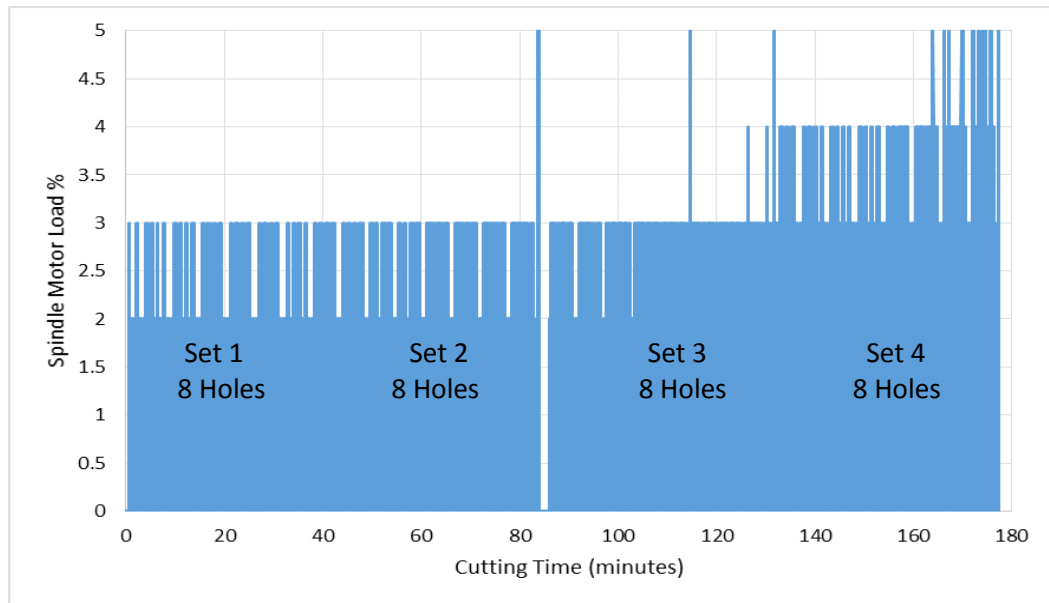


Figure 7.6 Spindle motor load percentage vs cutting time/series 10.6

### 7.3.2 Spindle Motor Load Profile during Milling One Cylinder

In this study, two different movements were used to make the holes, discontinuous milling process on the periphery cutting edge and a continuous drilling process on the bottom cutting edge. The characteristics of these two cutting edges with the workpiece are different. Therefore, these two movements will be analysed separately.

The experimental observations reported in this section provide a significantly better understanding of the overall relationship between the cutting power and process parameters. This is because the information content of this particular output is relatively wealthy and provides valuable data to understand the mechanism of tool wear.

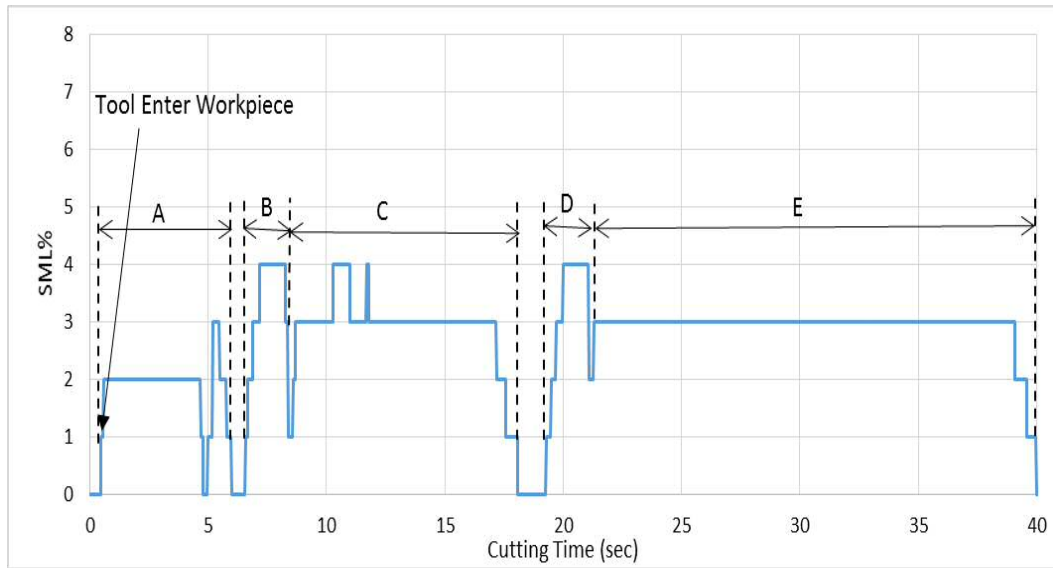
For this reason, the next section presents a detailed time-dependence analysis of spindle load motor output. Figures 7.7 and 7.8 present examples of the measured values of the spindle motor load profile obtained during cutting for the small, (Figure 7.7) and large cutters, (Figure 7.8) with variable feed rate, as shown in Table 4.4. As can be seen, numerous changes in tool force occur with changes to the cutting direction/tool paths and feed rate of cutting while cutting one cylinder.

This scale of analysis allows a very clear picture of how the tool interacts with the workpiece to make one cylinder. As noted in Figure 7.7, such a signal can be divided into five consecutive stages, which correspond to the regions “A”, “B”, “C”, “D” and “E”. The physical interpretation of each of them is given as follows:

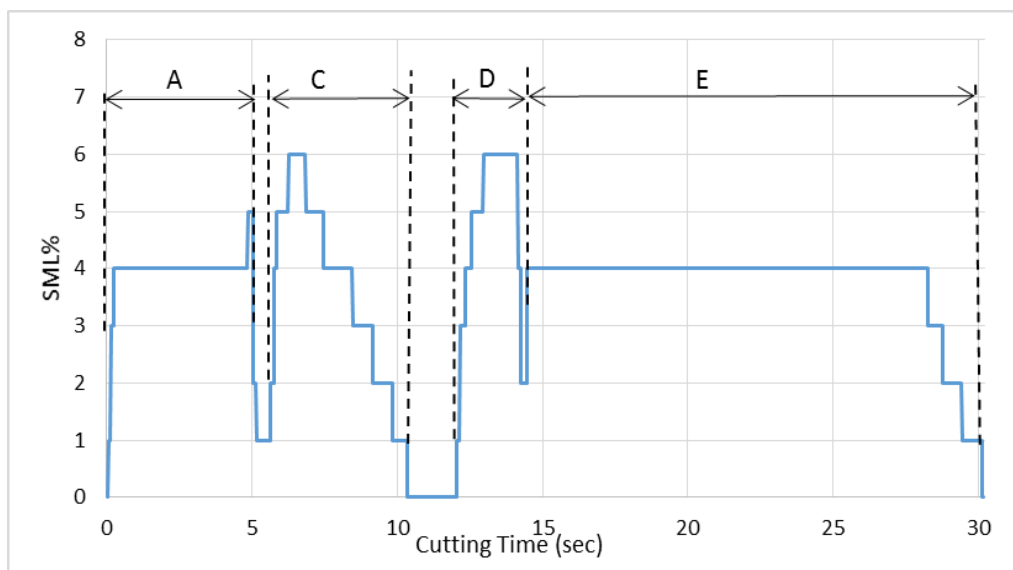
- 1- The first cycle/region A: This phase is started with an initial plunge into the centre of the workpiece down to 5mm depth. In this case, the cutter only works axially, and therefore the material at the bottom of the hole is removed by the bottom cutting edges. The total time for this cycle varies depending on the cutting speed, cutter diameter, and the feed rate. In this stage, the cutting is a continuing plunge process on the bottom cutting edges, and the cutter engages all bottom cutting edges in their entirety. As a result, the cutting force is

generated due to the resistance of the material to chip formation, this, in turn, leads to high stresses on the bottom cutting edge.

- 2- The second cycle /region B: At this stage, the cutter would then proceed to move out with the straight line at the same depth 5 mm as shown in Figure 4.5 b. This step was the shorter one compared with other cycles; it just takes approximately 1.9 – 2.68 seconds for a 10mm cutter. The amount of cutter travel is roughly 7 mm. In this process, the material will be removed from both front and periphery cutting edges at the same time. It should be noted that this stage was missed when using the 16 mm cutters.
- 3- The third cycle /region C: the cutter was opening out the initial bore by a radius increase of the same amount of the straight line in step number two. In this step, the feed per revolution was changed between 0.136 mm/rev to 0.2 mm/rev for 10 mm and 16 mm cutters respectively. In understanding this event, the material will be removed from both front and periphery cutting edges at the same time.
- 4- Fourth cycle /region D: In this stage, the cutter then proceeds to move out again with a straight line at the same depth 5 mm. The amount of cutter travel was changed from cutter to cutter; it is roughly in a range between 8 mm to 9 mm. This step took approximately 1.7 – 3 seconds for a 10 mm and a 16 mm cutter respectively. Regardless of the cutter diameters, the SML in this stage and stage B was the maximum. This is due to the tool being fully immersed; the radial depth of cut is equal to the cutter diameter.
- 5- Fifth cycle /region E: the cutter was opening out the remaining width left surrounding the cylinder by a radius increase of the same amount of the straight line in stage number four as shown in Figure 4.5 e. In this step, the feed per revolution for the cutter was the maximum. More specifically, it is typically in a range between 0.17 mm/rev to 0.25 mm/rev for a 10mm and a 16 mm cutter respectively. This procedure was the longer one compare with other cycles; it takes approximately 17 – 28.8 seconds for the 16 mm and the 10 mm cutter respectively.



**Figure 7.7** A schematic diagram of the power profile during milling one Cylinder for the small cutter /series 10.4 H1C1



**Figure 7.8** A schematic diagram of the power profile during milling one Cylinder for the large cutter /series 16.5 H1C1

It is observed that from the Figures 7.7 and 7.8 all 10 mm cutter profiles exhibit significantly lower SML than the 16 mm cutter profiles at the same volume removed. In addition, the effect of the tool path, as well as metal removal rate on the spindle load is pronounced for all cycles. For example, the SML in cycles B and D in Figure 7.7 is higher than other cycles A, C, and E and it is due to the increase metal removal rate.

Figure 7.8 showed that although increases in the cutter diameter translate to faster machining times, the loads on the spindle motor increase as well, resulting in higher power demand. Since our main interest is monitoring the spindle load in product manufacture, the trade-off between spindle load and machining time was analysed to show if the increased loads due to developing the tool wear were increasing the work done.

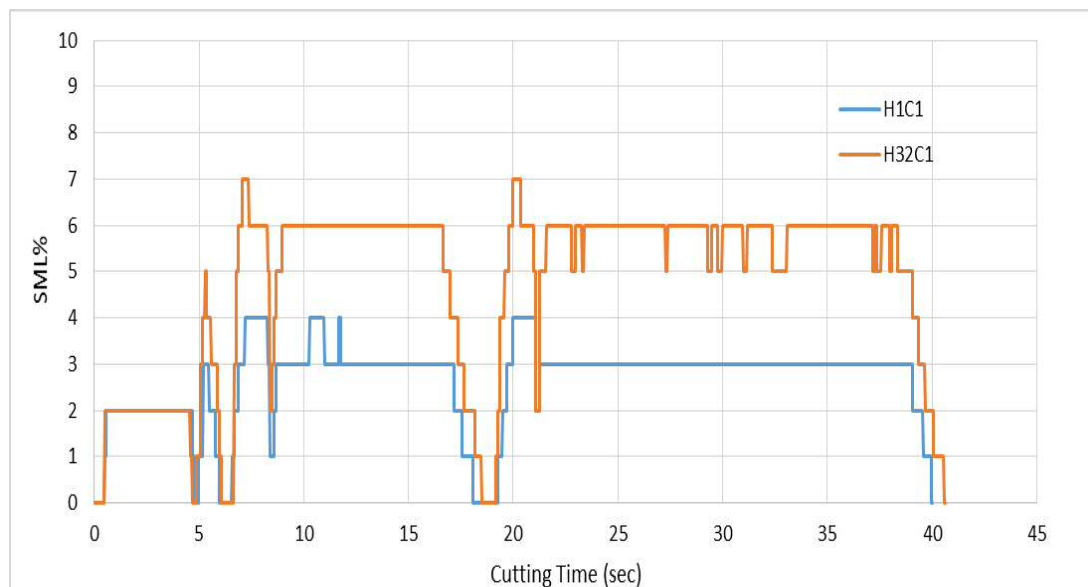
It can be seen in Figures 7.7 and 7.8 that the cutting power increases distinctly with the increase cutter diameter. For example, the SML in cycle A is 2% for the 10 mm cutter in Figure 7.7 and 4% for the 16 mm cutter in Figure 7.8. This is because the large cutter actually used more power due to the high rate of metal removed. Logically, as the tool is wearing, the cutting power will reduce because it removes less metal. However, by the time, and when the tool wear increases, the contact between the tool and the machined surface increases too. This will lead to an increase in the friction force between the tool and workpiece. As a result, the effect of tool wear will override the impact of the cutter size and more energy consumption is expected during a cutting process. Consequently, the condition of the tool is changing not just the diameter of the tool but the actual efficiency and effectiveness.

### **7.3.3 The Effect of Tool Wear on the Spindle Motor Load**

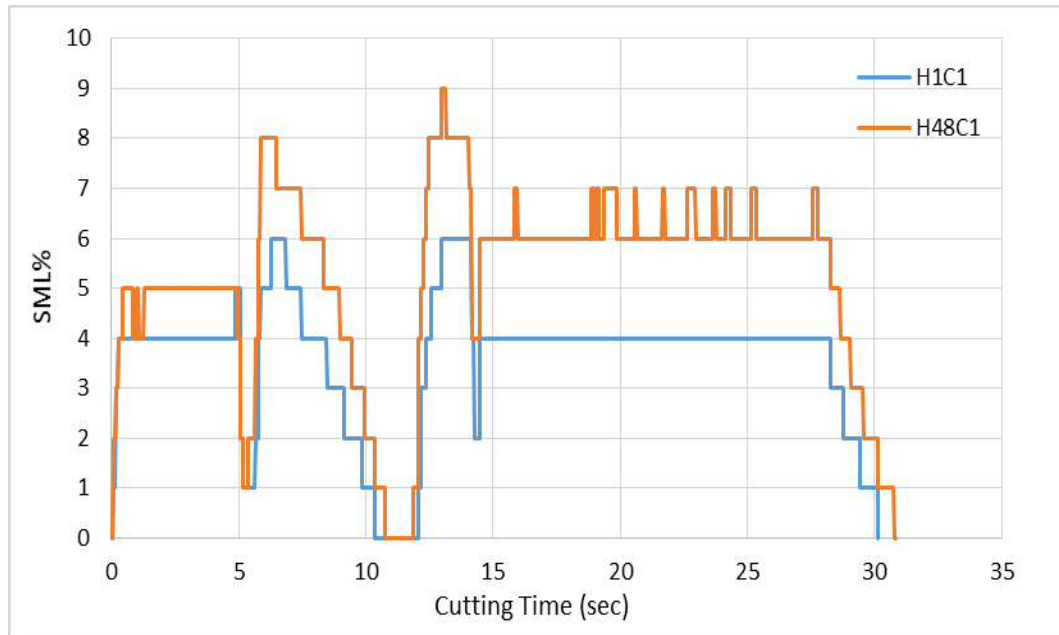
To illustrate the effect of tool wear on the SML, two profiles cycles can be compared in Figures 7.9 and 7.10 at the start and end of a set of tests. The blue lines refer to the reference point, they show the trends of the SML regarding the process parameters for a new cutter; the orange lines show the patterns of the SML in terms of the process

parameters under severe-wear conditions. The results show that the new and the worn cutter have the same profile. The power consumption of the machine tool increased with the cutting time and tool wear.

Concerning the reference condition Hole 1 C1 in Figures 7.9 and 7.10, the increase in the SML was in the same order during the tool wear and process parameters changes (cycles B, C, D, and E). Figure 7.9 shows that the impact of the flank wear on the SML was prominent for the 10 mm cutter. The SML in cycles C and E were 3% for new cutter and 6% for worn cutter. Whereas, for the 16 mm cutter, Figure 7.10, the case was different. The effect of flank wear on the SML was relatively small, compared to the influence of cutter diameter and cutting parameters. For example, the SML in cycle E was 4% for new cutter and 6% for worn cutter. The metal removal rate and the tool path had more significant influence than other process parameters on the SML at each level for the given cutting conditions, as shown in cycles B and D in Figures 7.9 and 7.10.



**Figure 7.9 The spindle motor load signal Vs. The time during milling one Cylinder for new (H1C1) and fully worn (H32C1) tool/series 10.4**



**Figure 7.10** The spindle motor load signal Vs. The time during milling one Cylinder for new (H1C1) and fully worn (H48C1) tool/series 16.5

### 7.3.4 Detecting Tool Breakage by the Spindle Motor Load

In this study, it is important to note that the spindle load identified that the tool breakage occurred in series 10.5, as shown in Figure 7.11 for health or brand new cutter and for the broken cutter in Figure 7.12. There is the potential to explore that method further to determine the reason for tool breakage. However, at the moment it is only able identify the tool has broken.



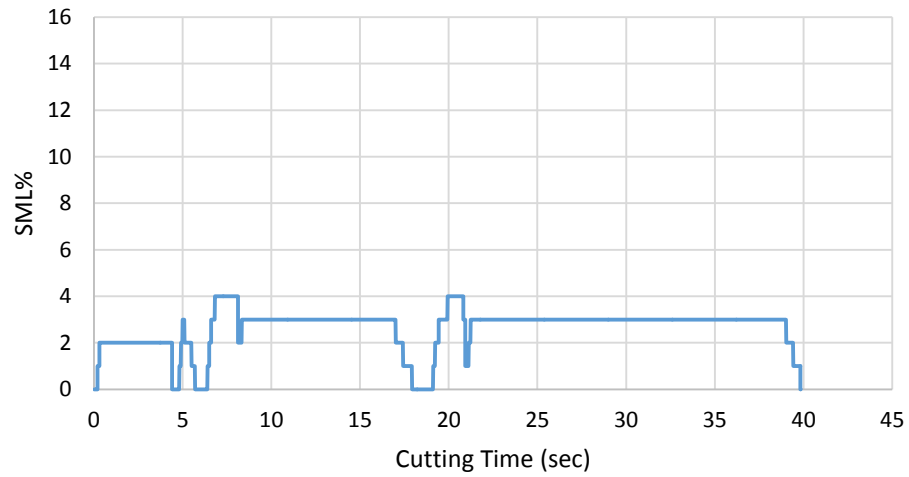


Figure 7.11 The spindle motor load signal for health cutter/series 10.5

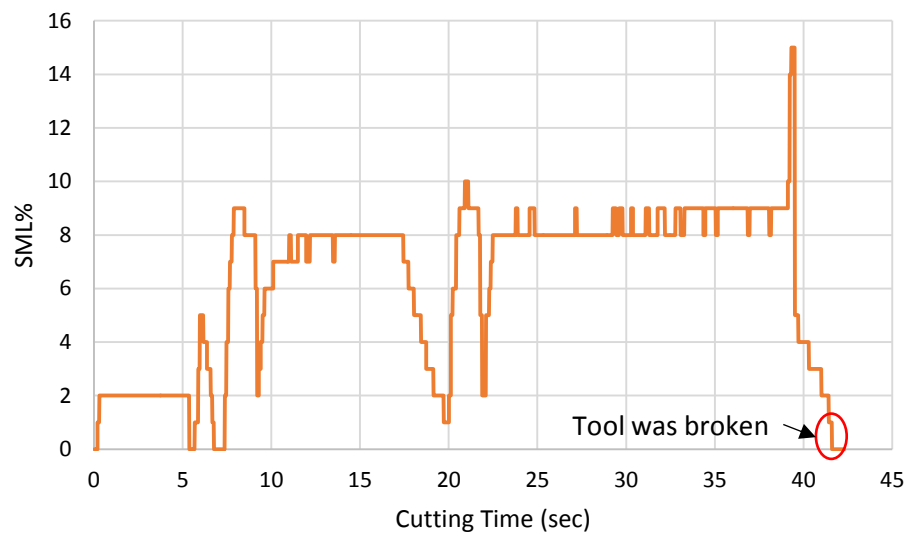


Figure 7.12 The spindle motor load signal for broken cutter/series 10.5

## 7.4 Assessment the Work Done by the Cutter

### 7.4.1 Cutting Time

As shown in Figure 7.4, the output data included the cutting time as well as the SML. Figure 7.13 summaries the cutting time for each segment of all regular series. The

cutting times for C1, C2, and C3 have been calculated based on the loop 2 / cycle E of the tool load applied to produce each cylinder.

As reported in chapter five, the bottom of the cutter worked harder and longer than other cutter segments. Consideration of the measured cutting times from the SML monitoring in Figure 7.13 confirms the estimated results from CMM in Figure 6.3 although there is a difference between those results up to 3%. This could be due to the machine controller adapted the tool path in order to reduce the tool wear and the load on the cutter. The bottom of the cutter C4 worked longer than the upper regions and removed more metal as will be discussed later. Therefore, the cutting time for C4 is the main parameter used in this initial analysis to monitor the cutting tool.

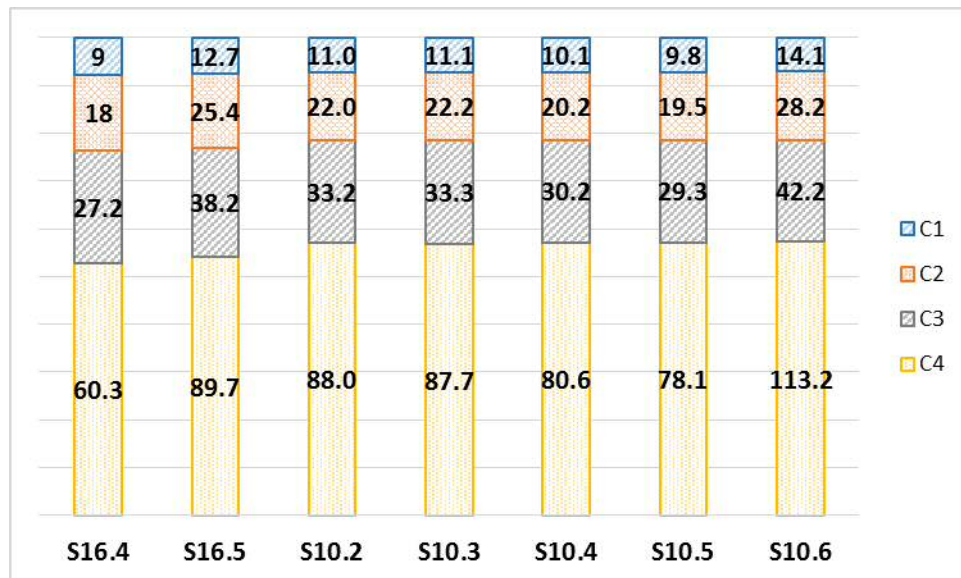


Figure 7.13 Total cutting time for each section (minutes)

#### 7.4.2 Calculate the Work Done

To prove the efficiency of using the spindle motor load to develop a monitor for tool life, it is necessary to transfer spindle load into a work done.

To achieve a work done value, the spindle output was analysed and the area under the curve of the load applied to produce each cylinder was calculated. All these calculations were done by using SUM function in Microsoft Excel 2013. Figure 7.14 shows the difference between the works done by each section as calculated based upon the area under the curve for the measured series.

The work done for C1, C2, and C3 was calculated based upon the area under the curve for loop 2 that applied to produce each cylinder. There is very little difference between the calculations from the CMM to the measurement from the SML regarding the metal removed and work done by each section reaches to 1%. Both methods are seen to confirm that the change in tool load reflects the tool condition and corresponds to the tool wear. The reason for the deviation can be due to the spindle load signal, which is measured in percentage.

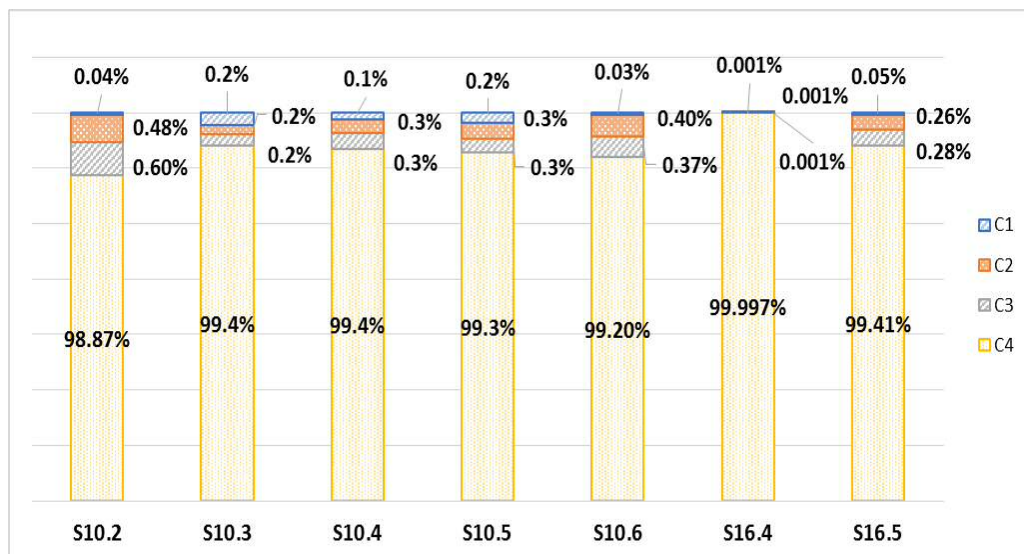
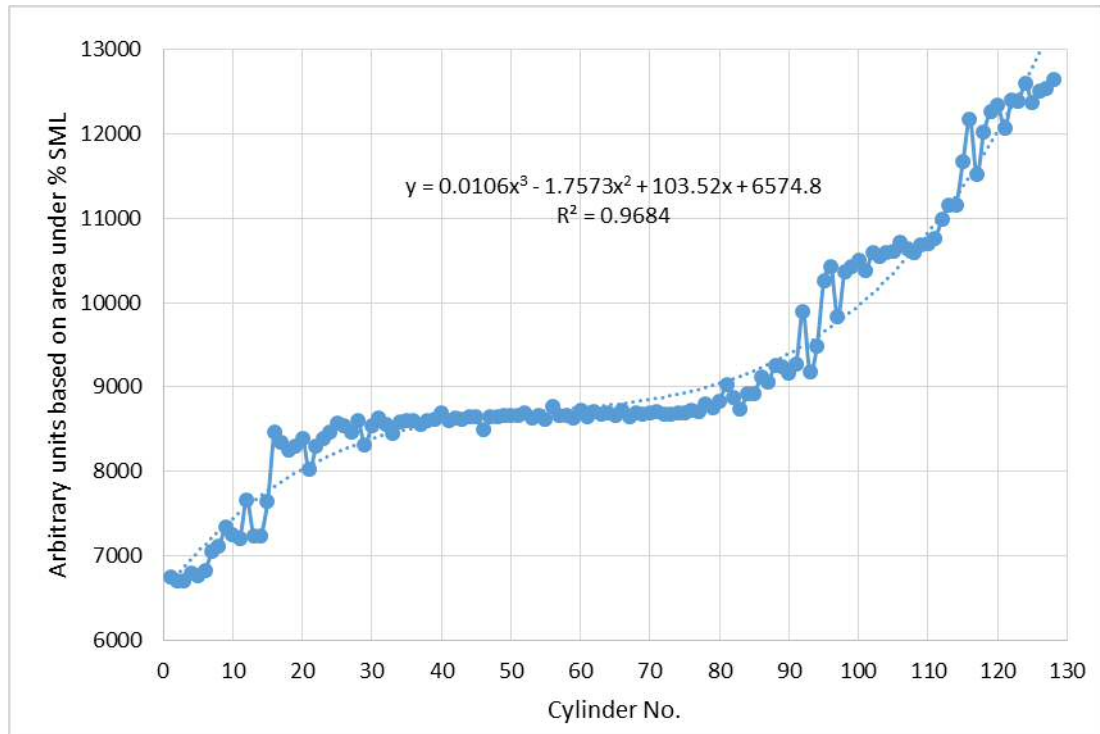


Figure 7.14 Percentage of the work done by each section

Figure 7.15 shows the work done by the bottom of the cutter C4 for the whole series 10.4. The results point out that the work done increases with time as the tool wear developed. The behaviour of the work done is similar to the typical tool wear curve shown in Figure 3.2. It rises initially, then reaches a plateau until the tool wear has higher values and from there on, the consumption increases again rather rapidly.

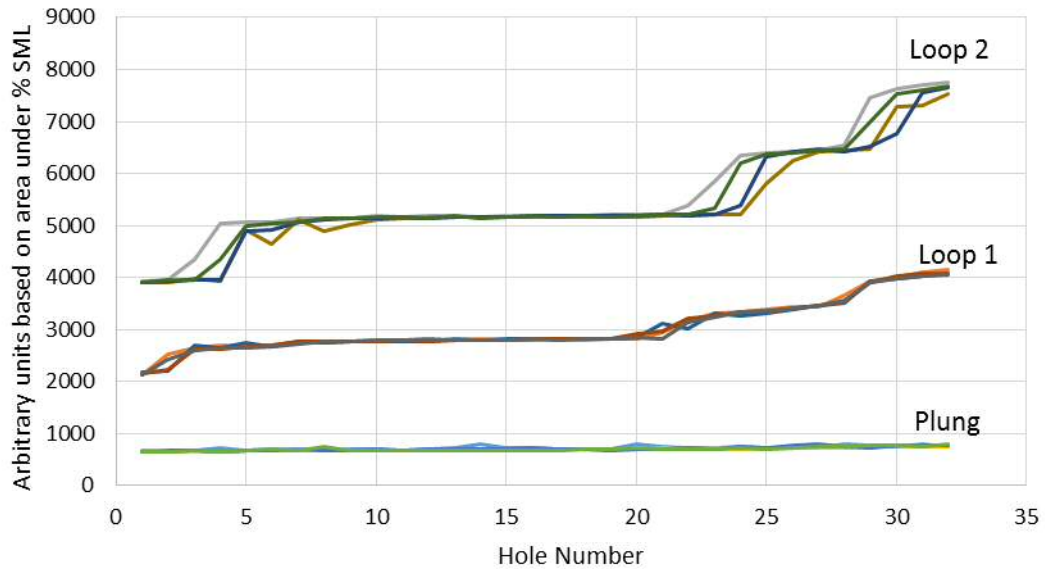


**Figure 7.15 The work done by C4/ series 10.4**

The Figure 7.16 shows how the values of the work done changes with the type of operation and the number of holes in series 10.4. P refers to plunge; Loop 1 relates to cycle 2, 3 and 4, Loop 2 refers to the cycle 5, as shown in Figures 4.5 and 4.6. The reason for dividing the cutting process into three parts is to show a clear picture for the work done in each cycle. The curve produced can clearly be seen to accurately follow the expected tool wear process. The benefits of having such a curve are considerable particularly when applying a tool management strategy aimed to preventing tool breakage. This will normally occur following the transition into the final section of this curve. It is observed that the overall increase in the work done from the start to the end of the series in the plunge, loop 1 and loop 2 is 21%, 90% and 97% respectively. These indicate much higher wear rates in periphery cutting edges compared with bottom cutting edges.

It is observed from Figure 7.16 that the magnitude of work done for loop 2 (Figure 4.6) is higher than other cycles (plunge and loop1), this could be due to the cutter in loop 1 will be under the effect of one cylinder work. However, the cutter will be under

the effect of more than one cylinder work in loop 2. There is not much variation in quantity in plunge cycle. This means that the tool wear at the front edges is minimal.



**Figure 7.16** The work done at different types of operation/series 10.4

Figure 7.17 shows the work done in plunge milling /cycle 1; it increases with developing the tool wear. The reason for the peaks may be due to such sudden changes or other factors that could include hard spots or inclusions in the workpiece material. However, these changes are still not highest than the force in loop 1 and loop 2 in Figure 7.16. The results obtained from Figures 6.24 and 6.25 confirm the output from Figure 7.14, which shows that the bottom cutting edges work less than the periphery cutting edges. Consequently, the wear rates in the periphery cutting edges are higher than the bottom cutting edges.

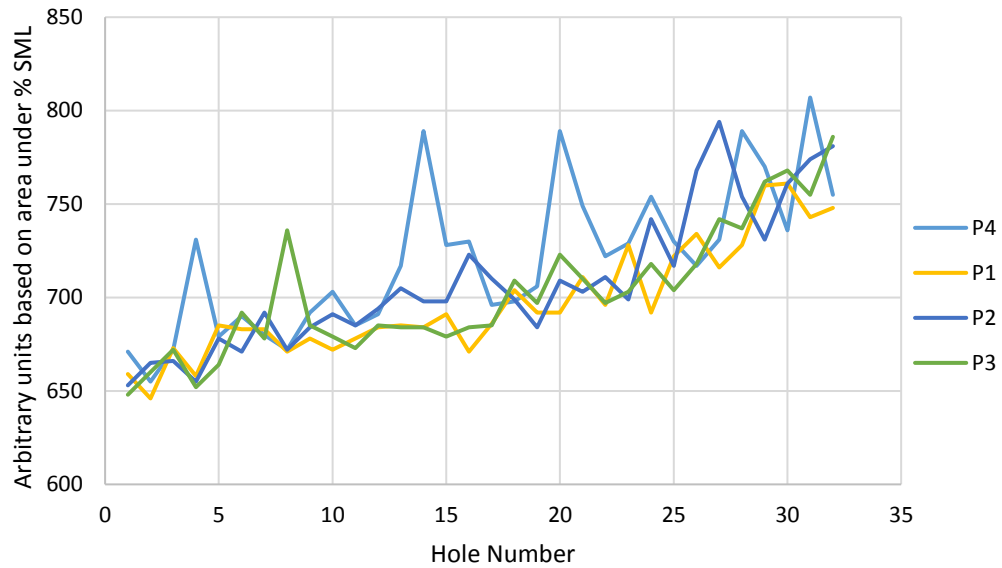


Figure 7.17 The work done in plunge operation/series 10.4

## 7.5 The Relationship between Spindle Motor Load and Tool Wear

The spindle motor load increased with the tool-flank wear, resulting in increasing the work done regarding the machining distance, hole number, and cutting time, Figures 7.18 and 7.19 show that relationship. However, the rate of the increase depended on the conditions or process parameters. The tool load will increase due to the change of the tool geometry, and the harsher cutting condition will be present for the cutting tool and lead to wear that is more serious.

Regarding the SML% and tool wear in Figures 7.18 and 7.19, there is a difference between the trends of both variables, although the general relationship between them is proportional. This can be attributed to the captured SML signal where it was in a percentage. The problem with the tool load measurement is its resolution. The resolution of the tool load is 1%. Therefore; small change can cause a significant difference. For example, if the spindle load is around 1.5 and drops to 1.4, the result will go down to 1, if it rises to 1.6, the result will go up to 2. This difference will effect

on the results accuracy. Figures 7.20 and 7.21 show that the trend between the tool wear calculated from the CMM and the work done, which is calculated from the area under the spindle load signal curve, look the same. The resulting signal was increased gradually when the wear value is increased.

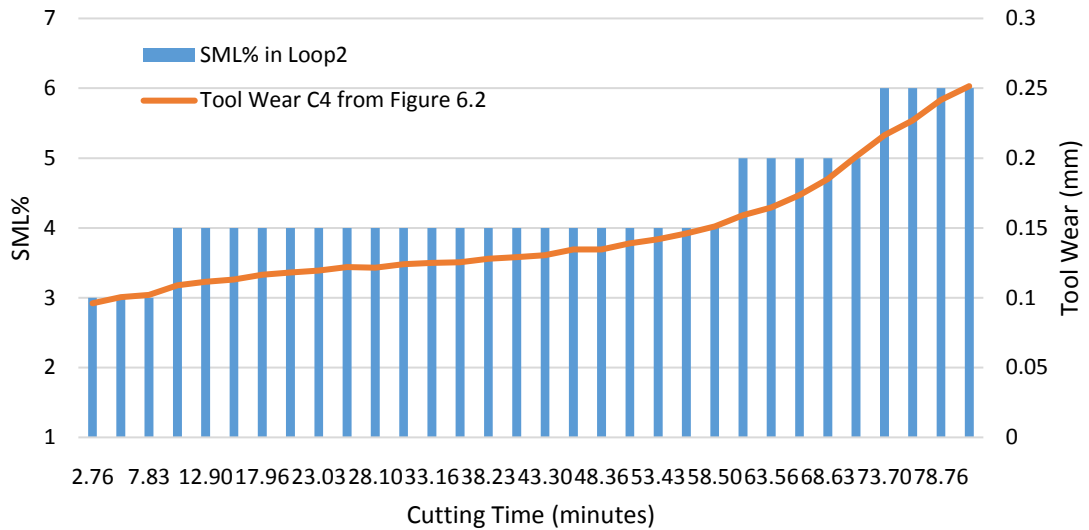


Figure 7.18 The relationship between the SML % and tool wear/series 10.4

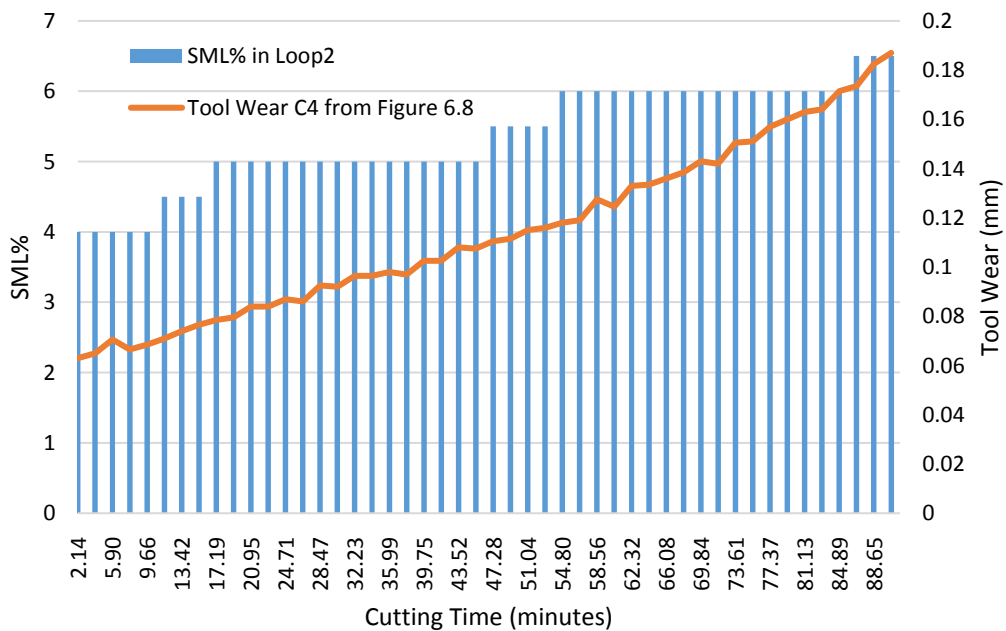


Figure 7.19 The relationship between the SML % and tool wear/series 16.5

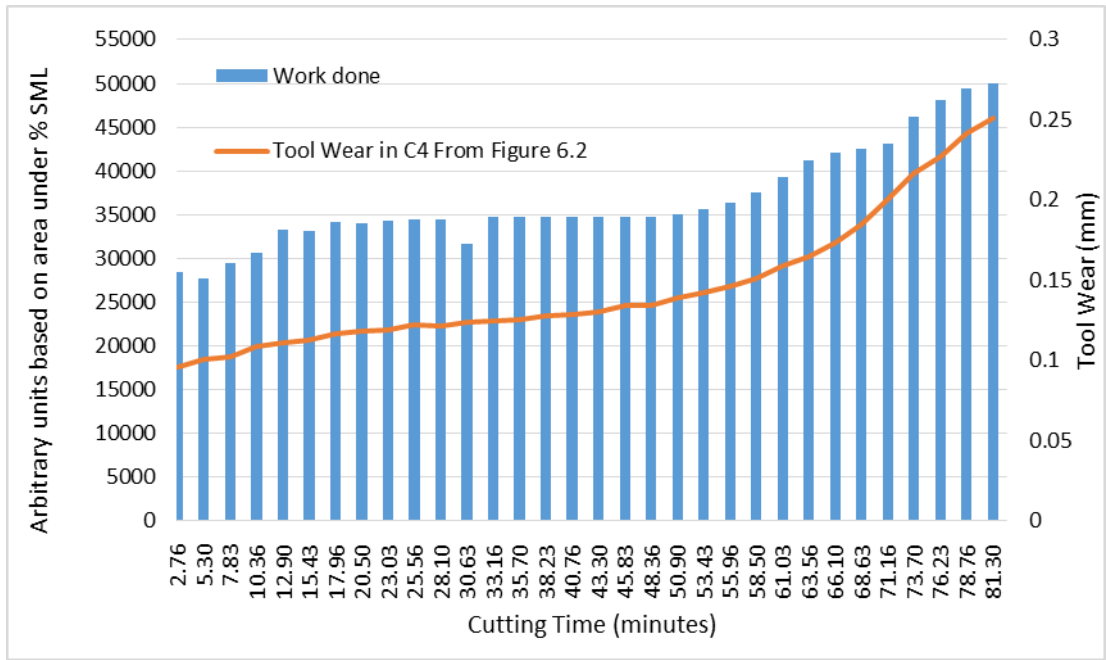


Figure 7.20 The relationship between the work done and tool wear/series 10.4

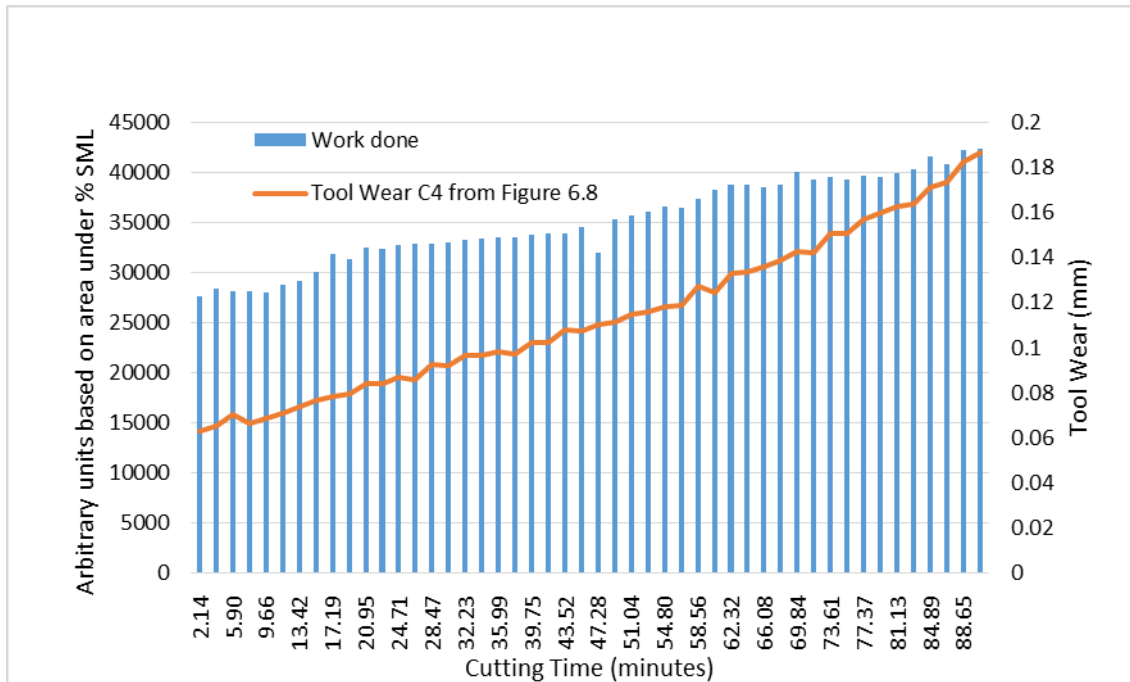


Figure 7.21 The relationship between the work done and tool wear/series 16.5



## 7.6 Summary

This chapter described the application of a spindle load based approach for monitoring online the effect and magnitude of cutting tool wear. In this study, the cutting load during milled 40 mm diameter holes at specific intervals of machining has been monitored. This relates tool load with radial tool wear meaning the method can indicate the level and rate of tool wear.

The main goal of this experimental study was to explain how the tool wear of the sequential processes influence the power consumption. It has been shown a sharp tool consumed less power than a used/worn tool. The power measurement routines using variable cutting speed, feed rate, and keeping the constant depth of cut of 5mm for each series carried out.

Current and power monitoring have been shown to potentially provide a good solution for indirect tool monitoring system since the material removal power is directly related to the tool load. However, the effect of the process parameters on the material-removal rate is more complicated. The use of spindle motor load for on-line control of a machine tool shows promise of leading to a new approach to tool condition monitoring. However, it does not adequately capture the tool force changes since it was in percentage.

The output results from the spindle motor load for monitoring the tool condition on-line show the validity of employing the CMM to measure the component geometry in case of monitoring the tool wear indirectly. The measuring cutting time from the spindle motor load agreed with that calculated from the CMM, although there is a difference up to 3%. In addition, the calculated work done by each section from the spindle motor load looks the same to the calculated volume removed by each section from the geometry, with a difference up to 1%. To this end, it is again emphasised that the in-process measurement of the machining state is even now far from completion, although understanding what are the leading issues in the establishment of some in-process measuring technologies for practical use with reasonable price.

# **Chapter 8**

## **Conclusions, Contributions and Future Work**

### **8.1 Introduction**

Milling is one of the most important machining processes in modern manufacture. It is a versatile machining process used to machine flat and irregular surfaces. It can also be used to make holes, cut gears and slots.

The main challenge for this study was to increase the accuracy of the tool wear estimate allowing for changes in cutting parameters and tool dimensions.

### **8.2 Conclusions**

In this investigation, the flank wear was measured indirectly based on the component measurement by using the CMM. In the final deployment the output signals (i.e. tool load) were acquired for online analysis using the spindle motor load.

The effect of the changes to the dimension of the tool has been considered using the component geometry. The results indicate that variations arise in tool dimensions and it is possible to measure the level of these changes. The established pattern of the tool

wear curve has been repeated and the previously defined three stages tool wear curve have been found to be applicable.

- Identifying the important and critical change point when the tool wear becomes rapid in it enters the third phase is essential. Determining this change allows the application of more careful tool management strategies.
- The results show when the tool is more likely to break. Therefore, it is important to identify this point, although there is no effective way to predict actual remaining life.
- The work has shown it is possible to extrapolate and identify potentially the end of useful tool life from the spindle load. Again, the context of useful tool life needs to be fully understood and better explored, which is stated as an important point in the future work.

The tool wear was calculated indirectly by using the CMM; the results were obtained in Chapter 5. It was clearly demonstrated that differential tool wear occurred in the tool. Not understanding this scenario will result in the under or overestimate of the remaining of tool life. Over-estimation of tool life can result in degraded product quality and damaged parts (in case of early breakage of the tool). Underestimation results in the early stoppage of the machining process and increased cost of production. Therefore, real-time tool wear estimation in machining processes is a key research topic in automated manufacturing.

The cutting time for each segment was calculated by using equations (4.2-4.4). The CMM results indicated that the bottom of the cutter (C4) works longer and harder than other segments and removes the most of the material as shown in Figures 6.3 and 6.23.

- The results in this study concluded that there is differential tool wear, which impacts on the incorrect assessment of the degree of tool life since previous research calculated average diameter as the input into the tool life calculations. This value will affect the accuracy of the component. In addition, the geometric

form of a component machined using the unevenly worn cutter will be less than the optimal.

The potential error associated with the non-allowance for differential tool wear was presented in section 6.4. When using the average value of the level of the tool wear, the error in assessing the remaining useful life reaches to 20%. Table 6.2 shows the effect of differential tool wear on the component geometry quantitatively.

A new method to calculate the metal removed by each section of the cutter depending on the component geometry by using simple volumetric measurements as explained in Chapter 4, has been explored. Based on such data, the work done by each section was evaluated, as presented in section 6.6.

- The results concluded that the bottom of the cutter (C4) works harder than other segments and removes more than 99% of the material, as shown in Figures 6.23 and 6.24.

It is important to note that there are accelerating rates of tool wear in the C1, C2, and C3 sections despite the short working time. This behaviour could be related to removing a small cut that leads to rubbing the metal, or due to the change of the local condition of the material due to the work hardening.

- This research identified that the rapid tool wear in the upper segments of the cutter has occurred, but the actual mechanism and consequences of that was not fully explored.

In this study, the author set out to calculate the tool wear in the bottom of the cutter by measuring the depth of each hole. However, the results were inconclusive. This could be due to the reference plane P0 from which feature depth could be measured. The data relies on the transfer of the reference point and assume it is the same for all sets.

Measuring the geometry gives a good indication and is helpful, but it is hard to distinguish what happens just from the measurement and more information is needed.

Therefore, a preliminary study was undertaken to look at tool life as indicated by the amount of work done. The acquired spindle load against time signal was used to do this.

Based upon the work done that calculated from the area under the curve of the spindle measurement approach, the last segment of the cutter (C4) was shown to work harder and remove most of the material, as shown in Figures 7.11 and 7.12. Comparisons indicated that the online spindle set up does replicate what was measured offline. The need for offline measurement was necessary in order to calibrate the online measurements. The experiments conducted are thus an important being for future work.

The behaviour of the work done by the bottom of the cutter measured using the spindle load approach, is similar to the tool wear curve that was calculated from the CMM results. It could be concluded that the work done is increased when the wear value is increased. Chapter 7 shows that there is a good correlation between the behaviour of the tool as indicated by the CMM and spindle load. The relationship between the change in spindle load and cutting condition is promising.

- It is also important to note that the spindle load identified that the tool breakage occurred. There is the potential to explore that method further to determine the reason for tool breakage. But at the moment it is only able identify the tool has broken, as presented in Chapter 7.
- The spindle load approach offers more potential. It is the first step to showing the tool wear and tool load relationship exists and it is a promising area to take forward.

### 8.3 Contributions

To estimate the tool wear two kinds of indirect acquisition methods were used, namely, post process and in-process. Post process includes measuring the component geometry by using the CMM. The in-process method requires the acquisition of a process variable from which tool wear can be estimated using a known relationship such as the spindle load.

The following original contributions were made:

- A method was developed and tested to calculate the tool wear indirectly based on measuring the component geometry by using the CMM.
- The CMM results were used to establish the tool wear behaviour and for identifying the important change in the rate of tool wear. The method can show when the tool goes into the third phase. The transition point was detected by using some analysis with the range when the change occurs. The same method could use spindle load to establish the transition point.
- The established method of the machining cylinders and associated measurement technique on the CMM was used to calibrate the online measurement based upon the spindle load.
- The results that were established off-line by using the CMM have shown that there was differential tool wear in the cutter. This has a specific and discernible effect on the estimated remaining tool life. In addition, it has an effect on the accuracy of the component geometry.
- The remaining useful life of a cutter has been estimated using the tool wear curve. The results show that this value differs significantly depending on the selected reference point of the cutter.
- The top segments of the cutter suffer from accelerating the rate of tool wear. This behaviour may be related to taking a small cut, which leads to rubbing the metal. It could also be due to the change of the local condition of the material due to the work hardening.

- A new system uses a spindle load has potential. It has been established by the method linking work done to that related to the metal removed.
- The basis for good agreements between the values of the cutting time and the percentage of volume removed has been evaluated by the analysis using CMM and those obtained by using a spindle load.

#### **8.4 Future Work and Recommendations**

This research has produced some original contributions and findings in the field of cutting material operations. However, the following research lines have been identified as the basis of future investigations in this area:

- Experimental Investigations to study the causes of accelerating the tool wear in C1, C2, and C3.
- Experimental investigations of the hole quality based upon the surface roughness measurements.
- Improve the resolution of the spindle motor load since it limited by the percentage.
- Further investigation to study the suitability of using the proposed spindle motor load model to evaluate the tool condition monitoring on different operations as well as remaining useful tool life.
- Find a suitable method for assessing the depth of hole as well as the tool wear in the bottom cutting edges.

# References

- Abbass, J. K. and Al-Habaibeh, A. 2015. A comparative study of using spindle motor power and eddy current for the detection of tool conditions in milling processes. *13th International Conference on Industrial Informatics (INDIN) 2015 IEEE*. Cambridge, UK, July 22-24. pp. 766-770.
- Abele, E. and Altintas, Y. and Brecher, C. 2010. Machine tool spindle units. *CIRP Annals-Manufacturing Technology* 59(2), pp. 781-802.
- Al-Sulaiman, F. A., Baseer, M. A. and Sheikh, A. K. 2005. Use of electrical power for online monitoring of tool condition. *Journal of Materials Processing Technology* 166(3), pp. 364-371.
- Alamin, B. B. 1996. *Tool life prediction and management for an integrated tool selection system*. Durham University.
- Altintas, Y. 1992. Prediction of Cutting Force and Tool Breakage in Milling Feed Drive Current Measurements. *ASME Journal Engineering for Industry* 114(4), p. 386.
- Armarego, E. and Brown, R. H. 1969. The machining of metals. *Prentice-hall inc, englewood cliffs, n. J., 1969, 437 P,*
- Astakhov, V. P. 2004. The assessment of cutting tool wear. *International Journal of Machine Tools and Manufacture* 44(6), pp. 637-647.
- Astakhov, V. P. 2006. *Tribology of metal cutting*. Elsevier.
- Astakhov, V. P. 2007. Effects of the cutting feed, depth of cut, and workpiece (bore) diameter on the tool wear rate. *The International Journal of Advanced Manufacturing Technology* 34(7-8), pp. 631-640.
- Axinte, D. and Andrews, P. 2007. Some considerations on tool wear and workpiece surface quality of holes finished by reaming or milling in a nickel base superalloy. *Proceedings of the Institution of Mechanical Engineers, Part B: Journal of Engineering Manufacture* 221(4), pp. 591-603.
- Axinte, D. and Gindy, N. 2004. Assessment of the effectiveness of a spindle power signal for tool condition monitoring in machining processes. *International journal of production research* 42(13), pp. 2679-2691.



- Aykut, Ş., Bağcı, E., Kentli, A. and Yazıcıoğlu, O. 2007. Experimental observation of tool wear, cutting forces and chip morphology in face milling of cobalt based super-alloy with physical vapour deposition coated and uncoated tool. *Materials and design* 28(6), pp. 1880-1888.
- Bajić, D., Celent, L. and Jozić, S. 2012. Modeling of the influence of cutting parameters on the surface roughness, tool wear and the cutting force in face milling in off-line process control. *Strojniški vestnik-Journal of Mechanical Engineering* 58(11), pp. 673-682.
- Barrow, G. 1972. Tool-life equations and machining economics. *Proceedings of the Twelfth International Machine Tool Design and Research Conference*. Springer.
- ben Wang, H. P. and Wysk, R. A. 1986. An expert system for machining data section. *Computers and Industrial Engineering* 10(2), pp. 99-107.
- Bhattacharyya, P. and Sengupta, D. and Mukhopadhyay, S. 2007. Cutting force-based real-time estimation of tool wear in face milling using a combination of signal processing techniques. *Mechanical Systems and Signal Processing* 21(6), pp. 2665-2683.
- Bhattacharyya, P., Sengupta, D., Mukhopadhyay, S. and Chattopadhyay, A. 2006. Current Signal Based Continuous On-line Tool Condition Estimation in Face Milling. *IEEE International Conference on Industrial Technology, ICIT 2006*.
- Bhattacharyya, P., Sengupta, D., Mukhopadhyay, S. and Chattopadhyay, A. 2008. On-line tool condition monitoring in face milling using current and power signals. *International journal of production research* 46(4), pp. 1187-1201.
- Black, J. T. and Kohser, R. A. 2017. *DeGarmo's materials and processes in manufacturing*. John Wiley & Sons.
- Byrne, G., Dornfeld, D., Inasaki, I., Ketteler, G., König, W. and Teti, R. 1995. Tool condition monitoring (TCM)—the status of research and industrial application. *CIRP Annals-Manufacturing Technology* 44(2), pp. 541-567.
- Caldeirani Filho, J. and Diniz, A. 2002. Influence of cutting conditions on tool life, tool wear and surface finish in the face milling process. *Journal of the Brazilian Society of Mechanical Sciences* 24(1), pp. 10-14.

- Carrilero, M., Bienvenido, R., Sanchez, J., Alvarez, M., Gonzalez, A. and Marcos, M. 2002. A SEM and EDS insight into the BUL and BUE differences in the turning processes of AA2024 Al–Cu alloy. *International Journal of Machine Tools and Manufacture* 42(2), pp. 215-220.
- Castejon, M., Alegre, E., Barreiro, J. and Hernández, L. 2007. On-line tool wear monitoring using geometric descriptors from digital images. *International Journal of Machine Tools and Manufacture* 47(12), pp. 1847-1853.
- Chandgude, S. and Sadaiah, M. 2014. Microcontroller Based Tool Wear Monitoring during End Milling of Hardened Steel. *International Journal of Emerging Technology and Advanced Engineering* 4(5),
- Chen, J. C. M. 2003. *In-process tool wear prediction system development in end milling operations*. Iowa State University.
- Childs, T., Maekawa, K., Obikawa, T. and Yamane, Y. 2000. *Metal machining: theory and applications*. Butterworth-Heinemann.
- Choudhury, S. and Kishore, K. 2000. Tool wear measurement in turning using force ratio. *International Journal of Machine Tools and Manufacture* 40(6), pp. 899-909.
- Choudhury, S. and Rath, S. 2000. In-process tool wear estimation in milling using cutting force model. *Journal of Materials Processing Technology* 99(1), pp. 113-119.
- Choy, H. and Chan, K. 2003. A corner-looping based tool path for pocket milling. *Computer-Aided Design* 35(2), pp. 155-166.
- Colding, B. N. 1961. Machinability of metals and machining costs. *International Journal of Machine Tool Design and Research* 1(3), pp. 220-248.
- Coromant, S. 1994. *Modern Metal Cutting. A practical handbook* Tofters Tryckery AB, 1994.
- Creese, R. 1999. *Introduction to manufacturing processes and materials*. CRC Press.
- Cuppini, D., D'errico, G. and Rutelli, G. 1990. Tool wear monitoring based on cutting power measurement. *Wear* 139(2), pp. 303-311.
- Čuš, F. and Župerl, U. 2011. Real-time cutting tool condition monitoring in milling. *Strojniški vestnik-Journal of Mechanical Engineering* 57(2), pp. 142-150.

- Dasarathi, G. 2016. *CNC: Work hardening, and how it affects CNC machining*. Available at: <https://www.cadem.com/single-post/work-hardening-cnc-machining> [Accessed: 21/3/2018].
- Davoodi, B. and Eskandari, B. 2015. Tool wear mechanisms and multi-response optimization of tool life and volume of material removed in turning of N-155 iron–nickel-base superalloy using RSM. *Measurement* 68, pp. 286-294.
- Diaz, N., Ninomiya, K., Noble, J. and Dornfeld, D. 2012. Environmental impact characterization of milling and implications for potential energy savings in industry. *Procedia CIRP* 1, pp. 518-523.
- Diaz, N., Redelsheimer, E. and Dornfeld, D. 2011. Energy consumption characterization and reduction strategies for milling machine tool use. *Glocalized solutions for sustainability in manufacturing*, pp. 263-267.
- Dimla, D. E. 2000. Sensor signals for tool-wear monitoring in metal cutting operations—a review of methods. *International Journal of Machine Tools and Manufacture* 40(8), pp. 1073-1098.
- Dong, J., Subrahmanyam, K., San Wong, Y., Hong, G. S. and Mohanty, A. 2006. Bayesian-inference-based neural networks for tool wear estimation. *The International Journal of Advanced Manufacturing Technology* 30(9-10), pp. 797-807.
- Drouillet, C., Karandikar, J., Nath, C., Journeaux, A. C., El Mansori, M. and Kurfess, T. 2016. Tool life predictions in milling using spindle power with the neural network technique. *Journal of Manufacturing Processes* 22, pp. 161-168.
- Fairbrother, P. 2010. *HSS vs. Carbide*. Available at: <https://www.rcgroups.com/forums/showthread.php?1324233-HSS-vs-Carbide> [Accessed: 20/4/2017].
- Gokulachandran, J. and Mohandas, K. 2012. Application of regression and fuzzy logic method for prediction of tool life. *Procedia Engineering* 38, pp. 3900-3912.
- Groover, M. P. 2010. *Fundamentals of modern manufacturing: materials processes, and systems*. John Wiley & Sons.
- Gu, J., Barber, G., Tung, S. and Gu, R. J. 1999. Tool life and wear mechanism of uncoated and coated milling inserts. *Wear* 225, pp. 273-284.

Hao, Z., Gao, D., Fan, Y. and Han, R. 2011. New observations on tool wear mechanism in dry machining Inconel718. *International Journal of Machine Tools and Manufacture* 51(12), pp. 973-979.

Hill, J. L., Prickett, P. W. and Grosvenor, R. I. 2018. *CNC spindle signal investigation for the prediction of cutting tool health. PHM Society European Conference.*

Hilscher. 2015. *PC Cards cifx, PCI (CIFX 50-XX, CIFX 50-2XX, CIFX 50-2XX\XX), PCI Express (CIFX 50E-XX) Low Profile PCI Express (CIFX 70E-XX, CIFX 100EH-RE\CUBE).* Available at: [https://www.hilscher.com/fileadmin/cms\\_upload/ja/Resources/pdf/PC\\_Cards\\_CIFX\\_50\\_50E\\_70E\\_100EH\\_UM\\_46\\_EN](https://www.hilscher.com/fileadmin/cms_upload/ja/Resources/pdf/PC_Cards_CIFX_50_50E_70E_100EH_UM_46_EN). [Accessed: 11/2/2017].

Hocheng, H. and Tsao, C. 2006. Effects of special drill bits on drilling-induced delamination of composite materials. *International Journal of Machine Tools and Manufacture* 46(12), pp. 1403-1416.

Hoffman, E. G. 1984. *Fundamentals of tool design.* Society of Manufacturing Engineers.

Hogmark, S. and Olsson, M. 2008. *Wear Mechanisms of HSS Cutting Tools.* GearSolutions. Available at: <http://www.gearsolutions.com/article/detail/5809/wear-mechanisms-of-hss-Cutting> [Accessed: 16/4/2018].

Hongqi, L., Yaoqiang, W., Hongliang, T., Xinyong, M. and Kuanmin, M. 2010. Reconstruction the milling force based on the feed motor current signal. 2010 *International Conference on Mechanical and Electrical Technology (ICMET2010)*, pp. 765-768.

Huang, S., Tan, K., Wong, Y., De Silva, C., Goh, H. and Tan, W. 2007. Tool wear detection and fault diagnosis based on cutting force monitoring. *International Journal of Machine Tools and Manufacture* 47(3), pp. 444-451.

Huo, D., Chen, W., Teng, X., Lin, C. and Yang, K. 2017. Modeling the influence of tool deflection on cutting force and surface generation in micro-milling. *Micromachines* 8(6), p.p 1-10.

Ikua, B. W., Tanaka, H., Obata, F. and Sakamoto, S. 2001. Prediction of cutting forces and machining error in ball end milling of curved surfaces-I theoretical analysis. *Precision Engineering* 25(4), pp. 266-273.

Iliescu, D., Gehin, D., Gutierrez, M. and Girot, F. 2010. Modeling and tool wear in drilling of CFRP. *International Journal of Machine Tools and Manufacture* 50(2), pp. 204-213.

ISO8688-2. 2016. *Tool life testing in milling — Part 2: End milling*. Available at: <https://www.iso.org/obp/ui/#iso:std:iso:8688:-2:ed-1:v1:en> [Accessed: 25/10/2017].

Jawaid, A., Koksai, S. and Sharif, S. 2001. Cutting performance and wear characteristics of PVD coated and uncoated carbide tools in face milling Inconel 718 aerospace alloy. *Journal of Materials Processing Technology* 116(1), pp. 2-9.

Jindal, A. 2012. Analysis of Tool Wear Rate in Drilling Operation Using Scanning Electron Microscope (SEM). *Journal of Minerals and Materials Characterization and Engineering* 11(01), p. 43-54.

John, E. and Grosvenor, R. 2000. Failure data analysis: the application of Excel spreadsheet add ins as an aid to curve fitting. *Quality and Reliability Engineering International* 16(2), pp. 81-89.

Jozic S. and and, B. D. and S., T. 2012. Flank wear in down and up milling. *Proceedings of the 23rd International DAAAM Symposium*, 23(1), pp. 251-254.

Juneja, B. 2005. *Fundamentals of metal cutting and machine tools*. New Age International.

Kalpakjian, S. 1984. *Manufacturing processes for engineering materials*. Pearson Education India.

Kalpakjian, S. and Schmid, S. R. 2014. *Manufacturing engineering and technology*. Pearson Upper Saddle River, NJ, USA.

Karandikar, J. M. Abbas, A. E. and Schmitz, T. L. 2014. Tool life prediction using Bayesian updating. Part 1: Milling tool life model using a discrete grid method. *Precision Engineering* 38(1), pp. 9-17.

Kim, D. and Jeon, D. 2011. Fuzzy-logic control of cutting forces in CNC milling processes using motor currents as indirect force sensors. *Precision Engineering* 35(1), pp. 143-152.

Kim, G., Kim, B. and Chu, C. 2003. Estimation of cutter deflection and form error in ball-end milling processes. *International Journal of Machine Tools and Manufacture* 43(9), pp. 917-924.

Kim, G., Kwon, W. and Chu, C. 2005. Indirect cutting force measurement and cutting force regulation using spindle speed motor current. *International Journal for Manufacturing Science and Technology* 1, pp. 50-64.

Kim, G. D. and Chu, C. N. 1999. Indirect cutting force measurement considering frictional behaviour in a machining centre using feed motor current. *The International Journal of Advanced Manufacturing Technology* 15(7), pp. 478-484.

Kim, T.-Y. and Kim, J. 1996. Adaptive cutting force control for a machining center by using indirect cutting force measurements. *International Journal of Machine Tools and Manufacture* 36(8), pp. 925-937.

Kiran, D. S. R. and Kumar, S. P. 2013. Multi objective optimization of tool life and total cost using 3-level full factorial method in CNC end milling process. *International Journal of Mech. Eng. & Rob. Res.(IJMERR)* 2(3), pp. 2278-0149.

Koren, Y., Ko, T.-R., Ulsoy, A. G. and Danai, K. 1991. Flank wear estimation under varying cutting conditions. *Journal of dynamic systems, measurement, and control* 113(2), pp. 300-307.

Krain, H., Sharman, A. and Ridgway, K. 2007. Optimisation of tool life and productivity when end milling Inconel 718TM. *Journal of Materials Processing Technology* 189(1), pp. 153-161.

Kramer, T. R. 1992. Pocket milling with tool engagement detection. *Journal of Manufacturing Systems* 11(2), pp. 114-123.

Kronenberg, M. 1970. Replacing the Taylor formula by a new tool life equation. *International Journal of Machine Tool Design and Research* 10(2), pp. 193-202.

Kurada, S. and Bradley, C. 1997. A review of machine vision sensors for tool condition monitoring. *Computers in industry* 34(1), pp. 55-72.

Lau, W., Venuvinod, P. and Rubenstein, C. 1980. The relation between tool geometry and the Taylor tool life constant. *International Journal of Machine Tool Design and Research* 20(1), pp. 29-44.

Layegh, S., Lazoglu, I. and Erdim, H. 2013. Tool deflection in five-axis milling. *International Conference and Exhibition on Design and Production of Machines/Dies/Molds*, p.p 1-7.

Lee, B. 1999. Application of the discrete wavelet transform to the monitoring of tool failure in end milling using the spindle motor current. *The International Journal of Advanced Manufacturing Technology* 15(4), pp. 238-243.

Lee, I. H. and Kwon, W. T. 2001. Development of torque monitoring system of induction spindle motor using graphic-programming. *Journal of the Korean Society for Precision Engineering* 18(10), pp. 184-193.

Lee, K. J., Lee, T. M. and Yang, M. Y. 2007. Tool wear monitoring system for CNC end milling using a hybrid approach to cutting force regulation. *The International Journal of Advanced Manufacturing Technology* 32(1-2), pp. 8-17.

Li, A., Zhao, J., Luo, H., Pei, Z. and Wang, Z. 2012. Progressive tool failure in high-speed dry milling of Ti-6Al-4V alloy with coated carbide tools. *The International Journal of Advanced Manufacturing Technology* 58(5), pp. 465-478.

Li, B. 2012. A review of tool wear estimation using theoretical analysis and numerical simulation technologies. *International Journal of Refractory Metals and Hard Materials* 35, pp. 143-151.

Li, H., He, G., Qin, X., Wang, G., Lu, C. and Gui, L. 2014. Tool wear and hole quality investigation in dry helical milling of Ti-6Al-4V alloy. *The International Journal of Advanced Manufacturing Technology* 71(5-8), pp. 1511-1523.

Li, W., Singh, H., Salahshoor, M. and Guo, Y. 2010. The development of a novel on-line optical inspection system for tool conditions in machining processes. *ASME 2010 International Manufacturing Science and Engineering Conference*. American Society of Mechanical Engineers.

Liang, M., Yeap, T., Rahmati, S. and Han, Z. 2002. Fuzzy control of spindle power in end milling processes. *International Journal of Machine Tools and Manufacture* 42(14), pp. 1487-1496.

Lin, S., Lin, J., Lin, C., Jywe, W. and Lin, B. 2006. Life prediction system using a tool's geometric shape for high-speed milling. *The International Journal of Advanced Manufacturing Technology* 30(7), pp. 622-630.

Lin, S. and Lin, R. 1996. Tool wear monitoring in face milling using force signals. *Wear* 198(1-2), pp. 136-142.

Liu, X., Zhang, C., Fang, J. and Guo, S. 2010. A New Method of Tool Wear Measurement. *2010 International Conference on Electrical and Control Engineering (ICECE)*, p.p 2606-2609.

Manufacturing-Terms. 2007. *Coordinate Measuring Machine (CMM)*. Manufacturing Terms. Available at: [https://www.manufacturingterms.com/Coordinate-Measuring-Machine-\(CMM\).html](https://www.manufacturingterms.com/Coordinate-Measuring-Machine-(CMM).html) [Accessed: 11/2/2018].

Mazakus.com. *VERTICAL CENTER SMART 430A*. Available at: <https://www.mazakusa.com/machines/vertical-center-smart-430a/> [Accessed: 16/1/2018].

Milfelner, M., Cus, F. and Balic, J. 2005. An overview of data acquisition system for cutting force measuring and optimization in milling. *Journal of Materials Processing Technology* 164, pp. 1281-1288.

Nagaanjeneyulu K., Avinash, M. and Shanmuka, S. M. 2015. Optimization of Cutting Tool Life Parameters by Application of Taguchi Method on A CNC Milling Machine. *International Journal of Innovative Research in Science, Engineering and Technology* 4(2), pp. 258-294.

Nee, J. G., Dufraigne, W., Evans, J. W. and Hill, M. 2010. *Fundamentals of tool design*. Society of Manufacturing Engineers.

Niaki, F. A., Ulutan, D. and Mears, L. 2015a. In-Process Tool Flank Wear Estimation in Machining Gamma-Prime Strengthened Alloys Using Kalman Filter. *Procedia Manufacturing* 1, pp. 696-707.

Niaki, F. A., Ulutan, D. and Mears, L. 2015b. Stochastic tool wear assessment in milling difficult to machine alloys. *International Journal of Mechatronics and Manufacturing Systems* 8(3-4), pp. 134-159.

Niklasson, G. 1962. Standardized milling test. *Proceedings of the 3rd International MTDR Conference, Birmingham, UK*. university of Birmingham,

Nouri, M., Fussell, B. K., Ziniti, B. L. and Linder, E. 2015. Real-time tool wear monitoring in milling using a cutting condition independent method. *International Journal of Machine Tools and Manufacture* 89, pp. 1-13.



Oliaei, S. N. B. and Karpat, Y. 2016. Influence of tool wear on machining forces and tool deflections during micro milling. *The International Journal of Advanced Manufacturing Technology* 84(9-12), pp. 1963-1980.

Pilafidis, E. 1971. Observations on Taylor n values used in metal cutting. *Annals CIRP* 19, pp. 571-577.

Prickett, P. and Johns, C. 1999. An overview of approaches to end milling tool monitoring. *International Journal of Machine Tools and Manufacture* 39(1), pp. 105-122.

Rassouli, H. 2011. *Conventional Metal Cutting - Understanding the Roles Played by Various Cutting Parameters - (b) Tool Material – HSS*. Available at: <http://www.brighthubengineering.com/manufacturing-technology/49448-high-speed-steel-versus-carbide-in-metal-cutting-why-hss-is-still-in-use>. [Accessed: 18/4/2017].

Reddy, S. M., Reddy, A. C. and Reddy, K. S. 2012. Latest developments in condition monitoring of machining operations. *Journal of Applied Sciences* 12, pp. 938-946.

SandvikCoromant. 2017. *Machining formulas and definitions*. Sandvik Coromant. Available at: <https://www.sandvik.coromant.com/en-gb/knowledge/machining-formulas-definitions/pages/drilling.aspx> [Accessed: 4/4/2018].

Saraie, H., Sakahira, M., Ibaraki, S., Matsubara, A., Kakino, Y. and Fujishima, M. 2003. Monitoring and adaptive control of cutting forces based on spindle motor and servo motor currents in machining centers. *Proc. of the International Conference on Leading Edge Manufacturing in 21st Century*.

Saranya, K. and Jegaraj, J. J. R. and Kumar, K. R. and Rao, G. V. 2016. Artificial Intelligence Based Selection of Optimal Cutting Tool and Process Parameters for Effective Turning and Milling Operations. *Journal of The Institution of Engineers (India): Series C*, pp. 1-12.

Sarhan, A. and Sayed, R. and Nassr, A. and El-Zahry, R. 2001. Interrelationships between cutting force variation and tool wear in end-milling. *Journal of Materials Processing Technology* 109(3), pp. 229-235.

Sarhan, A. A. and El-Zahry, R. 2011. Monitoring of tool wear and surface roughness in end-milling for intelligent machining. *International Journal of Physical Sciences* 6(10), pp. 2380-2392.

Shah, I. B. and Gaw, K. R. 2012. Optimization of Cutting Tool Life on CNC Milling Machine Through Design Of Experiments-A Suitable Approach—An overview. *International Journal of Engineering and Advanced Technology (IJEAT)* 4(1), pp. 188-194.

Shahabi, H. and Ratnam, M. 2009. In-cycle monitoring of tool nose wear and surface roughness of turned parts using machine vision. *The International Journal of Advanced Manufacturing Technology* 40(11-12), pp. 1148-1157.

Shao, H. and Wang, H. and Zhao, X. 2004. A cutting power model for tool wear monitoring in milling. *International Journal of Machine Tools and Manufacture* 44(14), pp. 1503-1509.

Shaw, M. C. 2005. *Metal cutting principles*. Oxford University Press.

Shin, B.c., Kim, G. h., Choi, J. h., Jeon, B. c., Lee, H., Cho, M. w., Han, J. y. and Park, D. s. 2006. A Web-based machining process monitoring system for E-manufacturing implementation. *Journal of Zhejiang University-SCIENCE A* 7(9), pp. 1467-1473.

Shyha, I., Aspinwall, D. and Soo, S. L. and Bradley, S. 2009. Drill geometry and operating effects when cutting small diameter holes in CFRP. *International Journal of Machine Tools and Manufacture* 49(12), pp. 1008-1014.

Sivasakthivel P.S., V. M. V. a. S. R. 2010. Prediction of Tool Wear from Machining Parameters by Response Surface Methodology in End Milling. *International Journal of Engineering Science and Technology* 6(2), pp. 1780-1789.

Spitler, D. and Lantrip, J. and Nee, J. G. and Smith, D. A. 2003. *Fundamentals of tool design*. Society of Manufacturing Engineers.

Stavropoulos, P., Chantzis, D., Doukas, C., Papacharalampopoulos, A. and Chryssolouris, G. 2013. Monitoring and control of manufacturing processes: A review. *Procedia CIRP* 8, pp. 421-425.

Stephenson, D. A. and Agapiou, J. S. 2016. *Metal cutting theory and practice*. CRC press.

Taylor, F. W. 1907. *On the art of cutting metals*. New York, The American Society of Mechanical Engineers,[1907]

Toh, C. 2006. Cutter path strategies in high speed rough milling of hardened steel. *Materials and design* 27(2), pp. 107-114.

Vallejo, A. J., Morales-Menéndez, R., Rodriguez, C. A. and Sucar, L. E. 2006. Diagnosis of a cutting tool in a machining center. *International Joint Conference on Neural Networks, 2006. IJCNN'06*. IEEE.

Vučina, D., Bajić, D., Jozić, S. and Pehnc, I. 2013. Evaluation Of 3D Tool Wear In Machining By Successive Stereophotogrammetry And Point Cloud Processing. *Tehnicki vjesnik/Technical Gazette* 20(3), pp. 1-10.

Wang, Y. C., Chen, C. H. and Lee, B. Y. 2014. Analysis model of parameters affecting cutting performance in high-speed machining. *The International Journal of Advanced Manufacturing Technology* 72(1-4), pp. 521-530.

Warfield, B. 2016. *Chip Thinning, Lead Angles, and Ballnose Compensation*. Available at: <http://s3.cnccookbook.com/CCChipThinning.htm> [Accessed: 28/3/2018].

Xiaoli, L. and Zhejun, Y. 1998. Tool wear monitoring with wavelet packet transform—fuzzy clustering method. *Wear* 219(2), pp. 145-154.

Xie, L. J., Schmidt, J., Schmidt, C. and Biesinger, F. 2005. 2D FEM estimate of tool wear in turning operation. *Wear* 258(10), pp. 1479-1490.

Xue, C. and Chen, W. 2011. Adhering layer formation and its effect on the wear of coated carbide tools during turning of a nickel-based alloy. *Wear* 270(11-12), pp. 895-902.

Yoon, H.-S. and Lee, J.-Y. and Kim, M.-S. and Ahn, S.-H. 2014. Empirical power-consumption model for material removal in three-axis milling. *Journal of cleaner production* 78, pp. 54-62.

Zhang, C., Liu, X., Fang, J. and Zhou, L. 2011. A new tool wear estimation method based on shape mapping in the milling process. *The International Journal of Advanced Manufacturing Technology* 53(1), pp. 121-130.

Zhang, C. and Zhou, L. 2013. Modeling of tool wear for ball end milling cutter based on shape mapping. *International Journal on Interactive Design and Manufacturing (IJIDeM)* 7(3), pp. 171-181.

Zhao, Q., Qin, X., Ji, C., Li, Y., Sun, D. and Jin, Y. 2015. Tool life and hole surface integrity studies for hole-making of Ti6Al4V alloy. *The International Journal of Advanced Manufacturing Technology* 79(5-8), pp. 1017-1026.

Zuperl, U., Cus, F. and Balic, J. 2011. Intelligent cutting tool condition monitoring in milling. *Journal of Achievements in Materials and Manufacturing Engineering* 49(2), pp. 477-486.

# APPENDIX A

## The Tool Details



HSS Milling Cutters 251E

### End Mills HSS-E – Type N Finishing Profile – Multi-Flutes

- DIN 844-B, Type N
- Right hand spiral 30°, 3 – 6 flutes
- Shank to DIN 1835-B (Weldon)
- Centre cutting up to Ø 20 mm



Standard Series

Size - Ø x L (mm)	Flute Length	Overall Length	Shank Ø x L	HERTEL Uncoated			HERTEL TiN Coated			DORMER PRAMET C298 Uncoated			DORMER PRAMET C677 Super G Coated		
				Ordering Code	Reg. Price	Offer Price	Ordering Code	Reg. Price	Offer Price	Ordering Code	Reg. Price	Offer Price	Ordering Code	Reg. Price	Offer Price
2.5	8	52	6	---	---	---	CAT-52225B	19.99	13.99	---	---	---	---	---	---
3.0	8	52	6	CAA-12180L	11.79	8.25	CAT-52103A	12.99	9.09	HSS-73806E	48.85	29.31	HSS-85200A	73.50	43.98
4.0	11	55	6	CAA-12184B	11.79	8.25	CAT-52104A	12.99	9.09	HSS-73807E	48.85	29.37	HSS-85201A	73.48	44.84
5.0	13	57	6	CAA-12185A	11.79	8.25	CAT-52105A	12.99	9.09	HSS-73808E	48.40	29.04	HSS-85202E	72.50	43.50
5.5	13	57	6	---	---	---	CAT-52106A	34.50	24.15	---	---	---	---	---	---
6.0	13	57	6	CAA-12186M	11.79	8.25	CAT-52106B	12.99	9.09	HSS-73809H	48.85	29.31	HSS-85203E	73.20	43.82
7.0	16	66	10	CAA-12187J	11.79	8.25	---	---	---	---	---	---	---	---	---
8.0	19	69	10	CAA-12188B	12.87	9.08	CAT-52106H	17.48	12.24	HSS-73804C	91.80	37.00	HSS-85204L	86.40	51.84
9.0	19	69	10	CAA-12189B	15.33	10.73	---	---	---	---	---	---	---	---	---
10.0	22	72	10	CAA-12190A	15.33	10.73	CAT-52110C	18.48	12.94	HSS-73805M	67.70	40.62	HSS-85205H	94.80	56.88
11.0	22	79	12	CAA-12191A	18.58	13.01	CAT-52110A	29.99	20.99	---	---	---	---	---	---
12.0	26	83	12	CAA-12192E	20.50	14.35	CAT-52112J	20.99	14.69	HSS-73806J	79.80	47.88	HSS-85206C	112.00	67.20
13.0	26	83	12	CAA-12193B	22.99	16.09	---	---	---	---	---	---	---	---	---
14.0	26	83	12	CAA-12194L	25.29	17.70	CAT-52114A	31.99	22.39	HSS-73807D	100.00	60.00	HSS-85207M	140.80	84.80
15.0	26	83	12	CAA-12195B	31.24	21.87	---	---	---	---	---	---	---	---	---
16.0	32	92	16	CAA-12196C	27.89	19.52	CAT-52116E	32.99	23.09	HSS-73808A	120.00	72.00	HSS-85208J	168.00	100.80
18.0	32	92	16	CAA-12197J	24.77	17.34	CAT-52116E	41.99	29.38	HSS-73809E	136.00	81.60	HSS-85209B	191.00	114.60
20.0	36	104	20	CAA-12198B	33.29	23.38	CAT-52120B	39.99	27.99	HSS-73810K	159.00	95.40	HSS-85210B	225.00	133.20
25.0	45	121	25	CAA-12195L	64.04	44.83	CAT-52125A	71.99	50.39	HSS-73811E	267.00	160.20	HSS-85212K	347.00	208.20

MILLING

### HERTEL End Mills HSS-E – Type N Ball Nosed Finishing Profile – Multi-Flutes

- Type N
- Right hand spiral 30°, 4 – 6 flutes
- HSS-Co8, uncoated and TiAlN coated
- Shank to DIN 1835-B (Weldon)
- Centre cutting
- Suitable to cut keyways to tolerance P9
- For sinking, copy and radius milling



Standard Series

Size - Ø x L (mm)	Flute Length	Overall Length	Shank Ø x L	No. of Flutes	UNCOATED			TiAlN COATED		
					Ordering Code	Reg. Price	Offer Price	Ordering Code	Reg. Price	Offer Price
8	19	69	10	4	HAA-40575C	19.99	13.99	HAT-40575C	27.48	19.23
10	22	72	10	4	HAA-40715C	36.99	21.68	HAT-40715C	37.28	26.10
12	26	83	12	4	HAA-40944M	36.99	25.89	HAT-40944M	42.73	29.91
16	32	92	16	4	HAA-40722A	67.99	47.59	HAT-40722A	78.56	53.58
20	38	104	20	4	HAA-40830J	85.99	60.19	HAT-40830J	93.20	65.24
25	45	121	25	6	HAA-40787B	138.33	96.83	HAT-40787B	164.32	115.02

### End Mills HSS-E – Type N Finishing Profile – Multi-Flutes

- DIN 844-B, Type N
- Right hand spiral 30°, 4 – 6 flutes
- HSS-Co8, uncoated and TiAlN coated
- Shank to DIN 1835-B (Weldon)
- Centre cutting up to Ø 20 mm
- Suitable to cut keyways to tolerance P9
- For materials up to 1600 N/mm2
- For profile and slot milling



Long Series

Size - Ø x L (mm)	Flute Length	Overall Length	Shank Ø x L	HERTEL Uncoated			HERTEL TiAlN Coated			DORMER PRAMET C273 Uncoated			DORMER PRAMET C699 Super G Coated		
				Ordering Code	Reg. Price	Offer Price	Ordering Code	Reg. Price	Offer Price	Ordering Code	Reg. Price	Offer Price	Ordering Code	Reg. Price	Offer Price
2	10	54	6	---	---	---	---	---	HSS-73400L	53.00	31.80	---	---	---	
3	12	56	6	CAA-22183B	11.49	8.04	---	---	HSS-73402E	50.00	30.00	---	---	---	
4	13	63	6	CAA-22184L	11.49	8.04	---	---	HSS-73404L	50.00	30.00	---	---	---	
5	24	65	6	CAA-22185B	11.49	8.04	---	---	HSS-73406C	48.50	29.70	---	---	---	
6	24	65	6	CAA-22186C	11.49	8.04	---	---	HSS-73408J	48.85	29.91	---	---	---	
7	30	80	10	CAA-22187M	22.99	16.09	CAT-62106E	14.99	10.49	---	---	---	---	---	
8	38	88	10	CAA-22188L	15.99	11.19	CAT-62108E	28.91	20.24	HSS-73410H	63.20	37.02	---	---	---
9	38	88	10	CAA-22189B	22.99	16.09	CAT-62109H	45.44	31.81	---	---	---	---	---	
10	45	95	10	CAA-22190A	46.99	32.89	CAT-62118H	23.31	16.32	HSS-73412K	69.20	41.52	---	---	---
12	53	110	12	CAA-22192X	17.89	12.59	CAT-62120A	27.55	19.20	HSS-73414E	81.80	49.08	HSS-79901M	115.00	69.00
13	53	110	12	---	---	---	---	---	HSS-73415L	106.00	65.40	---	---	---	
14	53	110	12	CAA-22194B	35.99	25.19	CAT-62114B	38.00	26.60	---	---	---	---	---	
16	63	123	16	CAA-22196B	32.99	23.09	CAT-62116E	45.99	32.19	HSS-73418M	123.00	75.80	HSS-79903D	173.00	103.90
18	63	123	16	CAA-22198M	46.99	32.89	CAT-62118H	61.87	43.38	---	---	---	---	---	
20	75	141	20	CAA-22120L	39.99	27.99	CAT-62120L	54.74	38.32	HSS-73420L	162.00	97.20	HSS-79905K	229.00	137.40
22	75	141	20	CAA-22192A	89.99	62.99	---	---	---	---	---	---	---	---	---
25	90	166	25	---	---	---	CAT-62125D	102.25	71.58	HSS-73422A	273.00	163.80	HSS-79906E	358.00	214.80
30	95	165	25	---	---	---	CAT-62130E	140.48	98.34	---	---	---	---	---	
32	108	185	32	---	---	---	CAT-62132A	190.76	126.53	---	---	---	---	---	

FREE PHONE 0800 66 33 55

www.msdirect.co.uk

FREE FAX 0800 58 00 58

251E

# APPENDIX B

## CMM Program

```
D:\Filtr\spepwp\My Files\Teaching15\Projects\Equator\Tool_Wear.dmi
DMISMN/'Start Template',05.2
FILNAM/'Start Template',05.2
DV(0)=DMESWV/'16,1,0,184'
UNITS/MM,ANGDEC
DECPL/ALL,DEFAULT
V(0)=VFORM/ALL,PLOT
DISPLY/TERM,V(0),STOR,DMIS,V(0)
SNSET/APPRCH,5
SNSET/CLRSRF,15
SNSET/DEPTH,0
D(0)=DATSET/MCS
MODE/MAN
T(CORTOL_X1)=TOL/CORTOL,XAXIS,-0.1,0.1
T(CORTOL_Y1)=TOL/CORTOL,YAXIS,-0.1,0.1
T(CORTOL_Z1)=TOL/CORTOL,ZAXIS,-0.1,0.1
T(DIAM_1)=TOL/DIAM,-0.1,0.1
RECALL/SA(RSP2_RSH250_3x30.1.30.3.A0.0-B0.0)
SNSLCT/SA(RSP2_RSH250_3x30.1.30.3.A0.0-B0.0)
$$ Manual Alignment $$
TEXT/OPER,'Take 4 Points on Top Plane Bores 1 3 5 7'
MODE/MAN
F(PLN001)=FEAT/PLANE,CART,0,0,25,0,0,1
MEAS/PLANE,F(PLN001),4
ENDMES
DATDEF/FA(PLN001), DAT(A)
D(1)=DATSET/DAT(A),ZDIR,ZORIG
TEXT/OPER,'Take 6 Points in Bore 1'
MODE/MAN
F(CYL001)=FEAT/CYLNDR,INNER,CART,0,0,0,0,0,1,40,-20
MEAS/CYLNDR,F(CYL001),6
```

```
ENDMES
TEXT/OPER, 'Take 6 Points in Bore 7'
MODE/MAN
F (CYL002)=FEAT/CYLNR, INNER, CART, 165.99, 0, 0, 0, 0, 1, 40, -20
MEAS/CYLNR, F (CYL002), 6
ENDMES
F (LINE001)=FEAT/LINE, UNBND, CART, 82.995, 0, 0, 1, 0, 0, 0, 0, 1
CONST/LINE, F (LINE001), BF, FA (CYL001), FA (CYL002)
DATDEF/FA (PLN001), DAT (A)
DATDEF/FA (LINE001), DAT (C)
DATDEF/FA (PLN001), DAT (A)
DATDEF/FA (LINE001), DAT (C)
DATDEF/FA (CYL001), DAT (B)
D (ISO8688-2)=DATSET/DAT (A), ZDIR, ZORIG, DAT (C), XDIR, DAT (B), XORIG, YORIG
TEXT/OPER, 'Move Probe to Safe Position Above Bore 1'
$$ CNC Alignment $$

MODE/PROG, MAN
F (PLN002)=FEAT/PLANE, CART, 0, 0, 0, 0, 0, 1
MEAS/PLANE, F (PLN002), 4
PTMEAS/CART, 26.449, 18.305, 0.001, -0.002, -0, 1, PCS, 96.013, 0.123, 174.476
PTMEAS/CART, 26.921, -21.934, -0.001, -
0.002, 0.001, 1, PCS, 95.977, 0.124, 174.511
PTMEAS/CART, 139.166, -16.721, 0.003, -
0.002, 0.002, 1, PCS, 96.059, 0.122, 174.429
PTMEAS/CART, 138.447, 19.667, -0.003, -0.001, -
0, 1, PCS, 96.03, 0.123, 174.458
ENDMES
DATDEF/FA (PLN002), DAT (D)
D (3)=DATSET/DAT (D), ZDIR, ZORIG
GOTO/CART, 0, 0, 10, HEADCS, 0, 0
MODE/PROG, MAN
F (CYL003)=FEAT/CYLNR, INNER, CART, 0, 0, 0, 0, 0, 1, 40, -20
MEAS/CYLNR, F (CYL003), 6
PTMEAS/CART, 0.237, 19.972, -2.473, 0.007, -
1, 0.002, PCS, 96.189, 0.12, 174.294
PTMEAS/CART, -18.344, 7.367, -
2.451, 0.993, 0.117, 0, PCS, 96.155, 0.121, 174.328
```

```

PTMEAS/CART,-16.812,-10.624,-2.413,0.591,0.806,-
0.001,PCS,96.179,0.12,174.304

PTMEAS/CART,9.384,-17.632,-2.392,-0.492,0.871,-
0.002,PCS,96.14,0.121,174.343

PTMEAS/CART,19.928,1.553,-2.429,-0.997,-0.077,-
0,PCS,96.204,0.12,174.279

PTMEAS/CART,14.311,13.955,-2.456,-0.699,-
0.715,0.001,PCS,96.179,0.12,174.303

ENDMES

GOTO/CART,0,0,10,HEADCS,0,0

GOTO/CART,165.99,0,10,HEADCS,0,0

MODE/PROG,MAN

F(CYL004)=FEAT/CYLNR,INNER,CART,165.99,0,0,0,0,1,40,-20

MEAS/CYLNR,F(CYL004),6

PTMEAS/CART,165.864,20.359,-2.619,0.007,-
1,0.002,PCS,96.173,0.12,174.309

PTMEAS/CART,149.756,11.968,-2.605,0.712,-
0.702,0.002,PCS,96.167,0.121,174.316

PTMEAS/CART,148.009,-8.145,-2.565,0.734,0.679,-
0.001,PCS,96.161,0.121,174.322

PTMEAS/CART,168.281,-19.43,-2.536,-0.208,0.978,-
0.002,PCS,96.177,0.12,174.305

PTMEAS/CART,185.006,-5.138,-2.562,-0.982,-
0.189,0,PCS,96.173,0.12,174.31

PTMEAS/CART,179.501,15.03,-2.605,-0.467,-
0.884,0.002,PCS,96.158,0.121,174.325

ENDMES

F(LINE002)=FEAT/LINE,UNBND,CART,82.995,0,0,1,0,0,0,0,1

CONST/LINE,F(LINE002),BF,FA(CYL003),FA(CYL004)

DATDEF/FA(PLN002),DAT(D)

DATDEF/FA(LINE002),DAT(F)

DATDEF/FA(PLN002),DAT(D)

DATDEF/FA(LINE002),DAT(F)

DATDEF/FA(CYL003),DAT(G)

D(4)=DATSET/DAT(D),ZDIR,ZORIG,DAT(F),XDIR,DAT(G),XORIG,YORIG

GOTO/CART,165.99,0,10,HEADCS,0,0

GOTO/CART,0,0,10,HEADCS,0,0

$$ Start of Measurement $$

P(PArc8)=PATH/ARC,CART,0,0,0,0,0,1,20,0,360,1,0,0

P(PArc9)=PATH/ARC,CART,0,0,-2.5,0,0,1,20,0,360,1,0,0

MODE/PROG,MAN

```



```
F (CYL006) =FEAT/CYLNR, INNER, CART, 0, 0, 0, 0, 0, 1, 40, -20
MEAS/CYLNR, F (CYL006), 6
PAMEAS/DISTANCE, 0.5, SCNVEL, MMPS, 100, P (PArc8), -1, 0, 0
PAMEAS/DISTANCE, 0.5, SCNVEL, MMPS, 100, P (PArc9), -1, 0, 0
ENDMES

P (PArc10) =PATH/ARC, CART, 0, 0, -5.5, 0, 0, 1, 20, 0, 360, 1, 0, 0
P (PArc11) =PATH/ARC, CART, 0, 0, -8, 0, 0, 1, 20, 0, 360, 1, 0, 0
MODE/PROG, MAN
F (CYL007) =FEAT/CYLNR, INNER, CART, 0, 0, 0, 0, 0, 1, 40, -20
MEAS/CYLNR, F (CYL007), 6
PAMEAS/DISTANCE, 0.5, SCNVEL, MMPS, 100, P (PArc10), -1, 0, 0
PAMEAS/DISTANCE, 0.5, SCNVEL, MMPS, 100, P (PArc11), -1, 0, 0
ENDMES

P (PArc12) =PATH/ARC, CART, 0, 0, -10.5, 0, 0, 1, 20, 0, 360, 1, 0, 0
P (PArc13) =PATH/ARC, CART, 0, 0, -13, 0, 0, 1, 20, 0, 360, 1, 0, 0
MODE/PROG, MAN
F (CYL008) =FEAT/CYLNR, INNER, CART, 0, 0, 0, 0, 0, 1, 40, -20
MEAS/CYLNR, F (CYL008), 6
PAMEAS/DISTANCE, 0.5, SCNVEL, MMPS, 100, P (PArc12), -1, 0, 0
PAMEAS/DISTANCE, 0.5, SCNVEL, MMPS, 100, P (PArc13), -1, 0, 0
ENDMES

P (PArc14) =PATH/ARC, CART, 0, 0, -15.5, 0, 0, 1, 20, 0, 360, 1, 0, 0
P (PArc15) =PATH/ARC, CART, 0, 0, -18, 0, 0, 1, 20, 0, 360, 1, 0, 0
MODE/PROG, MAN
F (CYL009) =FEAT/CYLNR, INNER, CART, 0, 0, 0, 0, 0, 1, 40, -20
MEAS/CYLNR, F (CYL009), 6
PAMEAS/DISTANCE, 0.5, SCNVEL, MMPS, 100, P (PArc14), -1, 0, 0
PAMEAS/DISTANCE, 0.5, SCNVEL, MMPS, 100, P (PArc15), -1, 0, 0
ENDMES

GOTO/CART, 0, 0, 10, HEADCS, 0, 0
GOTO/CART, 0, -71, 10, HEADCS, 0, 0
P (PArc24) =PATH/ARC, CART, 0, -71, 0, 0, 0, 1, 20, 0, 360, 1, 0, 0
P (PArc25) =PATH/ARC, CART, 0, -71, -2.5, 0, 0, 1, 20, 0, 360, 1, 0, 0
MODE/PROG, MAN
F (CYL014) =FEAT/CYLNR, INNER, CART, 0, -71, 0, 0, 0, 1, 40, -20
MEAS/CYLNR, F (CYL014), 6
```

```
PAMEAS/DISTANCE,0.5,SCNVEL,MMPS,100,P(PARc24),-1,0,0
PAMEAS/DISTANCE,0.5,SCNVEL,MMPS,100,P(PARc25),-1,0,0
ENDMES
P(PARc26)=PATH/ARC,CART,0,-71,-5.5,0,0,1,20,0,360,1,0,0
P(PARc27)=PATH/ARC,CART,0,-71,-8,0,0,1,20,0,360,1,0,0
MODE/PROG,MAN
F(CYL015)=FEAT/CYLNR,INNER,CART,0,-71,0,0,0,1,40,-20
MEAS/CYLNR,F(CYL015),6
PAMEAS/DISTANCE,0.5,SCNVEL,MMPS,100,P(PARc26),-1,0,0
PAMEAS/DISTANCE,0.5,SCNVEL,MMPS,100,P(PARc27),-1,0,0
ENDMES
P(PARc28)=PATH/ARC,CART,0,-71,-10.5,0,0,1,20,0,360,1,0,0
P(PARc29)=PATH/ARC,CART,0,-71,-13,0,0,1,20,0,360,1,0,0
MODE/PROG,MAN
F(CYL016)=FEAT/CYLNR,INNER,CART,0,-71,0,0,0,1,40,-20
MEAS/CYLNR,F(CYL016),6

PAMEAS/DISTANCE,0.5,SCNVEL,MMPS,100,P(PARc28),-1,0,0
PAMEAS/DISTANCE,0.5,SCNVEL,MMPS,100,P(PARc29),-1,0,0
ENDMES
P(PARc30)=PATH/ARC,CART,0,-71,-15.5,0,0,1,20,0,360,1,0,0
P(PARc31)=PATH/ARC,CART,0,-71,-18,0,0,1,20,0,360,1,0,0
MODE/PROG,MAN
F(CYL017)=FEAT/CYLNR,INNER,CART,0,-71,0,0,0,1,40,-20
MEAS/CYLNR,F(CYL017),6
PAMEAS/DISTANCE,0.5,SCNVEL,MMPS,100,P(PARc30),-1,0,0
PAMEAS/DISTANCE,0.5,SCNVEL,MMPS,100,P(PARc31),-1,0,0
ENDMES
GOTO/CART,0,-71,10,HEADCS,0,0
GOTO/CART,55.33,0,10,HEADCS,0,0
P(PARc32)=PATH/ARC,CART,55.33,0,0,0,0,1,20,0,360,1,0,0
P(PARc33)=PATH/ARC,CART,55.33,0,-2.5,0,0,1,20,0,360,1,0,0
MODE/PROG,MAN
F(CYL018)=FEAT/CYLNR,INNER,CART,55.33,0,0,0,0,1,40,-20
MEAS/CYLNR,F(CYL018),6
PAMEAS/DISTANCE,0.5,SCNVEL,MMPS,100,P(PARc32),-1,0,0
PAMEAS/DISTANCE,0.5,SCNVEL,MMPS,100,P(PARc33),-1,0,0
```

```
ENDMES
P (PArc34)=PATH/ARC,CART,55.33,0,-5.5,0,0,1,20,0,360,1,0,0
P (PArc35)=PATH/ARC,CART,55.33,0,-8,0,0,1,20,0,360,1,0,0
MODE/PROG,MAN
F (CYL019)=FEAT/CYLNDR,INNER,CART,55.33,0,0,0,0,1,40,-20
MEAS/CYLNDR,F (CYL019),6
PAMEAS/DISTANCE,0.5,SCNVEL,MMPS,100,P (PArc34),-1,0,0
PAMEAS/DISTANCE,0.5,SCNVEL,MMPS,100,P (PArc35),-1,0,0
ENDMES
P (PArc36)=PATH/ARC,CART,55.33,0,-10.5,0,0,1,20,0,360,1,0,0
P (PArc37)=PATH/ARC,CART,55.33,0,-13,0,0,1,20,0,360,1,0,0
MODE/PROG,MAN
F (CYL020)=FEAT/CYLNDR,INNER,CART,55.33,0,0,0,0,1,40,-20
MEAS/CYLNDR,F (CYL020),6
PAMEAS/DISTANCE,0.5,SCNVEL,MMPS,100,P (PArc36),-1,0,0
PAMEAS/DISTANCE,0.5,SCNVEL,MMPS,100,P (PArc37),-1,0,0
ENDMES
P (PArc38)=PATH/ARC,CART,55.33,0,-15.5,0,0,1,20,0,360,1,0,0
P (PArc39)=PATH/ARC,CART,55.33,0,-18,0,0,1,20,0,360,1,0,0
MODE/PROG,MAN
F (CYL021)=FEAT/CYLNDR,INNER,CART,55.33,0,0,0,0,1,40,-20
MEAS/CYLNDR,F (CYL021),6
PAMEAS/DISTANCE,0.5,SCNVEL,MMPS,100,P (PArc38),-1,0,0
PAMEAS/DISTANCE,0.5,SCNVEL,MMPS,100,P (PArc39),-1,0,0
ENDMES
GOTO/CART,55.33,0,10,HEADCS,0,0
GOTO/CART,55.33,-71,10,HEADCS,0,0

P (PArc40)=PATH/ARC,CART,55.33,-71,0,0,0,1,20,0,360,1,0,0
P (PArc41)=PATH/ARC,CART,55.33,-71,-2.5,0,0,1,20,0,360,1,0,0
MODE/PROG,MAN
F (CYL022)=FEAT/CYLNDR,INNER,CART,55.33,-71,0,0,0,1,40,-20
MEAS/CYLNDR,F (CYL022),6
PAMEAS/DISTANCE,0.5,SCNVEL,MMPS,100,P (PArc40),-1,0,0
PAMEAS/DISTANCE,0.5,SCNVEL,MMPS,100,P (PArc41),-1,0,0
ENDMES
P (PArc42)=PATH/ARC,CART,55.33,-71,-5.5,0,0,1,20,0,360,1,0,0
```

```
P (PArc43)=PATH/ARC,CART,55.33,-71,-8,0,0,1,20,0,360,1,0,0
MODE/PROG,MAN
F (CYL023)=FEAT/CYLNDR,INNER,CART,55.33,-71,0,0,0,1,40,-20
MEAS/CYLNDR,F (CYL023),6
PAMEAS/DISTANCE,0.5,SCNVEL,MMPS,100,P (PArc42),-1,0,0
PAMEAS/DISTANCE,0.5,SCNVEL,MMPS,100,P (PArc43),-1,0,0
ENDMES
P (PArc44)=PATH/ARC,CART,55.33,-71,-10.5,0,0,1,20,0,360,1,0,0
P (PArc45)=PATH/ARC,CART,55.33,-71,-13,0,0,1,20,0,360,1,0,0
MODE/PROG,MAN
F (CYL024)=FEAT/CYLNDR,INNER,CART,55.33,-71,0,0,0,1,40,-20
MEAS/CYLNDR,F (CYL024),6
PAMEAS/DISTANCE,0.5,SCNVEL,MMPS,100,P (PArc44),-1,0,0
PAMEAS/DISTANCE,0.5,SCNVEL,MMPS,100,P (PArc45),-1,0,0
ENDMES
P (PArc46)=PATH/ARC,CART,55.33,-71,-15.5,0,0,1,20,0,360,1,0,0
P (PArc47)=PATH/ARC,CART,55.33,-71,-18,0,0,1,20,0,360,1,0,0
MODE/PROG,MAN
F (CYL025)=FEAT/CYLNDR,INNER,CART,55.33,-71,0,0,0,1,40,-20
MEAS/CYLNDR,F (CYL025),6
PAMEAS/DISTANCE,0.5,SCNVEL,MMPS,100,P (PArc46),-1,0,0
PAMEAS/DISTANCE,0.5,SCNVEL,MMPS,100,P (PArc47),-1,0,0
ENDMES
GOTO/CART,55.33,-71,10,HEADCS,0,0
GOTO/CART,111,0,10,HEADCS,0,0
P (PArc48)=PATH/ARC,CART,110.66,0,0,0,0,1,20,0,360,1,0,0
P (PArc49)=PATH/ARC,CART,110.66,0,-2.5,0,0,1,20,0,360,1,0,0
MODE/PROG,MAN
F (CYL026)=FEAT/CYLNDR,INNER,CART,110.66,0,0,0,0,1,40,-20
MEAS/CYLNDR,F (CYL026),6
PAMEAS/DISTANCE,0.5,SCNVEL,MMPS,100,P (PArc48),-1,0,0
PAMEAS/DISTANCE,0.5,SCNVEL,MMPS,100,P (PArc49),-1,0,0
ENDMES
P (PArc50)=PATH/ARC,CART,110.66,0,-5.5,0,0,1,20,0,360,1,0,0
P (PArc51)=PATH/ARC,CART,110.66,0,-8,0,0,1,20,0,360,1,0,0
MODE/PROG,MAN
F (CYL027)=FEAT/CYLNDR,INNER,CART,110.66,0,0,0,0,1,40,-20
```

```
MEAS/CYLNDR, F (CYL027) , 6
PAMEAS/DISTANCE, 0.5, SCNVEL, MMPS, 100, P (PArc50) , -1, 0, 0
PAMEAS/DISTANCE, 0.5, SCNVEL, MMPS, 100, P (PArc51) , -1, 0, 0
ENDMES

P (PArc52) =PATH/ARC, CART, 110.66, 0, -10.5, 0, 0, 1, 20, 0, 360, 1, 0, 0
P (PArc53) =PATH/ARC, CART, 110.66, 0, -13, 0, 0, 1, 20, 0, 360, 1, 0, 0
MODE/PROG, MAN
F (CYL028) =FEAT/CYLNDR, INNER, CART, 110.66, 0, 0, 0, 0, 1, 40, -20
MEAS/CYLNDR, F (CYL028) , 6
PAMEAS/DISTANCE, 0.5, SCNVEL, MMPS, 100, P (PArc52) , -1, 0, 0
PAMEAS/DISTANCE, 0.5, SCNVEL, MMPS, 100, P (PArc53) , -1, 0, 0
ENDMES

P (PArc54) =PATH/ARC, CART, 110.66, 0, -15.5, 0, 0, 1, 20, 0, 360, 1, 0, 0
P (PArc55) =PATH/ARC, CART, 110.66, 0, -18, 0, 0, 1, 20, 0, 360, 1, 0, 0
MODE/PROG, MAN
F (CYL029) =FEAT/CYLNDR, INNER, CART, 110.66, 0, 0, 0, 0, 1, 40, -20
MEAS/CYLNDR, F (CYL029) , 6
PAMEAS/DISTANCE, 0.5, SCNVEL, MMPS, 100, P (PArc54) , -1, 0, 0
PAMEAS/DISTANCE, 0.5, SCNVEL, MMPS, 100, P (PArc55) , -1, 0, 0
ENDMES

GOTO/CART, 111, 0, 10, HEADCS, 0, 0
GOTO/CART, 111, -71, 10, HEADCS, 0, 0
P (PArc56) =PATH/ARC, CART, 110.66, -71, 0, 0, 0, 1, 20, 0, 360, 1, 0, 0
P (PArc57) =PATH/ARC, CART, 110.66, -71, -2.5, 0, 0, 1, 20, 0, 360, 1, 0, 0
MODE/PROG, MAN
F (CYL030) =FEAT/CYLNDR, INNER, CART, 110.66, -71, 0, 0, 0, 1, 40, -20
MEAS/CYLNDR, F (CYL030) , 6
PAMEAS/DISTANCE, 0.5, SCNVEL, MMPS, 100, P (PArc56) , -1, 0, 0
PAMEAS/DISTANCE, 0.5, SCNVEL, MMPS, 100, P (PArc57) , -1, 0, 0
ENDMES

P (PArc58) =PATH/ARC, CART, 110.66, -71, -5.5, 0, 0, 1, 20, 0, 360, 1, 0, 0
P (PArc59) =PATH/ARC, CART, 110.66, -71, -8, 0, 0, 1, 20, 0, 360, 1, 0, 0
MODE/PROG, MAN
F (CYL031) =FEAT/CYLNDR, INNER, CART, 110.66, -71, 0, 0, 0, 1, 40, -20
MEAS/CYLNDR, F (CYL031) , 6
PAMEAS/DISTANCE, 0.5, SCNVEL, MMPS, 100, P (PArc58) , -1, 0, 0
```

```
PAMEAS/DISTANCE,0.5,SCNVEL,MMPS,100,P(PARc59),-1,0,0
ENDMES
P(PARc60)=PATH/ARC,CART,110.66,-71,-10.5,0,0,1,20,0,360,1,0,0
P(PARc61)=PATH/ARC,CART,110.66,-71,-13,0,0,1,20,0,360,1,0,0
MODE/PROG,MAN
F(CYL032)=FEAT/CYLNR,INNER,CART,110.66,-71,0,0,0,1,40,-20
MEAS/CYLNR,F(CYL032),6
PAMEAS/DISTANCE,0.5,SCNVEL,MMPS,100,P(PARc60),-1,0,0
PAMEAS/DISTANCE,0.5,SCNVEL,MMPS,100,P(PARc61),-1,0,0
ENDMES
P(PARc62)=PATH/ARC,CART,110.66,-71,-15.5,0,0,1,20,0,360,1,0,0
P(PARc63)=PATH/ARC,CART,110.66,-71,-18,0,0,1,20,0,360,1,0,0
MODE/PROG,MAN
F(CYL033)=FEAT/CYLNR,INNER,CART,110.66,-71,0,0,0,1,40,-20
MEAS/CYLNR,F(CYL033),6
PAMEAS/DISTANCE,0.5,SCNVEL,MMPS,100,P(PARc62),-1,0,0
PAMEAS/DISTANCE,0.5,SCNVEL,MMPS,100,P(PARc63),-1,0,0
ENDMES

GOTO/CART,111,-71,10,HEADCS,0,0
GOTO/CART,167,0,10,HEADCS,0,0
P(PARc64)=PATH/ARC,CART,165.99,0,0,0,0,1,20,0,360,1,0,0
P(PARc65)=PATH/ARC,CART,165.99,0,-2.5,0,0,1,20,0,360,1,0,0
MODE/PROG,MAN
F(CYL034)=FEAT/CYLNR,INNER,CART,165.99,0,0,0,0,1,40,-20
MEAS/CYLNR,F(CYL034),6
PAMEAS/DISTANCE,0.5,SCNVEL,MMPS,100,P(PARc64),-1,0,0
PAMEAS/DISTANCE,0.5,SCNVEL,MMPS,100,P(PARc65),-1,0,0
ENDMES
P(PARc66)=PATH/ARC,CART,165.99,0,-5.5,0,0,1,20,0,360,1,0,0
P(PARc67)=PATH/ARC,CART,165.99,0,-8,0,0,1,20,0,360,1,0,0
MODE/PROG,MAN
F(CYL035)=FEAT/CYLNR,INNER,CART,165.99,0,0,0,0,1,40,-20
MEAS/CYLNR,F(CYL035),6
PAMEAS/DISTANCE,0.5,SCNVEL,MMPS,100,P(PARc66),-1,0,0
PAMEAS/DISTANCE,0.5,SCNVEL,MMPS,100,P(PARc67),-1,0,0
ENDMES
```

```
P (PArc68)=PATH/ARC,CART,165.99,0,-10.5,0,0,1,20,0,360,1,0,0
P (PArc69)=PATH/ARC,CART,165.99,0,-13,0,0,1,20,0,360,1,0,0
MODE/PROG,MAN
F (CYL036)=FEAT/CYLNR,INNER,CART,165.99,0,0,0,0,1,40,-20
MEAS/CYLNR,F (CYL036),6
PAMEAS/DISTANCE,0.5,SCNVEL,MMPS,100,P (PArc68),-1,0,0
PAMEAS/DISTANCE,0.5,SCNVEL,MMPS,100,P (PArc69),-1,0,0
ENDMES
P (PArc70)=PATH/ARC,CART,165.99,0,-15.5,0,0,1,20,0,360,1,0,0
P (PArc71)=PATH/ARC,CART,165.99,0,-18,0,0,1,20,0,360,1,0,0
MODE/PROG,MAN
F (CYL037)=FEAT/CYLNR,INNER,CART,165.99,0,0,0,0,1,40,-20
MEAS/CYLNR,F (CYL037),6
PAMEAS/DISTANCE,0.5,SCNVEL,MMPS,100,P (PArc70),-1,0,0
PAMEAS/DISTANCE,0.5,SCNVEL,MMPS,100,P (PArc71),-1,0,0
ENDMES
GOTO/CART,167,0,10,HEADCS,0,0
GOTO/CART,167,-71,10,HEADCS,0,0
P (PArc72)=PATH/ARC,CART,165.99,-71,0,0,0,1,20,0,360,1,0,0
P (PArc73)=PATH/ARC,CART,165.99,-71,-2.5,0,0,1,20,0,360,1,0,0
MODE/PROG,MAN
F (CYL038)=FEAT/CYLNR,INNER,CART,165.99,-71,0,0,0,1,40,-20
MEAS/CYLNR,F (CYL038),6
PAMEAS/DISTANCE,0.5,SCNVEL,MMPS,100,P (PArc72),-1,0,0
PAMEAS/DISTANCE,0.5,SCNVEL,MMPS,100,P (PArc73),-1,0,0
ENDMES
P (PArc74)=PATH/ARC,CART,165.99,-71,-5.5,0,0,1,20,0,360,1,0,0
P (PArc75)=PATH/ARC,CART,165.99,-71,-8,0,0,1,20,0,360,1,0,0
MODE/PROG,MAN
F (CYL039)=FEAT/CYLNR,INNER,CART,165.99,-71,0,0,0,1,40,-20
MEAS/CYLNR,F (CYL039),6
PAMEAS/DISTANCE,0.5,SCNVEL,MMPS,100,P (PArc74),-1,0,0
PAMEAS/DISTANCE,0.5,SCNVEL,MMPS,100,P (PArc75),-1,0,0
ENDMES
P (PArc76)=PATH/ARC,CART,165.99,-71,-10.5,0,0,1,20,0,360,1,0,0
P (PArc77)=PATH/ARC,CART,165.99,-71,-13,0,0,1,20,0,360,1,0,0
```

```

MODE/PROG,MAN
F (CYL040)=FEAT/CYLNDR,INNER,CART,165.99,-71,0,0,0,1,40,-20
MEAS/CYLNDR,F (CYL040),6
PAMEAS/DISTANCE,0.5,SCNVEL,MMPS,100,P (PArc76),-1,0,0
PAMEAS/DISTANCE,0.5,SCNVEL,MMPS,100,P (PArc77),-1,0,0
ENDMES
P (PArc78)=PATH/ARC,CART,165.99,-71,-15.5,0,0,1,20,0,360,1,0,0
P (PArc79)=PATH/ARC,CART,165.99,-71,-18,0,0,1,20,0,360,1,0,0
MODE/PROG,MAN
F (CYL041)=FEAT/CYLNDR,INNER,CART,165.99,-71,0,0,0,1,40,-20
MEAS/CYLNDR,F (CYL041),6
PAMEAS/DISTANCE,0.5,SCNVEL,MMPS,100,P (PArc78),-1,0,0
PAMEAS/DISTANCE,0.5,SCNVEL,MMPS,100,P (PArc79),-1,0,0
ENDMES
GOTO/CART,167,-71,10,HEADCS,0,0
GOTO/CART,0,0,40,HEADCS,0,0
RECALL/SA (Surf_Finish.1.170.8.A0.0-B0.0)
SNSLCT/SA (Surf_Finish.1.170.8.A0.0-B0.0)
GOTO/CART,-80,-40,60,HEADCS,0,0
T (S_1)=TOL/SURFINISH,UPLIMIT,FILTER,GAUSS,SHORT,0.003,LONG,0.8,RA,1
T (S_1)=TOL/SURFINISH,UPLIMIT,FILTER,GAUSS,SHORT,0.003,LONG,0.8,RA,1
SNSET/APPRCH,5
SNSET/RETRCT,5
F (LINE006)=FEAT/LINE,BND,CART,-11.382,-35.52,-5,-16.182,-35.52,-5,0,0,1
MODE/PROG,MAN
SCNSET/VENDOR,TOL,T (S_1)
P (PLin8)=PATH/LINE,BND,CART,START,-11.381563,-35.520417,-5,END,-16.181563,-35.520417,-5,VEC,0,-1,0
F (SURFINISH004)=FEAT/SURFINISH,F (LINE006)
MEAS/SURFINISH,F (SURFINISH004),6
GOTO/CART,-11.382,-35.52,4.4,PCS,-180,90,180
PAMEAS/DISTANCE,1,SCNVEL,MMPS,1,P (PLin8),0,0,1,REMOVE,DIST,0.4,0.4
ENDMES
OUTPUT/FA (SURFINISH004),TA (S_1)
T (S_2)=TOL/SURFINISH,UPLIMIT,RA,3
T (S_2)=TOL/SURFINISH,UPLIMIT,FILTER,GAUSS,SHORT,0.003,LONG,0.8,RA,3

```



```
SNSET/APPRCH, 5
SNSET/RETRCT, 5
F(LINE007)=FEAT/LINE, BND, CART, 8.317, -34.98, -5, 3.52, -34.797, -5, 0, 0, 1
MODE/PROG, MAN
SCNSET/VENDOR, TOL, T(S_2)
P(PLin10)=PATH/LINE, BND, CART, START, 8.316838, -34.980239, -5, END,
3.520346, -34.7967$
7, -5, VEC, -0.038223, -0.999269, 0
F(SURFINISH005)=FEAT/SURFINISH, F(LINE007)

MEAS/SURFINISH, F(SURFINISH005), 6
GOTO/CART, 8.317, -34.98, 4.4, PCS, 177.809, 90, 180
PAMEAS/DISTANCE, 1, SCNVEL, MMPS, 1, P(PLin10), 0, 0, 1, REMOVE, DIST, 0.4, 0.4
ENDMES
OUTPUT/FA(SURFINISH005), TA(S_2)

PAUSE
ENDFIL
```

# APPENDIX C

## The Depth of the Holes

### C.1 For The Large Cutter Series

Hole No.	The Depth of Hole for				
	S16.1	S16.2	S16.3	S16.4	S16.5
1	20.11	20.022	20.015	20.026	20.007
2	20.082	19.992	20.033	20.023	20.044
3	20.096	20.025	19.977	20.029	19.953
4	20.059	20.002	19.995	20.029	19.99
5	20.095	20.06	19.949	20.059	19.915
6	20.051	20.026	19.969	20.046	19.959
7	20.12	20.13	19.958	20.118	19.912
8	20.07	20.073	19.978	20.09	19.951
9	20.125	20.008	20.027	20.021	20.034
10	20.111	19.967	20.04	20.031	20.017
11	20.104	19.975	19.96	19.985	20.008
12	20.062	19.944	19.985	19.999	19.995
13	20.075	19.974	19.938	19.973	20.012
14	20.071	19.938	19.959	19.979	19.992
15	20.116	20.006	19.945	19.989	20.048
16	20.105	19.962	19.968	19.986	20.016
17	20.122	20.017	20.036	20.002	20.029
18	20.126	20.06	20.01	20.059	19.997
19	20.087	19.958	19.981	19.984	19.999
20	20.085	20.005	19.98	20.06	19.974
21	20.08	19.939	19.963	19.989	19.995
22	20.069	19.974	19.956	20.088	19.96
23	20.109	19.959	19.988	20.046	20.016
24	20.091	19.979	19.967	20.141	19.97
25	20.184	20.002	20.019	20.028	20.035
26	20.132	19.992	20.032	20.11	20.051
27	20.126	19.927	19.969	20.031	19.999
28	20.074	19.927	19.988	20.127	20.029
29	20.086	19.904	19.951	20.063	20.003
30	20.038	19.895	19.969	20.159	20.031
31	20.087	19.921	19.976	20.126	20.032
32	20.03	19.902	19.99	20.221	20.053
33	20.07				20.033
34	20.058				20.001

35	20.036				20.008
36	20.025				19.98
37	20.029				20.005
38	20.008				19.965
39	20.057				20.027
40	20.03				19.973
41					20.04
42					20.027
43					20.014
44					20.002
45					20.01
46					19.99
47					20.029
48					19.996

## C.2 For The Small Cutter Series

Hole No.	The Depth of Hole for					
	S10.1	S10.2	S10.3	S10.4	S10.5	S10.6
1	20.015	20.039	20.039	20.047	20.028	20.016
2	20.074	20.034	19.981	19.921	20.001	20.032
3	20.004	20.044	20.037	20.053	20.014	19.977
4	20.066	20.04	19.973	19.914	19.976	19.99
5	20.006	20.049	20.031	20.07	20.005	19.948
6	20.082	20.078	19.98	19.936	19.968	19.965
7	20.068	20.082	20.076	20.143	20.031	19.964
8	20.145	20.017	20.001	20.001	19.988	19.977
9	20.034	19.963	20.012	20.045	20.035	20.043
10	20.045	19.945	20.038	19.977	20.063	20.014
11	20.013	19.89	19.959	20.029	20.005	20.025
12	20.022	19.883	19.974	19.976	20.031	19.991
13	19.993	19.834	19.919	20.037	19.988	20.015
14	20.002	19.859	19.944	19.989	20.02	19.984
15	20.004	19.805	19.926	20.094	20.004	20.046
16	20.012	20.02	19.939	20.04	20.039	20.01
17	20.035	20.015	20.032	20.049	20.039	20.046
18	20.026	19.974	20.079	19.973	20.099	20.037
19	20.011	19.971	20.002	20.049	20.022	20.037
20	20.008	19.937	20.047	19.974	20.079	20.026
21	20.011	19.946	19.989	20.07	20.01	20.034
22	20.01	19.952	20.036	20.002	20.081	20.02
23	20.043	19.95	20.014	20.147	20.039	20.061
24	20.039		20.062	20.066	20.111	20.042

---

25			20.019	20.021	20.049	20.045
26			19.83	20.049	20.06	20.058
27			19.884	19.954	20.004	20.029
28			19.719	19.995	20.032	20.046
29			19.809	19.926	20.002	20.041
30			19.636	19.956	20.031	20.053
31			19.767	19.929	20.009	20.078
32			19.573	19.954		20.084

# APPENDIX D

## Calculate the Metal Removal Rate

### D.1 Introduction

The next paragraph shows the sample of how calculated the feed rate, cutting time, and the volume of metal removed for each cycle for 10mm and 16 mm cutters.

### D.2 10mm Cutter: series 10.6

#### D.2.1 Cycle 1: Plunge Milling

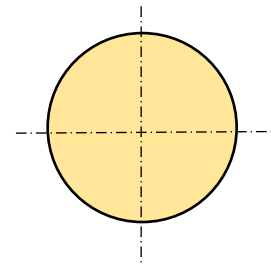


Figure D. 1

$$N= 1035 \text{ rpm} = 1153/60 = 19.22 \text{ rev/sec}, \quad = 0.068 \text{ mm/rev}$$

According to Eq. (3.9), the feed rate in Cycle 1 is

$$= \quad = 0.068 * 19.22 = 1.3 \text{ mm/sec}$$

According to Eq. (4.2), the cutting time in Cycle 1 (Plunge in) is

$$= 5/1.3 = 3.85 \text{ sec}$$

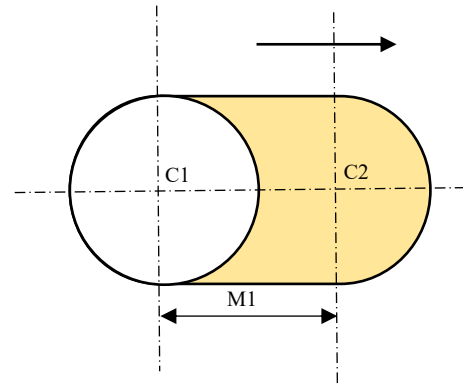
The area of the plunger is equal to the cylinder area

$$= 3.149 \cdot (5)^2 = 78.54 \text{ mm}^2$$

The Volume Removed is

$$= 78.54 \cdot 5 = 392.7 \text{ mm}^3.$$

**D.2.2 Cycle 2 Move Out**



$$= 0.136 \text{ mm/rev}, \quad = 7 \text{ mm}$$

$$= 0.136 \cdot 19.22 = 2.6 \text{ mm/sec}$$

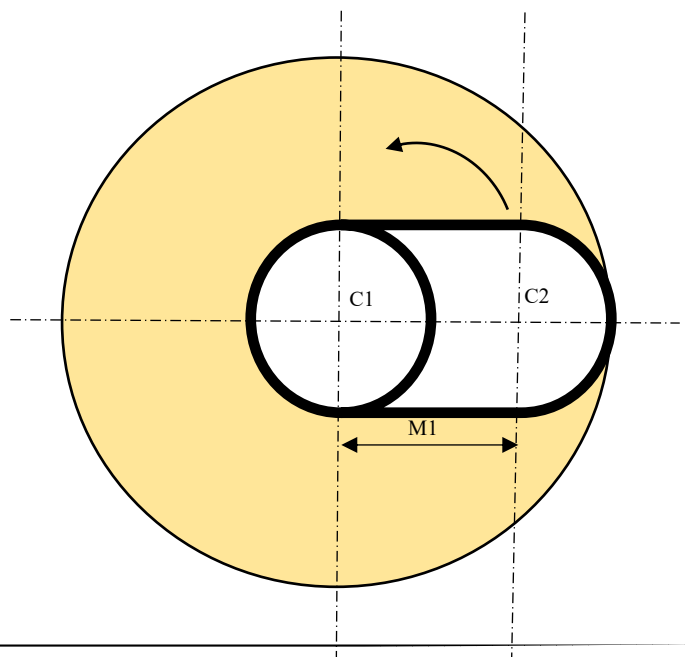
Figure D. 2

$$= 10 \cdot 7 = 70 \text{ mm}^2$$

$$= 350 \text{ mm}^3$$

$$= 7 / 3.45 = 2.68 \text{ sec.}$$

**D.2.3 Cycle 3 Circular Cut**



$$= 0.136 \text{ mm/rev}$$

Figure D. 3

$$= 0.136 * 19.22 = 2.6 \text{ mm/sec}$$

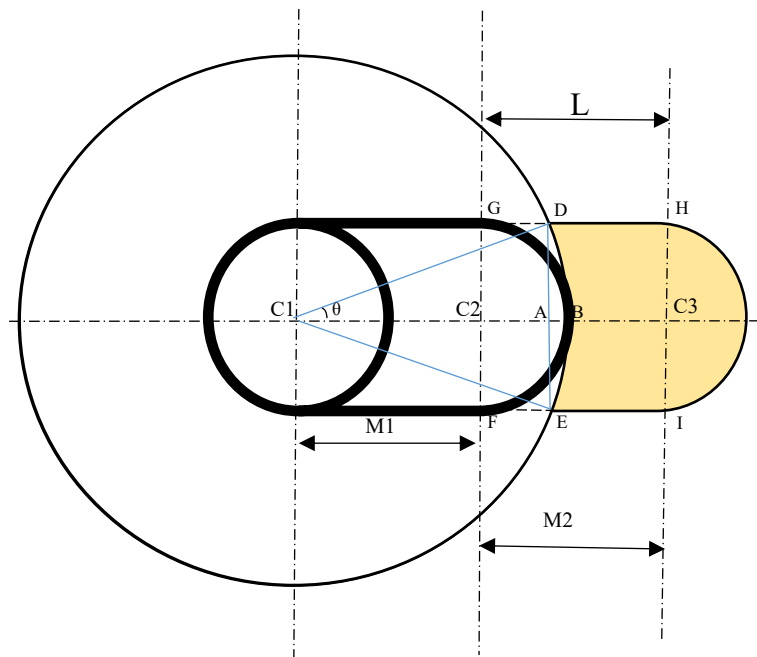
$$= \pi * (5)^2 * 70 = 303.85 \text{ mm}^2$$

$$= 1519.3 \text{ mm}^3$$

According to Eq. (4.4), the cutting time is:

$$= (2 * \pi * 7) / 2.6 = 16.8 \text{ sec}$$

#### D.2.4 Cycle 4 Move Out



$$= 0.17 \text{ mm/rev}, \quad = 8 \text{ mm}$$

Figure D. 4

$$= 0.17 \times 19.22 = 3.26 \text{ mm/sec}$$

$$= 8 / 3.26 = 2.45 \text{ sec}$$

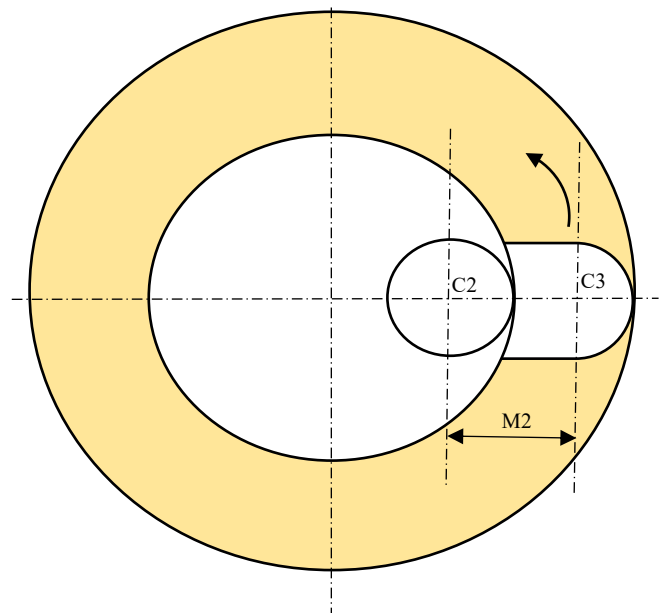
To calculate

$$= \text{Arc Length of BD}$$

$$= 73 \text{ mm}^2$$

$$= 365 \text{ mm}^3$$

**D.2.5 Cycle 5 Circular Cut**



$$= 0.17 \text{ mm/rev}$$

**Figure D. 5**



$$= 0.17 * 19.22 = 3.26 \text{ mm/sec}$$

$$= \pi * 15^2 = 706.86 \text{ mm}^2$$

$$= 3655 \text{ mm}^3$$

According to Eq. (4.4b), the cutting time in Cycle 3 (circular path) is

$$= 2 * \pi * 15 / 3.26 = 28.87 \text{ sec.}$$

### D.3 16mm Cutter: series16.4

#### D.3.1 Cycle 1 Plunge Milling

$$N = 1035 \text{ rpm} = 1035/60 = 17.25 \text{ rev/sec}, \quad f = 0.1 \text{ mm/rev}, \quad \theta = 16 \text{ mm}$$

The feed rate is:

$$= 0.1 * 17.25 = 1.725 \text{ mm/sec}$$

The cutting time is:

$$= 5 / 1.725 = 2.898 \text{ sec}$$

The area of the plunge is equal to the cylinder area

$$= 3.149 * (16/2)^2 = 201.06 \text{ mm}^2, \text{ which approximate } 2 \text{ cm}^2.$$

The Volume Removed is:

$$= 201.06 * 5 = 1005.3 \text{ mm}^3, \text{ which approximate } 1 \text{ cm}^3.$$

**D.3.2 Cycle 2 Circular Cut**

$$= 0.2 \text{ mm/rev}$$

$$= 0.2 * 17.25 = 3.45 \text{ mm/sec}$$

$$= \pi * (11)^2 * 201 = 179 \text{ mm}^2$$

$$= 895 \text{ mm}^3$$

The cutting time is:

$$= 2 * \pi * 3 / 3.45 = 5.46 \text{ sec}$$

**D.3.3 Cycle 3 Move Out**

$$= 0.25 \text{ mm/rev}, \quad = 9 \text{ mm}$$

$$= 0.25 * 17.25 = 4.3 \text{ mm/sec}$$

$$= 16 * 3 = 133.6 \text{ mm}^2$$

$$= 668 \text{ mm}^3$$

$$= 9 / 4.3 = 2 \text{ sec}$$

**D.3.4 Cycle 4 Circular Cut**

$$= 0.25 \text{ mm/rev}$$

$$= 0.25 \times 17.25 = 4.3 \text{ mm/sec}$$

$$= \pi \times 12 \times 4.3 = 742.8 \text{ mm}^2$$

$$= 3714 \text{ mm}^3$$

The cutting time is:

$$= 2 \times \pi \times 12 / 4.3 = 17.48 \text{ sec}$$